Scalable base station switching framework for green cellular networks

Thesis

SCALABLE BASE STATION SWITCHING FRAMEWORK FOR GREEN CELLULAR NETWORKS

ATM Shafiul Alam

B.Sc. (Honours), M.Sc.

A thesis submitted in fulfilment of

the requirements for the degree of Doctor of Philosophy

Department of Computing and Communications

Faculty of Mathematics, Computing & Technology
The Open University
Milton Keynes

August 2014

Statement of Originality

This is to certify that to the best of my knowledge and belief, all materials presented in this thesis is the original work of the author, unless otherwise stated. The content of this thesis has not been previously submitted as a part of any academic qualification to any other university or institution.

ATM Shafiul Alam
August, 2014

Abstract

With the recent unprecedented growth in the wireless market, network operators are obliged not only to find new techniques including dense deployment of *base stations* (BSs) in order to support high data rate services and high user density, but also to reduce the operating costs and energy consumption of various network elements. To solve these challenges, powering down certain BSs during low-traffic periods, so-called *BS sleeping,* has emerged as an effective green communications paradigm. While *BS sleeping* offers the potential to significantly lower energy consumption, it also raises many challenges, since when a BS is switched off, this can lead to, for example, coverage holes, sudden degradation in *quality of service* (QoS), higher transmit power dissipation in off-cell *mobile stations* (MSs), an inability to rapidly power up/down equipment and finally, a failure to uphold regulatory requirements. In order to realise greener network designs which both maximise energy savings whilst guaranteeing QoS, innovative *BS switching* mechanisms need to be developed.

This thesis presents a novel *BS switching framework* which improves *energy efficiency* (EE) in comparison with existing approaches, while guaranteeing the minimum QoS and seamless services. The major technical contributions in this framework are: *i*) a new BS to *relay station* (RS) switching model where certain BSs are switched to RS mode rather than being turned off, firstly using a *fixed threshold based switching* algorithm utilizing temporal traffic diversity, and *ii*) then subsequently by means of an *adaptive threshold* by exploiting the inherently asymmetric traffic profile between cells, *i.e.*, by exploiting both the temporal and spatial traffic diversity; *iii*) a *traffic-and-interference-aware BS switching* strategy that considers the impact of inter-cell interference in the decision making process to dynamically determine the best BS set to be kept active for improved EE; and finally *iv*) a novel *scalable multimode BS switching* model which enables each BS to operate in different power modes *i.e.*, macro/micro/sleep to explore energy savings potential even at higher traffic conditions.

The thesis findings conclusively confirm this new *BS switching framework* provides significant EE improvements from both BS and MS perspectives, under diverse network conditions and represents a notable step towards greener communications.

Dedication

my respected parents

my lovely sisters, Sumi and Lithu

Acknowledgements

This thesis could not have been produced without the inspirations, encouragement and support from many people, to whom I am greatly indebted. First and foremost, I would like to express my earnest tribute to my respected parents, A. K. Fazlul Hoque and Asafa Khatun and my lovely sisters, Sumi and Lithu. Their unconditional and immeasurable sacrifices, encouragement, blessings, and prayers have empowered me to reach this stage and successfully complete this thesis. With the deepest gratitude, I dedicate this thesis to them.

My sincere gratitude also goes to my principal supervisor, Professor Laurence S. Dooley, who was very generous to accept guiding me throughout this research. Professor Laurence's in-depth knowledge, unfailing advice, and uplifting moral support helped me to overcome many moments of depression. His constructive feedback immensely helped me in formulating and crystallizing ideas. Professor Laurence's philosophy of scientific research and advice on the art of scientific writing, tremendously contributed towards the production of this thesis. I am also indebted to my co-supervisor Dr. Adrian S. Poulton for his constant support and cooperation throughout this entire research. This work is in its current shape only through their numerous supports, insistence and attention to detail.

I would like to thank Professor Yusheng Ji, National Institute of Informatics (NII), Tokyo for giving me the opportunity to work in her lab during my internship at NII. I would also like to thank Dr. Faisal Tariq, University of Bedfordshire, for his effective instructions, discerning suggestions and insightful technical advice.

I also wish to thank Dr. Patrick Wong and Dr. Soraya Kouadri Mostéfaoui for their valuable advices, as well as all of my colleagues from the *neXt Generation Multimedia Technologies* (XGMT) Group at The Open University. In particular, Bola, John, Jonny, Eugen, Parminder, Dimitris, Udo, Hnin, Smarti, and George were really generous in providing me a friendly research environment. Thanks to all the administrative staff in the department and the research school with special appreciation for Donna Deacon, Anita and Paula. Last, but by no means the least, I would like to thank all my friends and family members for their encouraging supports and love.

Table of Contents

Chapter 3: Simulation and Evaluation Methodology

Chapter 4: Relay-Assisted Base Station Switching – A Fixed Threshold Approach

List of Figures

List of Tables

List of Acronyms

3G	Third Generation
4G	Fourth Generation
5G	Fifth Generation
3GPP	Third Generation Partnership Project
AC	Alternating Current
AF	Amplify-and-Forward
AI	Antenna Interfaces
APC	Area Power Consumption
BBU	Baseband Unit
BS	Base Station
CAPEX	Capital Expenditure
CC	Central Controller
CDF	Cumulative Distribution Function
CO_2	Carbon Dioxide
CoMP	Coordinated Multi-Point
CR	Cognitive Radio
DC	Direct Current
DF	Decode-and-Forward
DL	Downlink
DPD	Digital Pre-Distortion
DSO	Digital Switchover
DTA	Dynamic Traffic-Aware
DTIA	Dynamic Traffic-and-Interference Aware
DTV	Digital TV
DTX	Discontinuous Transmission
E2E	End-to-End Efficiency
EB	Exabyte
FCPC	Fully-Compensated Power Control
EE	Energy Efficiency
eNB	e-Node B
EPS	Evolved Packet System
FFT	Fast Fourier Transform
GPRS	General Packet Radio Service
GSM	Global System for Mobile Communications

ICI	Inter-Cell Interference
ICT	Information and Communication Technology
IF	Intermediate Frequency
IP	Internet Protocol
ISD	Inter-Site Distance
ITU	International Telecommunication Union
KPI	Key Performance Indicator
LOS	Line-of-Sight
LP	Low-Power
LTE	Long Term Evolution
LTE-A	LTE-Advanced
M2M	Machine-to-Machine
MAC	Medium Access Control
MAF	Mode Activity Factor
MIMO	Multiple-Input Multiple-Output
MMBS	Multimode Base Station Switching
mmWave	Millimetre Wave
MNO	Mobile Network Operators
MS	Mobile Station
MSC	Mobile Switching Centre
NLOS	Non-Line-of-Sight
OFDM	Orthogonal Frequency Division Multiplexing
OPEX	Operational Expenditure
PA	Power Amplifier
PDF	Probability Density Function
PL	Path-Loss
PRB	Primary Resource Block
PSTN	Public-Switched Telephone Network
QoE	Quality of Experience
QoS	Quality of Service
RAN	Radio Access Network
RAT	Radio Access Technology
RF	Radio Frequency
RNC	Radio Network Controller
RRM	Radio Resource Management
RS	Relay Station

SIM	Subscriber Identity Modules
SINR	Signal-to-Interference-plus-Noise Ratio
SON	Self-Organizing Networks
TDMA	Time Division Multiple Access
TVWS	TV White Space
UE	User Equipment
UHF	Ultra High Frequency
VHF	Very High Frequency
UL	Uplink
UMTS	Universal Mobile Telecommunications System
WCDMA	Wideband Code Division Multiple Access
WiMAX	Worldwide Interoperability for Microwave Access
XG	Next Generation
x-RS	Switched Relay Station

List of Variables

α	Cell-Specific PL Compensation Factor
δ	Tolerance Margin
γ_0	SINR Threshold
λ	Traffic Intensity
μ^{-1}	Mean Service Time
σ	Standard Deviation
ρ	Set of Traffic Load Profiles
ρ_b	Traffic Profile of $\mathcal{B}_b$
$\rho_{\max}$	Maximum Permitted Traffic Load
ρ_{th}	Switching Threshold
$\rho_{th}^{(c)}$	Switching Threshold in Cluster *c*
ξ	Load Factor
Ψ_{bm}	Shadow Fading Effect
η_{EE}	Energy Efficiency
Φ	Cumulative Distribution Function
Γ_{bm}	SINR between $\mathcal{B}_b$ and MS *m*
a_{BS}	BS Power Scaling Factor
$\mathcal{A}$	Network Area
A_b	Mode Activity Factor of $\mathcal{B}_b$
$\mathcal{B}_b$	Base Station
$\mathcal{B}_b^{(c)}$	Base Station in Cluster *c*
$\mathcal{B}$	Set of BSs in the Network
$\mathcal{B}^{\text{on}}$	Set of Active BSs
d_{bm}	Propagation Distance between $\mathcal{B}_b$ and MS *m*
E_{AO}	Network Energy Consumption with "*always-on*" mode
E_{ES}	Network Energy Savings
g	Ratio of RS to BS Energy Consumption
G	Antenna Gain
I_b	Interference Term in $\mathcal{B}_b$
$\mathcal{M}_b$	Set of MS in $\mathcal{B}_b$

$\mathcal{M}$	Set of MS in the Network
M_m	Number of Primary Resource Block
$\mathcal{N}_b$	Neighbour BS Set of $\mathcal{B}_b$
N_0	Noise Power
N_c	Total Number of Channels in each Cell
N_{BS}	Total Number of BSs
N_{BS}^{off}	Number of Dormant BSs
N_{BS}^{on}	Number of Active BSs
N_{MS}	Total Number of MS in the Network
N_{RB}	Total Number of available Channels or PRB in each Cell
N_T	Total Number of Switching Instances per Day
$p_{rx,bm}$	Received Power at MS m in $\mathcal{B}_b$
$p_{tx,bm}^{BS}$	Transmit Power of $\mathcal{B}_b$ for MS m
$p_{tx,rm}^{RS}$	Transmit Power of RS for MS m
P_f^{BS}	Fixed/Static Power Consumption
P_{dyn}^{BS}	Dynamic Power Consumption
P_0	User-Specific Power Offset Parameter
P_{APC}	Area Power Consumption
P_{block}	Blocking Probability
P_C	Probability of Collisions
P_{out}	Signal Outage Probability
P_T	Total Network Power Consumption
P_{T_b}	Total Power Consumption of $\mathcal{B}_b$
$P_{T,BS}$	Total BS Power Consumption
$P_{T,UL}$	Total MS Power Consumption
$P_{tx,\max}^{BS}$	Maximum BS transmit power
$P_{tx,m}^{MS}$	MS Transmit Power
$P_{tx,\max}^{MS}$	MS Maximum Transmit Power
P_f^{BS}	Fixed or Static Power Consumption of BS

$P_{tx,b}^{BS}$	Total Power Consumed by $\mathcal{B}_b$
$PL(d_{bm})$	Path-Loss over Distance d_{bm}
r_m	User Throughput
$r_{\min}$	Minimum Data Rate Requirements
R_b	Overall Cell Throughput
R_{ma}	Macrocell Coverage Radius
R_{rs}	Relay Coverage Radius
T_0	Minimum Mode Holding Time
$\mathcal{U}(\mathcal{B}_b)$	Utility Function for $\mathcal{B}_b$
$\boldsymbol{w}$	Weighted Vector for Received Interference
W	Channel Bandwidth
W_{max}	Maximum Cell Bandwidth

Chapter 1

Introduction

1.1 Overview

Cellular communications have become an integral part of our daily lives. The mobile market has grown dramatically in the past two decades, surpassing the number of wireline subscribers as far back as 2002 (Anon, 2014). At the same time, mobile phones have become much more than mere communication devices. With the popularity of *Third Generation* (3G) and *Fourth Generation* (4G) cellular communication technologies supporting several megabits per second data rates, mobile devices are now multimedia-enabled, delivering a variety of applications from music, interactive games and video-streaming to web-browsing and email. Concurrently, the wireless industry has also witnessed explosive and sustained growth, with the key drivers for this growth being ubiquitous network coverage, allied with easy and cheap access and the emergence of a wide range of support applications.

Recently, several innovative technologies have been introduced to increase the data rates in cellular networks including for example: spatial reuse of spectrum (Novlan et al., 2011), deploying smaller and more cells (Richter et al., 2009), distributed antennae systems (DAS) (Choi & Andrews, 2007; Hosseini et al., 2013), coordinated multi-point (CoMP) transmissions (Lee et al., 2012), optimization of resource allocations and relays. Despite providing significantly higher data rates, cellular communication technologies have still struggled to meet the ever increasing demands that new services need in terms of data rates. Not only this, but the consequence of achieving these higher data rates raise the fundamental sustainability question of cellular networks, both from an economic and environmental point of view. Operators must deliver an economically sustainable capacity and performance growth by offering both improved coverage and a superior user experience at a lower cost than is currently provided by existing systems. Since growth in

cellular communications also increases the overall energy consumption of the networks, which has a greater impact on carbon emissions, addressing the energy efficiency of emerging wireless technologies is of immediate concern. Key limitations are the inherently inefficient network design which is based solely on peak-traffic demands and the inefficient management of *base station* (BS) operation. As BS switching technique is recognized as one of major focuses in *next-generation* (XG) greener cellular networks to lower overall energy consumption (Marsan et al., 2011; 3GPP, 2010a), the development of new innovative energy efficient strategies and paradigms represents a fertile area of research.

1.2 Energy Efficiency in Cellular Networks

The main design objective of early mobile radio systems was to achieve a large coverage area by using a single, high-powered transmitter with an antenna mounted upon a tower. Due to restrictions imposed by government regulatory bodies on the allocation of specific radio spectrum and its capacity limit (Tse & Viswanath, 2005), as well as the explosive growth in cellular network data traffic (Cisco, 2013), it became imperative to restructure the cellular systems in order to achieve higher capacity with limited spectrum, while covering large areas.

The massive data demand for cellular services within a limited radio spectrum, with ever increasingly high data rate requirements for new data intensive mobile applications like multimedia streaming, forced operators in the last decade to more densely deploy BSs to fulfil this demand. It is expected that the cellular data traffic will continue to grow in the future, so BSs will need to be even more densely deployed to service the higher capacity (Cisco, 2013). Correspondingly, energy consumption as well as the *Carbon Dioxide* (CO_2) footprint of cellular networks will also inevitably increase at an excessive rate leading to higher network *operating expenditure* (OPEX) and more public and political pressure to reduce CO_2 emissions (Huawei, 2011). Ever-increasing energy costs are of equal concern

to both cellular network operators and vendors (Edler & Lundberg, 2004; Huawei, 2011). For instance, among the energy consuming industries, the *information and communication technology* (ICT) industry contributes 2% of global total CO_2 emissions, and this is expected to double by 2020 (Shen, 2013). Recent studies have predicted that although the overall carbon footprint of ICT is expected to less than double from 2007 to 2020, it will triple for cellular networks in the same time frame (Fehske et al., 2011; Oh et al., 2013). However, existing cellular architectures have been designed primarily for optimizing network coverage and data throughput, while generally ignoring the energy efficiency aspect. It has thus now become imperative to include energy efficiency as a major performance indicator in both the planning and the operational stages of XG green cellular networks.

In current cellular systems, the BS in the *radio access network* (RAN) is the dominant energy consuming equipment, with typically between 60% and 80% of the whole network energy consumption (Marsan et al., 2009). In contrast, the energy requirement for *mobile stations* (MSs) lies in the range of only 1% to 10% (Peng et al., 2011; Ge et al., 2010), so any reduction in the net BS energy consumed can lead to considerable improvements in the overall network energy efficiency. To meet the challenge of improving the energy efficiency in cellular networks, it is imperative to resort to new paradigm-shifting technologies, such as energy efficient network architectures and protocols, transmission techniques and energy efficient resource management. In addition, from the network operator's perspective, reducing the overall network energy consumption can be translated into lower OPEX.

Traditionally, BSs operate in a 24 hours a day/7 days a week "*always-on*" mode and are generally designed based on peak-traffic loads, irrespective of either the time of day or traffic profile. In practice, the cellular network traffic generation exhibits a high-degree of temporal-spatial variation (Oh et al., 2011; Peng et al., 2011). Due to the significant traffic

diversity in both time and spatial domains and "*always-on*" mode of BS operation, many BSs remain significantly under-utilized for large portions of a day, resulting in system-wide energy inefficiency at BS (Oh et al., 2011; Peng et al., 2011). They have become a prime candidate for the adoption of energy efficient approaches in many networking scenarios such as BS sleep operation, multi-operator network sharing and advanced energy efficient communication technologies. This is evidenced by many recent solutions which have been developed for energy efficient cellular network including Marsan et al., (2009), Oh & Krishnamachari, (2010), Chiaraviglio, et al., (2008), Peng et al., (2011), Gong et al., (2012), Deruyck et al., (2014). There thus exists the prospect to exploit these opportunities and devise new innovative BS operation mechanisms to manage cellular networks in a more energy efficient way than is currently implemented, without importantly compromising the *quality of service* (QoS) provision.

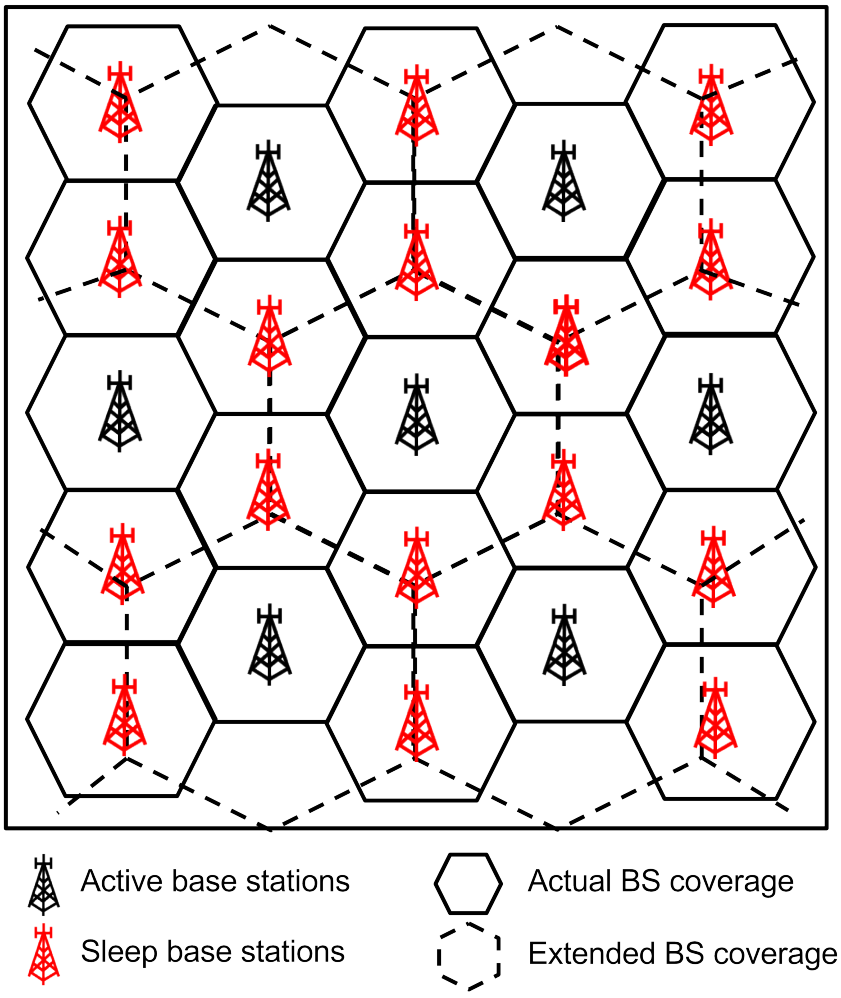

Figure 1-1: Example of *BS sleeping* scheme with coverage extension.

1.3 Research Motivation

In order to reduce the BS energy consumption, *BS sleeping* operation, in which selected BSs can switch to a *sleep* mode has been considered as a promising solution for green cellular networks (Louhi, 2007; Marsan et al., 2009; Zhou et al., 2009; Niu et al., 2010; Marsan et al., 2011; Oh et al., 2013). The design criterion for *BS sleeping* operation is to *minimize the energy consumption while guaranteeing the availability of wireless access over the service area and maintaining a minimum QoS*. An illustration of the *BS sleeping* operation is shown in Figure 1-1, where certain BSs are switched to *sleep* mode, whilst others extend their coverage to maintain the requisite services in the sleeping cells. Although the *BS sleeping* approach can significantly reduce energy dissipation, there are still many design challenges to resolve in realising an efficient and practical BS switching operation. Some of the key issues to be addressed include:

- In making the switching decision, the number of BSs to be switched to *sleep*/*active* mode has to be considered. This is important because frequent BS mode switching requires fast coverage adjustments and some BSs will always have to be kept in *active* mode to guarantee the required QoS.

- Turning off certain BSs may result in coverage holes due to shadowing and fading effects, especially close to other sleeping BSs, because radio propagation is strongly affected by the environment and the distance between BS and MS when the transmit power is restricted. So guaranteeing cell coverage when some BSs are switched to *sleep* mode is challenging.

- The BS switching decision can not only be made based on the load conditions of a BS itself, but it also needs to consider the load of neighbouring BSs. Therefore, BS cooperation is essential in order to guarantee the availability of wireless access over the service area.

- The specific system parameters used for making the switching decision, have to be determined. Since in low-traffic periods, most BSs will be able to be easily switched to *sleep* mode, identifying the best BS set to switch off is a major challenge. Furthermore, consideration needs to be given to key parameters which directly impact on network performance, such as traffic load and interference.

- While traffic dynamics provide opportunities for energy savings, pragmatically these can only be exploited during low-traffic periods, while almost no savings are achievable during periods of medium and high-traffic loads. To attain any savings during these demanding traffic periods, new BS switching design strategies and models need to be developed.

These various challenges and the general aim of increasing BS energy efficiency without compromising QoS highlighted in *Section 1.2* were the main motivations for this research. It is an important requirement from both a social and economic perspective, and arises as a direct consequence of the persistent performance gap existing between traditional BS operation and current BS switching mechanisms like *BS sleeping*. This provided the context for the overarching thesis research question and related objectives which are distilled in the next section.

1.4 Research Question and Objectives

From the discussion in *Section 1.3*, the main research question was framed:

How can the energy consumption of traditional cellular networks be minimized without compromising the required QoS?

The energy consumption of a cellular network can be reduced by improving the *energy efficiency* (EE) from every aspect from hardware design enhancements through to optimal deployment strategies, cooperative techniques, and adoption of innovative *BS sleeping* techniques, which will be fully discussed in *Section 2.7*. Following the detailed literature

review to survey existing solutions and models, and an evaluation of suitable potential technologies and strategies in Chapter 2, *BS switching* was identified as a particularly rich topic area for investigation as it has considerable potential to achieve the desired significant reductions in network energy consumption. As a consequence, the following set of three research objectives was framed to underpin the above overarching question:

1. To critically analyse the potential of traffic dynamics to minimise energy consumption while upholding QoS, especially for off-cell users.

Justification: This addresses the potential of natural cellular traffic dynamics and the vital coverage holes problem inherent in all *BS sleeping* approaches. As well as guaranteeing comparable QoS to normal "*always-on*" BS mode, the objective is to develop new solutions such that the overall network energy consumption is minimized and off-cell users cannot distinguish any service differences before and after switching. Under-utilized BSs could be placed into dormant mode based upon the service requirements, with cell coverage being maintained by adopting new techniques. Above all the framework would include a switching mechanism that reflects the impact of the asymmetric nature of practical cellular traffic profiles to enhance further energy savings. In other words, any switching decision criterion has to be sufficiently flexible to manage instantaneous network traffic scenarios.

2. To develop and critically evaluate new *BS switching* mechanisms which jointly address the impact of traffic load and interference.

Justification: Interference can seriously impact the choice of which BSs are to have their operating modes changed, so the nexus between the best BS set selection to be kept *active* and the impact of interference will be thoroughly analysed. New switching techniques thus need to be developed which are able to make switching decisions based not only upon the existing traffic conditions, but on other key network performance parameters like interference, in determining the best set of BSs to switch operating modes.

3. To critically synthesise a scalable BS switching solution able to dimension network capacity according to traffic demands and across diverse load conditions.

Justification: Switching off particular BS during either low or no traffic periods requires the load to be sufficiently small so that user performance is not compromised. There are still however, energy saving opportunities beyond low-traffic conditions, so new BS switching models need to be investigated such that the network can be dimensioned into different capacity scales depending upon the prevailing traffic conditions, to maximise energy savings. It is important to stress that both the service coverage and QoS must always be maintained at the required level.

In summarising, the overall aim is to develop a flexible *BS switching* paradigm which minimizes energy consumption in cellular access networks by adopting dynamic BS operating mechanisms which exploit the inherent spatial-temporal traffic diversity for greener cellular networks.

1.5 Contributions

To fulfil the aforementioned objectives, this thesis presents a new robust *BS switching framework* which comprises four original scientific contributions to the field of green cellular networks. The framework includes two separate network models namely, *multimode BS switching* (MMBS) and *BS-to-relay station* (*RS*) or *BS-RS switching* models, and three switching algorithms namely, *fixed* and *adaptive threshold based* and *dynamic traffic-and-interference aware* (DTIA) algorithms. The first two algorithms are designed by only considering traffic load and are thus termed as *dynamic traffic-aware* (DTA) switching algorithms, while the third technique innovatively considers both the traffic and interference. Figure 1-2 illustrates the layout of the objectives and original achievements of this thesis using different colours. The framework, which is based on the key system parameters of traffic profiles and interference, represents a paradigm shift for green cellular networks as it not only provides significant energy savings under a range of traffic

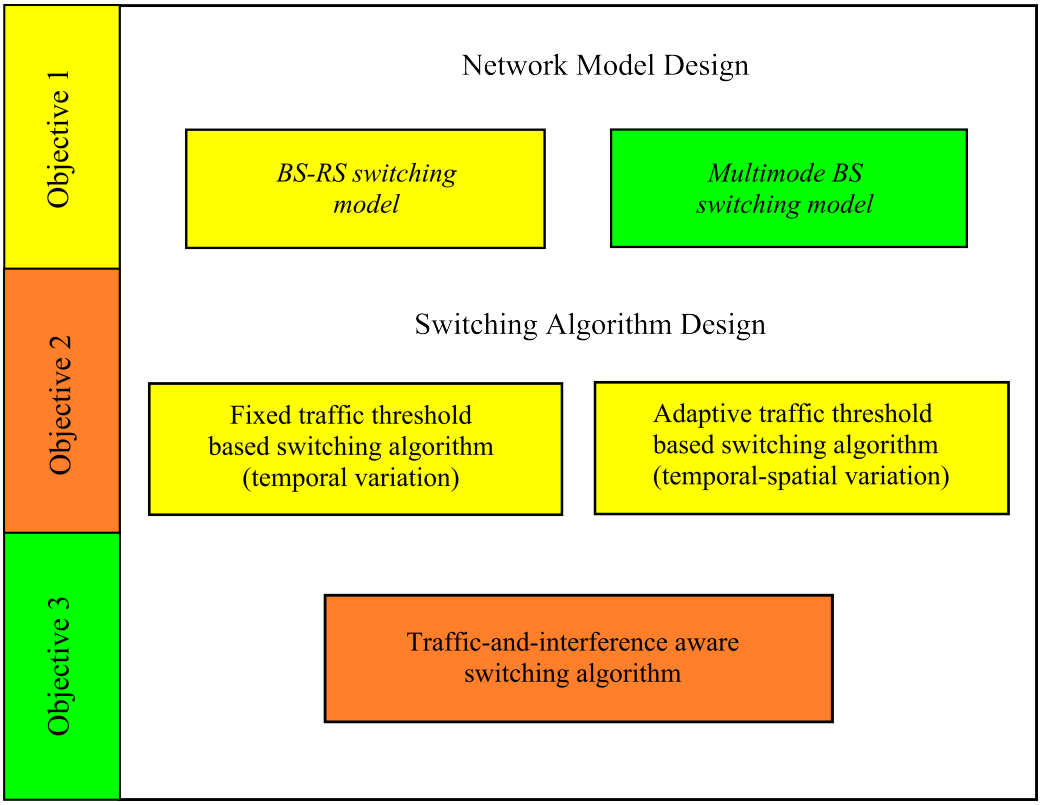

Figure 1-2: Layout of the objectives and achievements in this thesis.

scenarios but crucially does so, without compromising the users' QoS.

To summarise, the following contributions have been made in this thesis:

i) A new *BS-RS switching* model is introduced and critically analysed, as a partial realisation of *Objective 1* (yellow blocks in Figure 1-2), addressing the potential of cellular traffic dynamics for energy savings and the issues of coverage holes, by keeping either a BS or a RS *active* all the time in every cell, instead of putting a cell completely to *sleep*. A generalised power consumption model is derived and the corresponding switching conditions based on a predefined *fixed threshold based BS switching* algorithm established for both the new *BS-RS switching* and existing *BS sleeping* models. Moreover, this chapter has contributed to both network model and switching algorithm designs as highlighted by the yellow blocks in Figure 1-2. The energy savings and off-cell user performance are comparatively analysed along with the traditional "*always-on*" approach.

ii) A new *adaptive threshold based BS switching* algorithm (Figure 1-2) is presented as fulfilment of *Objective 1* (yellow blocks in Figure 1-2). This reflects the fact that in practical network situations, cellular traffic significantly varies between cells. Using a cooperative BS strategy, the adaptive algorithm first determines the switching threshold based on the instantaneous traffic profiles of all BSs at each decision instant. The switching choice for each BS then employs the same criterion which was applied in the *fixed threshold* algorithm in i), and this technique can be seamlessly integrated into both the *BS-RS switching* and other existing *BS sleeping* models. Furthermore, the proposed adaptive algorithm is proven to have consistently superior energy saving performance compared with the *fixed threshold* algorithm.

iii) To successfully realise *Objective 2*, the impact of network interference together with the traffic dynamics has to be resolved in the BS switching mechanism, and this is achieved by means of a new DTIA algorithm, which is in the switching algorithm design part of the framework (Figure 1-2, orange blocks). By continually monitoring both the instantaneous traffic profile and the level of interference, the best set of BSs to be kept in *active* mode is identified at any particular time. The DTIA algorithm bases its decision on the *fixed threshold based switching* algorithm in i), always ensuring that priority is given to switch those BSs generating the highest interference to other network users. Particularly significant is that due to the finer granularity involved, DTIA achieves reliably higher energy savings than the DTA algorithm.

iv) Finally, in considering *Objective 3*, a new MMBS model is presented as shown in Figure 1-2, green blocks, which enhances energy savings under all traffic conditions, since existing *BS switching* solutions only achieve savings during low-traffic periods. The MMBS model functions such that each BS can switch its

operating mode into three different power modes in a scalable fashion depending upon the cell traffic demands. This leads to a novel *scalable BS switching framework* which has been shown to effectively overcome many of the limitations of existing solutions in achieving energy reductions beyond the normal low-traffic conditions, while upholding minimum QoS requirements.

1.6 Thesis Structure

The rest of the thesis is organized as follows:

- *Chapter 2* presents a thorough literature review of the state-of-the-art cellular technologies relating to green cellular networks. It also surveys existing BS switching mechanisms, designs and operational challenges; the generalised power consumption model available for various BS types and other associated research activities. A comprehensive study of the fundamental approaches to green cellular networks is also presented to buttress the overarching thesis research question defined in *Section 1.4*.

- *Chapter 3* focuses upon the research methodology adopted in this thesis including the modelling requirements and system-level simulation methodology. It also discusses the choice of simulation test platform, the new framework's validation procedures and the key performance metrics applied to critically assess the comparative performance of all new models and algorithms.

- *Chapter 4* details the *BS-RS switching* model, which dynamically changes BS operation modes between *active* (normal BS mode) and RS mode. The *BS-RS switching* model aims to both guaranteed coverage and to deliver similar QoS levels for off-cell users as that of the "*always-on*" BS operating mode. The model's performance is critically evaluated and compared with the *BS sleeping* approach in terms of energy efficiency using a *fixed threshold based switching*

algorithm to trigger a BS into RS mode, reliably ensuring an over 25% energy saving. Work from this chapter has been published in Alam *et al.*, (2012).

- *Chapter 5* leverages from the findings of using the *fixed switching threshold* in *Chapter 4*, to extend the idea and exploit the asymmetric traffic dynamics among cells to further improve the level of energy saved in the *BS-RS switching* and the *BS sleeping* models. A dynamic mechanism for changing BS modes is described based on an *adaptive threshold based switching* algorithm, with a rigorous comparative performance evaluation being presented to support the theoretical basis of the algorithm. This *adaptive threshold based switching* algorithm will be shown to achieve energy savings of greater than 50% and 30% respectively when applied in the *BS-RS switching* and *BS sleeping* models. Work from this chapter has been published in Alam *et al.*, (2012).

- *Chapter 6* considers the network impact of both traffic load profiles and interference in the BS switching decision process and proposes a new DTIA switching algorithm. This applies the *fixed threshold based switching* algorithm developed in *Chapter 4*, to prioritise the best set of BSs which are to be switched to dormant mode based upon their interference impacts upon other users. The DTIA algorithm is robustly evaluated and compared with an existing dynamic traffic only aware BS switching technique, with results revealing an energy efficiency improvement of greater than 20%. Work from this chapter has also been published in Alam *et al.*, (2013).

- *Chapter 7* proposes a novel robust, scalable MMBS model which exploits opportunities during all traffic conditions to reduce the overall energy consumption. While earlier switching models are founded on the assumption that a BS can switch between *active* and dormant modes only if specific switching threshold conditions are met, the MMBS model dimensions network capacity

according to traffic demand, so enabling certain BSs to switch to intermediate low-power mode, even under high-traffic conditions to secure further energy savings. Results confirm a more than 50% energy reduction for low-traffic conditions and up to 7% during demanding high-traffic conditions. Work from this chapter has been accepted for presentation at the IEEE Wireless Communications and Networking Conference 2015 (Alam & Dooley, 2015).

- *Chapter 8* summarises some feasible enhancements and extensions to the new *scalable BS switching framework* together with identifying some other potential future research directions in green cellular networks.

- *Chapter 9* summarises the key findings and original contributions presented in this thesis.

1.7 Summary

This chapter has formulated the three principal research objectives addressed in this thesis by highlighting the high energy under-utilization of existing cellular networks and exceptionally growing energy expenditure according to the statistical evident. A concise overview of the main research question, related objectives, contributions made and the thesis structure have been provided. The following chapter presents a comprehensive literature survey on green cellular networks and their associated technologies.

Chapter 2

Green Cellular Networks – A Literature Review

2.1 Introduction

The rapid growth of wireless communications is good news for the wireless industry as it is one of the major contributors to the global economy (GSMA, 2013). Not only that, it also provides an excellent experience for mobile users who expect high-speed internet access anywhere and anytime with any device to be provided by *XG* wireless networks. There have been considerable efforts over the last two decades to improve the cellular system's capacity by deploying more BSs, multiple antennas, and so on. However, the drawback is that there is an enormous energy consumption associated with the wireless infrastructure as it has been overlooked in the past. This chapter discusses the overview of cellular architecture, the necessity of green cellular networks and their energy expenditures, high level power model for different types of BSs and existing energy saving techniques toward green cellular networks as well as the related projects and standardization initiatives. The goal of this chapter is to allow reader to get an up to date overview of the literature on green cellular networks.

2.2 Overview of Cellular Communication Systems

The cellular concept was a major breakthrough in solving the problem of spectral congestion and user capacity (Rappaport, 2001). It is a system-level idea which calls for replacing a single, high power transmitter (covering a large area) with many low power transmitters covering small geographic areas called *cells* that are represented as a hexagon. Each cell is served by a BS providing coverage to only a small portion of the service area. The BS is located at a fixed position and connected to a *mobile switching centre* (MSC) in *Time Division Multiple Access* (TDMA) based *Global System for Mobile* (GSM) or a *radio network controller* (RNC) in *Wideband Code Division Multiple Access* (WCDMA) based

Universal Mobile Telecommunications System (UMTS). An MSC or RNC is in charge of a cluster of BSs, and through them, mobile devices are connected to the *public-switched telephone network* (PSTN) and the Internet (*i.e.* external networks). GSM was developed to carry real time services, in a circuit switched manner and then develop towards an *internet protocol* (IP) based packet switched solution with the evolution of GSM to *General Packet Radio Service* (GPRS). In UMTS, a circuit switched connection is used for real time services and the IP based packet switched connection is for data services. *Third Generation Partnership Project* (3GPP) *Long Term Evolution* (LTE) *Evolved Packet System* (EPS) is purely an IP based technology. The BS in UMTS and LTE are referred to as NodeB, and e-NodeB (eNB), respectively, while MS as *user equipment* (UE). However, the eNB in LTE embeds its own control functionality, rather than using an RNC. Figure 2-1(a) illustrates a cellular network architecture of GSM, UMTS and EPS/LTE systems connected to external networks. The eNB are interconnected with each other by means of the X2 interface, which supports the exchange of signalling information between eNB for coordination and cooperation purposes (3GPP, 2008). This is illustrated in Figure 2-1(b). It might be appropriate to mention that there is no interface between BS in GSM/UMTS cellular systems. The NodeB or eNB and UE will be referred as BS and MS, respectively throughout this thesis. Both BS and MS are equipped with a transceiver. Thus, LTE has a flatter and much more distributed architecture with each BS having more functionality compared to GSM/UMTS systems.

Cellular systems are limited to the overall system capacity[1] (Caire et al., 1998), which can be increased by employing various strategies such as multiple antenna techniques, higher-order modulations, and deploying more cells. The simplest way of increasing the overall system capacity is to deploy more cells of smaller size such that the limited radio spectrum can be reused again and again without any significant interference. Traditionally, cellular

[1] System capacity is a measure of the number of users per cell which can be supported for a given QoS.

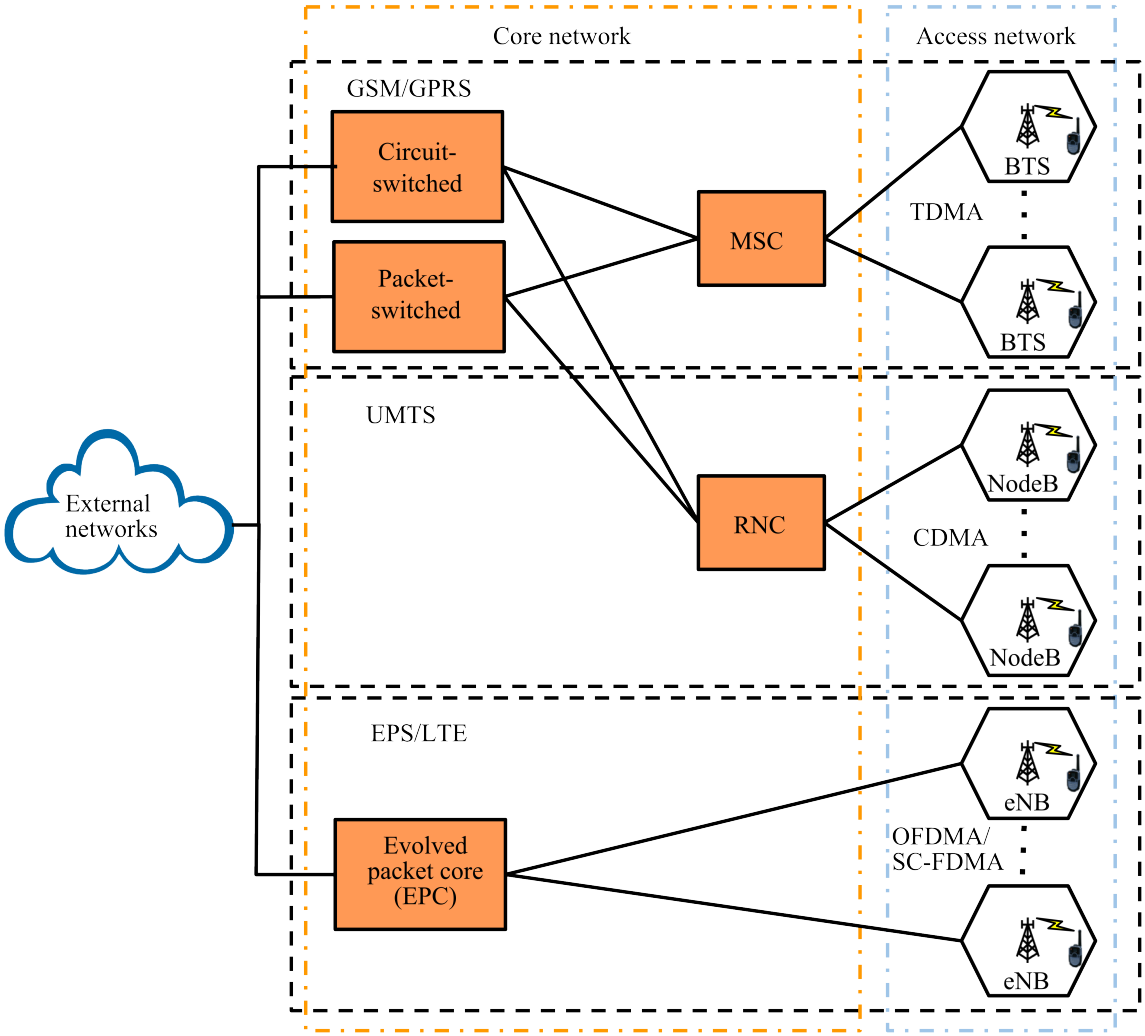

(a)

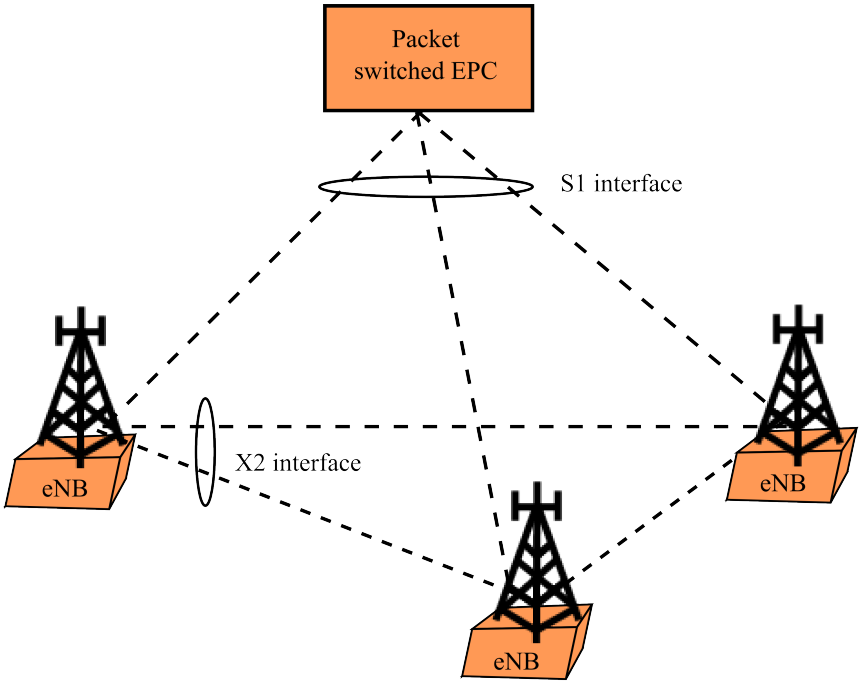

(b)

Figure 2-1: (a) Network solutions from GSM to LTE; and (b) LTE architecture with interfaces.

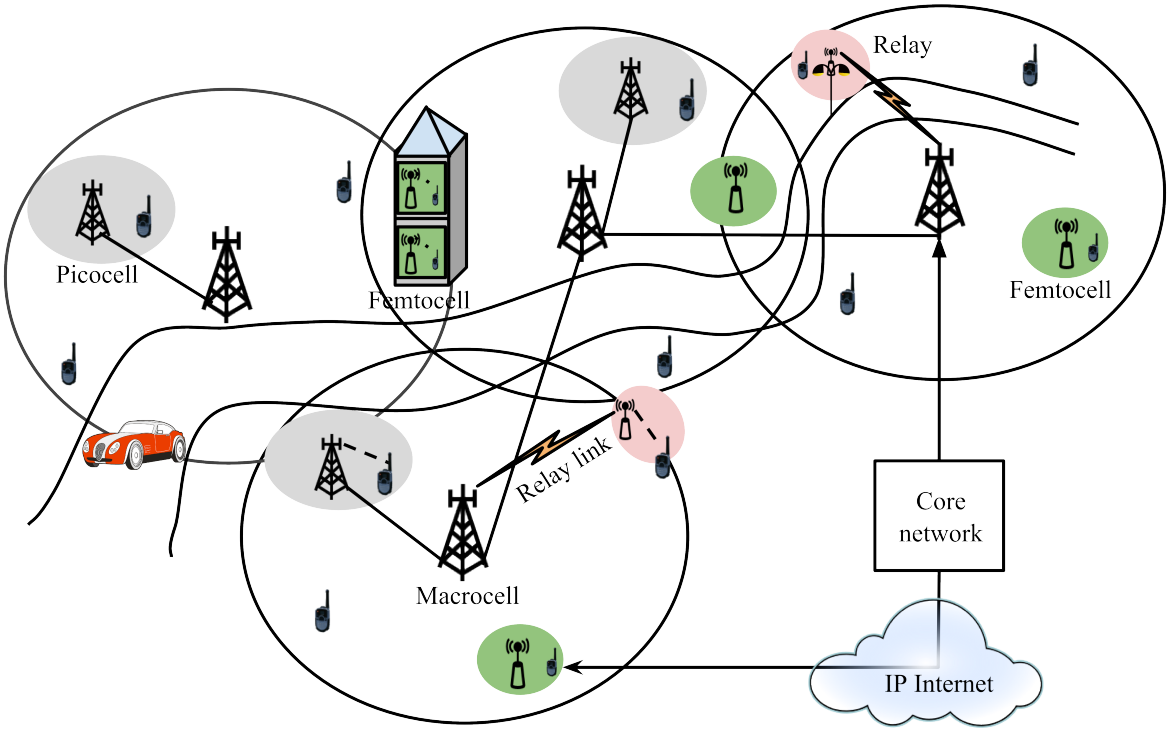

Figure 2-2: An illustration of a multi-tier (heterogeneous) cellular network topology.

networks adapt a single-tier network, *i.e.*, only a single type of BSs is deployed (usually macro BSs) and the network is known as a homogeneous network. Due to the poor signal coverage especially for indoor users, poor cell-edge throughput, increased *Inter-Cell Interference* (ICI) and high transmit power requirements, *XG* cellular architecture such as LTE and *Worldwide Interoperability for Microwave Access* (WiMAX), have embraced the concept of a multi-tier network consisting of a mix of macrocells and small cells such as microcells, picocells, femtocells and relays. A multi-tier network has a potential in substantially improving the capacity and coverage (Yeh et al., 2011), though it is considerably less planned unlike typical single-tier macrocell networks (Ashraf et al., 2011). These multi-tier networks are usually known as heterogeneous networks (Ghosh et al., 2012). An example of a typical heterogeneous cellular network is illustrated in Figure 2-2.

2.3 Rationale for Green Cellular Networks

The energy consumption problem in the ICT sector has become crucial during the past years (Lannoo et al., 2013). As a result, governments and industries have recently shown

keen concerns on the critical issues related to the energy efficiency in the ICT sector. Among the energy consuming industries, the ICT industry takes 2% of global total CO_2 emissions, which is expected to double by 2020 (Shen, 2013). As a percentage, the role of ICT could be thought to be small; the reality is, however, different for many reasons as ICT plays a key role in reducing energy consumption in many sectors such as transportation, power generation and distribution, agriculture, etc., which are the major contributors to the rise of global CO_2 emission (Neves & Krajewski, 2012). For example, a company that converts 100 meetings a month to wireless teleconferences would reduce its CO_2 emissions by 720,000 kilograms per year (Pescovitz, 2004). More specifically, the cellular mobile industry itself is also a contributor of CO_2 emission through network operations, mobile equipment and so on due to its tremendous growth and massive involvement in almost every sector. For example, cellular networks are estimated to be responsible for 0.5% of world-wide electrical energy consumption (Fettweis & Zimmermann, 2008). As most of the energy produced today is still generated from non-renewable energy sources, networks are correspondingly responsible for a significant amount of CO_2 emissions, which is estimated at between 0.5% and 1% of the entire world carbon footprint (Fettweis & Zimmermann, 2008).

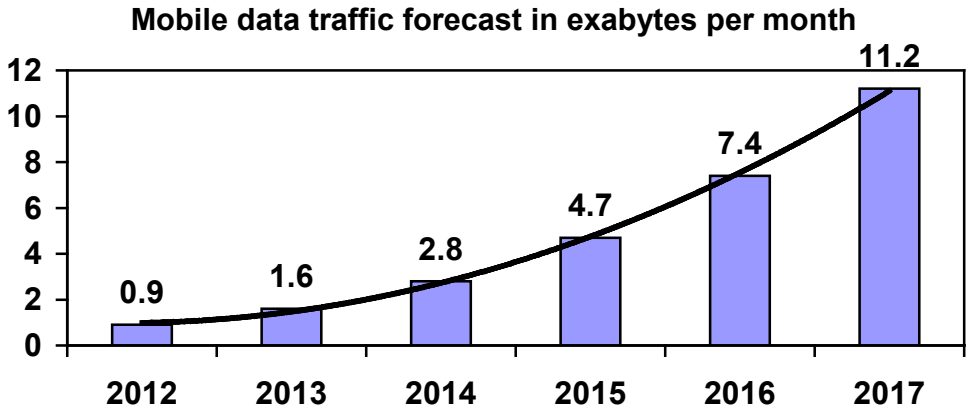

Figure 2-3: Global mobile data traffic, 2012 to 2017, forecasted by Cisco VNI Mobile (Cisco, 2013).

The increasing number of wireless devices such as smartphones and high-end wireless devices including tablets, laptops, *machine-to-machine* (M2M) nodes, and gaming consoles is spawning a raft of data intensive applications that are accessing mobile networks worldwide. This is one of the primary drivers behind the tremendous growth in data traffic. According to (Cisco, 2013), the global mobile data traffic grew 70% in 2012 and is expected to reach 11.2 Exabytes[2] (EB) per month by 2017, which is a 13-fold increase over 2012 as evidence in Figure 2-3. This Figure also reveals that the mobile data traffic will continue to grow at a compound annual growth rate[3] (CAGR) of 66%. To accommodate this massive traffic demand, a dense deployment of BSs is required, which correspondingly increases the overall network energy consumption. For example, there are already more than five million BS sites deployed worldwide, with the number expected to grow to more than 11 million BS sites worldwide by 2020 (Anon, 2012a). The problem is further aggravated by considering financial constraints from the operator's point of view, as higher capacity and better QoS come at the cost of higher capital expenditure (CAPEX) and OPEX. In Lister, 2009, it has been pointed out that the energy bill accounts for approximately 18% of the OPEX in the mature European market and at least 32% in India. So, network energy consumption is a significant portion of the OPEX. With mobile network operators spending around $15 billion on energy use annually, energy efficiency is a strategic priority for them globally (Anon, n.d.). As mobile use expands, so does the demand for energy, particularly by the network infrastructure. Since the RAN or BS is the most dominant energy consuming equipment estimated around 60-80% of the whole network energy consumption (Marsan et al., 2009), a large electricity bill results from the huge energy consumption of the BS. An illustration of power consumption of a typical cellular network is shown in Figure 2-4. It gives an insight into the possible research

[2] 1 Exabyte = 1Billion Gigabytes (10^{18} bytes)

[3] $\text{CAGR} = \left(\frac{\text{Ending value}}{\text{Starting value}}\right)^{\left(\frac{1}{\#\text{of years}}\right)} - 1$

avenues for reducing energy consumption in cellular networks. Therefore, the radio access needs to be the main focus of energy efficiency measures.

Moreover, from the mobile user's point of view, mobile users need to charge their mobile devices much more often due to the dramatic demand for high-rate wireless communication data and multimedia services, especially with the popularity of smartphones, tablets and other smart mobile devices. As the high data rate increases, so does the transmission power requirement. However, battery capacity has not improved much over the years (Miao et al., 2009) and there is an increasing gap between the mobile terminal demand for energy and the offered battery capacity. As a result, it is also necessary to reduce energy consumption by the mobile devices to attract mobile users to stay connected for a longer time.

The mobile industry is one of the major contributors to the world economy (GSMA, 2013). In 2012, revenues of mobile network operators (MNO) contributed $1 trillion or 1.4% of the world's GDP. MNO have been investing billions of dollars in developing network infrastructures needed to support the surging data traffic. The problem is that the growth of mobile data volumes are beginning to outstrip the growth in revenues, and importantly, a mobile operator's cost structure is defined more by mobile data volumes than by the

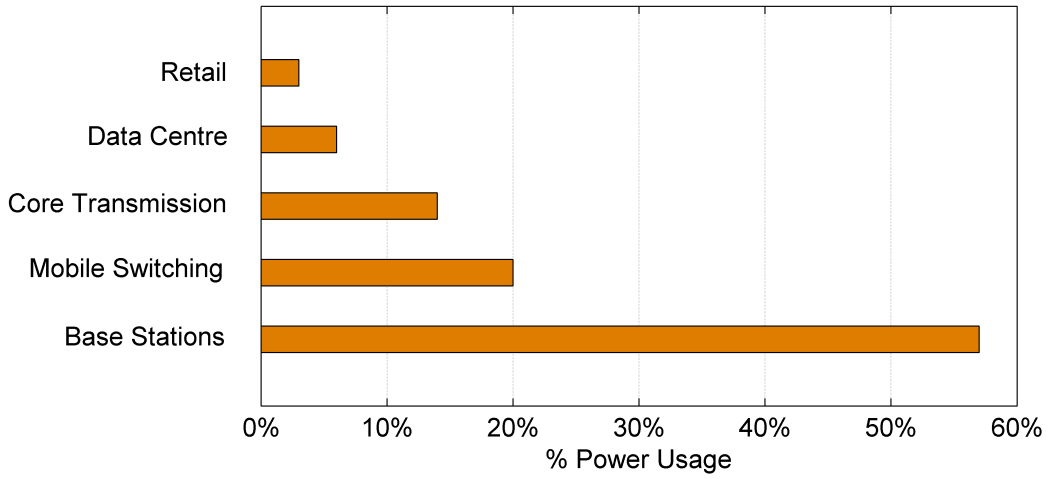

Figure 2-4: Power consumption of a typical wireless cellular network (Vodafone) (Han et al., 2011).

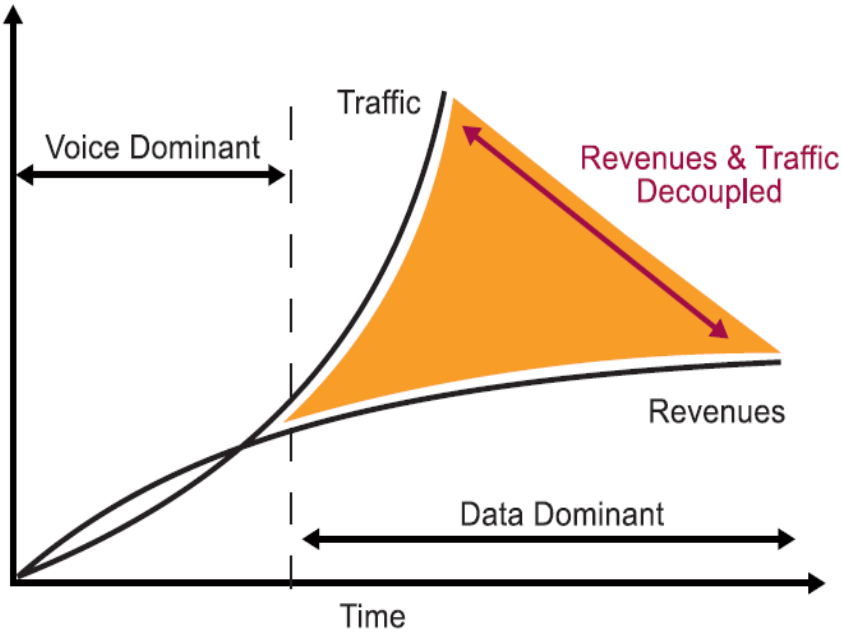

Figure 2-5: Growing gap between the mobile network operator revenue and global mobile data traffic[4].

number of subscribers. Figure 2-5 illustrates the growing gap between the MNO revenue and mobile data traffic growth, especially in the data dominant region. As this gap widens, mobile operators will be increasingly challenged to maintain profitability and fund future network expansions. New business plan and reduction in network energy consumption can help to close the widening revenue gap shown in Figure 2-5.

Green cellular networks are becoming a necessity to bolster environmental, social and economic sustainability (Alam, 2011). Recently, there has been a surge in interest in energy savings in cellular networks due to both the rising energy costs and the environmental awareness, which have led to an emerging trend of addressing energy efficiency amongst the cellular network operators and regulatory bodies such as 3GPP and *International Telecommunication Union* (ITU) (3GPP, 2009a; ITU-T, 2010). This is why green cellular networks have received much attention recently in both industry and academia. For example, British Telecom has announced CO_2 emission reduction target of 80% against the 1996 baseline by 2020 while the operators AT&T and Verizon have

[4] *Source: Unstrung Pyramid Research 2010.*

already started research toward their "green plan" agenda (Webb, 2008; E. Hossain et al., 2012). According to the "*Green Action Programme*" taken by China Telecom and China Mobile, power consumption per traffic in 2010 is 40% lower than that of 2005 (E. Hossain et al., 2012). Deutsche Telekom AG and France Telecom are committed to reduce CO_2 emissions by 20% below 2006 levels by 2020 (Webb, 2008). Some UK mobile phone operators including Vodafone have announced CO_2 emission reductions by 50% against the 2006/07 baseline by March 2020 (Anon, 2012d).

With considering the energy consumption issues of cellular networks, adoption of energy efficient technologies could reap both private and social rewards, in the form of economic, environmental, and other social benefits from reduced energy consumption. As part of the advancement of wireless technologies, it is therefore obvious to reduce energy consumption per data bit carried which forces researchers to innovate new technologies in wireless communications for sustainability. With pressure ever increasing to conserve energy and reduce carbon emissions and the opportunity of wireless to save energy in other industries, the imperative for green cellular networks becomes very clear.

2.4 Main Sources of Energy Consumption in Cellular Networks

The typical energy usage (in percentage) for operating a cellular network is illustrated in Figure 2-4. The energy expenditure within the RAN according to Nokia Siemens Networks is shown in Figure 2-6, which interestingly shows only 15% of the energy, is used for forwarding bits. This means that 85% of the energy is dissipated and is not used for revenue generation, since most energy is expended on fans and cooling systems, heating and lighting, uninterruptable and other power supplies, and in running idle resources (Anon, 2013). As only a small percentage of energy within RAN is utilized to transfer bits, there is clearly real potential and opportunities to reduce these secondary usages of energy to substantially improve the overall energy efficiency of a network. It was stressed in *Section 2.3* that the main source of energy consumption in cellular networks is RAN or BS,

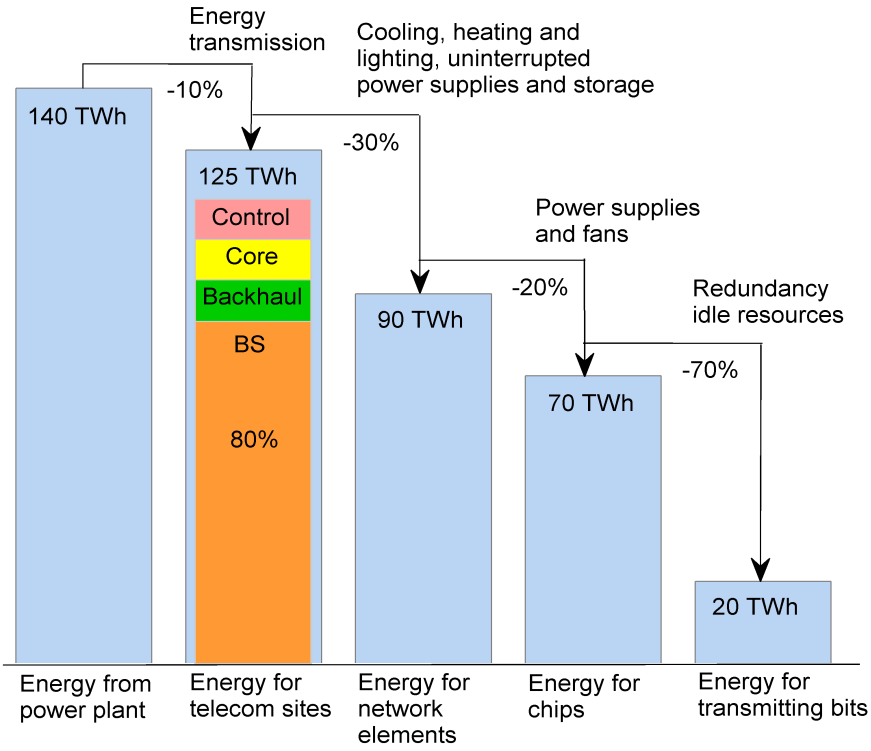

Figure 2-6: Where energy is consumed in a network (Anon, 2013) (calculations based on published operator figures in 2012).

consuming 80% of all energy as confirmed in Figure 2.6 (energy for telecom sites bar). As a result, BS efficiency is one of the key areas in which energy efficiency is ripe for improvement. The components of different types of BSs and their power models will be described in the following section.

2.5 Power Consumption Models of Different Base Station Types

As BSs represent a dominant share of the total network energy consumption, a convenient BS energy consumption model is required, providing estimates of the energy consumption in different scenarios in order to study energy reduction techniques. Traditional cellular networks are designed to cater to large coverage areas, which often fail to achieve the expected throughput to ensure seamless mobile broadband. In order to improve the coverage and the capacity in the cellular networks, heterogeneous networks have been introduced in the *XG* cellular networks, where low-power BSs such as micro/pico/femtocell BSs are deployed while macrocells are also deployed as umbrella cells. It is seen (Figure 2-6) that energy consumption for the radio transmission part only

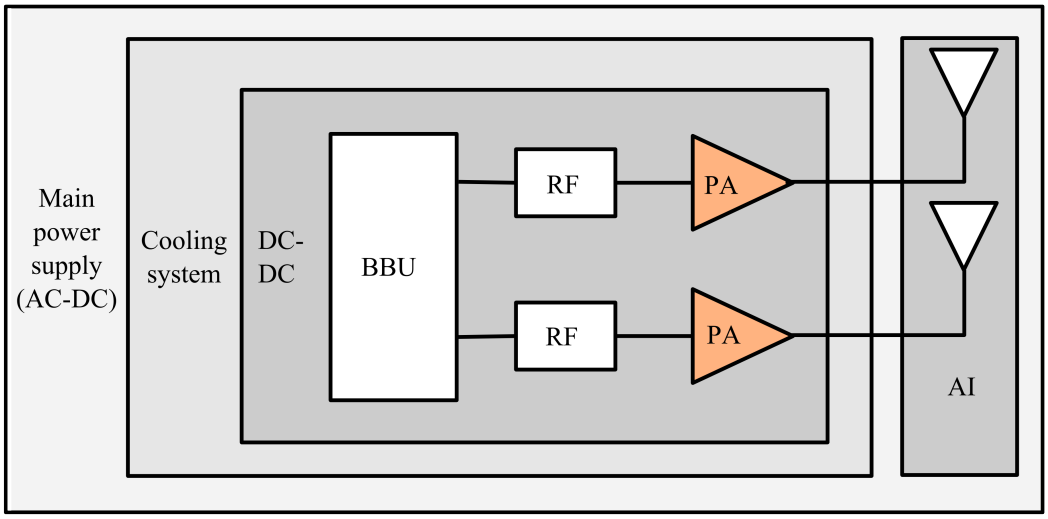

Figure 2-7: A simplified block diagram of a base station with its main power consuming components.

constitutes a small fraction of total energy consumption according to manufacturer data (Anon, 2013; Weng et al., 2011). As a result, each BS typically consists of different power consuming components and the amount of component energy consumption varies depending on the type of BSs. Figure 2-7 shows a simplified block diagram of a complete BS that can be generalized for all BSs types. A BS is comprised of a number of antenna interfaces (AI), power amplifiers (PA), radio frequency (RF) transceiver sections, a baseband unit (BBU), a direct current (DC)-DC power supply, an active cooling system, and an alternating current (AC)-DC (main) supply (Auer et al., 2012). In practice, a BS can be serving multiple cells by sectorization. In this case, few components can be shared among cells. For example, a single cooling system may be used to house the electronics for all sectors. However, for the purpose of modelling, it is assumed that a BS only serves a single cell and thus, the energy consumption of a BS with multiple cells can be calculated as the sum of the individuals.

The power consumption of a BS can be influenced by the type of antenna used and is usually modelled by a certain amount of losses, including the feeder, antenna band-pass filters, multiplexers, and matching components. For a macro BS, a feeder loss of about 3dB needs to be added, while the feeder loss for smaller BS types is typically negligible (Auer

et al., 2012). The feeder loss of a macro BS can be mitigated by mounting the PA at the same physical location as the transmit antenna. The PA are the most dominant energy consuming component of a BS system, being responsible for as much as 80% of the total BS consumption and are also the most power inefficient components (Frenger & Moberg, 2011; Mancuso & Alouf, 2011). However, the PA efficiency can be improved by using advanced technology such as *digital pre-distortion* (DPD) or envelop tracking techniques for wideband signals, which have been put in practice such as Doherty PA (Hirata et al., 2010). The PA of a small cell BS is less efficient as it does not use DPD compared to the PA of a macro BS where DPD is used. A traditional PA has an efficiency of typically between 20% and 30% (Joung, Ho, et al., 2014). The portion of the power that is not converted to useful signal is dissipated as heat. This means PA with low efficiency have high levels of heat dissipation, which could be a limiting factor in a particular design. Moreover, since PA operate in either *active* or *idle* mode and their power consumptions are different, the PA power consumption also depends on the system traffic load and hence, on the transmission power.

The BBU performs digital baseband signal processing, which includes digital up/down conversion including filtering, Fast Fourier Transform (FFT)/inverse-FFT for orthogonal frequency division multiplexing (OFDM), modulation/demodulation, DPD (only in downlink (DL) and for large BS), signal detection (synchronization, channel estimation, equalization, compensation of RF non-linearities) and channel coding/decoding (Auer et al., 2012). The digital baseband processing complexity and its power consumption increases with the BS size (Desset et al., 2012).

The RF architecture contains the different elements of a low-intermediate frequency (IF)/zero-IF architecture, in particular clock/carrier generation and distribution, modulator, mixers, low-noise amplifier, variable-gain amplifier, analog/digital converters, filters, buffer and pre-driver, and feedback chain. Power consumption of each of these elements

varies from element-to-element, but is independent of external factors. Some of the elements are not present in smaller BSs that can work from a lower supply voltage resulting in reduced power consumption after downscaling factor (Desset et al., 2012). Note, one RF transceiver is installed for each antenna chain, so RF power consumption scales with the number of antenna chains.

Interestingly, a relevant portion of the power consumption in a BS is due to the cooling system, DC-DC power supply and main supply losses (Desset et al., 2012; Auer et al., 2012; Arnold et al., 2010), which is computed as a fixed power component linearly depending on the total power consumption of other components. Note, there are no active cooling systems in small cell BSs (micro/pico/femto). According to (Auer et al., 2012), the main constituent is the PA that dominates the total power consumption due to the high AI losses in macro BSs whereas in smaller BSs like pico and femto, it is the baseband part that dominates the overall power consumption.

As energy saving techniques will be explored in this thesis where only a few parameters are varied regularly, it is often unnecessary to derive the power consumption of a BS from the component level. In this thesis, a linear power consumption model is considered as many previous works such as (Arnold et al., 2010; Fehske et al., 2009; Richter et al., 2010; Richter & Fettweis, 2010; Alam, et al., 2012; Son, Kim, et al., 2011) have already considered the same linear model for analysing the power consumption of a BS. According to this model, the total power consumption ($P_{T,BS}$) of a BS consists of two parts: a fixed or static power (P_f^{BS}) and a dynamic power consumption (P_{dyn}^{BS}). The fixed part P_f^{BS} is the consumption independent of loads or transmission power which consists of the DC-DC power supply and main supply losses as well as the cooling system, which are reliant on the type of BSs. On other hand, the dynamic part P_{dyn}^{BS} is the load/transmit power dependent power consumption such as PA, digital signal processing, feeder losses and site cooling. The power consumption due to the site cooling system can be considered to

impact on both the transmit power dependent and the transmit power independent power components due to the thermal radiation caused by both categories of equipments. The relationship between the transmit power and the total consumed power of a BS can be generalized as follows (Richter et al., 2009; Fehske et al., 2009):

$$\begin{aligned} P_{T,BS} &= P_{dyn}^{BS} + P_{f}^{BS} \\ &= a_{BS}.P_{tx,BS} + P_{f}^{BS} \end{aligned} \tag{2.1}$$

where $P_{tx,BS}$ denote the transmission power of a BS, while a_{BS} is a BS power scaling factor which reflects both amplifier and feeder losses. Since some macrocells may be sectorized and use multiple antennas, both P_{dyn}^{BS} and P_{f}^{BS} for macro BSs increase with the number of sectors per macro site and the number of antennas per sector. The values of a_{BS} and P_{f}^{BS} mainly depend on the BS technology and model. However, the assumption is that the parameter values for all BSs of same type are same and, hence, consume the same amount of power for a given traffic load. Intuitively, smaller scale BSs such as micro, pico and femtocells will have lower a_{BS} and P_{f}^{BS} values compared with a macrocell BS as they neither require large power amplifiers nor major cooling equipment (Auer et al., 2012; Fehske et al., 2009; Ambrosy et al., 2012). The power model parameters are chosen according to Richter et al., 2009 and Fehske et al., 2009, where two power models are considered both for macro/micro BSs and RS deployed in this thesis, which are tabulated in Table 2.1. For macro BSs, the power consumption values are calculated based on a three sector cell arrangement with two antennas per sector. Since each BS is limited to a maximum transmission power, $P_{tx,\max}^{BS}$ and the transmission power depends on load factor, ξ, so, $P_{tx,BS} = \xi.P_{tx,\max}^{BS}$. Based on Table 2.1, Figure 2-8 shows the load-dependency in the power model (2.1), where the power consumption values are calculated using the aforementioned three sector cell for a macro BS. For example, $P_{T,BS}$ = 783.4 W for macro

Table 2.1: Power model parameters.

Power models	Base station types	a_{BS}	P_f^{BS} [W]
Model 1 (Richter et al., 2009)	Macro	21.45	354.44
	Micro	42.60	36.50
Model 2 (Fehske et al., 2009)	Macro	32.00	412.40
	Micro	5.50	22.60
Model 3 (Lee et al., 2011)	Relay station	7.84	71.50

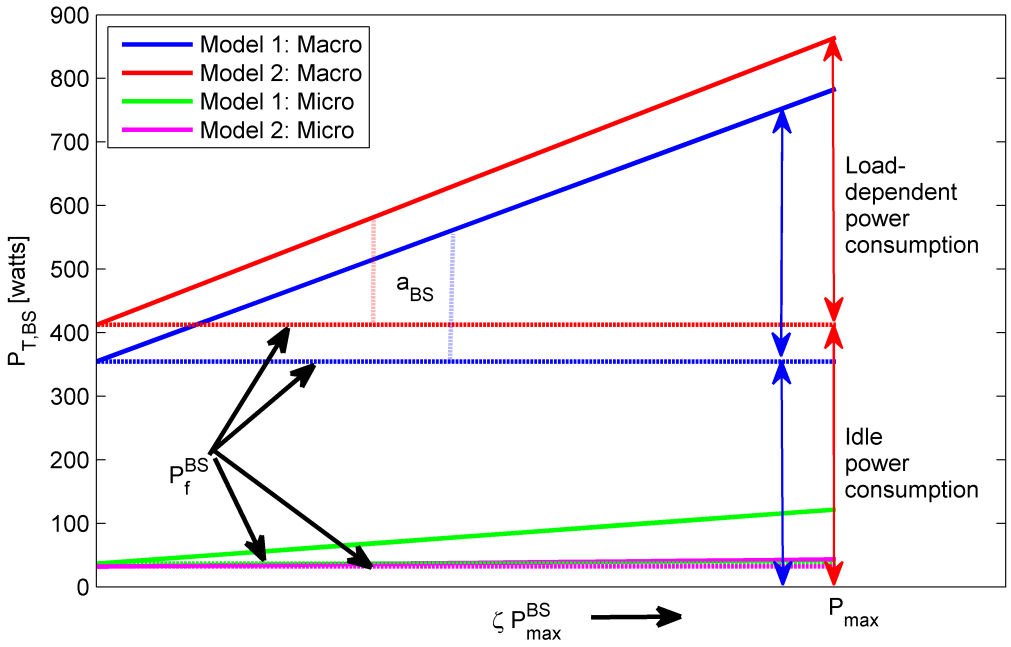

Figure 2-8: Load-dependent power model for a BS.

BSs with the transmission power of 43 dBm or 20 W in the case of Model 1 being used. The power also shows that only 15.6%[5] of the total power spent in a BS is used for bit transmission, which is fully congruent with the earlier finding on the real BS efficiency shown in Figure 2-6. This shows that a macro BS consumes significant energy even at zero load, *i.e.*, for $\xi = 0$ and macro BSs are also heavily depends on load factor compared to the microcell BSs.

[5] $\text{Efficiency} = \frac{20W}{783.4W} \text{x} 100\% \text{ x } 3 \text{ x } 2 = 15.6\%; \quad (3 \text{ sectors/} 2 \text{ antennas})$

2.6 Cellular Traffic Analysis and Opportunities

In order to find any energy efficient solution, it is important to understand the dynamics of cellular traffic. There have been several studies carried out for characterizing the traffic generation of individual BS as well as that of the aggregate network (Shafiq et al., 2011; Willkomm et al., 2008). Recently, several network operators have come forward to disclose their normalized daily traffic patterns (Kyuho; Son et al., 2011). Most of the studies have clearly identified that there are significant traffic variations in both temporal and spatial domains across a day. It has also been pointed out that the peak-time traffic load is much higher (~20 times) than that of at off-peak times (Peng et al., 2011). In the following subsections, traffic dynamics in both temporal and spatial domains will be broadly described.

2.6.1 Temporal Traffic Diversity

Real network data from an anonymous mobile network operator in a metropolitan urban area analysed in (Oh et al., 2011) was considered to understand the traffic dynamics. The graph shown in Figure 2-9 is produced from the real dataset available in (Kyuho; Son et al., 2011). The graph shows the normalized traffic trace averaged with a resolution of 30min from five BSs during one week. It can be observed that the traffic in each cell is a periodic sinusoidal profile and notice that the traffic during daytime (11am – 9pm) or peak periods is much higher than that at night times (10pm – 9am). The temporal variation also depends on the natural life styles and locations. For example, the business areas may be heavily loaded during daytimes but only lightly loaded at nighttimes. Additionally, the traffic profile during weekends/holidays, even during peak hours, is much lower than that of a normal weekday. So, weekdays and weekends appear to show distinct trends (Figures 2-9 and 2-10). During daytimes, the peak traffic period is only a small portion of the whole day while the low activity period can be significant. Based on the traffic profile in Figure 2-9, the percentage of time that the traffic is below x percent of weekday peak during

weekdays and weekends, for x = 5, 10, 20 is shown in Table 2.2. For instance, during weekdays, just over 30 percent of the time the traffic is less than 10 percent of the peak while this low activity period increases to 43% of the time during weekends and holidays (Oh et al., 2011). As a result, some cells will always have traffic loads much lower than the network capacity for a large fraction of time in a day (8~10 hours), which indicates the underutilization of each BS in the temporal domain. Indeed, this will result in network wide energy inefficiency at BSs.

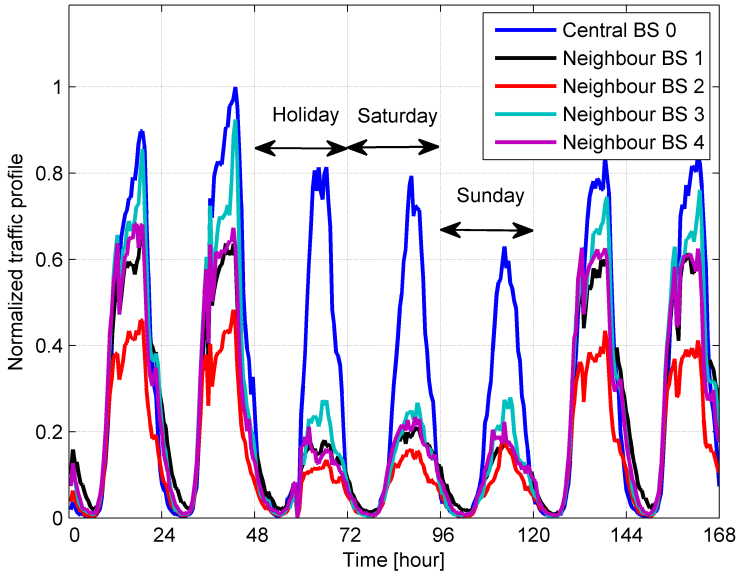

Figure 2-9: Cellular traffic dynamics over one week in both time and spatial domains (Oh et al., 2011).

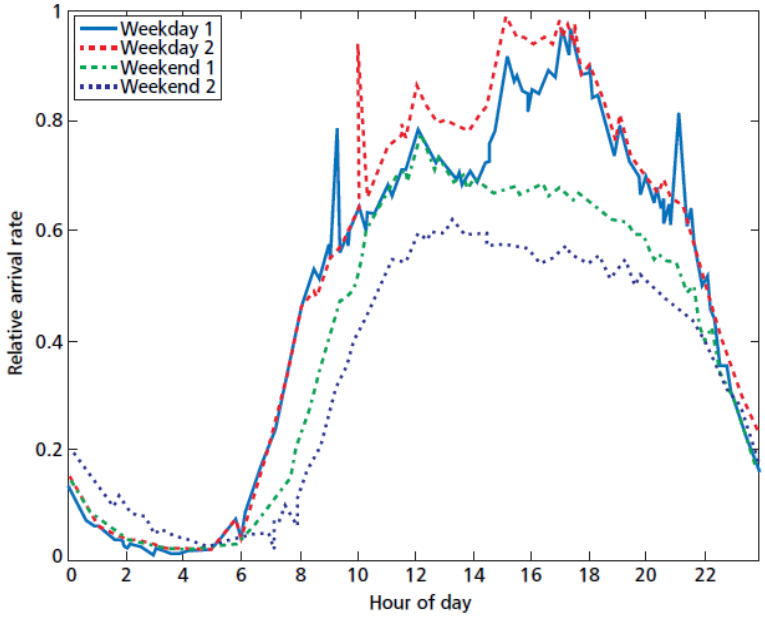

Figure 2-10: Normalized average call arrival rates during for different days (Willkomm et al., 2009).

Table 2.2: Analysis of sample cellular traffic load profiles – percentage of time the traffic is below *x* percent weekday peak during weekdays and weekends, for *x* = [5, 10, 20, 30].

% of the weekday peak	Weekdays	Weekends	Average
5	22.9	30.0	26.4
10	30.4	42.6	36.5
20	38.9	64.9	51.9
30	45.1	88.9	67.0

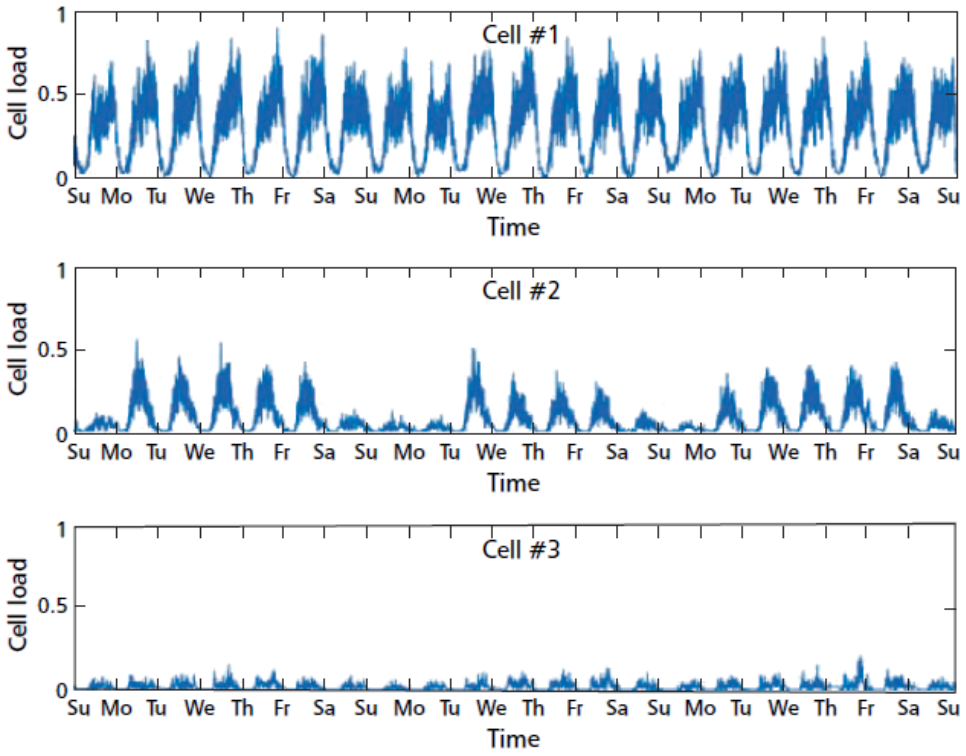

Figure 2-11: Normalized load of three different cell sectors over three weeks showing high load (Cell#1), varying load (Cell#2) and low load (Cell#3) (Willkomm et al., 2009).

2.6.2 Spatial Traffic Diversity

The traffic in different regions can be very different due to user mobility, the behaviour and activities of mobile subscribers on the temporal scale and demands for data and video applications. In the city centre (hot spots), traffic demands are very high during the day time whereas the traffic demand may not be the same in residential areas. Similarly, the traffic demands in cells near railway stations are very high compared to other areas. So, the traffic loads can vary greatly even in neighbouring cells. The normalized traffic over three consecutive weeks taken from three different cells of the same network was investigated

in (Willkomm et al., 2009) and the results are plotted in Figure 2-11. It shows clear evidence of the spatial diversity as the traffic generation is much lower in cell#3 compared to the other two. It can also be seen from Figure 2-9 that the central BS always has higher traffic than that in neighbour BS 2 and the gap is much larger during both peak-time and weekend/holiday periods.

In summary, the traffic in a cellular network is quite diverse over time and space. Such strong temporal and spatial traffic diversity indicates the underutilization of BS resulting in both system- and network-wide energy inefficiencies at BS. However, the traffic dynamics can provide significant opportunities for energy savings. For example, if the traffic variation can be traced and the resource allocation strategy for individual or the whole network is adopted accordingly, a significant amount of energy could be saved. From the above discussion, it can be concluded that the variation of traffic density in cellular networks in both the temporal and spatial domains shows significant under-utilization of system capacity given the network being designed based on the peak-traffic scenarios.

2.7 Energy Saving Techniques within Cellular Networks: Opportunities and Trends

There is considerable scope for significant improvement in energy efficiency of cellular networks to secure both environmental and financial benefits. Improvement of energy efficiency in cellular networks involves energy reduction of all elements, such as mobile core networks, mobile switching centres, BS, backhaul networks, and MS (Wu, 2012). In fact, BSs are the most energy consuming elements of the cellular system, and are often under-utilized during low traffic periods. However, the subject of energy savings in cellular networks only came to prominence a few years ago (Louhi, 2007). Since then, a number of strategies have been proposed to reduce the carbon footprint of BSs, ranging from the use of renewable energy sources (Han & Ansari, 2012; Grangeat et al., 2010; Gong et al., 2013), to the improvement of hardware component (Brubaker, 2009), to the optimum network deployments (Bhaumik et al., 2010; Kyuho Son, Oh, et al., 2011), to the

optimization of resource management and transmission techniques (e.g. *multiple-input multiple-output* (MIMO), CoMP transmission etc.) (Han & Ansari, 2012; Cui et al., 2005), to cell zooming techniques (Niu et al., 2010), to the adoption of *BS sleep* modes (Chiaraviglio, Ciullo, et al., 2008). In the following subsections, different energy saving techniques for BSs in literature will be described.

2.7.1 Efficient Hardware Design

The energy consumption of a typical BS can be reduced by improving the BS hardware design. A general overview of such hardware improvement is provided in (Ferling et al., 2010, 2012). Typically, 80% of the total energy use at a BS site is consumed by the PA (Frenger & Moberg, 2011), so the PA efficiency can play a significant role in reducing the BS energy consumption. Modern BSs are inefficient due to their need for PA linearity and high *peak-to-average power ratios*. Existing PA with new efficient devices using DPD or envelope tracking techniques for wideband signals allow up to 50% energy saving overall (Mancuso & Alouf, 2011). Designing more efficient PA such as switch-mode amplifiers based on gallium nitride transistors can potentially reduce the energy cost of a BS. Usually, PA perform better at maximum output power in order to maintain the required signal quality. However, during low traffic periods or for small cell BSs with low output power, a lot of energy is routinely wasted. Therefore, flexible PA design, which can adapt to the required output power, is essential to reduce BS energy consumption further. Moreover, modifications to BS architectures requiring less cooling or no cooling systems at all can save a great amount of energy. For example, Ericsson's Tower Tube, a new radio BS site concept, where the network equipment is placed at the top of the tower (next to the antennas) with the possibility of exploiting the wind as a passive cooling system can result in a 40% reduction of OPEX due to energy savings (Mancuso & Alouf, 2011).

2.7.2 Hybrid Energy Sources

BSs powered by renewable energy sources such as solar and wind are promising options, not only for saving on-grid energy consumed by BSs but also to help reduce carbon footprint caused by the BS. It is also appropriate to mention that some rural regions do not have on-grid energy but rely on the use of diesel generators, which are expensive, not environment-friendly and difficult to transport to remote areas. Adopting on-site renewable energy sources to power the network can be very effective. For example, Orange has already installed more than 900 solar powered BSs across Africa as of the year 2010. These stations are 100% solar-powered and save 1300 litres of fuel per year per station and produce a 25% energy surplus to help surrounding communities (Yvetot, 2010). However, due to the instability of renewable energy sources availability and the lack of required energy supply by means of renewable sources, a complete replacement is not possible in short terms. Hence, despite instability of the renewable sources, a consumption reduction strategy is strictly necessary to enable the deployment of renewable energy-powered BSs. As a result, hybrid energy supplies, which combine both the on-site renewable energy and on-grid energy has been proposed to power BSs recently (Han & Ansari, 2012; Gong et al., 2013).

2.7.3 Energy-Aware Network Planning and Deployments

There are substantial prospects of energy savings by network planning and optimum deployment that is designed to be scenario specific, such as dense urban, suburban and sparse rural areas. Network planning is a primary task, which locates and configures transmission facilities at a minimum cost including the energy cost reduction (Boiardi et al., 2014). Therefore, energy awareness must be incorporated at the network planning phase.

For network planning, the authors in Badic et al., (2009) studied the impact of reducing cell sizes on the energy performance in cellular networks. It has been shown that the

architecture of reducing cell sizes only can increase the number of delivered information bits per unit energy for a given user density. Another study in (Leem et al., 2010) showed similar results, stating that as the cell size becomes smaller, energy efficiency and system capacity can be increased. However, making cell sizes either too small or too large cannot improve the energy efficiency as optimal cell size from an energy perspective depends on a number of factors including the traffic demand. In (Richter & Fettweis, 2010), a network densification utilizing microcell BS is studied focusing on high load scenarios. The fundamental trade-off between the energy and deployment efficiency has been thoroughly investigated for future green cellular network planning under a simplified model in (Chen et al., 2010; Lee & Kim, 2012; Chen et al., 2011; He et al., 2012).

Besides energy efficient cell size design, emerging heterogeneous network deployment such as configuring the networks with various sizes of cells, relays and cooperative communications, as shown in Figure 2-2, are worth considering and are advantageous in reducing energy consumption and to increase the network capacity (Kyuho Son, Oh, et al., 2011; Lee et al., 2013; Chiaraviglio et al., 2012). Authors in (Kyuho Son, Oh, et al., 2011) presented an energy-aware hierarchical cell configuration framework with the objective to reduce the total energy consumption from the network deployments and operations point of view while limiting the capital expenses. The area power consumption (APC) and area spectral efficiency of homogeneous macro-sites, micro-sites and heterogeneous networks are compared in (Richter et al., 2010; Fehske et al., 2009) with differential energy efficiency being dependent on the target throughput. For higher throughput targets, additional deployment of micro-sites is beneficial. In (Lee et al., 2013), the authors proposed a spatial modelling to generate inhomogeneous traffic distribution for cellular networks. Based on the spatial traffic modelling, a network planning scheme, which adaptively deploys macro and micro BSs adapting to the in-homogeneity, was proposed with a considerable improvement in the performance of energy efficiency.

Similarly, picocells and femtocells are also promising deployment strategies in terms of cost-efficient services. Both cell types are usually deployed for better indoor coverage due to the poor indoor radio coverage of macro/micro cells because of high wall penetration and path-losses (PL) (Tariq, 2012). However, the macro-micro deployment strategy can save more energy than the energy saving of femto only deployment (Dufková et al., 2011). Relay and cooperative communications have also been considered as a cost-effective solution for providing services in hotspots, extending service coverage, improving cell-edge throughput, prolonging battery life of MS regardless of the transmission delay and energy consumption of RS (Lin et al., 2010; Ng & Yu, 2007; Pabst et al., 2004; Bulakci et al., 2013). Deploying an appropriate number of relays with proper locations can bring in potential improvements in the energy efficiency (Wu & Feng, 2012; Khirallah et al., 2011; Chandwani et al., 2010).

2.7.4 Efficient Network Operations and Management

Efficient network operations and management is one of the most significant approaches in reducing energy consumption of cellular networks. As discussed above in *Sections 2.2* to *2.5*, the BSs are the major energy consuming as well as the most energy inefficient part in the cellular network. Therefore, enhancing the energy efficiency of cellular networks largely depends on the effective operation and management of the BS. Turning off some BSs during low-traffic periods, called *BS sleeping*, is being considered as one of the most promising techniques. This can be confirmed from the emergence of a large number of *BS switching* schemes in recent years which has drawn more and more attention in literature (Niu et al., 2010; Hasan et al., 2011; Rao & Fapojuwo, 2013; Bolla & Bruschi, 2011; Feng et al., 2013; Boiardi et al., 2014) (Chiaraviglio, Ciullo, et al., 2008; Marsan et al., 2009; Oh et al., 2013; Oh & Krishnamachari, 2010; Morosi et al., 2013; Marsan et al., 2011).

The common idea of the *BS switching* in all the proposals is fairly simple and can be summarised as: *Depending on the instantaneous traffic conditions within cells and their*

spatial positions in a network, the number of active BSs (and hence the overall ***energy consumption****) is dynamically minimized, while the remaining active BSs provide the* ***radio coverage*** *and service provisioning (required* ***QoS****) for all users within the network*. In other words, the objective is to keep the number of *active* BSs within the network at any instant of time that makes the network energy consumption proportional to traffic. This is also the principal research focus of this thesis. More precisely, this thesis will focus on a *BS switching framework*, *i.e.*, an energy efficient operation of cellular BSs, which is a paradigm for *green cellular networks*.

Base station switching

In (Chiaraviglio, Ciullo, et al., 2008), the authors first proposed energy-aware UMTS access network management by reducing number of *active* BSs by half during the night zone (low-traffic periods) while keeping the blocking probability below a given target as described in Section 3.6.7. Authors in (Marsan et al., 2009) presented a static *BS sleep* pattern based on a deterministic traffic profile over a whole day period that neither considers the randomness nor the spatial variation of the traffic. In contrast, the authors in (Zhou et al., 2009) focused on a preliminary attempt at dynamic *BS switching*. Both centralized greedy and distributed algorithms were proposed to switch off certain BSs during low traffic periods. In this case, the complete traffic and channel information are assumed to be known in the centralized case and only local load information and user specific associate control are known in the decentralized algorithm. As an extension, they modelled the dynamic *BS switching* problem as a dynamic programming problem combining the cost function of energy consumption, switching cost and blocking probability penalty to avoid frequent mode switching to reduce signalling and delay overhead (Gong et al., 2012). In (Oh & Krishnamachari, 2010), a dynamic *BS switching* approach was proposed under the setting where the traffic pattern is not predictable day to day, but is modelled as sinusoidal with a period of 24hr. The authors have provided at first-

order analysis of energy saving based on the time varying characteristic of the traffic profile. It was shown that the mean and variance of the traffic profile and the BS density are the dominant factors that determine the amount of energy savings. This work has further been extended and a distributed SWitching-on/off based Energy Saving (SWES) algorithm has been proposed, without the need for a central controller (Oh et al., 2013). SWES algorithms are able to minimally affect the network as determined by the term *network-impact,* which takes into account the additional load increments brought to its neighbouring BSs.

A distance-aware *BS switching* algorithm was proposed in (Bousia, Kartsakli, et al., 2012) that exploits the knowledge of estimated distances between the BS and MS with priority being given to those BSs to switch off that have the maximum average distance. In (Han et al., 2013), four heuristic-based BS switch-off patterns were proposed that progressively turn more BSs off to save energy according to the offered traffic load while exploiting their corresponding coordination topology to provide service coverage of off-cell users.

Cell-zooming and energy-delay trade-off

Another similar approach but one that is even more flexible is the concept called "*cell-zooming*" that was presented in (Niu et al., 2010). In this approach, BS can adaptively adjust their cell sizes according to the traffic load, and the off-cell users can be served by the neighbouring *active* BSs by transmit power adjustment, antenna re-configurations, wireless relays and BS cooperation technologies. This interesting approach can not only provide a solution for traffic imbalance, *i.e.*, load balancing but also reduce the energy consumption. However, there are many challenges yet to be solved from a practical point of view such as trace of traffic fluctuations, compatibility, coverage holes, and the management of ICI. In order to mitigate some of the challenges, dynamic cell expansion closely similar to cell zooming was proposed for maintaining the service coverage of sleep cells in (Guo & O'Farrell, 2013). Dynamic antenna-beam tilting, frequency reuse,

distributed inter-cell coordination and cooperative transmission can be used for cell expansion.

Most of the aforementioned works focus mainly on the energy efficiency improvement of cellular networks with certain levels of optimization. However, the *BS sleeping* operation may lead to longer delay to users if the BS takes a longer time to wake up. In this context, authors in (Kyuho Son, Kim, et al., 2011) have investigated energy savings in dynamic BS operation and the related problems of user association with a single greedy on/off algorithm and an optimal user association policy that allows for a trade-off between flow-level performance and energy consumption. On other hand, Niu et al., 2012 and Wu et al., 2013 presented a comprehensive analysis on the energy-delay trade-off towards designing optimal sleeping parameter (sleep control) and power matching by developing various closed-form expressions. Recently, a framework was proposed to analyse the performance of *BS sleeping* while capturing the impacts of different scheduling and user association schemes (Tabassum et al., 2014).

Base station sleeping among multiple operators

Usually, urban areas are provided with cellular services by multiple competitive operators with all providing full coverage of the area. For example, there are multiple BSs deployed from different operators in a city centre while the BS coverage of one operator overlaps other operator's BS coverage. It is seen from the traffic dynamics in *Section 2.4* that cellular traffic varies significantly over time while each operator usually dimensions their networks based on the peak traffic of a day. Therefore, networks with overlapped coverage can cooperate with each other to reduce energy consumption (Marsan & Meo, 2010; Ismail & Zhuang, 2011; Marsan & Meo, 2011). When traffic load is low, the BS capacity from each operator becomes redundant and at some points all the traffic can be served by only one network in that area. In (Marsan & Meo, 2010), the authors presented a *BS sleeping* strategy incorporating cooperation between two operators. During low traffic periods, one

of two operators shares all traffic from both operators while the other network switches to *sleep* mode. Similar proposals involving more than two operators were also presented in (Ismail & Zhuang, 2011; Marsan & Meo, 2011). The potential of network cooperation in saving energy was evaluated under different settings in these schemes; however, none of them provided any algorithm or implementation framework.

Base station sleeping in self-organizing networks

Self-organizing networks (SON) can be useful in load-balancing as well as energy reduction by deciding when to disperse load for load-balancing and when to concentrate load for energy savings. For example, self-organizing capability is inherent in *BS switching* and *cell-zooming* techniques (Niu et al., 2010; F. Hossain et al., 2012), which are useful in both load-balancing and energy savings. In (M. F. Hossain et al., 2012), the authors have proposed three cooperation techniques, where cellular networks are dynamically reconfigured with a minimum number of *active* BSs, which are distributed and self-organizing in nature at the expense of computational cost.

2.7.5 Energy-Aware Radio Technologies

Smart Antenna technology

It has been seen that some energy efficient techniques such as *cell-zooming* and *BS switching* techniques require dynamic adjustment of parameters, including the transmission beam-width, beam-direction, transmission range of antennas, dual-band antennas, antenna-tilt, reconfigurable beam antennas and number of antennas (Anon, 2012c). Therefore, along with the *BS switching*, the role of smart antenna technology is also essential in terms of energy efficient communications.

Along with smart antenna technology, the transmission and reception of wireless signals with multiple antennas, referred to as MIMO, have been widely adopted in modern communications systems (Cho et al., 2010). There are several benefits of MIMO systems

over Single-Input Single-Output (SISO) such as higher data rates, lower error rates, improved *signal-to-noise ratio* at receivers, multipath rejection, and lower transmit power consumption for a given data rate requirement (Jain et al., 2011; Marzetta, 2010). For example, using *K* transmit antennas, the overall data rate compared to a single antenna system is enhanced by a factor *K* without requiring extra bandwidth or transmission power (Mietzner et al., 2009). However, the circuit power consumption of a MIMO system is more that for a SISO system as it has multiple RF chains and requires a high digital signal processing capability. The idea of *sleep* modes can also be applied to the MIMO system. Rather than using all installed antennas, a BS could deactivate some antennas when high capacities are not required (Pace, 2012).

Cognitive radio

Cognitive radio (CR) is a promising paradigm proposed to cope with the spectrum scarcity that has emerged as a result of the increased need for high data rate demands with 'anytime anywhere' connectivity (Haykin, 2005; Mitola & Maguire, 1999). CR is an intelligent and adaptive communication system that enables the radio spectrum to be utilized in a more efficient manner. CR is being intensively researched as an enabling technology for secondary access to *TV White Space* (TVWS) (Nekovee, 2010). Currently, some countries have planned to convert their TV stations from analogue to digital transmission, (Digital Switchover, DSO). DSO was completed in the US and the UK in 2009 and 2012, respectively, and is expected to be completed in other countries in near future. During DSO, some spectrum will become vacant due to the higher spectrum efficiency of digital TV (DTV). As a result, there will be a number of TV channels that are not used for DTV broadcasting in a given geographic area and these vacant channels are known as TVWS. As the TVWS spectrum comprises a large portion of the *ultra high frequency* (UHF)/*very high frequency* (VHF) spectrum with favourable propagation characteristics, these bands can be used for a wide range of potential new services, including last mile broadband

access, using CR technology. In (Sachs et al., 2010), the authors proposed a network architecture that enables spectrum sharing between a primary TV broadcast system and a secondary cellular system through the CR approach. However, using a radio spectrum on secondary basis can cause service degradation for primary users due to interference (Goldsmith et al., 2009; Jovicic & Viswanath, 2009). Adopting the concept of CR, a dynamic spectrum access scheme within a cellular network was proposed by sharing the cellular radio spectrum within the system using overlay cognitive approach in order to improve the spectral efficiency (Alam et al., 2011). CR can also be viewed as an enabling technique to provide a greener wireless solution by means of decreasing the electromagnetic emissions level by sending the right signal in the right direction with optimal power, only when it is necessary, for the same QoS (Gür & Alagöz, 2011; Alam, 2011; Grace et al., 2009; Palicot, 2009; Holland et al., 2010). In (Grace et al., 2009), the authors proposed an adaptive modulation scheme with virtually partitioning a set of channels to reduce the need for frequent spectrum sensing, thereby permitting energy savings by exploiting reinforcement learning. The authors in (Li et al., 2010) studied an energy-efficient transmission duration and power allocation methods in the CR networks with having knowledge of each channel. The CR not only adjusts modulation, coding, and transmission power, as with conventional adaptive modulation, but also adjusts component characteristics so that radio can operate with the highest energy efficiency (He et al., 2009).

Cooperative communications

Implementations of cooperative communications among various network elements have been previously demonstrated to improve the network capacity (Hossain et al., 2011). Recent studies (Hasan et al., 2011; Li et al., 2011) show that the application of cooperative communications can also minimize the network energy expenditure. For example, deployment of relays between the BS and MS can allow for significant reduction in the

total transmit power while enabling better signal reliability (Wu & Feng, 2012; Ku et al., 2013). Another possible approach to improve both the network reliability and energy efficiency is CoMP transmission, which has already been comprehensively studied in literature (Irmer et al., 2011; Sawahashi et al., 2010; Lee et al., 2012; Heliot et al., 2011) and has been identified as one of the major development paths for increased traffic demand. The CoMP transmission technique requires additional backhaul links and more complicated processing algorithms, leading to more energy consumption. However, the cell throughput can be significantly improved as well as the energy efficiency performance of the system. Since relaying technology will be adopted in this thesis, the more details of relaying will now be described in the following paragraphs.

In LTE-Advanced (LTE-A), relaying is considered as a tool to improve, for example, the coverage of high data rates, group mobility, temporary network deployment, the cell-edge throughput and/or to provide coverage in new areas (Bhat et al., 2012; 3GPP, 2010c). The relay node is wirelessly connected to the RAN via a donor cell. Relaying provides better fairness to users with homogeneous user experience, though this comes at the cost of additional donor BS access link resource being utilized for the relay backhaul and associated latency (Bhat et al., 2012). Moreover, there are commonly three types of relays depending on the underlying technologies used (Letaief & Zhang, 2009): i) *amplify-and-forwards* (AF); ii) *decode-and-forward* (DF); and iii) *compress-and-forward* (CF).

In AF relays, the relay simply amplifies and retransmits the noisy version of the transmitted signal (analog version) from the source. The advantage of this protocol is its simplicity, low-cost implementation and short processing delays associated with relaying. However, the relay amplifies the ICI and noise together with desired signal components thereby deteriorating the received *signal-to-noise ratio* (SINR) and reducing the throughput enhancing gain. This type of relay is also called Layer 1. In DF or Layer 2 relays, the relay decodes the received signals, re-encodes (regenerates) and retransmits an

exact copy of the original signal. This type of relay overcomes the drawback in AF relays of deteriorating the received SINR but incurs a delay associated with encoding/decoding. In CF, the relay regenerates an estimate of the received signal. This is then compressed, encoded and transmitted to create an estimated value that will assist in decoding the original codeword at the destination (Letaief & Zhang, 2009), however this leads to high processing delays due to amongst other things, user data regeneration processing.

Depending upon the operation of relays, two categories with respect to the relay node's usage of spectrum are (3GPP, 2010c):

i) *In-band*, in which case the relay backhaul (BS-RS) link shares the same carrier frequency with the access (RS-MS) links, as shown in Figure 2-12(a). In other words, one carrier is sufficient for both the relay and access links, which are multiplexed in time. The in-band relay needs to operate in half-duplex mode to avoid self-interference problem, unless sufficient physical isolation or interference cancellation is secured between transmit and receive antennas at the RS (Tran et al., 2012).

ii) *Out-band*, in which case the relay and access links use different carrier frequency, as shown in Figure 2-12(b), *i.e.*, the out-band approach requires multiple carriers and the links are multiplexed in frequency, so it can easily work in full-duplex mode.

While in-band relaying improves coverage, out-band relaying will also improve capacity (Bhat et al., 2012; Bou Saleh et al., 2010). In LTE-A and WiMAX, two types of RS have been defined, namely, Type 1 and Type 2 in LTE-A, and *transparent* and *non-transparent* in WiMAX (3GPP, 2010c; Anon, 2012b). According to the definition, the non-transparent relays in WiMAX and Type 1 relays in 3GPP LTE-A are same while transparent and Type 2 relays are also the same. In Type 1 relaying, the RS controls cells by having a cell identity of its own. For both relay and access links, the same carrier frequency is used, *i.e.*,

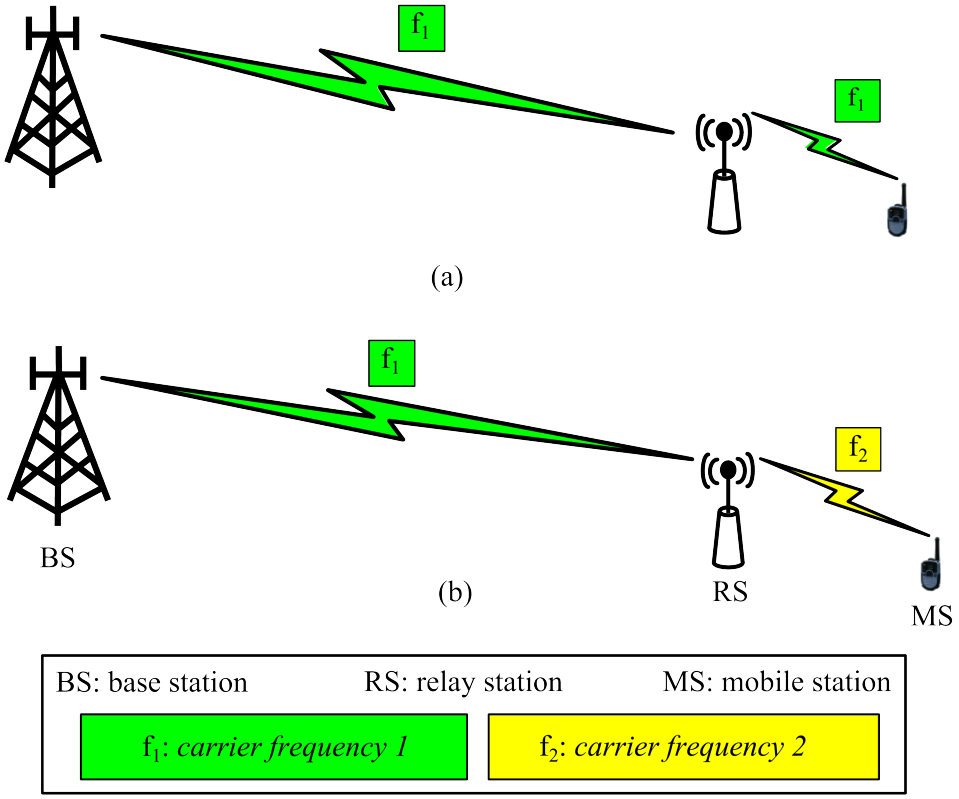

Figure 2-12: Relaying operations with respect to spectrum usage: (a) *in-band* relaying; and (b) *out-band* relaying.

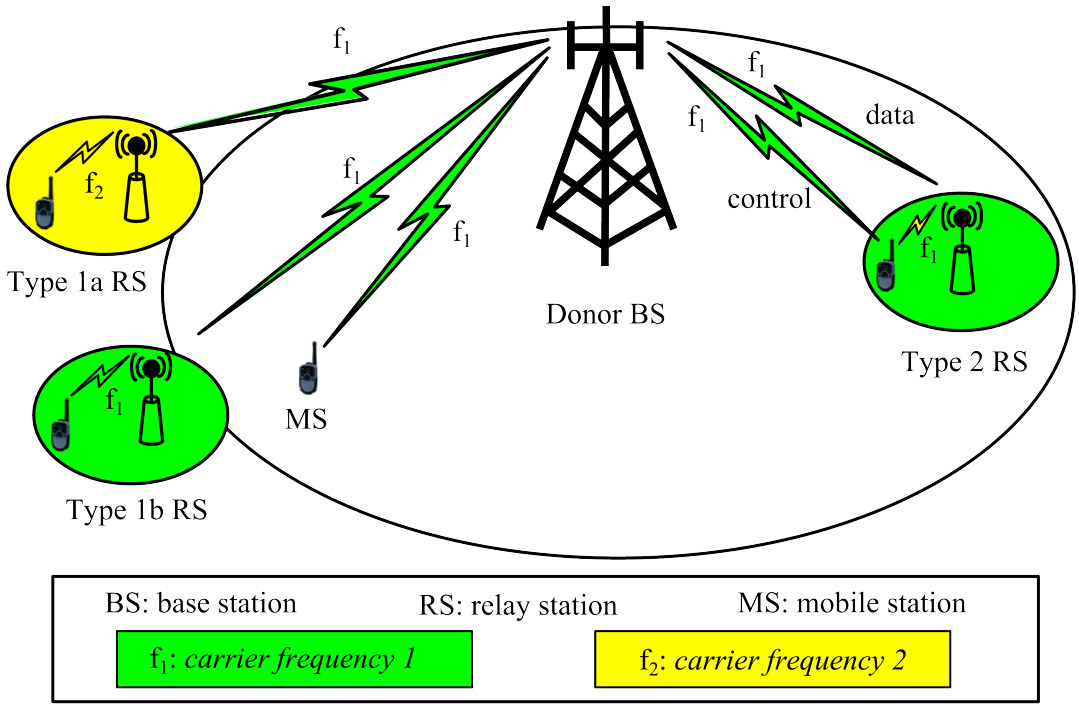

Figure 2-13: Different types of RS: *Type* 1*a*, *Type* 2*b*, and *Type* 2.

it operates in-band, thus a half-duplex solution. To avoid reduced performance associated with half-duplexing, two additional types of RS related to Type 1 are introduced in 3GPP

LTE-A: Type 1a and Type 1b, differing from the Type 1 only in the characteristics of the relay link. The Type 1a operates out-band while Type 1b operates in-band with enough isolation between the relay and access links to mitigate their mutual interference. Both Type 1a and Type 1b allow full-duplex operation. The Type 2 relays are characterized by being an in-band relay. The RS is part of the donor cell and the RS does not have a cell identity of its own. In this case, the MS is not aware of whether or not it communicates with the network via the RS, *i.e.*, the RS is transparent to MS. Figure 2-13 illustrates all types of relays. However, only Type 1 and Type 1a out of all these type of RS is being selected to be standardized as part of LTE-A (3GPP, 2011a).

For more surveys on green cellular networks, the reader is referred to (Feng et al., 2013; Bianzino et al., 2012; Hasan et al., 2011; Chen et al., 2011; Correia et al., 2010; McLaughlin et al., 2011) and the IEEE ComSoc *Best Readings Topics on Green Communications* (Anon, n.d.).

2.8 Global Research Activities and Standardizations

As discussed in *Section 2.3*, with the explosive growth of wireless data traffic, the energy efficiency performance of cellular networks has recently drawn increasing attention from both industry and academia. This leads to comprehensive efforts to design new energy efficient architectures, protocols and algorithms, network planning and deployments. As a result, there are several workshops, conferences and journal special issues especially dedicated to green communications and networking, which reflects current interest in green communication networks. For instance, green communications and networking topic has been included as one of the selected areas in communications symposium in flagship conferences such as GLOBECOM and ICC. Several international research projects on green communication networks around the globe have been initiated under different international research platforms in recent years. These include OPERA-Net (Anon, n.d.) and OPERA-Net 2 (Anon, n.d.), MVCE Green Radio (Anon, n.d.), EARTH (Anon,

2010a), GreenTouch (Anon, 2010b), GREENET (Anon, 2011) and 5GrEEn (Olsson et al., 2013) and their possible objectives and solutions are summarised in Table 2.3.

Table 2.3: Global green wireless research activities with their possible solutions.

Project Name	Possible objectives and solutions	Remarks
OPERA-Net	*Optimising Power Efficiency in mobile Radio Networks* **1. Mobile RAN end-to-end efficiency (E2E):** ▪ KPI (key performance indicator) for EE; ▪ Improve power efficiency from the management of: cell sizes, *sleep* mode, MAC, DC power, cooling systems, etc; **2. Link level:** ▪ Optimization technique for link level power efficiency; ▪ Energy aware device design; **3. Technology enablers:** ▪ Improvement of RF PA and energy recovery in BSs; **4. Network test-bed:** ▪ Integration of devices (proof of concept); ▪ Mobile RAN E2E.	Duration: 10/2008–10/2010 Total cost: 5.9 m€
OPERA-Net 2	*Optimising Power Efficiency in mobile Radio Networks 2* **1. E2E work package:** ▪ Evaluation methodology for life cycle analysis; ▪ Impact of efficiency on products and networks; ▪ Specific focus on cooling solutions; **2. Hybrid energy sites** ▪ Future energy usage and power sources; ▪ Modelling and optimization of energy supply; **3. Access network optimization:** ▪ Single and multi-user distributed MIMO; ▪ Energy-aware scheduling for optimizing energy consumption of extremely dense networks; **4. Architecture and hardware design:** ▪ Linear transmitters and PA for distributed/compact BSs; **5. Standardization:** ▪ Advanced ‘green’ solutions into the standardization of wireless networks.	Duration: 12/2011 – 11/2-14 Total cost: 7996 k€

MVCE Green Radio	*Mobile Virtual Centre of Excellence's Green Radio* **1. Energy metrics and models:** ▪ Energy metrics to accurately quantify consumption; ▪ Energy consumption model for RAN; ▪ 100x reduction in energy requirements for delivery of high data rate services; **2. Energy efficient architectures:** ▪ Large vs. small cell deployments; ▪ Relays and cooperative communications; ▪ Efficient backhaul strategy for a given architecture; ▪ Solar-powered architecture; **3. Energy efficient resource management:** ▪ SISO vs. MIMO packet scheduling; ▪ CR (dynamic spectrum access) and spectrum sharing; ▪ Adaptive reconfigurability – algorithms; **4. Power efficient hardware design:** ▪ Advanced PA techniques such as DSP; ▪ Masthead PA and passive cooling systems.	Duration: 01/2009 – 01/2012
EARTH	*Energy Aware Radio and Networks Technologies* **1. Energy efficient analysis, metrics and target:** ▪ Life cycle analysis of energy consumption by telecom products; ▪ Energy efficient metrics on system levels; ▪ Cut the energy consumption of 4G networks by 50%. **2. Energy efficient Architecture:** ▪ Optimization of cell size; ▪ Heterogeneous network deployments; ▪ Relay and cooperative communications; **3. Energy efficient resource management:** ▪ Dynamic load and transmission mode adaptation; ▪ Cooperative scheduling, interference coordination, joint power and resource allocation; ▪ Multi-RAT (radio access technology) coordination; **4. Radio Technologies and Components:** ▪ MIMO, OFDM, adaptive antennas, and CoMP; ▪ Power scalable transceiver and power control on component, front-end and system level.	Duration: 01/2010 – 06/2012 Total Cost: 14.8 m€ EARTH integrated solutions allow decreasing more than 50% energy consumption.
Green	**1. Mobile Networks:**	Duration: 01/2010 –

Touch	▪ Beyond cellular green generation - separating signalling (continuous and full coverage service) and data network (on demand service); ▪ Flexible power model of future BSs based on operation modes, component configuration, hardware technology and BS architecture; ▪ Green transmission technologies – fundamental trade-off between EE and spectrum efficiency, and between service delay and energy consumption; ▪ Large-scale antenna systems ▪ By 2015, increase network EE by a factor of 1000 compared to 2010 levels; **2. Standards and Policies:** ▪ Energy metrics for users; ▪ Green rating system for network operators and service providers; ▪ Taxonomy of communication applications for energy consumption and efficiency calculations; **3. Wired core and access networks:** ▪ Bit-interleaved passive optical network technology; ▪ Router power monitoring; ▪ Energy efficient content distribution and clouds for service delivery; ▪ Optimum end-to-end resource allocation; ▪ Low-power large photonic switch architecture and transmission; ▪ Service energy aware sustainable optical networks;	01/2015 Total cost: 502,500 k€ (a total of projects)
GREEN ET	**1. Novel energy efficient and low complexity PHY-layer technique:** ▪ Spatial modulation for generalized MIMO; **2. Energy efficient design of medium access control (MAC) and radio resource management (RRM) protocols:** ▪ Data aggregation schemes; ▪ Energy efficient collisions resolution, lightweight control packets and minimize listening; ▪ Energy efficient scheduling, *sleep* modes and interference management for heterogeneous networks; **3. Energy efficient network coded architecture:** ▪ Cross-layer design, network/channel coding; **4. Cognitive and cooperative networking:** ▪ Security mechanisms for cooperative networks;	Duration: 01/2011 – 12/2014 Total cost: 4.2 m€

	▪ Energy efficient cooperative spectrum sensing for CR;	
5GrEEn	*Towards Green 5G Mobile Networks* **1. Energy efficient architecture and metrics:** ▪ A new clean state architecture ▪ Appropriate metrics and accepted methodology ▪ Full connectivity, always available, and full service support with required *quality of experience* (QoE); **2. New PHY-layer signalling and higher layer protocols with minimizing energy consumption** **3. Traffic adaptive solutions and deployments strategies in 5G** **4. Optimizing the trade-off between QoE and EE.**	Duration: 2013 - 2014

Energy efficient communication techniques in wireless networks have been intensively studied across academia, industry, whilst standards bodies such as IEEE, IETF and 3GPP, and ICT-related government agencies and public institutions are working to develop regulation and standardization of EE metrics (ATIS, 2010; Christensen et al., 2010; Anon, 2010c; 3GPP, 2010a). There is an urgent need to have standards as a guideline to measure the EE of mobile networks.

2.9 Summary

This chapter presented the architecture of a typical cellular network of different generation cellular technologies with addressing the necessity for green cellular networks. The emergency of green cellular networks is not only due to the rising cost of energy and/or the energy conservation but also the reduction of their environmental impacts. The main sources of power consumption within a cellular network were identified, which are the BS and the power model for BS was then presented. An in-depth analysis of cellular traffic diversity was then presented while the traffic diversity of cellular networks indicates the underutilization of each BS for a large period of a day. This is mainly due to the traditional cellular network design assumptions and operations. Next, a comprehensive survey of energy saving techniques in cellular networks was provided, ranging from efficient hardware design to hybrid energy sources, to network planning and management, to

energy-aware radio technology. In particular, the *BS switching* technique was studied critically, as it has been considered as a promising technique to save energy and will be the main focus of this thesis. Other energy-aware communication techniques were also discussed with their energy conservation potentials. Finally, the global research activities in the context of green cellular networks were also studied with their possible solutions. The next chapter will present simulation and evaluation methodology together with the key performance metrics to evaluate the performance of new models and algorithms proposed in this thesis.

Chapter 3

Simulation and Evaluation Methodology

3.1 Introduction

Cellular communication systems are very complex in nature due to the architectures and the environments in which they are deployed. For example, the architecture of a wireless cellular system needs to be designed in such a way as to provide high data rates while satisfying constraints such as transmit power, bandwidth and minimum QoS requirements. The system often involves a large number of random events over time and space such as the location and the number of simultaneous mobile users, propagation conditions, interference and power level settings, and user traffic demand. This combination of system complexity and challenging variable environments leads to design and analysis of problems that are not analytically tractable by applying traditional, non-simulation based techniques (Tranter et al., 2003). Prototypes are often not available and testing different candidate features in the field would often prove to be too expensive and time consuming. Moreover, simulations of wireless systems such as LTE are essential in the research and standardization phases whenever a new technology is under development. Consequently, the most convenient way to evaluate the performance of the system is by computer simulations, which have become a widely adopted methodology (Kasch et al., 2009; ITU-R, 2009). This simulation-based approach not only reduces the high cost of actually implementing a real system, but also saves a significant development time.

Over the last two decades, the development of powerful and inexpensive computers together with robust software packages has grown rapidly. As a consequence, computer-aided design and analysis techniques are readily available, and are usually referred to as simulations. An important motivation for adopting a simulation approach in this thesis is that it provides a valuable insight into system behaviour and performance before

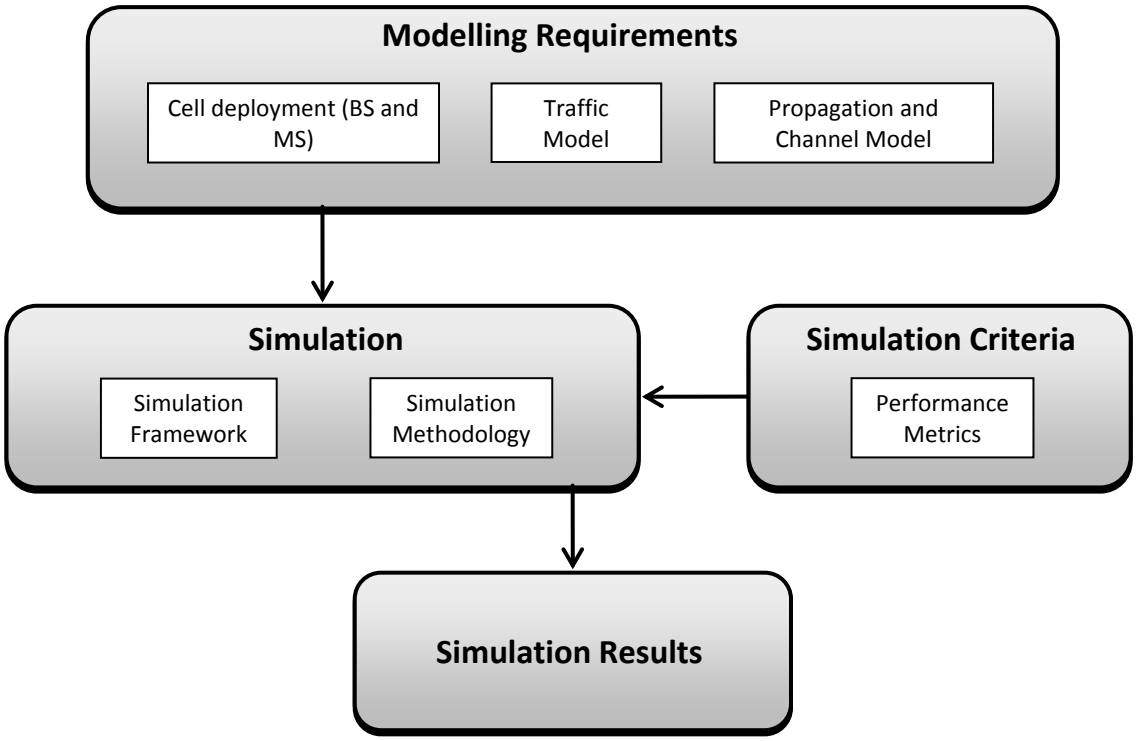

Figure 3-1: Simulation components.

considering expensive real implementation. In addition, the ITU has provided general guidelines for procedures and criteria which are to be used in evaluating any proposed advanced system (ITU-R, 2009). For this reason, the aim of this chapter is to present the evaluation guidelines specifying both the simulation methodology and tools used in assessing the overall performance of the proposed new *BS switching framework* for greener cellular networks.

3.2 General Evaluation Methodology

Most simulation problems involve the following basic steps (Tranter et al., 2003):

- Mapping a given problem into a simulation model or a logical representation of a complex entity, system phenomena or process,
- Decomposing the overall problem into a set of smaller problems,
- Selecting an appropriate set of modelling, simulation and estimation techniques and applying them to solve these sub-problems,

- Combining the results of the sub-problems to provide a solution to the overall problem.

Figure 3-1 illustrates the simulation components of cellular systems which are described subsequently. The mapping of the design and/or the performance estimation problem into a simulation model is one of the most difficult steps in the methodology. In this regard, ITU have defined general evaluation guidelines, relevant figures of merit, test environments, scenarios, and corresponding channel models (ITU-R, 2009), which will be reviewed.

The simulation methods are divided into link-level and system-level simulations (Roche et al., 2013). The link-level simulation focuses on defining simple scenarios consisting of one transmitter and one receiver, while the system-level simulation aims to study the global characteristics of a communication system comprising a network of multiple BSs and MSs. In this thesis, system-level simulations are the primary focus so as to be able critically evaluates the expected system performance of the proposed new *BS switching framework*.

3.3 Model Requirements for Simulations

The simulation methodology of a cellular network involves many modules, including the cell deployment, channel modelling, radio resource allocation, interference modelling, traffic modelling, and other key factors. In the following subsections, the simulation requirements of these various modules will be discussed in detail.

3.3.1 Cell Deployment

For homogeneous deployments, macrocells are deployed uniformly in a large area with each BS having hexagonal cell coverage. Throughout the thesis, it is assumed the BSs are located at the centre of each cell, and the terms cell and BSs are used interchangeably. For each macrocell, different cases representing a mix of *inter-site distance* (ISD), system bandwidth and other system simulation parameters such as BSs and RS transmit powers are applied, and which are formally defined in Table 3.1.

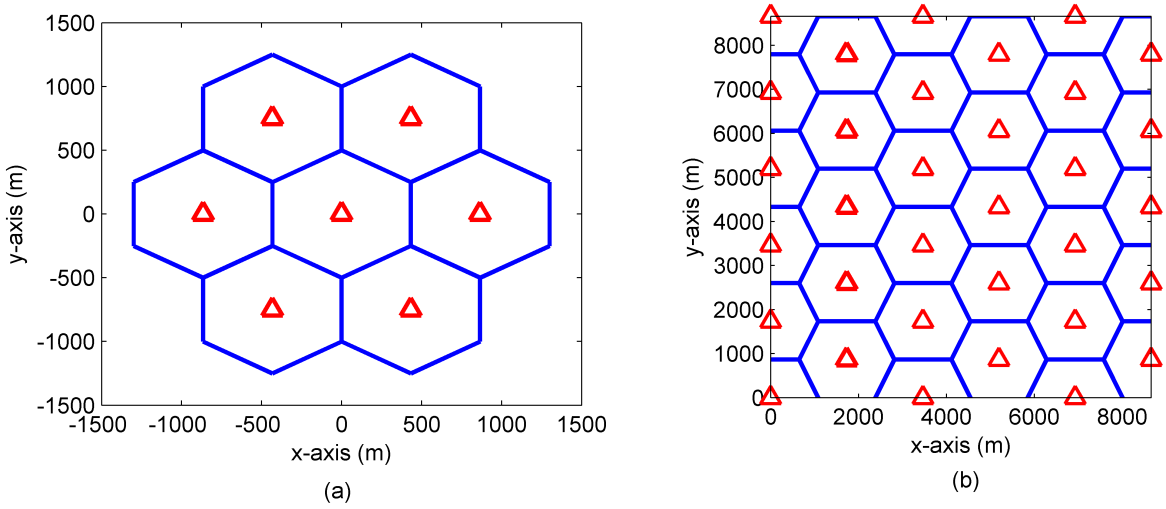

Figure 3-2: Example of homogeneous cellular network layouts consisting of (a) a 7-cell cluster; and (b) 5x5 grids with ISD of 1000m and 1735m, respectively, with the red triangles representing the BS.

For numerical evaluation, the network configuration consists of N_{BS} BSs ranging from a 7-cell cluster to the 5x5 hexagonal grid arrangements as shown in Figure 3-2. The 7-cell cluster has been used for proof-of-concept solutions, while the 5x5 cell arrangement has been used for capturing a more realistic network scenario. An ISD for the homogeneous deployment ranging from 500m to 2800m is assumed (3GPP, 2010c) and the cell radius is calculated as $\frac{ISD}{\sqrt{3}}$. A minimum distance between the BS and MS of 35m is assumed.

For the case of microcells employed in the proposed *scalable BS switching framework* presented in *Chapter 7*, the cell layout for a micro BS is the same as a macro BS with corresponding parameters being specified in Table 3.1. The cell radius for microcell BSs of 200m is fixed for all scenarios while each BS has an omni-directional antenna unless otherwise stated. In addition, RS are also deployed at the edge of each cell for some scenarios in order to improve the cell edge throughput, although the RS deployed cellular network scenario is only considered in *Chapter 5*.

3.3.2 Backhaul Assumptions

In the proposed *BS switching framework*, cooperation among BSs is an essential condition underpinning the development of the new models and algorithms. As a result, BSs are assumed to be interconnected, which is one of the integral features of LTE cellular systems via the X2 interface for coordination purposes, which does not have any centralised intelligence controllers (3GPP, 2008), as illustrated in Figure 2-1(b). The performance of a system which needs cooperation between BSs in regard to such matters as, exchange of signalling information and/or forwarding protocol data units to the respective endpoints is very sensitive to the backhaul capacity and latency. The X2 backhaul latency between BSs is highly-deployment dependent for example, on whether there is a dedicated X2 fibre network or a generic IP network (3GPP, 2010c). Cells with dedicated X2 fibre links provide low latency (3GPP, 2010c), which may reasonably be assumed to be negligible. In this context, it is assumed that there are dedicated X2 fibre links in existence between BSs for all the various network scenarios considered in this thesis, so the issue of latency can be ignored.

3.3.3 Traffic Generation Model

The traffic model adopted assumes that user traffic is distributed in each cell and that it arrives according to a Poisson process with traffic intensity λ, *i.e.*, the number of simultaneous calls per unit time. The traffic distribution among cells can either be symmetric (evenly distributed, *i.e.*, each cell has the same traffic) or asymmetric (unevenly distributed, *i.e.*, unequal traffic in all cells) depending upon the scenario being considered, while the traffic within each cell is assumed to be uniformly distributed (Gong et al., 2012). Two traffic generation profiles have been used in this thesis: approximated sinusoidal traffic profile and a rate function based traffic. The former is adopted from Oh & Krishnamachari (2010) and is employed in *Chapters 4* and *5*. The rate function based traffic profile generation technique is adopted from Hossain et al. (2013), which provides a

more realistic traffic profile as practical cellular network and is used in *Chapters 6* and *7*. The formal traffic generation models will formally be described in each individual chapter. All MS arrive randomly and then remain stationary until the transmission is finished. The transmission duration of each MS follows an exponential distribution with mean μ^{-1} (Gong et al., 2012) and the model parameters used for system performance evaluations are given in Table 3.1.

3.3.4 Propagation and Channel Models

A good understanding of channel characteristics is important for both determining the coverage and QoS of a wireless cellular system. A defining characteristic of a wireless channel is the time and frequency variations in signal strength (Tse & Viswanath, 2005; Roche et al., 2013). These variations can be divided into two types: (*i*) *large-scale fading:* caused by the signal PL as a function of distance and shadowing by large objects like buildings and hills; and (*ii*) *small-scale fading*, due to the constructive and destructive interference of multiple signal paths between the transmitter and receiver. In the new proposed framework the former will be assumed, with the latter being averaged out, since long time-scale performance is considered (Gong et al. 2013).

The modified IEEE 802.16d propagation model (IEEE, 2007) is used with three different categories (*Types A, B* and *C*) depending on the density of obstructions between the transmitter and receiver in macrocell urban/suburban areas. The PL for the IEEE 802.16 system contains the basic models for an air interface for fixed broadband wireless access system and an additional PL associated with RSs (IEEE, 2007). The PL equation relating to the modified IEEE 802.16 model is given by (IEEE, 2007; Alam et al., 2012):

$$PL(d) = \begin{cases} 20\log\left(\dfrac{4\pi d}{\lambda_w}\right) & for \quad d \le d_0' \\ A + 10\gamma\log\left(\dfrac{d}{d_0}\right) + C_f + C_h \ for & d > d_0' \end{cases}$$

where d is the distance between BS/RS and MS,

$\lambda_w =$ wavelength,

$\gamma = x_1 - x_2 h_{TX} + x_3 / h_{TX}$,

$h_{TX} =$ transmit antenna height,

$d_0 =$ reference distance (100m),

x_1, x_2, and x_3 are the three model parameters used for intermediate PL conditions which are heuristically set as 4, 0.0065 and 17.1, respectively. A, C_f, C_h and d_0' are functions of the wavelength, antenna heights and reference distance respectively, as given in (IEEE, 2007).

In order to capture a more realistic propagation model, a log-normal distributed random variable Ψ with mean zero and standard deviation σ of 8dB is added (Zeng & Zhu, 2008). Similarly, the PL model for links between the BS and RS is also based on the IEEE 802.16d (IEEE, 2007). Hence, PL and shadowing effects are the main sources of performance degradation in this thesis unless otherwise specified.

3.4 Simulation Framework and Parameter Settings

The simulation framework used for this thesis has been designed based upon the cellular network architecture specifications of international standard bodies including ITU-T, WiMAX and LTE (ITU-R, 2009; 3GPP, 2010d, 2010c). This will be considered throughout the thesis as the ground truth baseline model, and is consistently applied as a comparator in critically evaluating the performance of the new *BS switching framework* and the suite of algorithms developed in subsequent chapters. A system-level simulation will be the main focus of the new framework following the guidelines defined in ITU (ITU-R, 2009) and the IEEE 802.16m Evaluation Methodology Document (IEEE, 2009b). The reason for this is that the research focus, as explained in *Chapter 1*, is to study the global energy consumption characteristics of a cellular system involving multiple links, cells and MS. Moreover, modelling all links allows the mutual interference between

Table 3.1: General system simulation baseline parameters and their normal values or characterization.

Parameters	Characterization/Values
Cellular layout	Hexagonal grid
Deployment scenarios	Homogeneous deployments
Carrier frequency [GHz]	2.0
Carrier bandwidth, $W_{\max}$ [MHz]	5, 10
Cell ISD [m]	[500, 750, 1000, 1500, 1732, 2800]
Microcell radius [m]	200
Scheduler	Round-robin
BS model (3GPP, 2010d)	
Max. BS power $P_{tx,\max}^{BS}$ [dBm]	43 (macro BS), 33 (micro BS)
Min. BS power per user [dBm]	15
Noise figure [dB]	7
Noise power [dBm]	-106
Antenna gain [dBi]	16
Antenna height [m]	32
Receiver sensitivity [dBm]	-103
RS model	
Backhaul	Air-interface (deployed RS) X2 interface (collocated *RS* only)
RS per macrocell	6
Max. RS power [dBm]	24, 30
Antenna height [m]	10
MS model	
Max. MS power $P_{tx,\max}^{MS}$ [dBm]	21, 23
Min. MS power [dBm]	-50
Noise figure [dB]	9
Antenna gain [dBi]	0
Antenna height [m]	1.5
Receiver sensitivity [dBm]	-99
Channel propagation model (IEEE, 2007)	
Path-loss model	(IEEE 802.16d): Type B
BS-MS/RS-MS link	Type B (urban/suburban, terrain Type B)
Shadowing effect [dB]	Log-normal fading with σ =8
Traffic model (3GPP, 2010c)	
User arrival	Poisson process with arrival rate λ
Mean service time, μ^{-1} [sec]	180

multiple links to be considered, which is an important limiting factor of system performance (Roche et al., 2013). All the contributions presented in this thesis are based upon homogeneous deployment scenarios, with all the parameter choices and their values used in the simulation framework being formally defined in Table 3.1. The system-level methodology will now be described.

3.5 System-Level Evaluation Methodology

The system-level simulation procedure to investigate the QoS requirements of both the baseline model and new *BS switching framework* are based on snapshots, where the MSs are randomly placed on a predefined two-dimensional area. At each snapshot, the statistics of the performance metrics to the given BSs and MS are computed, by taking user locations and propagation conditions into account, with the *uplink* (UL) and DL being simulated independently. A series of snapshots is simulated for performance evaluation in order to generate a sufficiently large sample set so that statistically valid results are achieved using a Monte Carlo simulation for each snapshot produced by the model. The following steps are considered in system-level simulations (ITU-R, 2009):

- Define the network layout within a predefined two-dimensional area, including BS placements.
- MS are randomly placed within this predefined area, with each MS corresponding to an active user session that runs for the duration of the drop.
- MS are randomly assigned to different channel conditions (*line-of-sight* (LOS)/non-LOS) based on the propagation and channel models as discussed in *Section 3.3.4*.
- The BS assignment to a MS is based on the strongest link for the available radio resources, while each BS employs a “Round-robin” scheduler that assigns an equal share to all MS.

- For a given drop, the simulation is run and then the process is repeated with users dropped at new random locations. A sufficient number of drops are simulated to ensure convergence in the user and system performance metrics.
- All cells in the system are assumed to have dynamic channel properties using a wrap-around technique and the performance statistics are collected for all MS in each cell.

By processing the results of the simulation, the performance of the overall cellular system can be estimated in terms of the key performance indicators, which will be discussed in *Section 3.6*. In order to reduce the complexity of these simulations, they are divided into separate link and system simulations with a specific *link-to-system interface* (ITU-R, 2009) or *PHY abstraction* (Roche et al., 2013; IEEE, 2009b). For the simulation of RS, the link from a RS to a MS is modelled using the same models as the conventional link between a BS and a MS.

3.6 Performance Metrics

To appraise the performance of any system, it is very important to choose the most appropriate and equitable assessment metrics. In evaluating how the performance of the proposed *BS switching framework* makes a contribution towards green cellular networks, the first obvious question is that what actually is meant by green? How can the degree of 'greenness' in cellular networks be defined and measured? The carbon footprint and/or CO_2 emissions, which are both by-products of the network energy consumption, would naturally be considered as a measure of greenness. Another motivation behind green cellular networks includes economic benefits (lower energy costs) and better practical usage (increased battery life in mobile devices), so a comprehensive evaluation of network energy savings or measuring the network EE is a more pertinent choice to reflect 'greenness'. Similarly, in measuring the energy savings, it is necessary to satisfy some defined QoS provision such as the data rate and/or blocking probability, since these are

well-accepted performance metrics by the community (IEEE, 2007; ITU-R, 2009; Imran et al., 2012; Auer et al., 2012). As a result, both the data rate and blocking probability have been used in this thesis as benchmarks to validate all the performance results. Therefore, a range of performance parameters need to be applied to equitably assess the network performance in this thesis. These are now briefly described.

3.6.1 Signal-to-Interference-and-Noise Ratio

Signal-to-interference-and-noise ratio (SINR) plays an important role in multiuser systems, and is a fundamental parameter for measuring the channel quality of each user. Accordingly, the received SINR Γ_{bm} of a MS m from $\mathcal{B}_b$ can be written as (Yang & Niu, 2013):

$$\begin{aligned}\Gamma_{bm} &= \frac{G \cdot 10^{-PL(d_{bm})/10} \cdot \Psi_{bm} \cdot p_{tx,bm}^{BS}}{\sum_{b' \in \boldsymbol{\mathcal{B}}, b' \neq \mathcal{B}_b} G \cdot 10^{-PL(d_{b'm})/10} \cdot \Psi_{b'm} \cdot p_{tx,b'm}^{BS} + N_0} \\ &= \frac{G \cdot 10^{-PL(d_{bm})/10} \cdot \Psi_{bm} \cdot p_{tx,bm}^{BS}}{\sum_{b'} I_{b'} + N_0}\end{aligned} \tag{3.1}$$

where $p_{tx,bm}^{BS}$ is the transmission power of $\mathcal{B}_b$ with the distance between $\mathcal{B}_b$ and MS m being d_{bm}; $\boldsymbol{\mathcal{B}}$ is the set of BSs; $PL(d_{bm})$ and Ψ_{bm} are the associated PL and shadow fading effects, respectively; N_0 and G are the noise power and antenna gains. The first term in the denominator is the interference term and is simply denoted by $I_{b'}$ from the interfering BS $\mathcal{B}_{b'}$ to the MS m.

For multi-hop communications, such as relays, the SINR between $\mathcal{B}_b$ and MS m via a RS k in two time-slots is given by (Fallgren, 2012):

$$\begin{cases}\Gamma_{bk} = \dfrac{G \cdot 10^{-PL(d_{bk})/10} \cdot \Psi_{bk} \cdot p_{tx,bk}^{BS}}{\sum_{b'} I_{b'} + N_0} \\ \Gamma_{km} = \dfrac{G \cdot 10^{-PL(d_{km})/10} \cdot \Psi_{km} \cdot p_{tx,km}^{RS}}{\sum_{b'} I_{b'} + N_0}\end{cases} \tag{3.2}$$

where Γ_{bk} and Γ_{km} are the SINR for the *relay-link* (BS-RS) and for the *access-link* (RS-MS) respectively, and $p_{tx,km}^{RS}$ is the transmission power of RS.

3.6.2 User Throughput

The data rate or throughput of a MS *m* is defined as the number of information bits per second successfully delivered or received and this is an important performance metric in terms of QoS. According to the classical Shannon formula, the attainable user throughput (bits/second) between $\mathcal{B}_b$ and MS m are given by:

$$r_m = \frac{W_{\max}}{N_c} \log_2 \left(1 + \Gamma_{bm}\right) \tag{3.3}$$

where $W_{\max}$ is the maximum cell bandwidth, which is divided into a number of orthogonal channels in a reuse-1 system and N_c is the total number of channels with each channel bandwidth being $W = \frac{W_{\max}}{N_c}$. Assuming the maximum number of active concurrent MS in a cell is the same as N_c. Now, for relay-assisted communications between $\mathcal{B}_b$ and MS *m* via RS *k*, the data rate of MS *m* under the DF scheme is given by (Uddin et al., 2012):

$$r_m = \frac{W_{\max}}{2N_c} \min\left\{\log_2\left(1+\Gamma_{bk}\right),\ \log_2\left(1+\Gamma_{bm}+\Gamma_{km}\right)\right\} \tag{3.4}$$

where the ½ scaling factor reflects the transmission between $\mathcal{B}_b$ and MS *m* occupies two time-slots. Consequently, the overall system throughput of $\mathcal{B}_b$ is given by:

$$R_b = \sum_{m \in \mathcal{M}_b} r_m \tag{3.5}$$

where $\mathcal{M}_b$ is the set of MS in cell $\mathcal{B}_b$.

3.6.3 Energy Efficiency

Energy efficiency (EE) is a key performance indicator in this thesis as it reflects the network energy (or equivalent power) consumed relative to the system capacity. EE (η_{EE}) in *bits per joule* is the ratio of the achievable throughput (bits/second) to the total network power consumption, which can be derived as (Alam et al., 2012):

$$\eta_{EE} = \sum_{b \in \mathcal{B}} \frac{R_b}{P_{T_b}} \tag{3.6}$$

where P_{T_b} is the total power consumption of $\mathcal{B}_b$.

3.6.4 Percentage of Network Energy Savings

To measure the percentage energy savings, it is important to ascertain the network energy consumed when all BSs are all *active* or in "*always-on*" mode (E_{AO}). The network energy consumption in this mode for a time period $D = 24hr$ is expressed as (Tranter et al., 2003):

$$E_{AO} = \sum_{b \in \mathcal{B}} \int_0^D P_{T_b}(t)dt \tag{3.7}$$

Assuming the network energy consumption of the proposed *BS switching framework* is E_{NEW} , then the percentage energy savings achieved with respect to the "*always-on*" mode is given by:

$$E_{ES} = \left(1 - \frac{E_{NEW}}{E_{AO}}\right) \text{x} 100\% \tag{3.8}$$

3.6.5 Area Power Consumption

To comparatively evaluate the energy performance of the proposed *BS switching framework* within an area $\mathcal{A}$, the APC is an insightful metric for different traffic variations as cell coverage always changes when a BS switches its operational mode. This is defined

as the ratio of the average total consumed power to the corresponding network area measured in watts per km^2 (Fehske et al., 2009):

$$P_{A\ P} = \frac{P_T}{T\ o\ a\ t\ \text{n}, \text{A}} \quad \text{watts/km}^2 \tag{3.9}$$

where $P_T = \sum_{b \in \mathcal{B}} P_{T_b}$ is the total power consumption.

3.6.6 Cumulative Distribution Function

In probability theory, the *cumulative distribution function* (CDF) is defined as the probability that an occurred event is below or equal to a given value. The CDF is related to the *probability density function* (PDF) in the following manner:

$$F_X(x) = \int_{-\infty}^{x} f(y)d \ . \tag{3.10}$$

where $F_X(x)$ is the CDF of x and $f(x)$ is the PDF of x. The main purpose of using the CDF is to obtain the statistical behaviour of the large amount of data produced by conducting Monte Carlo simulation, which has been used to calculate the signal outage probability of the *BS switching framework* and is described in the following subsection.

3.6.7 Call Blocking and Signal Outage Probabilities

Communications between the BS and MS can be disrupted due to two reasons:

i) *Call blocking probability*, due to the lack of required radio resources for newly arrived users;

ii) *Signal outage probability*, due to the received signal strength *i.e.*, the received SINR, Γ_{bm} is less than a predefined threshold γ_0.

Both these probabilities are important parameters that reflect the performance of the framework, with the former measuring system performance while the latter measures the link quality between the transmitter and receiver. Now, the call blocking probability for a

cell, which has N_c channels with the offered traffic load being ρ Erlang can be estimated as (Norris, 1998):

$$P_{block} = \frac{\frac{\rho^{N_c}}{N_c!}}{\sum_{n=0}^{N_c} \frac{\rho^n}{n!}} \tag{3.11}$$

When a cellular system is designed, the blocking probability should be less than a particular predetermined value, P_{th} = 1% (Gong et al., 2012).

Given that a user request is not rejected or blocked due to limited radio resources, *i.e.*, a link have been established between the user and a BS, if then the instantaneous SINR levels of the established link is lower than a predefined threshold γ_0 which guarantees the minimum required transmission rate due to the channel fading, then a signal outage will occur. The outage probability is defined as the probability of the received SINR Γ_{bm} being less than a predefined threshold, so p% outage value means (100 – p)% users are performing at or above the threshold. Let $P_{out}(d_{bm})$ denote the outage probability at the MS m with a distance d_{bm} between the MS and the served BS. The signal outage probability at distance d_{bm} is then given by (Cao et al., 2010; Alam et al., 2012):

$$\begin{aligned} P_{out}(d_{bm}) &= \Pr\left(\Gamma_{bm} \le \gamma_0\right) \\ &= P\left(\frac{G \cdot 10^{-PL(d_{bm})/10} \cdot \Psi_{bm} \cdot p_{tx,bm}^{BS}}{N_0 + \sum_{\hat{b}} I_{\hat{b}}} \le \gamma_0\right) \\ &= \Phi\left(\frac{10}{\sigma} \log_{10}\left(\frac{\gamma_0 \cdot \left(N_0 + \sum_{\hat{b}} I_{\hat{b}}\right)}{G \cdot 10^{-PL(d_{bm})/10} \cdot p_{tx,bm}^{BS}}\right)\right) \end{aligned} \tag{3.12}$$

where $\Phi(*)$ is the CDF of standard normal distribution with standard deviation σ.

3.6.8 Base Station Switching Overheads

As *BS switching* techniques involve changing between different BS operating modes, they will inevitably consume some energy, even if this is very small. While the switching energy costs will be negligible in most of models proposed in this thesis, the BS switching overhead is an important parameter in critically evaluating the performance of the *MMBS framework* in *Chapter 7*. This is because the *MMBS framework* will incur a higher number of switching instances due to its multi-mode operation.

If N_T is the total number of instances over time period D per BS at which the algorithms are executed by $\mathcal{B}_b$, then, the average percentage of instances at which switching occurs can be expressed as (Hossain et al., 2013a):

$$N_{SW} = \frac{1}{N_{BS}N_T}\sum_{b=1}^{N_{BS}}\left[\sum_{t=1}^{N_T} XOR\left(A_b(t), A_b(t-1)\right)\right] \text{x}100\%\,;\ A_b(t) = \{0,1\}, \forall b \qquad (3.13)$$

where $A_b(t)$ is the operating mode of $\mathcal{B}_b$, which will be explaining in *Section 4.2.1*, and XOR is the exclusive OR operation between the current and previous modes of $\mathcal{B}_b$.

BS switching delay can be considered as a contributory factor to the QoS in any *BS switching* technique. Since the switching decisions will be taken based on a predefined interval between two consecutive switches, *i.e.*, T_0 = 1hr in *Chapter 4* and T_0 = 15min in the other chapters, and switching decisions are made only if certain conditions are fulfilled within the interval T_0, it is reasonable to assume that switching delays between two switches will be negligible and so can be ignored. Moreover, there can be some delay in exchanging traffic information among BSs, though this delay has also been ignored because as discussed in Section 3.3.2, it is assumed there are dedicated links between BSs.

3.7 Simulation Platform

Over the past years, a variety of software packages has been developed, which have been widely used to simulate communication systems. Simulation models can be built using a

Table 3.2: Simulation platform specifications.

MATLAB Version	PC Specifications	
MATLAB 7.10/R2010a	Processor	Intel® Core™ 2 Duo E7500 (2.93GHz, 1066MHz FSB, 3MB L2 Cache)
	RAM	3GB
	Hard Disk	160GB, 8MB Cache, 7200 RPM
	OS	Windows XP Professional SP3 (64-bit)

general-purpose programming language such as C/C++, Java or FORTRAN and writing the appropriate code, or by using a graphical model builder such as SIMULINK or OPNET. The graphical model builders are relatively simple to use by clicking and dropping functional blocks on the computer screen and linking them together to create a simulation model in a hierarchical block diagram form. However, models can have a number of representations ranging from floating-point sub-routines to bit-level implementations of sub-routine models.

As an alternative to using a graphical block diagram editor for model building, one could use an intermediate (pseudo) language such as the MATLAB command language, which is one of the popular numerical computing environments and programming languages. MATLAB was chosen as the main system modelling tool for this thesis to demonstrate original concepts, for problem solving, and for rigorous comparison with the baseline model described in *Section 3.3*. There are a number of persuasive reasons for adopting MATLAB. Firstly, it combines excellent computational capabilities with easy-to-use graphical capabilities. It also contains a rich library of pre-programmed functions (m-files) for generating, analysing, processing and displaying signals together with specially developed add-on libraries (toolboxes) for communications and signal processing. It is also easy for MATLAB users to generate new m-files for user-dependent applications.

Additionally, MATLAB code is very concise, making it possible to express complex digital signal-processing (simulation) algorithms using relative few lines of code and although MATLAB is relatively slow compared to the basic C/C++ or Java, running the MATLAB codes in powerful computers can overcome these slow execution speeds. For this thesis, the PC specifications and MATLAB version used are summarized in Table 3.2.

3.8 Performance Validation

Verification and validation techniques were applied throughout the simulator development process of the new proposed framework. Using MATLAB, the design was refined through rapid iterations and verification cycles in an interactive test environment. Early in the development process, design and coding errors such as integer overflow, division by zero, and dead logic in models were detected using formal verification methods (Mathworks, n.d.).

In order to validate the system simulator, the performance of the baseline cellular model was firstly estimated through Monte-Carlo simulations by properly setting the system simulator parameters in verifiable test scenarios. A performance evaluation methodology was followed according to the ITU-T evaluation guidelines (ITU-R, 2009), discussed in *Section 3.3* and *3.4*. For verification purposes, hexagonal cells without any coverage gaps between consecutive cells were considered, while the traffic arrival process was modelled as a Poisson process, and as discussed in *Section 3.3.3*, this is normal practice in cellular traffic modelling.

The initial approach to the simulator validation was to test the operation of the baseline system using appropriate system parameter setting which were congruent with the 3GPP LTE (3GPP, 2010d) according to a number of logical consistency checks. For example, the corresponding LTE performance bounds such as capacity CDF, power and simulated radio behaviour as a function of distance were established for validation purposes and checked so as to establish suitable confidence levels when evaluating the results and

verifying the performance of the proposed *BS switching framework* under different test scenarios. The advantage of using 3GPP LTE standard values as the test parameters is that the proposed *BS switching framework* can be validated against the performance limits of a baseline LTE system. Moreover, the assessment metrics described in *Section 3.6*, were determined and compared with the baseline performance for each of the presented scenarios. Detailed critical performance analysis is provided in every respective chapter upon the behaviour of the developed systems and models.

3.9 Summary

This chapter describes how the system modelling tasks are conducted in this thesis. The system model methodology, simulation framework, tools used and the key performance indicators have been formally presented in this chapter. MATLAB has been adopted as the main simulation tool and a Monte-Carlo simulation approach applied to generate statistically meaningful results, with all results being compared with a baseline model for each scenario. Finally, a brief discussion on the verification of the simulation approach has been provided. The next chapter will present the first contribution to the new *BS switching framework*.

Chapter 4

Relay-Assisted Base Station Switching – A Fixed Threshold Approach

4.1 Introduction

This chapter discusses energy reduction in cellular networks by exploiting the dynamic nature of cellular traffic load profiles. Recently, (Marsan et al., 2009, 2011; Zhou et al., 2009; Oh & Krishnamachari, 2010; Niu et al., 2010; Weng et al., 2011; Elayoubi et al., 2011) have proposed the *BS sleeping* strategy in various forms to reduce energy consumption in network operations by either powering down or putting certain BSs to *sleep* during low-traffic periods. While such dynamic schemes regulate the EE by switching the BS to *active*/*sleep* mode depending on network traffic variations, sustaining QoS provision to the cells that have been switched off raises major design challenges. For example, ensuring regulatory constraints are upheld, protecting spatial coverage, and the inevitable increasing transmit power consumption to service those MS, called off-cell MS, located in sleeping cells. Therefore, the *active* neighbouring BSs must guarantee to protect spatial coverage, which requires the neighbouring BSs to increase their transmission power to serve the off-cell MS.

A literature survey on the *BS sleeping* strategy was discussed in *Section 2.7.4*. The main focus of the *BS sleeping* strategy has been to improve the EE of cellular networks either by minimizing the number of *active* BSs with certain QoS constraints or proposing different switching schemes and critically analysing their relative performance. For example, most existing *BS sleeping* strategies are based on the assumption that each BS is able to fully cover its neighbouring cells, which may not be practical given both the limited transmit power and current cell deployment, thus creating coverage holes. Another assumption is that each MS is required to maintain a minimum QoS, but this may not be the same as when all BSs are *active*, which is usually higher than the minimum QoS. As a result, by

employing the *BS sleeping* approach, some MSs will get better QoS when they are located within the *active* cell coverage, while others located in a sleeping cell will have a reduced QoS. In other words, the network can be seen as a worse service provider due to the reduced QoS when it decreases the number of *active* BSs for conserving energy while network operators are keen to provide the best QoS to users in a competitive market. From the sustainable business point of view, providing reduced QoS for energy savings is neither an acceptable nor a viable solution. In addition, from a MS power consumption perspective, the energy consumption for off-cell MS will be increased due to the higher transmit power dissipation for the increased propagation distance between the serving neighbouring BSs and the off-cell MS. As a result, the battery lifetime for off-cell MS will be significantly reduced during low-traffic periods when some BSs turn to *sleep* mode, as the main constituent is transmission power. Although most existing approaches are able to provide a certain level of energy saving, the aforementioned discussion and literature review (*Chapter 2*) confirms there is a gap between protecting the service coverage and upholding the QoS for off-cell MS. It is therefore, imperative to develop a new solution which guarantees the service coverage without degrading the QoS of off-cell MS within the *BS switching* model.

Recently, relays (Yang et al., 2009; Wu & Feng, 2012) have been considered as a low-cost solution not only for extending coverage, but also for improving the QoS. Besides, the low-cost and low-powered relay technology has been pursued very actively by *XG* broadband systems such as LTE-A (3GPP, 2010b; Iwamura et al., 2010) and IEEE 802.16j mobile WiMAX (IEEE, 2009a; Yang et al., 2009). In the above context and by taking advantage of relay technology, this chapter develops a *BS switching framework* for enhancing the EE as well as for providing better QoS for the off-cell MS. In this framework, a RS is deployed in each cell and is collocated with the corresponding BSs. The BSs and RSs operate in opposite modes, so at any time instant, when a BS is in *sleep* mode, the collocated RS operates in *active* mode and vice-versa. As a result, it can be said

that each BS can operate in either an *active* (standard BS operation) or RS modes at any instant and is able to alter its operating modes between them. The new proposed *BS switching* paradigm is termed the *BS-RS switching* model and is illustrated in Figure 4-1(a) for a 7-cell cluster scenario. Within a cluster, only the centre BS is in *active* mode, while the other six BSs can be in RS mode during low-traffic conditions.

The rationale for switching from a BS to RS mode is to ensure those MS that would be served by the switched off-cell and may for instance suffer deep fading, are still able to receive a similar level of QoS. Furthermore, as the propagation distance has been shortened between the off-cell MS and serving BSs via the RS as shown in Figure 4-1(b), the required MS transmit power is concomitantly reduced compared with the existing *BS sleeping* model (Marsan et al., 2009, 2011; Zhou et al., 2009; Oh & Krishnamachari, 2010; Niu et al., 2010; Weng et al., 2011; Elayoubi et al., 2011; Bousia, Antonopoulos, et al., 2012). A comparative transmission strategy for both the *BS-RS switching* and *BS sleeping* models is also presented in *Appendix A* for completeness.

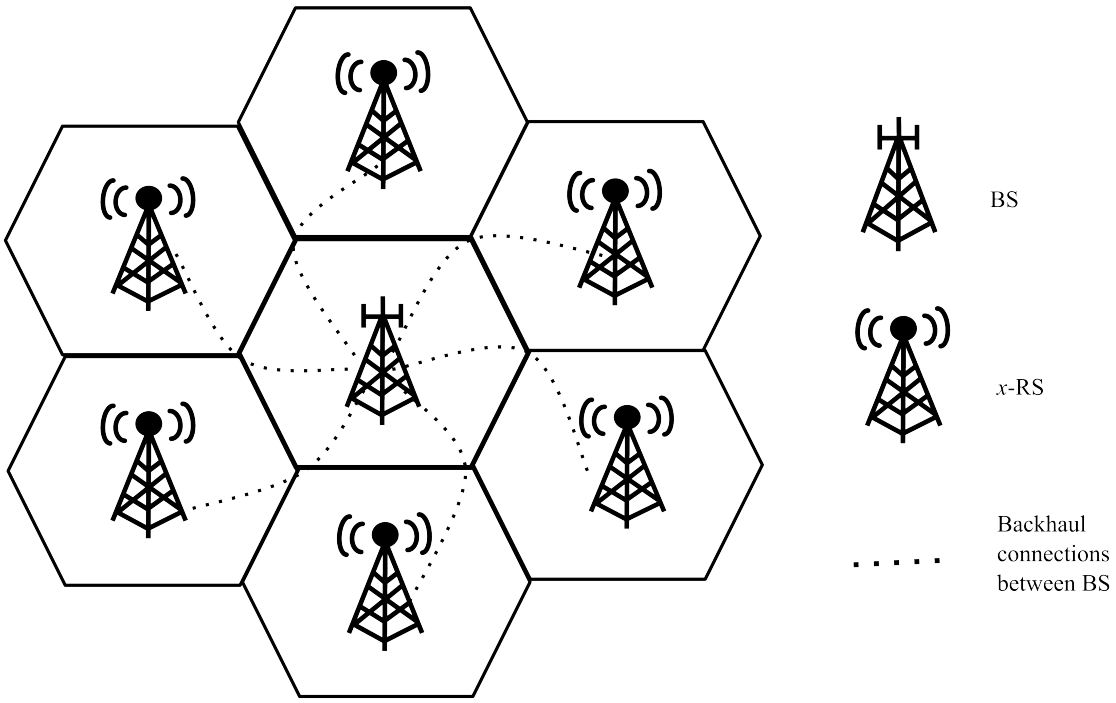

(a)

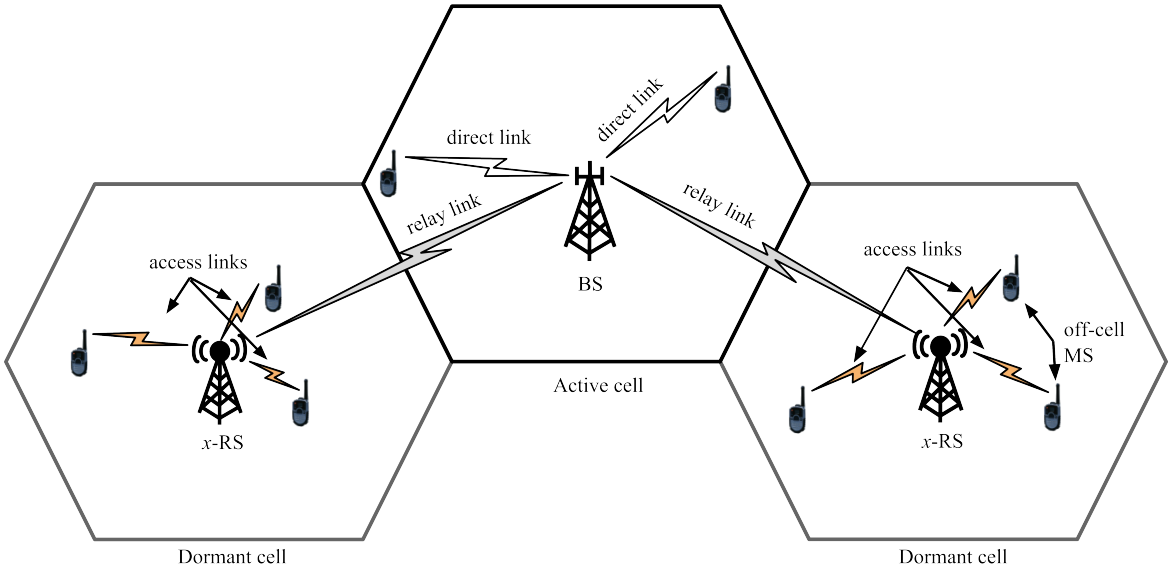

(b)

Figure 4-1: (a) Example layout showing the base station (BS) and switched relay station (*x-RS*) arrangement; and (b) Transmission strategies for the *BS-RS switching model* at low-traffic conditions.

4.2 System Model, Assumptions and Problem Formulation

4.2.1 System Model and Assumptions

The network scenario shown in Figure 4-1(a) is a cluster of 7-cells without sectoring for simplicity, and is assumed for the analysis of the proposed *BS-RS switching* model. Both the system model and the associated assumptions used in this chapter are summarized below:

1) Each BS within the cluster is denoted by $\mathcal{B}_b$ for b = 1, 2,…, and 7, with the set of BSs denoted by $\boldsymbol{\mathcal{B}}$ where $\mathcal{B}_1$ is the centre BS of the cluster and $\mathcal{B}_2$, …, $\mathcal{B}_7$ are the neighbouring BSs of $\mathcal{B}_1$.

2) Within a cluster, the centre BS is always in *active* mode, with the other BSs having the capability to switch to *active* and *sleep* modes depending on their traffic conditions.

3) In each cell, a RS is deployed and is collocated with the corresponding BS. The RS also has the capability to switch between *active* and *sleep* modes. When the RS is in operational mode, the maximum coverage of a RS is the same as the BS.

4) When a BS is switched to *sleep* during low-traffic periods, the corresponding collocated RS is triggered to switch into *active* mode. This means that each BS can switch its operating mode between the *active* and RS mode while both always operate in opposite mode. In other words, for simplicity, each BS has two modes: *active*, $A_b = 1$ and RS mode, $A_b = 0$, where A_b is the *mode activity factor* (MAF) of $\mathcal{B}_b$. The switched RS is denoted as *x-RS* throughout the thesis as shown in Figure 4-1(b), so as to distinguish it from the other RS deployed within a particular cell.

5) All BSs are interconnected via dedicated connections as described in *Section 3.3.2* to share information to support any usage in the cluster. Additionally, Kanesan & Ng (2012) showed that radio-over-fibre techniques are possible as an alternative to a wireless interface structure between the BS and RS. In this case, the dedicated links between the BS and RS can be utilized as the relay link (between BS and RS) and is an exemplar of avoiding severe propagation fading caused by the wireless relay link.

When any BS is in the RS mode, the off-cell MS are successfully handed over to the neighbouring *active* BSs, with any handover delay ignored. Therefore, the off-cell MS are served by the centre BS either directly or via the *x-RS* under the transmission strategy for the *BS-RS switching* model illustrated in Figure 4-1(b). For the *x-RS* assisted communications between the BS and off-cell MS, an *amplify-and-forward* (AF) relay protocol is adopted in this chapter due to its simplicity, low-cost implementation and very short delay. This relay-assisted BS switching model not only reduces the transmission power but also improves off-cell MS throughput. However, BS switching between the

active and dormant[6] modes is, in general, critically dependent on when and which BS should be switched to *active*/dormant mode and under what conditions the switching decision is determined. Before formally introducing the problem and the *BS switching* strategy, the power consumption model for the new *BS-RS switching* model is described in the following subsections.

4.2.2 Power Consumption Model

According to the power consumption model described in *Section 2.5*, a linear model predicts the power consumption of $\mathcal{B}_b$. Since each BS operates in two modes (*active* and RS mode) in the *BS-RS switching* model, with each mode consuming different powers, the total power consumed by $\mathcal{B}_b$ in (2.1) can be expressed by incorporating the MAF A_b as:

$$\begin{aligned} P_{T_b} &= P_{T,BS} + P_{T,RS} \\ &= A_b \cdot \left(a_{BS} \cdot P_{tx,b}^{BS} + P_f^{BS}\right) + \left(1 - A_b\right) \cdot \left(a_{RS} \cdot P_{tx,b}^{RS} + P_f^{RS}\right) \end{aligned} \tag{4.1}$$

where the first expression is for the BS power consumption and is the same as (2.1), while the second term reflects corresponding transmission power, scaling factor and fixed power components of the *x-RS* as signified by $P_{tx,b}^{RS}$, a_{RS}, and P_f^{RS}, respectively. For both the BS and *x-RS*, the maximum transmission power constraint must be satisfied, *i.e.*, $P_{tx,b}^{BS} \le P_{tx,\max}^{BS}$ and $P_{tx,b}^{RS} \le P_{tx,\max}^{RS}$, where $P_{tx,\max}^{BS}$ and $P_{tx,\max}^{RS}$ are the maximum transmit power of each BS and the *x-RS*. Since the RS is a simple, low-powered radio station with comparatively less complex equipment, both the scaling factor and fixed power consumption parameters of the *x-RS* are much less than for the macro BS as shown in Table 2.1, *i.e.*, $a_{BS} > a_{RS}$ and $P_f^{BS} > P_f^{RS}$ (Lee et al., 2011; Richter et al., 2009).

[6]When a BS changes from active to either sleep (*BS sleeping*) or RS mode (*BS-RS switching*), it switches from *active* to *dormant* mode.

The power model in (4.1) is also a function of the MAF A_b for $\mathcal{B}_b$, so the total power consumption is dependent upon the operating mode of $\mathcal{B}_b$. When $A_b = 1$, $\mathcal{B}_b$ is *active* and the second term in (4.1) which accounts for the *x-RS* is zero. The reverse is also true when $A_b = 0$. Moreover, since the performance of the new *BS-RS switching* model is to be compared with the existing *BS sleeping* model in order to study the effectiveness of the new model, the power model expression in (4.1) can also be seen as a generalized power model for both cases. This means that (4.1) can also be applied to the *BS sleeping* model, in which there is no *x-RS*, so the second term, $P_{T,RS}$ in (4.1) can simply be set to zero.

From the MS power consumption perspective, the main constituent is transmission power, which increases with the distance between the MS and the serving BS due to PL and shadowing effects. It is assumed that each MS is capable of autonomously adapting its transmit power according to the LTE uplink (open-loop) power control scheme (3GPP, 2009b; Bulakci et al., 2013) that is given in *dBm* as:

$$P_{tx,m}^{MS} = \min\left(P_{tx,\max}^{MS},\ P_0 + 10\log_{10} M_m + \alpha \cdot PL(d_m)\right) \tag{4.2}$$

where $P_{tx,m}^{MS}$ is the transmit power of the MS *m*,

$P_{tx,\max}^{MS}$ is the maximum allowed transmit power of the MS,

P_0 is the user-specific (optionally cell-specific) power offset parameter that is used for controlling the received signal power target to ensure a minimum QoS,

M_m is the number of *primary resource block* (PRB) in LTE allocated to each MS,

α is a cell-specific PL compensation factor that can be set to 0 and between 0.4 and 1 with a step size of 0.1, and

$PL(d_m)$ is the DL PL estimate between the MS *m* and the BS/RS.

If $\alpha = 1$, the PL is fully compensated in order to reach the target received power P_0 and the resulting scheme is called *fully-compensated power control* (FCPC). This means all MS receive signals with the same power at the BS irrespective of their locations. For a given P_0 value, FCPC improves the cell-edge user performance at the cost of increased ICI due to higher transmit power levels. Assuming that there are N_{MS} MS in the network, then the total MS power consumption can be expressed by using (4.2) as:

$$P_{T,UL} = \sum_{m=1}^{N_{MS}} P_{tx,m}^{MS} \tag{4.3}$$

It can be seen both from (4.2) and (4.3) that the required total transmission power for MS to communicate with the associated BS/RS depends on their channel conditions, which are related to the distance between the transmitter and receiver. The closer the MS is located to its receiver, the less transmission power is required for successful communication between them.

4.2.3 Problem Formation and Solution

Assume the number of available channels (equivalent to the total number of PRB) in every cell is N_{RB} for transmission with a channel bandwidth of $W = \frac{W_{max}}{N_{RB}}$, where W_{max} is the maximum cell bandwidth. For simplicity, it is assumed that each user is allocated to one PRB so the maximum number of users in a cell $\mathcal{B}_b$ is $N_{MS} = N_{RB}$ and different frequency bands are used by adjacent cells so ICI can be ignored. The overall throughput of $\mathcal{B}_b$ is thus the aggregate of the capacity of each MS *m* served in the coverage area of $\mathcal{B}_b$ and can be derived using Shannon formula (Shannon, 1948) as:

$$R_b = W \sum_{m=1}^{N_{MS}} \log_2 \left(1 + \Gamma_{bm}\right) \tag{4.4}$$

where Γ_{bm} is defined in (3.1). In the case of the *BS-RS switching* model, off-cell MS will be served by neighbouring *active* BSs via the corresponding *x-RS*. As such, the achievable throughput for the off-cell MS *m* can be determined from (3.4) and (3.5).

To analyse the MS power consumption, it is assumed that each MS *m* can achieve a prescribed minimum data rate $r_{\min}$. If $P_{tx,m}^{MS}$ is the MS transmission power, which guarantees $r_{\min}$ for the MS *m* with the propagation distance d_m between the serving BS and the MS *m*, then according to Shannon formula it must satisfy the following:

$$r_{\min} = W \log_2 \left(1 + \frac{\eta_0 \cdot P_{tx,m}^{MS} \cdot 10^{\xi_m/10}}{d_m^n} \right) \tag{4.5}$$

where $\eta_0 = \frac{G_0}{N_0}$ includes the effect of the antenna gain G_0 and thermal noise N_0. The signal attenuation at the distance d_m is given by d_{bm}^{-n} where n is the PL exponent, and the shadow fading $10^{\Psi_m/10}$ follows a lognormal distribution $\Psi_m \sim \mathcal{N}\left(0, \sigma^2\right)$. Therefore, (4.5) can be written as:

$$P_{tx,m}^{MS} = \frac{\left(2^{r_{\min}/W} - 1\right) \cdot d_m^n}{\eta_0 \cdot 10^{\Psi_m/10}} \tag{4.6}$$

(4.6) reveals the transmission power depends on d_m, so to achieve a given $r_{\min}$, the aim is to always maintain the minimum distance between the transmitter and receiver to reduce propagation attenuation. In the *BS-RS switching* model, since the RS is collocated with the BS, each off-cell MS will experience the same propagation distance between the neighbour serving BS and the MS, whenever the BS is switched to RS mode. On the other hand, this distance can be significant on other models (Marsan et al., 2009, 2011; Zhou et al., 2009; Oh & Krishnamachari, 2010; Niu et al., 2010; Weng et al., 2011; Elayoubi et al., 2011; Bousia, Antonopoulos, et al., 2012), which will ultimately force both the BS and MS to use higher transmission powers.

From (4.1) and (4.4), the EE of a cell (3.6) in *bits per joule* is:

$$\eta_{EE} = \sum_{b=1}^{|\mathcal{B}|} \frac{R_b}{P_{T_b}} \tag{4.7}$$

where $|\mathcal{B}|$ denotes the size of the set $\mathcal{B}$. To attain a high EE while concurrently guaranteeing the QoS for each user, the design objective is to turn off as many BSs as feasible and switch to the RS mode during *zero-to-medium* traffic periods. Thus, to maximize the EE, a design problem can be formulated with a minimum data rate and transmit power constraints as:

$$\max_{A_b} \quad \eta_{EE} \tag{4.8}$$

$$s.t. \qquad \sum_{k=1}^{N_{RB}} p_{tx,k}^{BS} = P_{tx,b}^{BS} \le P_{tx,\max}^{BS} \ , \ \forall \mathcal{B}_b \in \mathcal{B} \tag{4.8a}$$

$$W \log_2 \left(1 + \Gamma_{bm}\right) \ge r_{\min} \ , \ \forall m \tag{4.8b}$$

$$\text{and } A_b(x) \in \{0,1\}, \forall x \in \{t, t+1\} \tag{4.8c}$$

(4.8) is the objective function to maximize the EE of the model. The constraint (4.8a) defines the upper bound of the BS transmit power that cannot be violated, while constraint (4.8b) ensures the data transmission rate of each MS is larger than or equal to $r_{\min}$. The MAF of $\mathcal{B}_b$, A_b can only be in one mode at any given time instant as defined by (4.8c), so at time *t*, the EE maximization problem in (4.8) is to determine the set of *active* BSs subject to the transmit power, rate and load constraints. The *BS switching* depends upon the traffic load at time *t* and this is performed on an hourly basis throughout the day, so the MAF A_b for all $\mathcal{B}_b \in \mathcal{B}$ only changes every hour, *i.e.*, the minimum mode holding time, T_0=1hr. The objective function in (4.8) can be numerically solved using an exhaustive search algorithm based on the *BS switching* strategy described in *Section 4.3*. The minimum energy consumption performance of both the *BS-RS switching* and *BS sleeping*

models (Niu et al., 2010; Oh & Krishnamachari, 2010) will then be analysed. Note, in the case of *BS sleeping*, when the numerator of (4.7) for $\mathcal{B}_b$ in *sleep* mode is zero, *i.e.*, $P_{T_b} = 0$, while the corresponding R_b is also zero as all traffic is handed over to its neighbouring BSs, the resultant outcome of (4.7) is indeterminate. To avoid the unexpected situation, η_{EE} is set to zero when $A_b = 0$.

4.3 Base Station Switching Strategy

Since the *BS switching* depends on the instantaneous traffic profile of each cell and the traffic profile of $\mathcal{B}_b$, $\rho_b(t) = \lambda_b(t) \cdot h$ is a time varying function over a 24hr period, it is assumed as in Oh & Krishnamachari, (2010) that BSs only know the approximate sinusoidal traffic profile with mean, $\overline{X}$ and variance V, and is defined by (Oh & Krishnamachari, 2010):

$$\overline{\rho}_b(t) = V \cdot \cos\left(2\pi(t+\theta)/D\right) + \overline{X} \tag{4.9}$$

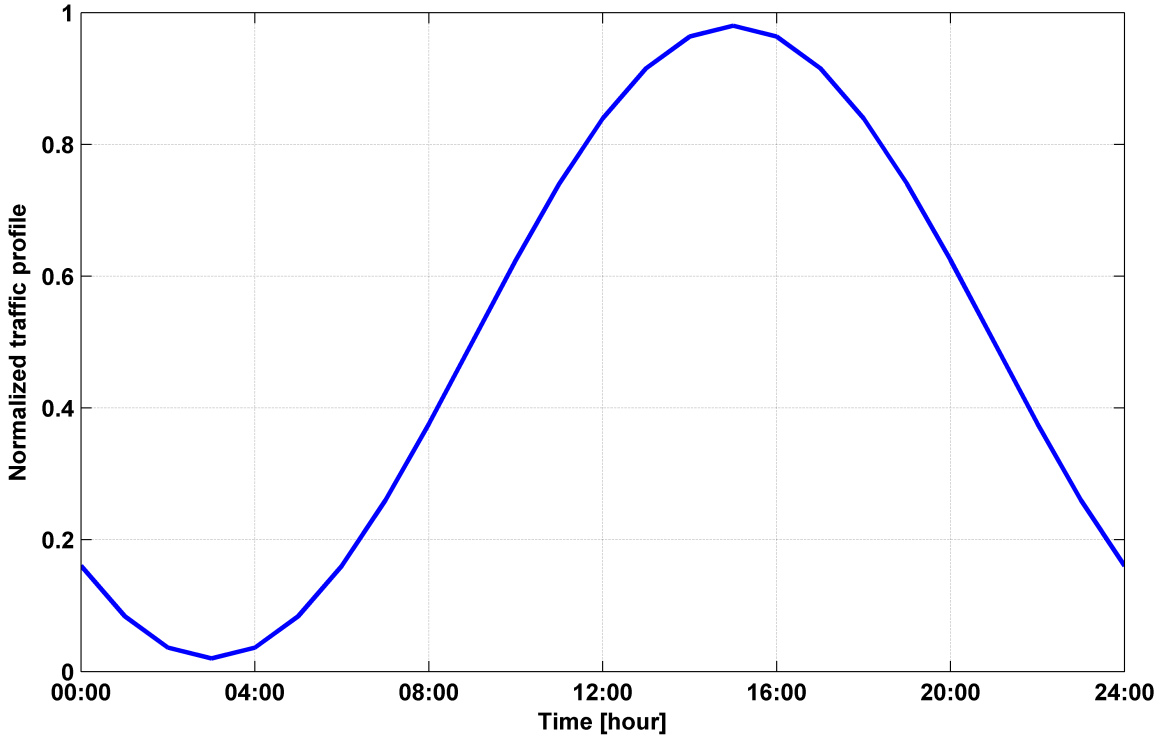

Figure 4-2: Approximate normalized traffic profile in an arbitrary cell with $\overline{X}$ = 0.5, V = 0.48, and D = 24hr.

An illustration of the approximate traffic profile over a 24hr period for an arbitrary cell with $\overline{X}$ = 0.5, V = 0.48 and D = 24hr is shown in Figure 4-2. The approximated traffic profile is normalized based on the 100% traffic handling capacity of a BS, which can be less than the peak-traffic load conditions within the cell. Since the switching decision will be taken on an hourly basis, there will be 24 time instants, *i.e.*, t = 1, …, 24. When the instantaneous traffic profile of $\mathcal{B}_b$ is lower than a predefined fixed threshold, called the switching threshold ρ_{th}, the BSs can be switched to RS mode, which potentially reduces network energy consumption. In this section, the rationale behind the *BS switching* strategy using a fixed switching threshold will be introduced, based on the work of Oh & Krishnamachari, (2010), before the switching assumption is subsequently relaxed in later chapters. In the context of a fixed threshold approach, two-load profile categories are defined on which the proposed *BS-RS switching* principle is modelled:

Case I**:** *Zero-to-medium traffic period*: During this period, certain BSs are switched off to conserve energy when their presence is not essential for the proper operation of the network, with low-powered, collocated RS alternatively being used to cover the area of the switched-off cell. For example, $\mathcal{B}_b$ can be switched to RS mode (*x-RS*) provided that a set of neighbouring *active* BSs, $\mathcal{N}_b$ of $\mathcal{B}_b$ are able to handle all the MS currently served by $\mathcal{B}_b$. When $\mathcal{B}_b$ is allowed to switch to RS mode at a decision instant t_b^{off}, the approximate handover traffic $\overline{\rho}(t_b^{off})$ of $\mathcal{B}_b$ is distributed among $\mathcal{N}_b$ according to their own traffic profiles. This means traffic loads $\rho_1'(t_b^{off}), \rho_2'(t_b^{off}), ..., \rho_{|\mathcal{N}_b|}'(t_b^{off})$ will be distributed to the 1^{st}, 2^{nd},…., $|\mathcal{N}_b|$-*th* neighbouring *active* BSs, respectively. For simplicity, the handover traffic is assumed to be equally distributed amongst the neighbouring *active* BSs for homogeneous traffic conditions among cells, so the handover traffic of each neighbouring *active* BS is approximated by:

$$\rho_1'(t_b^{off}) = \rho_2'(t_b^{off}) \ldots = \rho_{|\mathcal{N}_b|}'(t_b^{off}) = \overline{\rho}(t_b^{off}) / |\mathcal{N}_b|$$

The new cell traffic load for each of the neighbouring *active* BSs when $\mathcal{B}_b$ is switched to RS mode at t_b^{off} is then:

$$\overline{\rho}_i(t_b^{off}) = \overline{\rho}(t_b^{off}).\left(1+\frac{1}{|\mathcal{N}_b|}\right); \quad \forall i = 1,2,\cdots,|\mathcal{N}_b| \tag{4.10}$$

So in general, when $\mathcal{B}_b$ is switched to RS mode at decision time *t*, when the MAF A_b is actually set to 0, the following two conditions must be satisfied:

$$\overline{\rho}_i(t) = \overline{\rho}(t).\left(1+\frac{1}{|\mathcal{N}_b|}\right) < \rho_{\max}, \quad \forall i = 1,2,\cdots,|\mathcal{N}_b| \tag{4.11}$$

and

$$\overline{\rho}_b(t) < \rho_{th} \tag{4.12}$$

where $\rho_{\max}$ is the maximum traffic load that each neighbouring *active* BS is able to handle and ρ_{th} is the predefined fixed switching threshold. The choice of ρ_{th} is critical to performance as a higher switching threshold gives higher energy saving, but can become compromised by a higher blocking probability, and *vice-versa*. The most appropriate choice for ρ_{th} will be discussed in *Section 4.4.2*, in conjunction with the blocking probability constraint.

When switching back from dormant to *active* mode, *i.e.*, from *x-RS* to BS mode, the neighbouring BSs are required to keep track and share the received handover traffic for a specific cell, *i.e.*, $\mathcal{B}_b$. The basic process of turning on $\mathcal{B}_b$ is: when the total handover traffic $\overline{\rho}_b(t)$ from cell $\mathcal{B}_b$ to its neighbouring *active* BSs becomes equal to the threshold ρ_{th}, any of the neighbouring *active* BSs can request $\mathcal{B}_b$ to wake-up. Thus, the corresponding traffic profile condition to be upheld is:

$$\overline{\rho}_b(t) \geq \rho_{th} \tag{4.13}$$

Although a homogeneous traffic condition is considered amongst cells, all BSs are not switched to RS mode at the same time due to the service coverage guarantee and hence, there will be a varying number of *active* BSs at each decision time.

Case II: *High-traffic period*: In this scenario, all BSs actively provide services as most of the cells will have a traffic load greater than the switching threshold ρ_{th}.

There can be situations where some cells become more over crowded than others, which is a special case in real cellular networks (e.g., sporting or concert events). In this scenario, the blocking probability for the crowded cell can be very high. Since the *BS switching* strategy is based on the assumption that BSs have the ability to expand their service coverage depending on their traffic demand, this cell coverage expansion capability can be alternatively viewed as a *load balancing technique*. This is done by migrating some traffic from overly crowded to less crowded cells (Niu et al., 2010; Son et al., 2009). By applying *load balancing techniques*, the traffic load in a particular cell can be lowered to below ρ_{th}, which then satisfies the switching condition in (4.11) and (4.12). However, care must be taken for resource allocation due to the increased ICI. As the focus of this chapter is upon verifying the proof-of-concept behind the proposed *BS-RS switching* model, this particular *load balancing* issue is outside the scope of the chapter and will not be considered further, though a different view of the *load balancing techniques* will be exploited in the design of the comprehensive cellular model in *Chapter 7*.

The *BS switching* strategy described above can also be applied to the *BS sleeping* model where off-cell MS are served directly by the *active* neighbouring BSs whereas in the *BS-RS switching* they are served by the *active* neighbouring BSs with the help of the *x-RS*. A number of benefits ensue from adopting the new *BS-RS switching* model compared to the traditional *BS sleeping* approach (Niu et al., 2010; Oh & Krishnamachari, 2010). These include:

i) maximising the EE and minimising the average energy consumption in the *Case I* scenario for both the BS and MS;

ii) maintaining the similar coverage and QoS as with all BSs in full-working modes;

iii) lower outage probability.

The rationale is that the energy consumption of the proposed model can be minimised by switching high-powered macro BSs to low-powered RSs without degrading the QoS, which also results in maximising the EE. A similar level of QoS is maintained by keeping all MS at the same propagation distance from the BS via the *x-RS* compared to the *BS sleeping* model, which also results in lower signal outage.

4.4 Simulation and Results Analysis

4.4.1 Simulation Settings

To critically assess the performance of the new *BS-RS switching model*, a homogeneous network comprising of seven cells is considered, as shown in Figure 4-1(a), with both the BS and MS perspectives being analysed. All results are based on a cluster of seven cells with ISD of 500m unless otherwise specified. Table 3.1 details all the simulation environment parameters, which were chosen to be congruent with the specifications of international standard bodies (ITU-R, 2009; 3GPP, 2010d, 2010c). In this simulation, the maximum transmission power of 30dBm and 21dBm are considered for the RS and MS, respectively, *i.e.*, $P_{tx,\max}^{RS}$ = 30dBm and $P_{tx,\max}^{MS}$ = 21dBm while the power model 1 in Table 2.1 is considered for the linear power model parameters of a macro BS in (4.1). The power consumption parameters for the RS are chosen as a_{RS} = 7.84 and P_f^{RS} = 71.5W (Lee et al., 2011) and it is assumed that there can be up to 25 MS in each cell such that each MS can be allocated to at least 1PRB during peak periods while W_{max} =5MHz. Hourly time intervals were used in the analysis *i.e.*, the switching decision was taken once every hour and the MAF, $A_b, \forall b$ does not change within the one hour time slot. The various hourly

interval results for both *BS-RS switching* and the *BS sleeping* strategies were then averaged and compared across an entire day.

4.4.2 Simulation Results

Firstly, the feasibility of determining the predefined switching threshold, ρ_{th}, in the switching strategy presented in *Section 4.3*, was studied. The switching threshold is a key design parameter for energy efficient operation of a BS in a network (Oh & Krishnamachari, 2010; Oh et al., 2013). If ρ_{th} is set too high, then a higher number of BSs can be switched to dormant mode, which results in higher achievable energy savings. However, the higher the number of BSs in dormant mode would also be more likely to lead to users in the blocking region due to the creation of coverage holes, transmit power constraints, and lack of radio resources. Therefore, a trade-off between the number of BSs in dormant mode to conserve energy and the blocking probability for finding the switching threshold parameter ρ_{th} is necessary. In this analysis, a network comprising 7x7 hexagonal cells (Figure 3-1(b)) is assumed. To find a feasible switching threshold, Figure 4-3 illustrates comparative results between the number of dormant mode BSs and the blocking probability across an entire day for different ρ_{th}. The switching decisions are made according to the *BS switching* strategy described in *Section 4.3*. The results show that when ρ_{th} is set to 0.75, for example, almost 65% of BSs are in dormant mode, which incurs a greater energy saving. However, this greater energy saving comes at a cost of over 90% of users being in blocking region which is an unacceptable situation for any communications system. On the other hand, for ρ_{th}=0.3, there is negligible average blocking probability of ≈0.2%, though now only 32% of BSs are in dormant mode during the day. Since the objective is to have the maximum number of BSs in dormant mode throughout the day, this is best achieved by setting ρ_{th} to a higher value while maintaining the minimum required QoS (in terms of the blocking probability). If a network can tolerate a maximum blocking

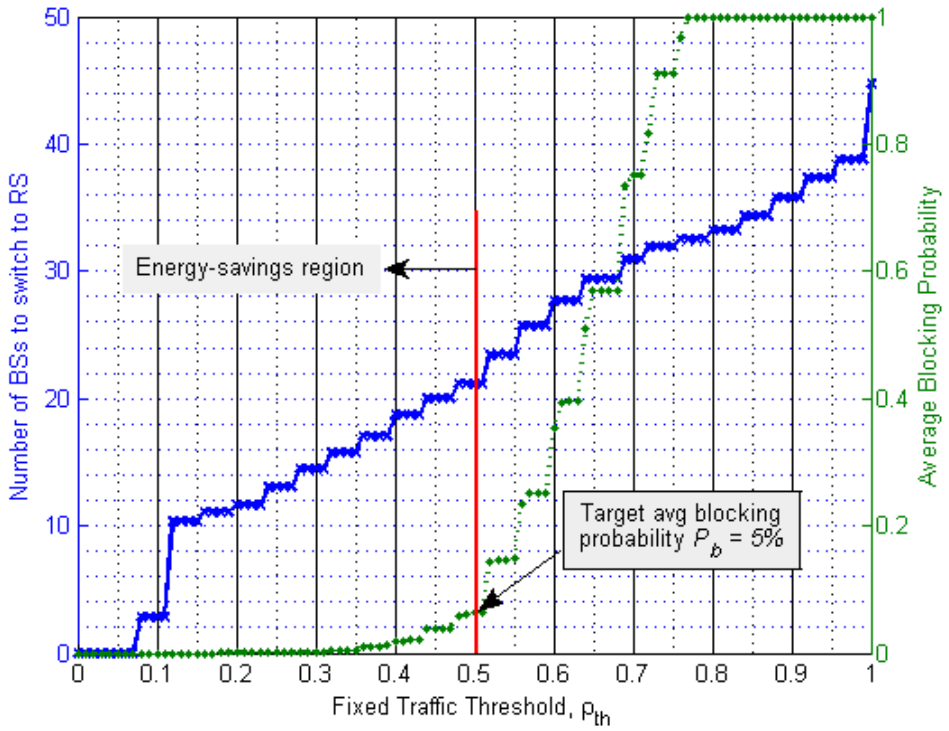

Figure 4-3: Number of BSs in dormant mode per day for different fixed traffic thresholds.

probability of up to 5%, the switching threshold ρ_{th} can be set to 0.5 indicated by the energy-savings region. However, one can choose a higher switching threshold for more energy savings by considering a higher target blocking probability. The increasing region of the average blocking probability for ρ_{th}>0.5 can be described as the QoS-limited region in Figure 4-3. This is because the QoS of the network is highly degraded within the region by applying the switching strategy for ρ_{th}>0.5. In other words, the right choice of the switching threshold determines the energy-savings region to be maximized without decreasing the network performance. The fixed value of ρ_{th}= 0.5 will be used for the rest of the analysis unless otherwise specified.

Now, the impact of introducing the *x-RS* in the new *BS-RS switching* model on the QoS level is analysed when certain BSs are switched to the *x-RS* mode rather than into *sleep* mode. The downlink SINR distributions for all target users are depicted in Figure 4-4(a), (b) and (c) with using "*always-on*", *BS sleeping* and *BS-RS switching* strategies, respectively, where red crosses indicate the dormant mode cells. When the network

operates in normal operation mode *i.e.*, "*always-on*" as shown in Figure 4-4(a), the SINR distribution in all cells are almost uniform. On the other hand, the SINR distributions, by employing the *BS sleeping* strategy, in certain cells in which the corresponding BSs are in *sleep* mode, are seriously degraded as shown in Figure 4-4(b), thus creating coverage holes. It is also noticed that the users around the centre area of all sleep cells are most likely to receive degraded SINR due to the high propagation PL distortions. However, the contour plot of SINR distribution in Figure 4-4(c) shows that a better SINR coverage in the switched cells can still be achievable even when certain BSs are switched to low-power RS mode to conserve energy, thus diminishing coverage holes. This was the main motivation to deploy an additional low-power RS (*x-RS*) collocated with the BS in each cell. Even though the BS is switched off, the off-cell users will still consistently receive superior SINR.

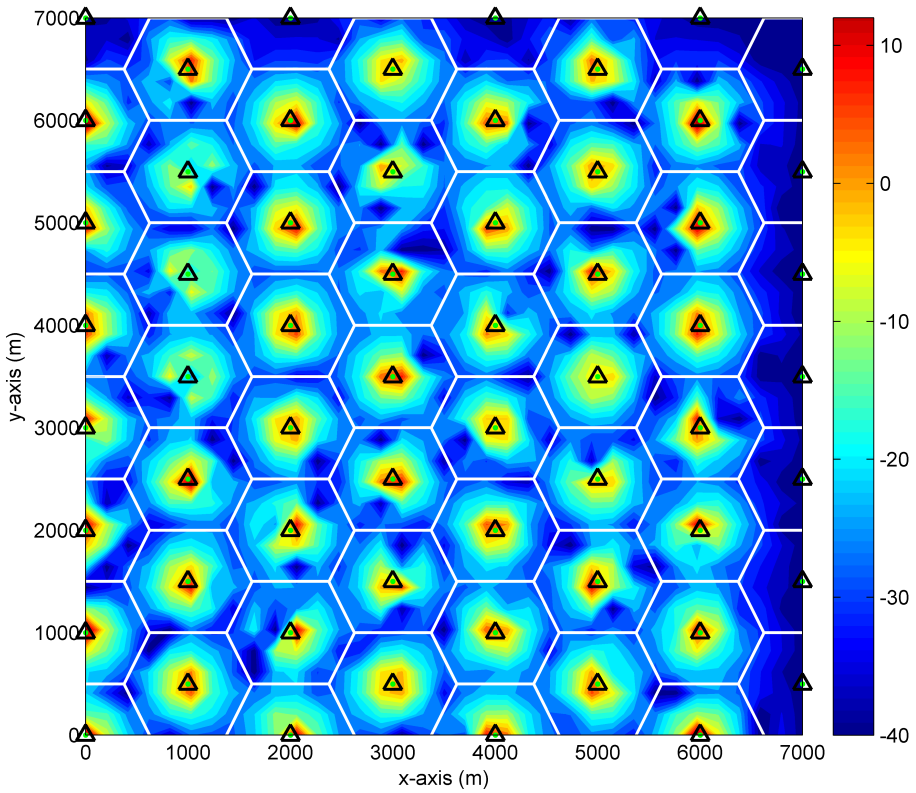

(a) Normal BS operation ("always-on") strategy

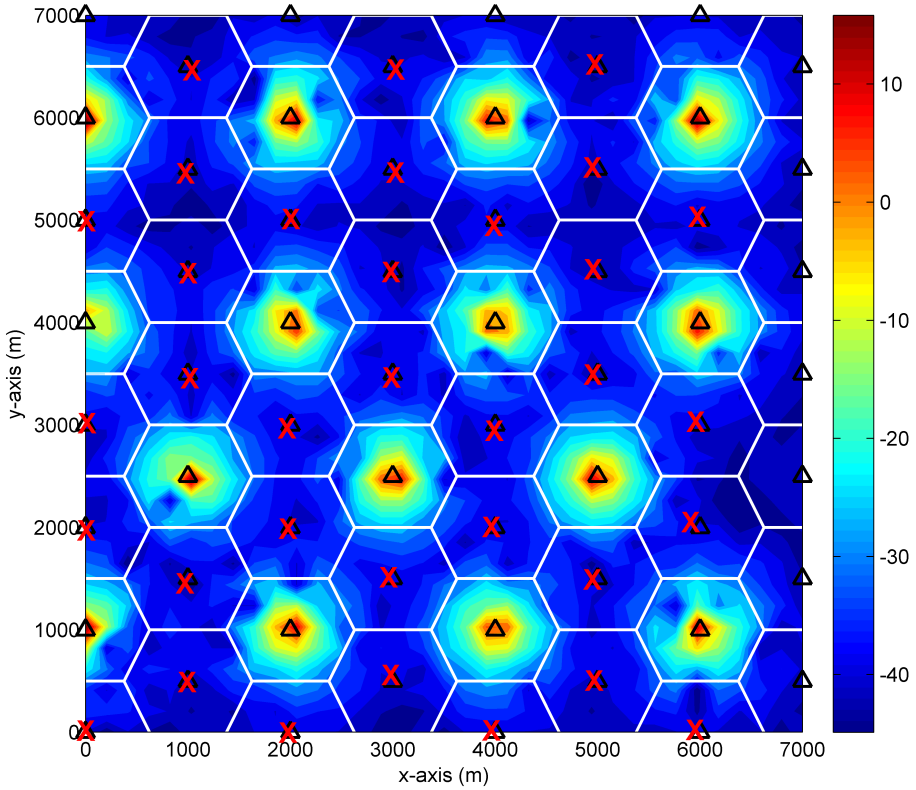

(b) BS sleeping strategy

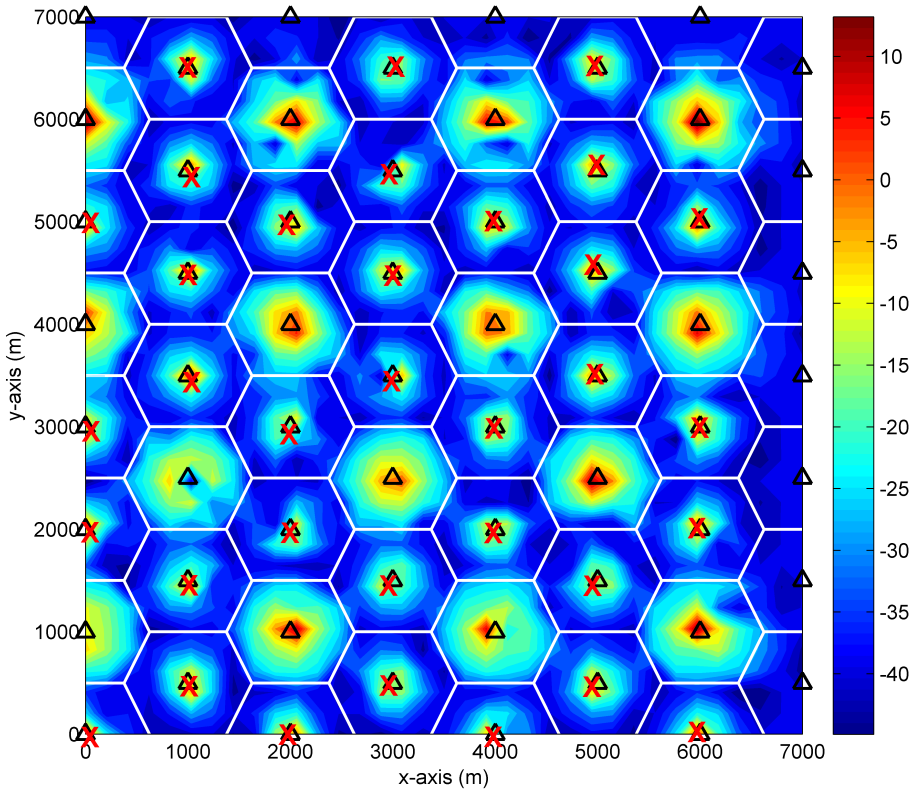

(c) *BS-RS switching strategy*

Figure 4-4: Contour plots of SINR distributions for different BS switching models with BS and RS transmission powers of 43dBm and 30dBm, respectively, and the ISD of 1000m being used in a 7x7 hexagonal cellular grid.

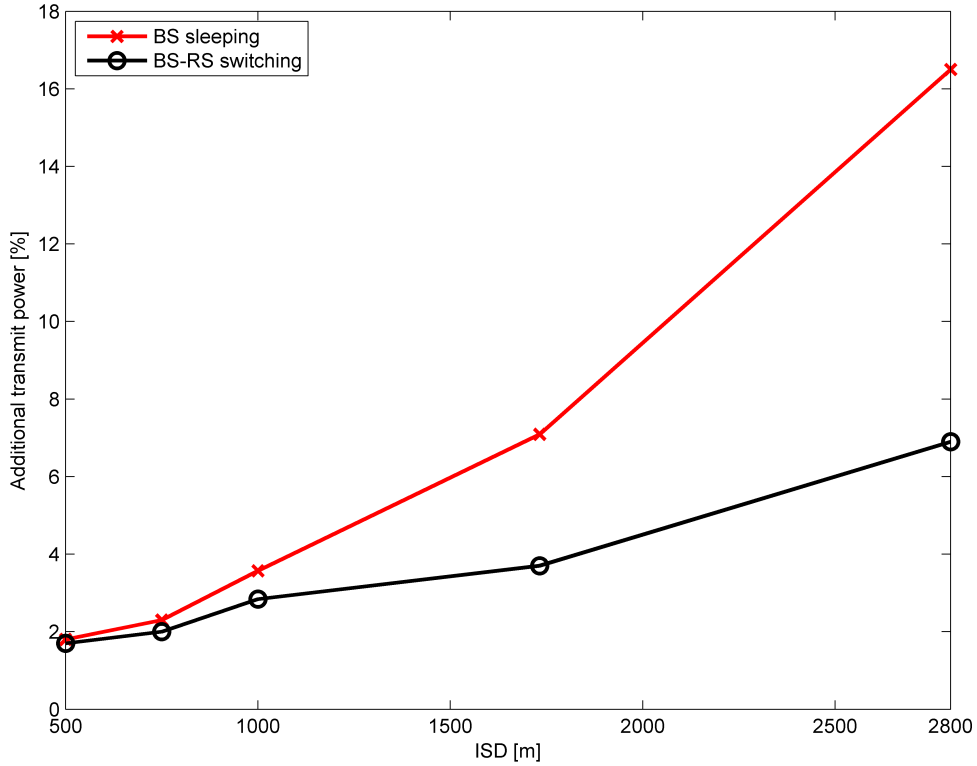

Figure 4-5: Additional average transmit power per BS to serve off-cell MS for a range of ISD values with their corresponding data rate requirements.

As the *active* BSs need to serve off-cell users located beyond their original coverage range, the *active* BSs are required to increase their transmit power to achieve data rate requirements for each off-cell MS. To estimate the required additional transmit power for each *active* BS, link budget analysis was used according to the PL model described in *Section 3.3.4*. The additional transmit power per BS required to serve off-cell MS is shown in Figure 4-5. Here, the analysis is based on different ISD of [500, 750, 1000, 1732, 2800] metres with the corresponding data rate requirements being [0.73, 0.65, 0.48, 0.41, 0.21] bps/Hz respectively according to 3GPP, (2006). It is seen that the required additional transmit power percentage of per-BS increases with the ISD. This is due to the increased propagation distance between the *active* BS and off-cell MS with the ISD. The longer propagation distance usually means a higher PL with shadowing effects leading to more transmission power. For example, in the case of ISD of 500m and 2800m, the worst-case location of an off-cell MS can be 500m and 2800m away from an *active* neighbouring BS, respectively. For the ISD of 500m, the *active* BS can normally be able to cover its

neighbouring cell with a small increase (≈2%) in its transmit power. It is required to increase the BS transmission power significantly (≈6.5% and over 16% depending on the model being used) to achieve the rate requirement for the latter case. It is mentioned earlier that the same propagation distance between off-cell MS and the serving neighbouring *active* BS can be maintained via the *x-RS* with the *BS-RS switching* model, less additional transmit power is required whereas the *BS sleeping* strategy requires higher transmission power due to the significant propagation distance. For example, for the ISD of 1732m, the additional transmit power requirement with the *BS-RS switching* and *BS sleeping* models are 3.7% and 7.09%, respectively. As a result, the addition deployment costs of the collocated RS (*x-RS*) compared to the *BS sleeping* model with no need for the *x-RS* deployment can be compensated with the higher additional transmit power costs of the *BS sleeping* model. It can be claimed that the deployment of a collocated low-cost RS together with each BS can be more beneficial in terms of the energy saving while ensuring improved signal quality for all users at all time.

In Figure 4-6, four hourly snapshots of the energy consumption in each cell of the cluster for different traffic scenarios in a day, for example, - (a) early morning at 3:00 am, (b) morning at 8:00 am, (c) afternoon at 15:00 pm, and (d) night at 20:00 pm are shown with the MAF A_b where b = 1, …, 7. The x-axis indicates $\mathcal{B}_b$ within the cluster where $\mathcal{B}_1$ is the centre BS, which is always *active i.e.*, A_1 = 1. In the early morning when the traffic loads in all cells are very low (as in Figure 4-2), only the centre BS is in *active* mode while it allows all its neighbours to switch into RS mode as indicated by the corresponding A_b = 0 in Figure 4-6(a). During the morning and night time when cell traffics are medium, only certain BSs are switched to RS mode, for example, [A_5, A_6, A_7] = [0, 0, 0] and [A_2, A_3, A_4] = [0, 0, 0] as shown in Figure 4-6(b) and 4-6(d), respectively. However, during the peak-traffic period in the afternoon, none of the BSs within the cluster are allowed to switch RS mode, *i.e.*, A_b = 1 for all b as described in *Section 4.3* (***Case II***). As a number of BSs

during each decision time are switched to low-power RS mode, the plots clearly reveal the improved energy consumption of each of the seven BSs when the *BS-RS switching model* is compared with retaining all BSs as *active* ("*always-on*" strategy). For example, in the early morning graph (Figure 4-6(a)), a higher energy reduction gain is achieved within the cluster while no energy reduction is achievable during the high-traffic period (Figure 4-6(c)). During medium-traffic periods shown in Figures 4-6(b) and 4-6(d), certain BSs are still able to reduce their energy consumption, though it is noted that the centre BS consumes more energy within the cluster with the proposed *BS-RS switching* strategy than no switching in all hours, if other BSs are in RS mode. This is due to the off-cell users' services provided by the centre BS when any of its neighbouring BSs is in RS mode. Therefore, maximum energy reduction is possible when only the centre BS is in *active* mode while no energy saving is feasible when all BSs are in *active* mode.

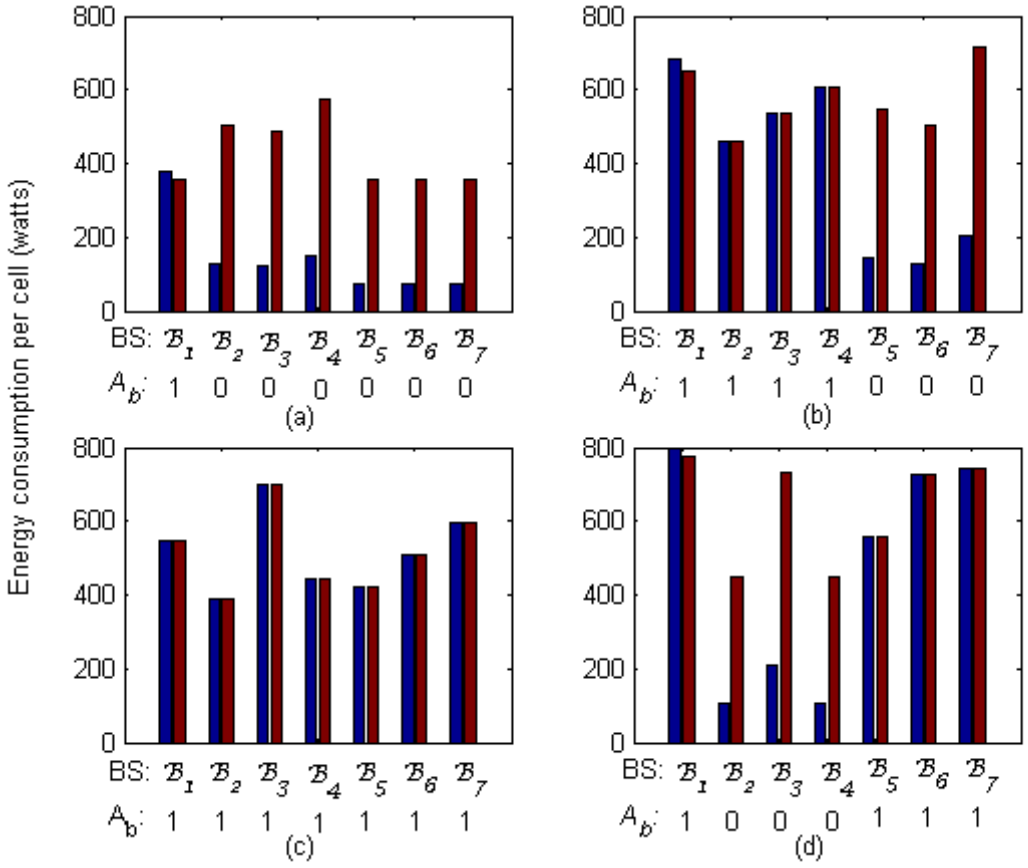

Figure 4-6: Energy consumption snapshots in each cell during four hours of a day (a) early morning (5:00 am); (b) morning (10:00 am); (c) afternoon (15:00 pm); and (d) night (20:00 pm). (blue bar – *BS-RS Switching* model, red bar – no switching).

To ascertain the energy saved in each cell by using the *BS-RS switching* paradigm compared with the traditional method, Figure 4-7 plots the corresponding average percentage of energy savings for both the DL (Figure 4-7(a)) and UL (Figure 4-7(b)) within a cluster of 7-cells. It can be observed that an overall energy saving of up to 30% (DL) has been achieved in different cells depending on the traffic load variations in those cells, whereas up to 38% average energy saving is achieved in the UL, which greatly increases the MS battery life. In the UL analysis, only the MS transmit power is considered and the transmit power was adjusted based on the FCPC scheme in (4.2) with P_0 =-91dBm, -102dBm and -103dBm for direct, access and relay links, respectively (Bulakci et al., 2013). Although additional energy will be consumed by the *x-RS* in the *BS-RS switching* model, this is compensated for by maintaining the same propagation distance between the serving BS and off-cell MS via the *x-RS*. This is because relay-assisted communication requires lower transmit power for a given data rate requirement. In contrast, the propagation PL for the *BS sleeping* approach are higher because of the longer propagation distances between the serving BS and off-cell MS, so the transmit powers are greater. Note, there is no energy saving feasible for the centre BS ($\mathcal{B}_1$) because it is always *active*.

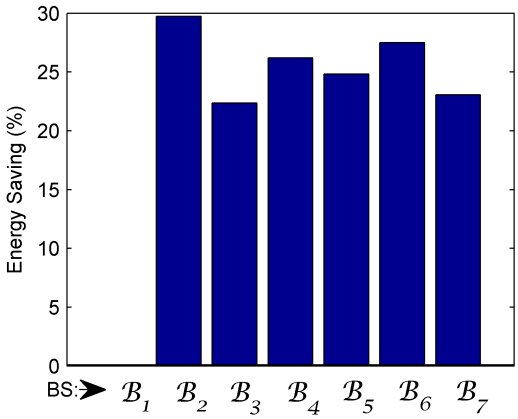

(a) The DL energy savings (when both the fixed and dynamic power consumptions are considered).

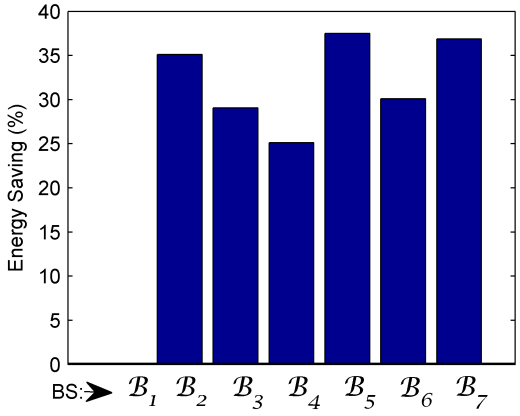

(b) The UL energy savings (only the transmit power of MS is considered).

Figure 4-7: Energy savings performance for the *BS-RS switching* model compared to the traditional method during a 24hr period.

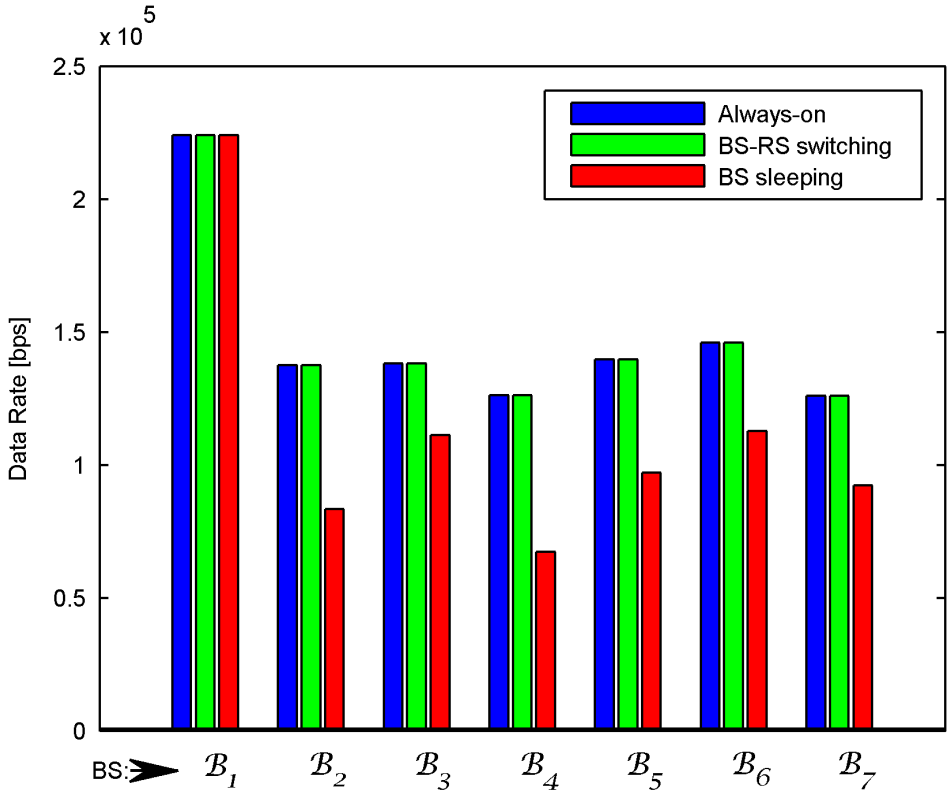

Figure 4-8: Average DL data rate for the *BS-RS Switching* model compared to the *BS sleeping* model over a 24hr period.

To ensure the minimum QoS provision is upheld, the average achievable DL data rate in each cell within the cluster was analysed across an entire day, with the corresponding results displayed in Figure 4-8. In this context, the maximum transmit power was considered, irrespective of the distance between BS and MS. Figure 4-8 reveals that the proposed *BS-RS switching* model improved the average data rate in each cell, with the exception of centre cell $\mathcal{B}_1$, which is kept *active*. The graph also confirms the data rates achieved by the new model are the same as those when all BSs are *active*, so there is no QoS compromise in securing significantly lower energy consumption. On the other hand, the *BS sleeping* strategy must compromise the QoS to achieve significant energy savings due the higher transmit power dissipations.

As discussed in *Section 3.6.7*, signal outage is one of the key performance evaluation parameters, which reflects the lack of signal strength at the receiver. To evaluate the corresponding signal outage performance in the UL, the CDF of the respective received

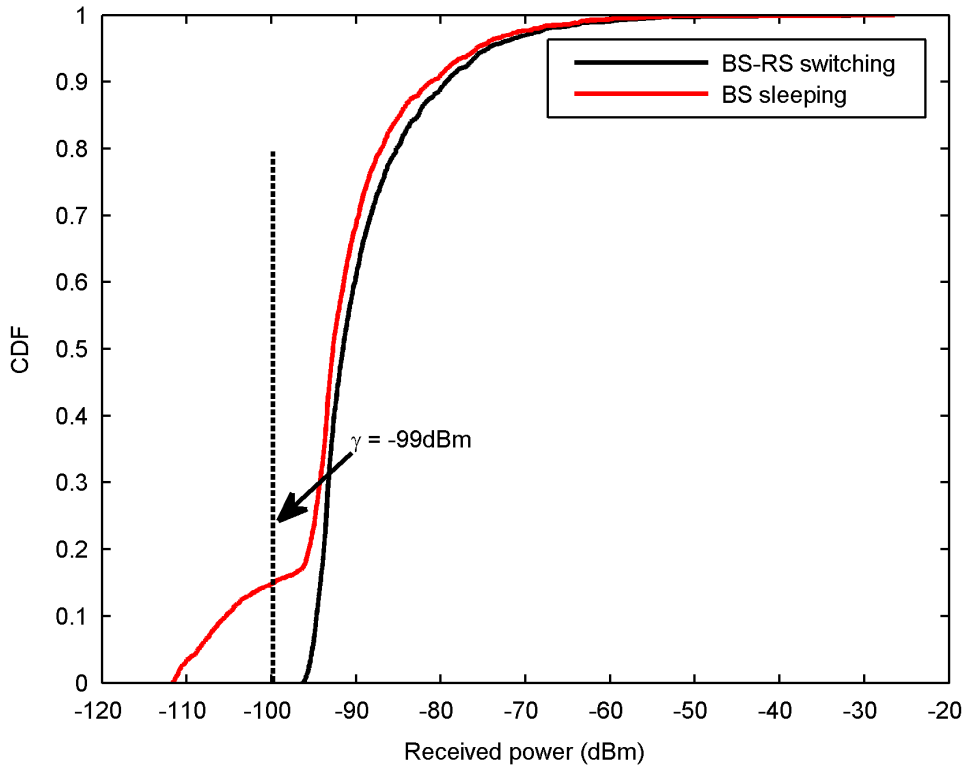

Figure 4-9: Comparative CDF of the received power for a maximum MS transmit power of 21dBm.

signal strengths are plotted in Figure 4-9, where the signal outage probability threshold is defined in accordance with the LTE specification (3GPP, 2011b). As the maximum MS transmit power is usually required in worst-case scenarios, the transmit power of each MS was set to $P_{tx,\max}^{MS}$ when calculating the signal outage. The corresponding results confirm that for the proposed *BS-RS switching* model, no users will be in the outage region compared to ≈15% when the *BS sleeping* strategy is applied.

In addition to absolute energy consumption, the EE is analysed for increasing cell loads as shown in Figure 4-10, where the EE is defined in (4.7) as the capacity per unit energy (bits/Joule) as described. It can be observed that the *BS-RS switching* model always affords a more efficient operation at any requested cell load. The EE improvement is due to the shorter propagation distance between the serving BS and off-cell MS via the *x-RS* which keeps a similar data rate for off-cell users as shown in Figure 4-8. As the cell load increases, the EE also increases because of the higher throughput for a given transmission

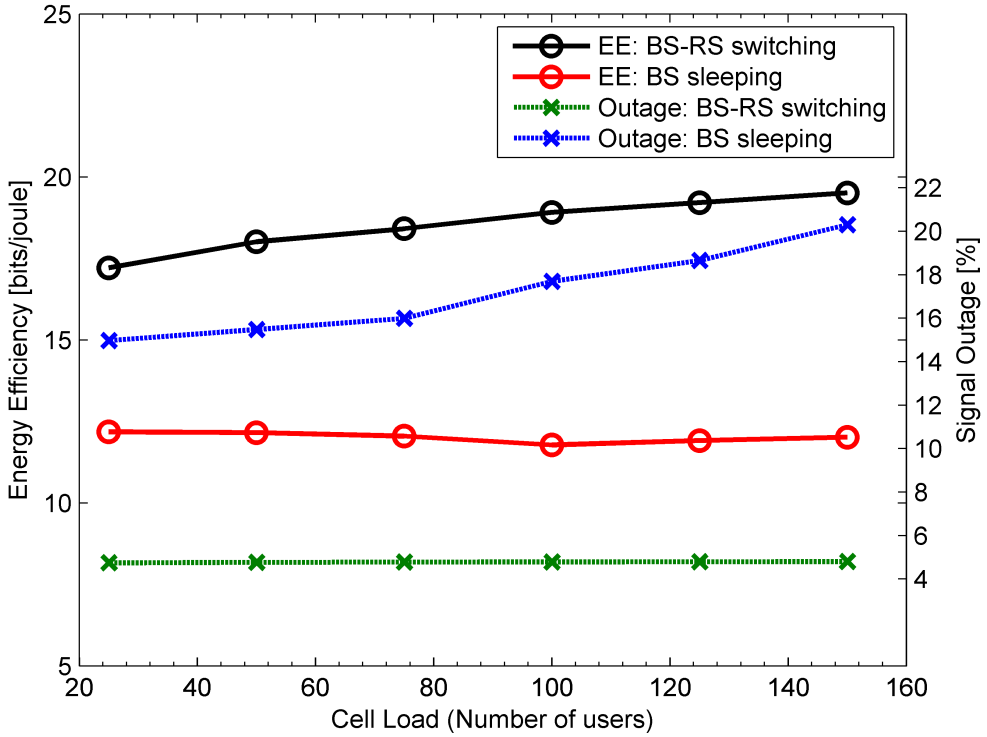

Figure 4-10: Energy efficiency/Signal outage vs. cell load.

power. This contrasts with the *BS sleeping* strategy, which has a slightly lower EE due to the increased transmission power for off-cell MS, offsetting any savings made by putting certain BSs to *sleep*. In addition, putting certain BSs in *sleep* mode means compromising the off-cell MS data rate as can be seen in Figure 4-8, which is also a factor in decreasing the EE as the cell load increases. This is the reason for the corresponding superior DL signal outage performance of the *BS-RS switching* model for all cell loads. However, users experience a higher signal outage with the *BS sleeping* for all cell loads compared with the *BS-RS switching* and it is even higher for high cell loads. This vindicates the rationale of adopting the *BS-RS switching* paradigm to achieve noteworthy improvements in the EE while concomitantly maintaining the QoS provision.

As has been seen in previous results, both the *BS-RS switching* and *BS sleeping* models are able to significantly improve the EE for a fixed threshold of $\rho_{th} = 0.5$. Both will now be analysed for a larger network scenario (7x7 hexagonal cells) for different switching threshold (ρ_{th}) as depicted in Figure 4-11. A lower value of ρ_{th} implies certain BSs are

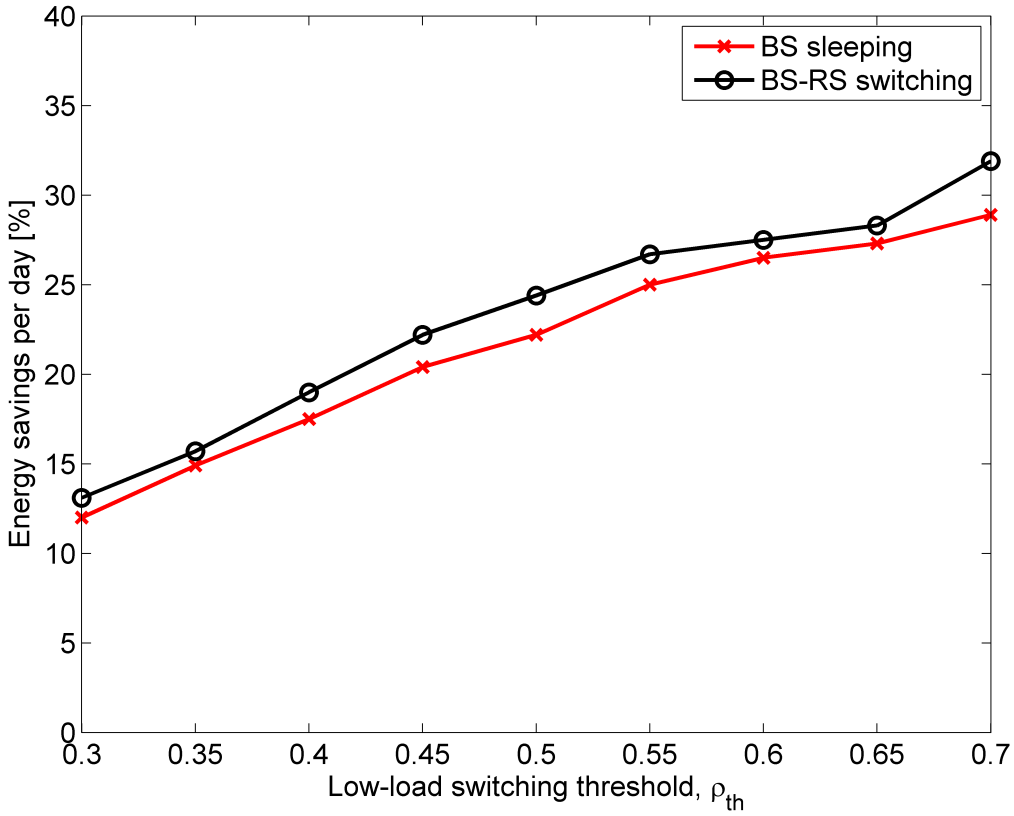

Figure 4-11: Daily network energy savings with both the *BS sleeping* and *BS-RS switching* models under homogeneous traffic among cells within a 7x7 hexagonal cell layout.

switched to dormant only for a small portion of time within a day, but each *active* BS can accept a higher amount of traffic from other BSs. Switching certain BSs to dormant for a short time implies lower energy savings. However, for higher ρ_{th} values, which let more BS switch to dormant mode for longer periods, a significant amount of network energy can be saved. For example, by setting ρ_{th} from 0.3 to 0.7, more than a doubling of energy saving is possible in both models, though the *BS-RS switching* model will always provide a higher energy saving percentage at a defined ρ_{th}.

Since every BSs can accept the same amount of traffic from off-cell BS, because homogeneous traffic loads are considered in all cells, the amount of network energy saved can vary if there is asymmetric traffic between cells. For example, if the homogeneous traffic profile of the 7 cells is [0.55, 0.65, 0.55, 0.70, 0.55, 0.75, 0.55], the BS switching strategy described in *Section 4.3* with ρ_{th} = 0.5 does not allow any BS to switch to dormant mode since none satisfy the switching condition (4.11). If however, ρ_{th} is set

marginally higher, say for example 0.56, then a number of BSs would be able to switch to dormant mode. As a result, the cellular network still has an over provision of capacity, as some BSs are still underutilized in such scenarios, even when the traditional fixed threshold based switching strategy is employed. It is therefore important to seek to develop a *BS switching* strategy that can both track and respond to network traffic demand with the aim of keeping the service provision to a minimum number of *active* BSs.

4.5 Summary

In this chapter, a new *BS switching* model together with its power model has been proposed as an alternative to the *BS sleeping* strategy to improve the network EE. The EE problem has been formally established for the proposed model and solved by an exhaustive search at high computational cost. As the EE depends on the number of *active* BSs at any instant of time, the BS switching conditions based on a fixed threshold have been defined. The new *BS-RS switching* model provides a solution to the shortcomings of the *BS sleeping* model, such as coverage holes and QoS degradation by using additional RS collocated with each BS. It has been found that energy consumption can be reduced by up to 30% compared to the traditional "*always-on*" mode of operation, especially at low-traffic loads. The rationale for the *BS-RS Switching* model is to guarantee undisrupted communications between the MS and BS and thereby ensure the similar QoS level. Using a fixed switching threshold for making decisions has one limitation, namely that certain BSs are not able to switch their modes even when there are opportunities to save more energy in scenarios where cells have different or asymmetric traffic loads. Fixed threshold based switching also restricts the mode holding time, which can be extended if the threshold was to be made more flexible, which will be the focus in the next chapter.

Chapter 5

Adaptive Base Station Switching – A Relay-Deployed Network Scenario

5.1 Introduction

This chapter proposes an adaptive threshold based BS switching algorithm for enhancing the energy saving in a relay-deployed cellular network and investigates both the *BS-RS switching* and *BS sleeping* models under this algorithm. In existing *BS sleeping solutions* (Niu et al., 2010; Oh & Krishnamachari, 2010; Oh et al., 2013) and even our proposed *BS-RS switching* solution (Alam et al., 2012) discussed in *Chapter 4*, the BS switching decisions are taken based on a fixed traffic threshold. This is not necessarily optimal in terms of exploiting the available resources (PRB) of neighbouring BSs. Motivated by the high traffic fluctuations over space and time, *i.e.*, the asymmetric nature of cellular traffic, a new *BS switching* algorithm based upon different traffic thresholds at each decision instant is proposed. In addition, shared relays (Panah et al., 2011; Kim et al., 2010) are deployed to both enhance the cell-edge users' throughput and support coverage extension during any BS switched to dormant mode as described in Section 2.7.5. The shared-RS has multiple antennas with each being associated with a BS.

5.2 Motivations and Related Works

As discussed in *Section 2.6*, current cellular networks are over provisioned due to their design criterion to satisfy services and quality requirements based on peak-traffic conditions. However, traffic conditions in a cellular network vary significantly both in temporal and spatial domains (Oh et al., 2011; Peng et al., 2011). As a result, the traffic fluctuations provide a significant margin to conserve the overall network energy by switching the underutilized BSs to dormant mode (Blume et al., 2010). However, the efforts toward energy awareness often come at the price of worsening the QoS as was seen in *Section 4.4.2* (see Figure 4-3, 4-4, and 4-8), with effects such as high blocking

probability, coverage holes, and off-cell user data rate degradation. The QoS issues have been dealt by proposing a new *BS-RS switching* model in *Chapter 4*. In both the *BS-RS switching* and *BS sleeping* models, the switching decisions are usually taken based on a fixed switching threshold (Oh & Krishnamachari, 2010; Niu et al., 2010; Oh et al., 2013; Zhou et al., 2009; Hossain et al., 2013a), no matter whether there are any possibilities of reducing further energy consumption. Since the traffic demand in a cellular network varies significantly from cell to cell (even in neighbouring cells), the fixed threshold based switching algorithm may still provide overprovision at certain times of a day. For example, for a given traffic demand, the fixed threshold based *BS switching* strategy employed in the area may only allow, say, one BS in five to switch to dormant mode, though this amount of traffic can be serviced by a single BS. As a result, the cellular network is still overprovisioned and some BSs are still underutilized during those scenarios even when the traditional fixed threshold based switching strategy is employed. It is therefore important to have a *BS switching* strategy that can track the network traffic demand and can keep the service provision to a minimum number of *active* BSs.

As already mentioned in section 2.7.5, relay technology can be used for network coverage extension and capacity enhancement due to its simplicity, flexibility, ease of deployment, and cost effectiveness. The relaying technology is not only able to provide extended coverage and improved cell-edge data rate, but is also able to reduce the overall network energy consumption (Pabst et al., 2004). By appropriately deploying RSs in the network, to reduce the propagation distances between BSs and MSs, the transmission power can be saved because of the smaller distances involved between transmitter and receiver and, thus, the reduction of propagation PL. Moreover, the "shared relay concept" where multiple BSs share the same RS, attributes the interference cancellation, if DF strategy is employed, with the minimal infrastructure requirements (Panah et al., 2011; Kim et al., 2010).

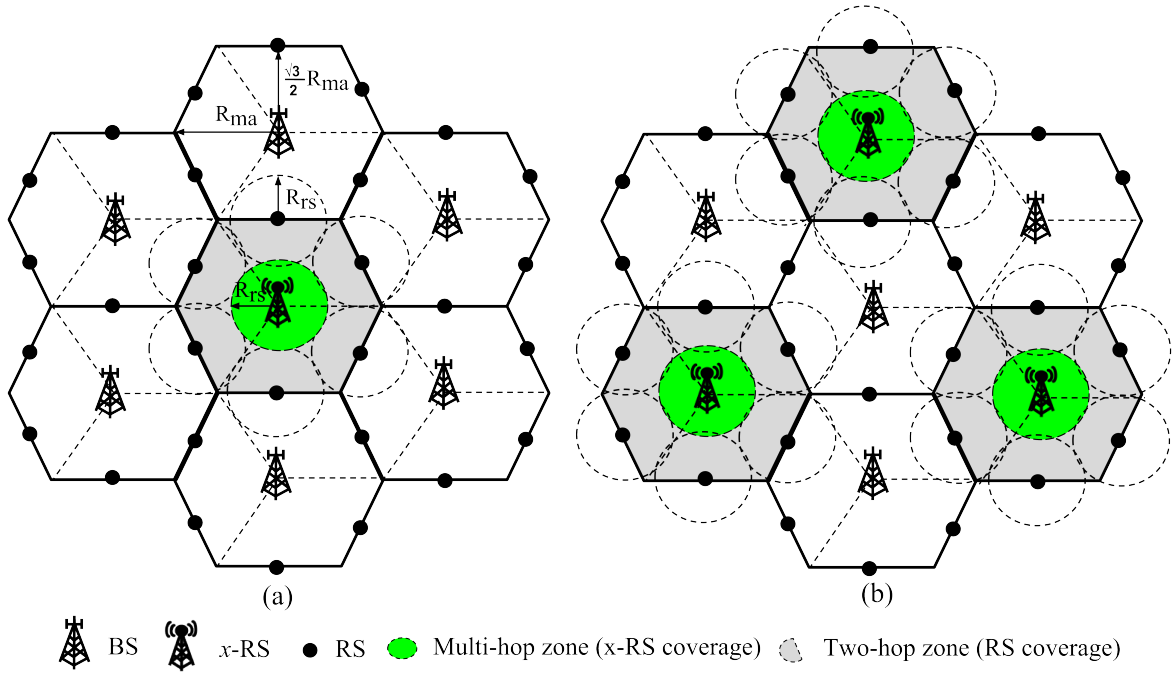

Figure 5-1: An example of proposed network model. (a) The centre BS is switched to relay (*x-RS*) mode; and (b) three BSs are switched to *x-RS* mode; where the *x-RS* serves users in the green area and shared RSs deployed at the edge of the cell serve users in the gray zone in the off-cells.

5.3 System Model and Problem Formulation

This section presents the proposed network model, relay selection and transmission strategies, and the problem formulation for energy conservation. In addition, the power model for the relay-assisted cellular network is also introduced.

5.3.1 Network Topology

A relay-assisted multi-hop network model is considered comprising multiple clusters of seven-cell configuration with every macro cell of radius R_{ma} as illustrated in Figure 5-1 (only one cluster is shown here). Let C be the set of clusters within the network. The BSs are located at the centre of a cell and each BS consists of three directional antennas, each serving a different sector of the cell, so each BS is able to provide a coverage area of $3\sqrt{3}R_{ma}^2/2$. The six shared RS are also deployed at the edge of each cell at a distance $\sqrt{3}R_{ma}/2$ from the centre of each cell with two RSs per sector in order to improve cell-edge throughput and to extend cell coverage. Two BSs that have a common cell edge in a

regular hexagonal cell grid share a single RS. It is assumed that there are N_{BS} BSs and each BS is denoted by $\mathcal{B}_b$ for all b = 1, …, N_{BS}. There is also a RS (*x-RS*) deployed and collocated with each BS, as described in *Section 4.2.1*, so the total number of collocated *x-RS* will be $N_{xRS} = N_{BS}$, and there are N_{RS} deployed RSs in the network. Each RS can provide a service coverage area of πR_{rs}^2, as shown in Figure 5-1. In this scenario, each BS is able to switch from *active* to *x-RS* mode during low traffic period as described in the previous chapter and the design model is called the *BS-RS switching* model. Therefore, the off-cell service coverage can be maintained by using the deployed RS and the *x-RS* if the coverage radius of each RS is assumed to be $R_{rs} = 0.5R_{ma}$.

Each deployed (shared) RS equipped with two antennas is able to connect with two neighbouring BSs one for each (Song et al., 2008; Peters et al., 2009). It is assumed that the deployed RSs can operate in either *in-band* or *out-band* as described in *Section 2.7.5* depending upon the operating modes of its associated BSs and MSs' locations within its coverage. When both the associated BSs for a RS are in *active* mode, the RS operates *in-band*. On the other hand, it operates in *out-band* to provide service coverage to off-cell MS, if either BS is in dormant mode while it associates with the other BSs. The relay link for *x-RS* is assumed to be connected by a dedicated backhaul connection, e.g., X2 or optical fibre connections. This assumption is reasonable as all BSs are interconnected by means of X2 connection in LTE (3GPP, 2008) (see Figure 2-1(b)).

5.3.2 Relay Selection and Transmission Strategy

The RS assists in communications between BS and MS by forwarding its data to the destination by either AF or DF relay protocols. In this chapter, for the relay transmission, the DF relay protocol is used because of its performance advantages over AF, which were identified in Section 2.7.5 (Hasan & Bhargava, 2013). In a DF relay, communications between BS and MS via a RS occurs in two time-slots. In the first, the RS decodes its

received signal, whereas it re-encodes the decoded data and then transmits it to the destination in the second time-slot (Fallgren, 2012). It is assumed that all off-cell MS are served by neighbouring *active* BSs via either the deployed RS or *x-RS*, *i.e.,* there is no direct communication link between the BS and off-cell MS. If it is assumed that each cell has N_{MS} users (MS) and N_{BS}^{off} BSs are switched to dormant mode at a specific time, then $N_{BS}^{on} = \left(N_{BS} - N_{BS}^{off}\right)$ *active* BSs need to jointly serve all $(N_{BS} \cdot N_{MS})$ MS within the network. The transmission between the *active* BS and MS within a cluster is done either directly (BS-MS) or via RS with DF relaying.

If direct transmission is adopted, the attainable user throughput between $\mathcal{B}_b$ and MS *m* can be measured by (3.3). When $\mathcal{B}_b$ serves a MS *m* via a RS *k* associated to it with DF relaying, the data rate of MS *m* can be given by (3.4). However, in order to maintain a given minimum data rate $r_{\min}$ for all MS, each BS must guarantee the constraint $r_m \geq r_{\min}$ to all MS. To develop the RS selection criteria, let us consider that all MS will be guaranteed $r_{\min}$. Therefore, the required BS transmission power for MS *m* is then, for a direct transmission case (Zhou et al., 2011):

$$p_m^{(b)} = \frac{\left(2^{r_{\min}/W} - 1\right) \cdot d_{bm}^{\alpha}}{\eta_0 \cdot 10^{\xi_m/10}} \tag{5.1}$$

In the case of relay-assisted communications, the transmit powers required for the associated BS and the RS *k* are (Zhou et al., 2011):

$$p_m^{(b)} = \frac{\left(2^{2r_{\min}/W} - 1\right) \cdot d_{bk}^{\alpha}}{\eta_1 \cdot 10^{\xi_k/10}} \tag{5.2}$$

and

$$p_m^{(k)} = \frac{\left(2^{2r_{\min}/W} - 1\right) \cdot d_{km}^{\alpha}}{\eta_2 \cdot 10^{\xi_m/10}} \tag{5.3}$$

The criterion for selecting RS or direct transmission is to minimize the transmission power. So, the MS *m* will be associated with the one that consumes the minimum transmit power, *i.e.*, $\mathcal{B}_{b*}(m) = \arg\min\left\{p_m^{(b)}, \left\{p_m^{(bk)} + p_m^{(km)}\right\}_{k=1}^{N_{RS}}\right\}$. Furthermore, the selection criteria for an off-cell MS to choose whether a deployed RS or *x-RS* depends on the location of the MS, *i.e.*, an off-cell MS chooses a RS based upon a distance dependent PL.

5.3.3 Power Consumption Model and Problem Formulation

By recalling (4.1), the power consumption model for the relay-assisted cellular network at time *t* with having N_{BS} BSs and N_{RS} RS can be expressed as (Lee et al., 2011; Alam et al., 2012):

$$P_T(t) = \sum_{b=1}^{N_{BS}}\left[A_b(t).\left(a_{BS}\cdot P_{tx,b}^{BS} + P_f^{BS}\right) + \left(1 - A_b(t)\right)\cdot\left(a_{RS}\cdot P_{tx,b}^{RS} + P_f^{RS}\right)\right] + \sum_{k=1}^{N_{RS}}\left(a_{RS}\cdot P_{tx,k}^{RS} + P_f^{RS}\right) \quad (5.4)$$

The first summation of (5.4) includes the power consumption of both BS and *x-RS* incorporating with the MAF A_b for each BS as in (4.1), whereas the deployed RS power consumption is included in the second summation term. (5.4) shows that the RS consumes a portion of the total power, so in order to measure the amount of energy consumed by the RS, it is important to establish a relationship with the BS power consumption. As a result, the power model parameters for RS, that is, a_{RS} and P_f^{RS} are replaced by $g.a_{BS}$ and $g.P_f^{BS}$, respectively, to calculate the influence of the RS power consumption in the proposed model relative to the BS energy cost. The factor *g* is the ratio of RS to BS power consumption so reflecting the actual cost of using the RS (Lee et al., 2011; Alam et al., 2012). Thus:

$$\begin{aligned} P_T(t) = \sum_{b=1}^{N_{BS}}\Big[a_{BS}\left\{A_b(t).P_{tx,b}^{BS} + g\left(1 - A_b(t)\right)P_{tx,b}^{RS}\right\} + \left\{A_b(t) + g\left(1 - A_b(t)\right)\right\}P_f^{BS}\Big] \\ + gN_{RS}\left(a_{BS}P_{tx,k}^{RS} + P_f^{BS}\right) \end{aligned} \quad (5.5)$$

Since the *x-RS* will only be *active* when the corresponding BS is in dormant mode, the power consumption of those *x-RS* varies depending on the number of BSs being dormant. It is also seen in *Section 4.4.2* that the additional energy cost incurred by the *x-RS* can be compensated by decreasing overall transmit power for off-cell MS by reducing their propagation distances between the associated neighbouring *active* BS and off-cell MS.

Let $\mathcal{M}_b$ denote the set of MS within $\mathcal{B}_b$, so $N_{MS} = |\mathcal{M}_b|$. From (5.4), the energy savings problem of the *BS switching* model that minimizes the network energy consumption with minimum data rate and transmit power constraints, can be formulated as:

$$\min_{A_b(t)} \; P_T(t) \tag{5.6}$$

$$s.t. \quad r_m \geq r_{\min}, \qquad \forall m \in \mathcal{M}_b$$

$$\sum_{m=1}^{|\mathcal{M}_b|} p_m^{(b)} = P_{tx,b}^{BS} \leq P_{tx,\max}^{BS} \quad , \quad \forall \mathcal{B}_b \in \mathcal{B}$$

$$\sum_{m=1}^{|\mathcal{M}_b|} p_m^{(k)} = P_{tx,k}^{RS} \leq P_{tx,\max}^{RS} \quad , \quad \forall k = 1, \cdots, N_{RS}$$

$$\text{and} \quad A_b(x) \in \{0,1\}, \forall x \in \{t, t+1\}$$

(5.6) is a mixed-integer linear programming problem, which is generally NP-hard (that is, non-deterministic polynomial-time hard). The optimal solution to (5.6) can be obtained by an exhaustive search, though this is computationally intensive. In this design, the *BS switching* decision is made at fixed time intervals of period T_0 based on the traffic variations between consecutive periods. Once the *BS switching* decision has been made using the new algorithm, (5.6) becomes a linear programming problem, whose optimal result can be obtained in linear calculation time. The following section proposes a centralized adaptive threshold based *BS switching* algorithm under varied traffic loads with lower complexity and provides the MAF $A_b(t), \forall b$ at each decision time *t*.

5.4 Adaptive Threshold based Base Station Switching

Existing *BS switching* techniques (Oh et al., 2013; Marsan et al., 2009; Alam et al., 2012) often use a fixed traffic threshold based approach for making switching decisions of a BS at any time instant *t*. This fixed threshold based *BS switching* strategy was mathematically developed in *Section 4.3*, more specifically, in (4.11) and (4.12). However, this may not necessarily be optimal in terms of exploiting the available resources (PRB) of neighbouring BSs due to the inherent asymmetric traffic profiles amongst cells. In other words, there are significant traffic variations among cells (referring to *Section 2.6*) creating opportunity gaps at certain time instants. For example, the fixed switching threshold based strategy to switch a BS to dormant mode cannot change ρ_{th} to a higher value even if neighbouring BSs will be able to handle more traffic. Intuitively, a higher switching threshold while maintaining the requisite QoS affords the possibility of a higher number of BSs staying in dormant mode for longer periods, thereby providing lower power operation and enhanced network energy savings (see Figure 4-11). As a result, it is necessary to embed an adaptive switching threshold, which will be determined prior to taking any switching decision in every time instant. This section will firstly present the basic idea behind a novel adaptive threshold based *BS switching* algorithm that dynamically finds the best switching threshold based on the instantaneous traffic profile of each BS within each cluster in a centralized manner. The algorithm is then formally presented with pseudo code and a flow chart.

5.4.1 Underlying Concept

Firstly, some notations are introduced to be used in the adaptive threshold based switching algorithm, which will dynamically change the switching threshold based on the instantaneous traffic loads. Let $\rho_b(t)$ be the traffic load profile of $\mathcal{B}_b$, $\forall b = 1, \cdots, N_{NB}$ and $\rho_{th}(t)$ be the switching threshold at time *t*. The BS must cooperate to share their current

traffic status in choosing $\rho_{th}(t)$. Interactions among BSs are primarily with the immediate neighbouring BSs and this is feasible given the current provision of X2 connections in LTE systems (see Figure 2-1(b)). The choice of $\rho_{th}(t)$ is made based on each cluster $c \in \boldsymbol{C}$ to avoid a large number of interactions. The traffic load of $\mathcal{B}_b^{(c)}$ within $c \in \boldsymbol{C}$ is denoted by $\rho_b^{(c)}$ and the corresponding switching threshold for *c* is denoted by $\rho_{th}^{(c)}(t)$. Initially, the MAF $A_b(t)$ for each $\mathcal{B}_b^{(c)}$ is set to 1 meaning that all BSs are in *active* mode and $\rho_{th}^{(c)}(t)$ is set to a low value, say, ρ_{th}.

In order to manage all interactions among BSs, a *central controller* (CC) is considered that receives the traffic condition in each cell, which is periodically updated by all BSs. To avoid unnecessary hardware as the CC, one of the *active* BSs within each cluster operates as the CC. A BS $\mathcal{B}_b^{(c)}$ with the highest traffic at any time instant *t* can be chosen as the CC for a number of time instants. If $\mathcal{B}_b^{(c)}$ needs to switch to dormant mode at any time, another *active* BS with the highest traffic load becomes the controller within the cluster.

Depending on the traffic profiles in all cells, the CC will set a switching threshold $\rho_{th}^{(c)}(t)$ for each cluster and then BS with traffic load lower than $\rho_{th}^{(c)}(t)$ will be switched to dormant mode. When $\mathcal{B}_b^{(c)}$ is switched to dormant mode at time *t*, then $A_b(t) = 0$ and vice-versa. Once certain BSs are in dormant mode, it is necessary to ensure that the off-cell MS are required to handover to their neighbouring *active* BSs in order to maintain the minimum QoS. It is also assumed that each $\mathcal{B}_b^{(c)}$ can carry a maximum load of ρ_{max} at any instant. In the following section, the adaptive threshold based *BS switching* algorithm will be described.

5.4.2 Adaptive Threshold based Switching Algorithm

The pseudo code of the adaptive threshold based *BS switching* is detailed in Algorithm 5.1. Initially, the CC first collects traffic load information from all BSs within the cluster *c* and $\boldsymbol{\rho}^{(c)}$ denotes the set of traffic loads within *c*. A predefined threshold ρ_{th} is set as the current threshold $\rho_{th}^{(c)}(t)$ at time *t* (*Line 5*). The CC then selects $\mathcal{B}_{b^*}^{(c)}$ whether to switch to dormant mode or not according to (4.11) and (4.12) considering the same switching threshold as in previous time instant, *i.e.*, $\rho_{th}^{(c)}(t-1)$ (*Line 7*). If the conditions in (4.11) and (4.12) are satisfied, all MS $\boldsymbol{\mathcal{M}}_{b^*}^{(c)}$ in $\mathcal{B}_{b^*}^{(c)}$ are distributed among the *active* neighbouring BSs $\boldsymbol{\mathcal{N}}_{b^*}^{(c)}$ (*Line 9*). Otherwise, the CC will compute a new switching threshold $\rho_{th}^{(c)}(t)$ based on the instantaneous traffic load in each cell within *c* (*Lines 11-16*). To find the adaptive threshold $\rho_{th}^{(c)}(t)$, the CC then firstly calculates the idle traffic capacity within *c* such that the traffic load of any dormant BS, $\mathcal{B}_{b^*}^{(c)}$ can be handed over to other *active* BSs, as follows:

$$\rho_{idle} = \rho_{\max} - \rho_{b^*}^{(c)}(t), \ \forall b \in \left\{ \boldsymbol{\mathcal{B}}^{(c)} - \mathcal{B}_{b^*}^{(c)} \right\} \tag{5.7}$$

where $\boldsymbol{\mathcal{B}}^{(c)}$ is the set of BSs within *c*. The idle capacity ρ_{idle} within *c* means that the *active* BSs within the cluster can accept more traffic up to ρ_{idle} at time instant *t*. Based on ρ_{idle}, the CC will then take the MAF decision of $\mathcal{B}_{b^*}^{(c)}$. Once a switching decision is made, the mode holds for a certain period T_0. As many MS will arrive during T_0, the CC will reserve traffic handling capability by the *active* BSs before setting a new threshold $\rho_{th}^{(c)}(t)$. Therefore, a tolerance margin δ is introduced in order to reduce the impact of sudden traffic changes (*Line 12*). If $\rho_{b^*}^{(c)}(t)$ is less than or equal to $\left(\rho_{idle} - \delta\right)$, then $\mathcal{B}_{b^*}^{(c)}$ will distribute its full traffic $\boldsymbol{\mathcal{M}}_{b^*}^{(c)}$ to BSs in $\boldsymbol{\mathcal{N}}_{b^*}^{(c)}$ (*Line 13*), *i.e.*, the traffic load in $\mathcal{B}_{b^*}^{(c)}$ satisfies the conditions to switch to dormant mode. Therefore, the number of dormant mode BSs

also depends on the choice of δ. A lower value of δ provides a higher number of dormant mode BSs at any time instant and vice-versa, *i.e.*, at δ = 0, the maximum number of BSs will be in dormant mode. For each decision made, the CC acknowledges an update $\left(\rho_{b^*}^{(c)}(t), \rho_{th}^{(c)}(t), A_b\right)$ to other *active* BSs within *c* (*Line 22*). When the switching decisions are made for all BSs at time *t*, optimize power allocation based on $\left(\hat{\rho}_b^{(c)}(t), A_b\right), \forall b \in \boldsymbol{\mathcal{B}}^{(c)}$ by solving problem (5.6) and calculate $P_T^{(c)}(t)$ within *c* (*Line 24*), where $\hat{\rho}_b^{(c)}(t)$ is the new traffic after handover.

For convenience, the complete flow-chart of the algorithm is also presented in Figure 5-2. The flow diagram is the extended version of the fixed threshold based *BS switching* described in *Section 4.3*. For comparing both the fixed and adaptive threshold based approaches in Figure 5-2, it is interesting to find the similarity between the two. Overall, they both rely on the fixed threshold based strategy satisfying the switching conditions (4.11) and (4.12) in the left decision box. The only difference is the additional adaptive threshold adjustment blocks (shaded box with dotted connections), which opportunistically adjust the switching threshold $\rho_{th}^{(c)}(t)$. Thus, the new algorithm is able to exploit the traffic dynamics that allows more BSs in dormant mode to conserve more energy.

Algorithm 5.1: Centralized Adaptive BS Switching

1: **Inputs:** $\boldsymbol{\mathcal{C}}$, $\subset$, ρ_{th}, $\boldsymbol{\mathcal{B}}$, $\boldsymbol{\mathcal{M}}$. **Outputs:** A_b.

2: **Initialize:** $c \in \boldsymbol{\mathcal{C}}$, $\boldsymbol{\mathcal{B}}^{(c)} \in \boldsymbol{\mathcal{B}}$, $\boldsymbol{\mathcal{B}}_{ON}^{(c)} \in \boldsymbol{\mathcal{B}}^{(c)}$, $\boldsymbol{\rho}^{(c)} \in \boldsymbol{\rho}$, $\rho_b^{(c)} \in \boldsymbol{\rho}^{(c)}$ $\mathcal{M}_b^{(c)} \in \boldsymbol{\mathcal{M}}$.

3: **FOR** each cluster *c* **DO**

4: The CC collects load profile set $\boldsymbol{\rho}^{(c)}$, $\forall b \in \boldsymbol{\mathcal{B}}^{(c)}$.

5: Initially: $\rho_{th}^{(c)}(t) = \rho_{th}$

6: **FOR** each $\mathcal{B}_b^{(c)}$ within *c* **DO**

7: Select a BS with minimum traffic load within *c*: $\mathcal{B}_{b^*}^{(c)} = \arg \min_{\mathcal{B}_b^{(c)} \in \boldsymbol{\mathcal{B}}^{(c)}} \left(\rho_b^{(c)}\right)$.

8: **IF** (4.11) & (4.12) are satisfied for $\mathcal{B}_{b^*}^{(c)}$ with $\rho_{th}^{(c)}(t)$ as switching threshold

9: Distribute all $\boldsymbol{\mathcal{M}}_{b^*}^{(c)}$ among $\boldsymbol{\mathcal{N}}_{b^*}^{(c)}$

10: **ELSE** // Finding an adaptive threshold

11: Compute the idle capacity, ρ_{idle} by (5.7)

12: **IF** $\rho_{b^*}^{(c)}(t) \leq \left(\rho_{idle} - \delta\right)$ **THEN**

13: Distribute all $\mathcal{M}_{b^*}^{(c)}$ among $\mathcal{N}_{b^*}^{(c)}$

14: Set $\rho_{th}^{(c)}(t) = \rho_{b^*}^{(c)}(t)$

15: **ELSE**

16: Set $\rho_{th}^{(c)}(t) = \rho_{th}^{(c)}(t-1) - \delta$

17: **END IF**

18: **END IF**

19: **IF** $\mathcal{M}_{b^*}^{(c)} = \phi$ **THEN**

20: $A_{b^*}(t) = 0;\ \rho_{b^*}^{(c)} = 0$

21: **END IF**

22: Update the status $\left(\rho_{b^*}^{(c)}(t), \rho_{th}^{(c)}(t), A_b\right)$ to the CC.

23: **END FOR**

24: Optimized power allocation based on $\left(\hat{\rho}_b^{(c)}(t), A_b\right),\ \forall b \in \mathcal{B}^{(c)}$ by solving problem (5.6) and calculate $P_T^{(c)}(t)$ within *c*.

25: **END FOR**

Since $A_b(t) \in \{0, 1\}$ is the operating mode or MAF of $\mathcal{B}_b^{(c)}$ at time *t*, the percentage of dormant mode BSs at time *t* can be given by:

$$P_{d,BS}(t) = \left[\frac{1}{|\mathcal{B}|}\sum_{b=1}^{|\mathcal{B}|}\{1 - A_b(t)\}\right] x\ 100\% \tag{5.8}$$

And the average percentage of dormant mode BSs over time D = 24hr with employing the proposed adaptive threshold based *BS switching* strategy can be given by:

$$P_d = \left[\frac{1}{D}\int_0^D P_{d,BS}(t)\,dt\right] x\ 100\% \tag{5.9}$$

In other words, these expressions also represent the probabilities of a BS to switch into dormant mode.

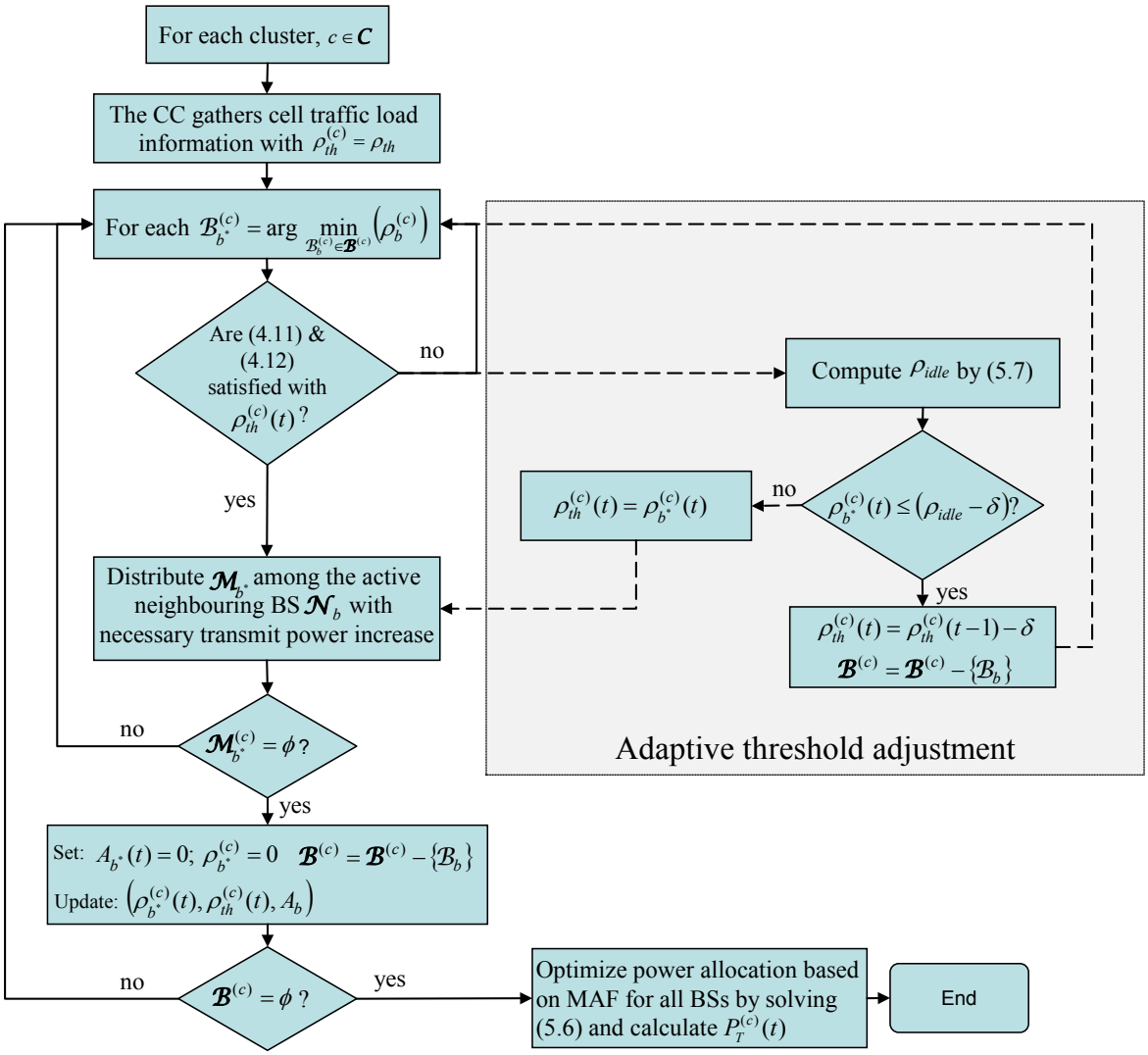

Figure 5-2: Flow diagram of the adaptive threshold based *BS switching* algorithm.

5.4.3 Distribution of Off-Cell Traffic

The switching decision is crucial and it is important to take into account three issues: the QoS should not be degraded, the cell service coverage should be maintained and the network operations must be stable. The QoS can be maintained by appropriately handing over off-cell MS to neighbouring *active* BSs, though this sometimes requires the increase of transmission power. As stated earlier, off-cell traffic from a dormant $\mathcal{B}_b^{(c)}$ need to be distributed to the best combination of the *active* neighbour BSs $\boldsymbol{\mathcal{N}}_b^{*(c)}$ which can support their traffic as well as maintain QoS within a target limit. It is assumed that there must be at least one *active* neighbour BS of $\mathcal{B}_b^{(c)}$ to support any off-cell MS that allows $\mathcal{B}_b^{(c)}$ to

switch to dormant mode. For example, in Figure 5-1, each dormant mode BS has at least one *active* neighbour BS.

To evaluate $\mathcal{N}_b^{*(c)}$, $\mathcal{B}_b^{(c)}$ first gathers the data of the idle traffic capacity by means of the number of available PRB in each of candidate neighbour BS set, $\mathcal{N}_b^{(c)}$. Based on the PRB allocation policy, the candidate neighbour BSs are required to support the MS of $\mathcal{B}_b^{(c)}$ and their own MS, which is needed to be calculated using BS cooperation. Similarly, the required addition transmit power for supporting the MS of $\mathcal{B}_b^{(c)}$ is also calculated from the available MS location data by feeding back from them to the serving BSs. Then, the candidate neighbour BSs with minimum additional transmit power are the probable best combination $\mathcal{N}_b^{*(c)}$. However, MS that are not supported by any $\mathcal{N}_b^{(c)}$ due to limited PRB and transmit power constraint will be blocked.

In the switching strategy, BSs with low traffic loads are more likely be in the dormant mode. As much traffic load as possible will be handed over to an *active* neighbouring BS, which currently has a higher traffic load. This is because the BSs with high traffic load will less likely be in dormant mode within that decision period, so there will not be multiple handover for the same off-cell MS. On the other hand, a BS with low traffic load may receive little or no handed over traffic, as it is likely one of the BSs has been switched to dormant mode next.

5.5 Numerical Results

5.5.1 Simulation Settings

In this section, the performance of the adaptive threshold based *BS switching* algorithm is evaluated and compared with the traditional fixed threshold based BS switching. Firstly, the simulation is based on three-sectored cells with each cell having an ISD of $\sqrt{3}$x750 m and six RS are deployed at $\sqrt{3}$x750/2 from the centre of each cell with two RS in each

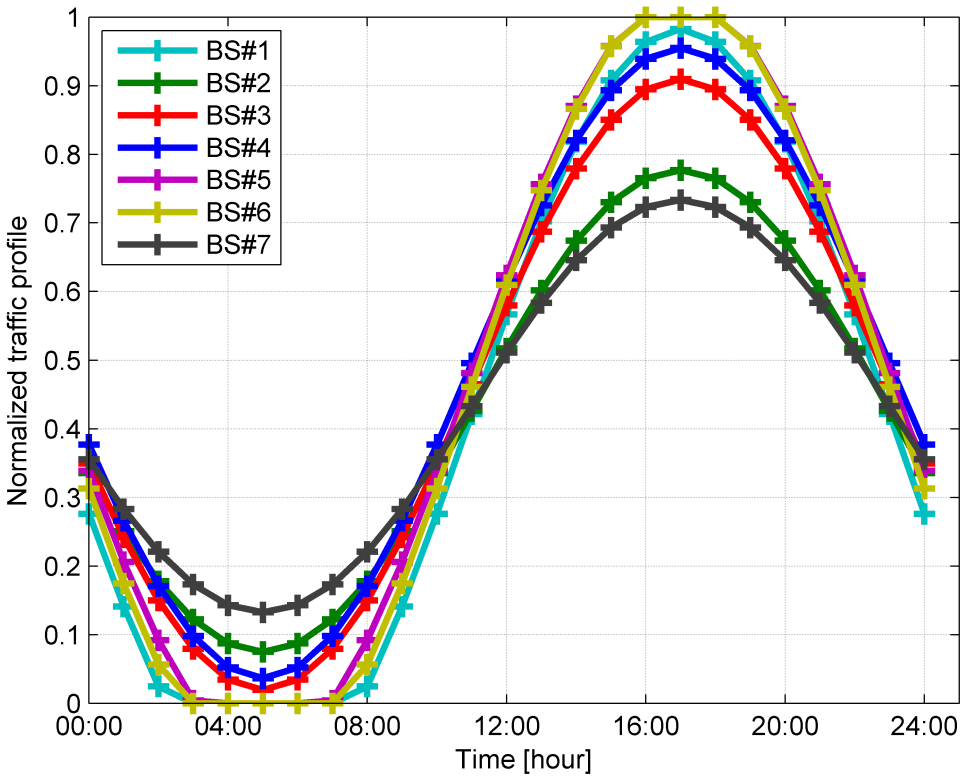

Figure 5-3: Asymmetric approximated traffic profiles of a cluster of seven cells.

sector as shown in Figure 5-1. Different approximated traffic profiles have been generated for different cells due to the asymmetric cellular traffic patterns in practice, according to (4.9) with different mean, $\overline{X}$ and variance, V. An illustration of the traffic profiles of a cluster (seven cells) is presented in Figure 5-3 whereas symmetric traffic profiles were considered in *Chapter 4*. Channel bandwidth = 5 MHz (*i.e.*, 25 PRB) per sector, RS transmit power = 37 dBm, and $|\mathcal{C}|$ = 3 are assumed while the power model 1 in Table 2.1 is used and the rest of the simulation settings are based on Table 3.1. To compare with the fixed threshold based BS switching, a threshold of 0.5 is assumed according to the chosen value in *Chapter 4*. In the following simulations, a 15min time resolution is considered, *i.e.*, T_0 = 15min, so the switching decision was taken once in every 15min and $A_b, \forall b$ was not changed within the period, T_0.

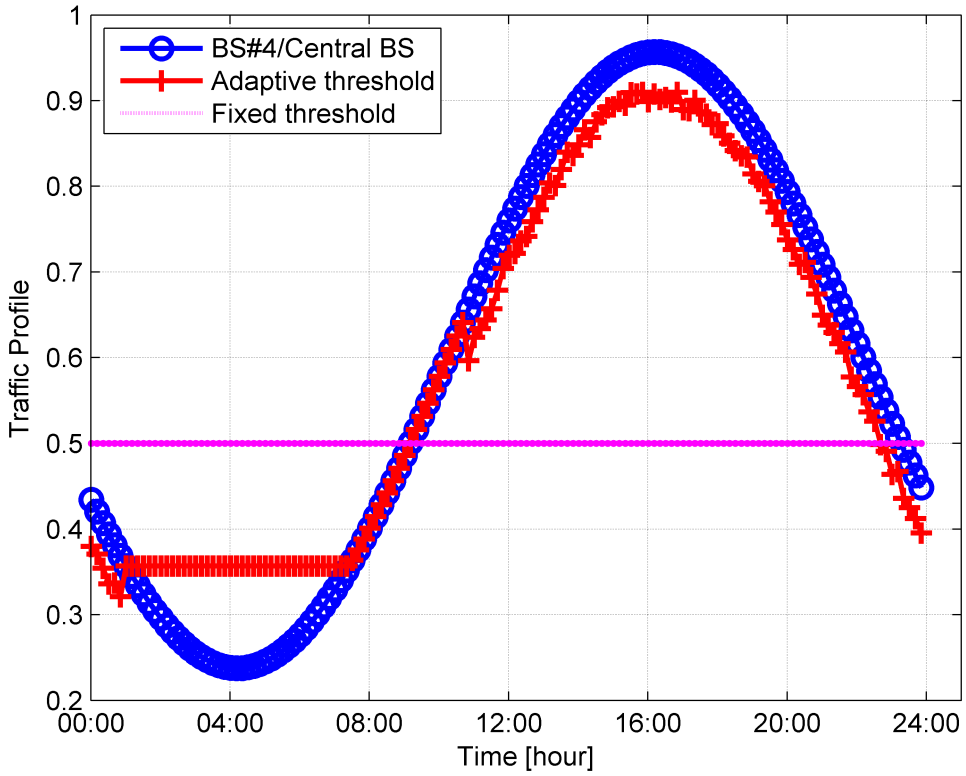

Figure 5-4: Illustrating the normalized traffic profile of a cell with fixed and adaptive switching threshold levels for $\delta = 0$.

5.5.2 Switching Threshold Adaptation

This subsection provides the threshold adaptation in each decision time *t*, as shown in Figure 5-4. The traffic profile of the central BS is shown as the reference with the fixed and adaptive threshold $\rho_{th}^{(c)}(t)$ levels. In the adaptive threshold algorithm, no switching is allowed in the first hour of the early morning even though the traffic load in the centre cell is low. This is because not enough resources or idle traffic capacity ρ_{idle} of neighbouring BSs to serve the traffic in the centre cell. In contrast, the *BS sleeping* allowed the BS to switch into *sleep* mode due to the switching conditions in (4.11) and (4.12) being upheld, which results in a higher number of MS being blocked. Interestingly, the results also show that the centre BS is allowed to switch to dormant mode even if its traffic profile is in a higher range, *e.g.*, $\rho_b^{(c)}(t) = 0.65$ at t = 10:30 am. The reason to allow the central BS to switch to dormant mode is that other *active* BSs within the cluster were happy to accept the

whole traffic currently serving by the central BS. In other words, since $\rho_{th}^{(c)}(t)$ is set to a new threshold value at each decision time (see the *adaptive threshold adjustment* block in Figure 5-2), the adaptive threshold $\rho_{th}^{(c)}(t)$ is able to track the traffic within a cell depending upon the available idle traffic capacity in other cells within the cluster. The CC within each cluster usually notifies the current $\rho_{th}^{(c)}(t)$ to other BSs.

Overall, this figure confirms that the adaptive threshold based algorithm provides a threshold level for BSs within each cluster, adapting to the instantaneous traffic profiles and following the traffic to obtain the maximum time a BS can be in dormant mode. On the other hand, the fixed threshold based algorithm will not allow the BS to switch to dormant mode if the traffic in the central BS is higher than the predefined fixed threshold ρ_{th}, *i.e.*, only if it satisfies the switching conditions in (4.11) and (4.12).

5.5.3 Percentage of Dormant Mode Base Stations

As discussed in *Section 5.4.2*, the impact of the tolerance margin δ in the adaptive threshold based *BS switching* algorithm plays a vital role in decreasing the number of *active* BSs, which in turn reduces the overall energy consumption. Figure 5-5 shows the percentage of dormant mode BSs P_d over a whole day in (5.9) for different values of δ. For δ = 0, the highest percentage of BSs is in dormant mode, *i.e.*, 45% and 59% of BSs for *BS sleeping* and *BS-RS switching* models, respectively. In this case, the proposed algorithm ignores any sudden changes in traffic loads within time period T_0. However, in real cellular traffic, there are sudden changes of incoming traffic loads varying cell to cell. To project such incoming traffic, the value of δ is required to set to a value other than 0. Now, for a higher value of δ, a lower number of BSs have the probability that their instantaneous traffic loads can be handed over to other *active* BSs. This is because the higher value of δ makes the new adaptive threshold $\rho_{th}^{(c)}(t)$ into lower value just to leave

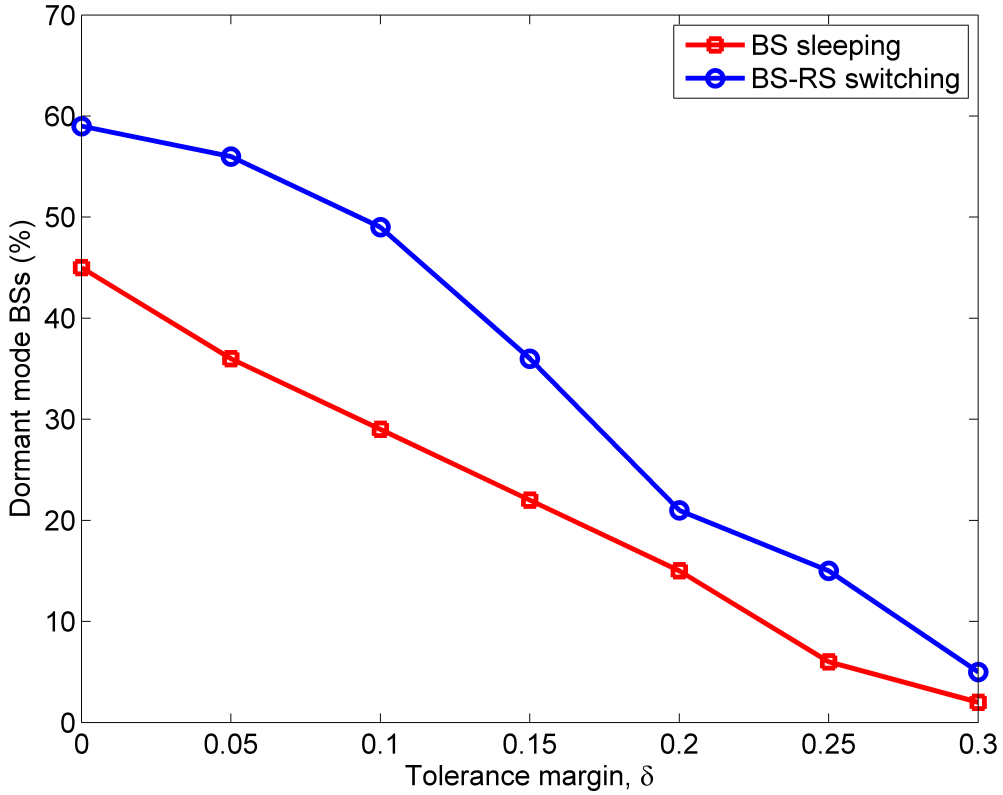

Figure 5-5: Percentage of dormant mode BSs over a whole day.

a gap between $\rho_{th}^{(c)}(t)$ and the actual idle traffic within the cluster. This means the algorithm works in a more conservative manner for higher δ. As a result, P_d decreases considerably with increasing δ. From the real cellular traffic analysis in *Section 2.6* and from the approximated traffic profile in Figure 5-3, the incoming traffic or the traffic variations within a cluster is not higher than 0.1 within the T_0 = 15min time resolution in most cases. Therefore, the rest of the analysis will be based on a tolerance margin value δ=0.1 unless otherwise specified. Moreover, for δ = 0.1, nearly 30% and 50% of BSs are in dormant mode with the *BS sleeping* and *BS-RS switching* models, respectively, which are respectable numbers from an energy conservation viewpoint. These results also suggest that the CC can set to the right δ depending on the traffic variations. For example, the CC can set δ=0.05 in rural areas, where the traffic variations is not significant whereas it may need to set δ=0.1 or higher in urban areas.

5.5.4 Energy Savings Performance

The total network power consumption corresponding to the new adaptive threshold based *BS switching* strategy for three different operation models is presented for a whole day period in Figure 5-6. In the traditional "*always-on*" mode, all BSs and RSs are *active* all the time irrespective of their traffic loads which consumes the most energy (100%). Since no *BS switching* is allowed in this mode of operation, the power consumption is independent of the threshold value. In contrast, both the *BS sleeping* and *BS-RS switching* models reduce energy consumption significantly compared to the "*always-on*" mode of operation. The proposed adaptive threshold based algorithm employed in both models reduces energy consumptions by more than 32% and 53%, respectively, compared to the fixed threshold based switching algorithm, which offers 20% and 39% savings, respectively. With both the fixed and adaptive threshold-based algorithms, the *BS-RS switching* model consistently outperformed the *BS sleeping* model. The results in Figure 5-6 are for a tolerance margin δ of 0.1. For convenience, more energy savings performance

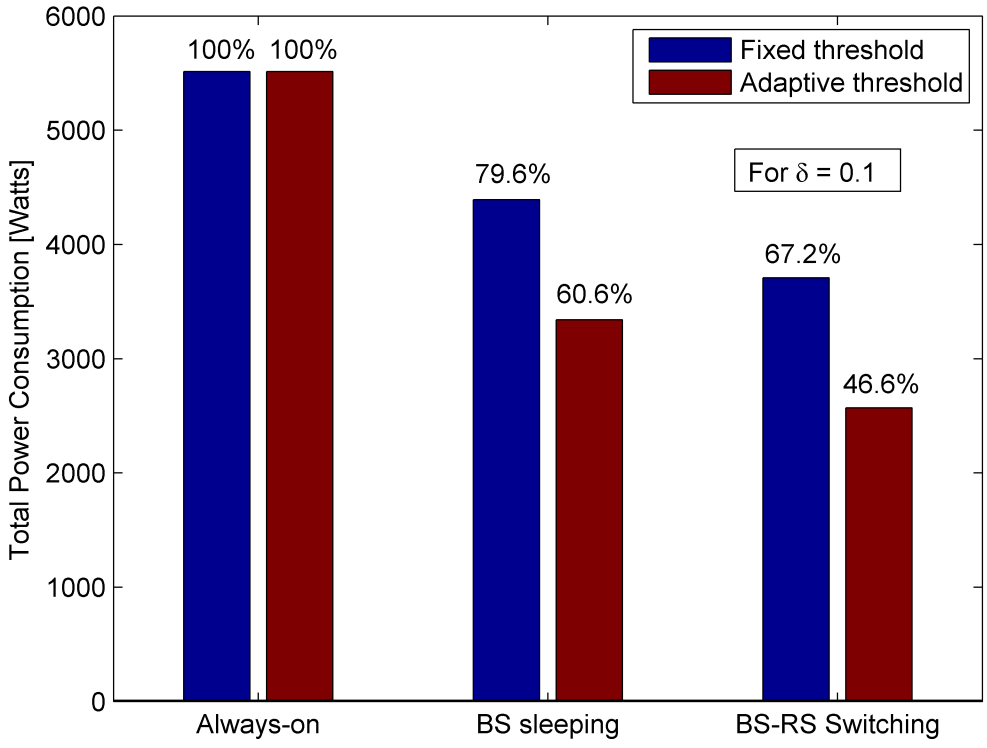

Figure 5-6: The percentage of energy consumption and savings in different BS operation modes for a whole day period with $\delta = 0.1$.

results are included in *Appendix B* for different δ values, where the adaptive threshold based algorithm for both *BS sleeping* and *BS-RS switching* models provided higher energy savings for δ=0 than that for δ=0.2.

5.5.5 The Impact of g

The percentage of energy savings with different strategies discussed above is also dependent on the amount of energy consumed by RS. The main reason for deploying RS is to improve the user throughput and extend coverage without additional transmit power of BSs, which is a significant amount of energy consumed by the *active* BSs as explained in Figure 4-5. The total energy consumed by the RS is assumed to be a fraction, g, of BS energy consumption, *i.e.*, the ratio of RS and BS energy consumption. To analyse the influence of RS energy consumption, the result relies on (5.5) and is shown in Figure 5-7. It can be seen that if RS consumes the amount of energy equivalent to g =0.07 (7%) of the BS energy, then the total energy consumption of the adaptive threshold based algorithm for both the *BS-RS switching* and *BS sleeping* models are almost the same as that of the traditional cellular networks ("*always-on*") without RS deployments. This means both models are taking the advantages of RS deployment in order to improve user throughput and coverage without spending extra energy if g=0.07. On the other hand, it is also possible to save energy by choosing $g < 0.07$.

Similarly, the fixed threshold based algorithm for both the *BS sleeping* and *BS-RS switching* models requires slightly lower g (5% and 6% of BS's energy, respectively) to achieve the same total energy as "*always-on*" operations without RS deployment. The lower RS energy requirement in the *BS sleeping* model is due to not using *x-RS*. However, the additional *x-RS* energy requirements in the *BS-RS switching* model can be compensated by reducing the transmission distance between the serving BS and off-cell MS as discussed in *Section 4.4*. In addition, the "*always-on*" mode of operation with RS deployments

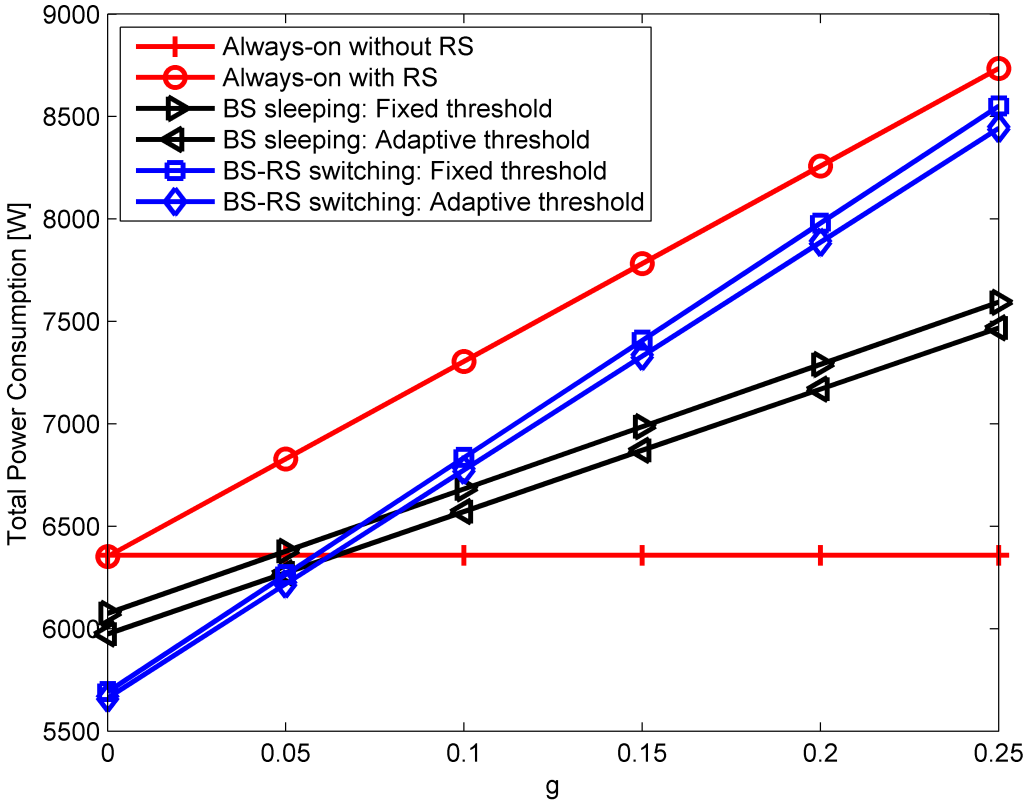

Figure 5-7: Total energy consumption with the variation of g (the ratio of RS and BS energy consumption) for a certain period in a day.

consumes the most energy as expected. As g increases, the total power consumption also increases. Therefore, the total power consumption has an impact of the RS power consumption, which is necessary to consider in designing RS for relay-assisted cellular networks. In this case, the RS power consumption should be less or equal to the mentioned percentages of BS's power consumption in order to have overall energy savings.

5.5.6 Off-Cell Users' Throughput

In *Section 4.4*, it has been seen that the off-cell MS experience a significant benefit (in terms of improving off-cell MS data rates) of switching a BS to *x-RS* (*BS-RS switching*) rather than entirely turning off a BS (*BS sleeping*) during low traffic periods. Similarly, the benefit of the new adaptive threshold based algorithm for both models is evidenced by the off-cell MS throughput curves displayed in Figure 5-8 with respect to different BS transmit powers. This clearly shows a significant improvement in off-cell user throughput with the adaptive threshold based algorithm in both models performing better than that with the

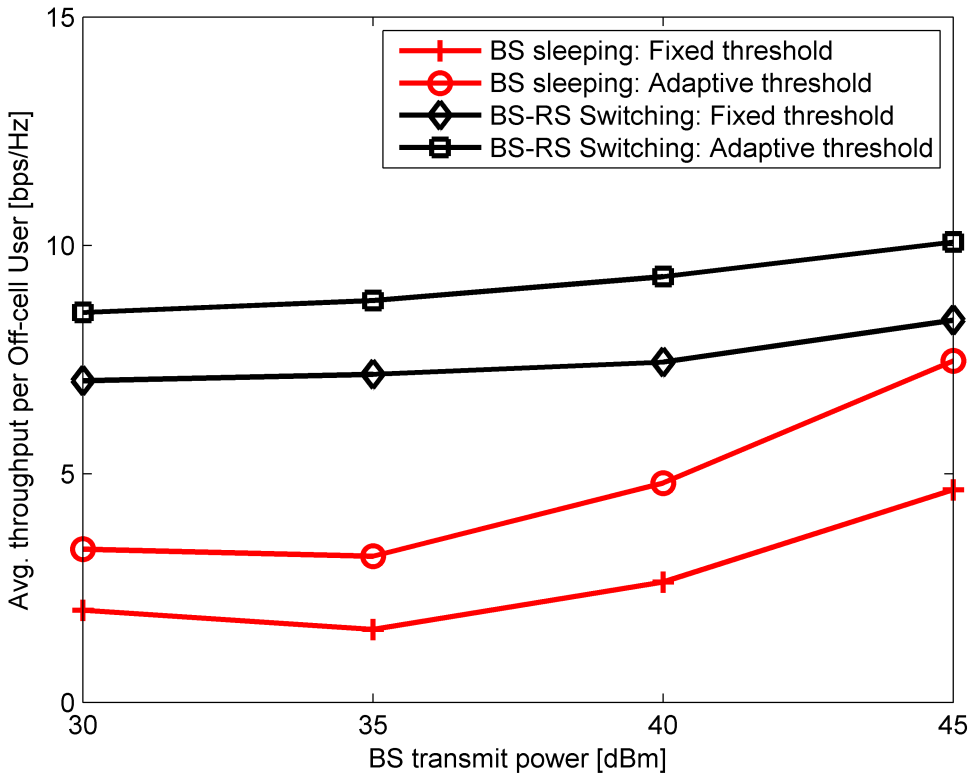

Figure 5-8: Average throughput of off-cell user during off-peak period for different BS transmission powers.

fixed threshold approach. For example, off-cell users experience an average throughput of up to 3.5bps/Hz and over 8bps/Hz in the *BS sleeping* and *BS-RS switching* models respectively, for a BS transmission power of 30dBm. This improvement is due to the service provided by *x-RS* to off-cell users located in the green zone (Figure 5-1), which are most likely either in a coverage hole or receive a degraded signal quality when a BS goes fully into *sleep* mode. Moreover, the improvements in the average off-cell users' throughput further increases with the BS transmit power up to 6bps/Hz and 10bps/Hz with the adaptive threshold based algorithm for both *BS sleeping* and *BS-RS switching* models, respectively. Overall, these results indicate that the adaptive threshold based *BS switching* algorithm consistently performs well in terms of maintaining a superior off-cell user experience in both models while it suits better for the *BS-RS switching* model.

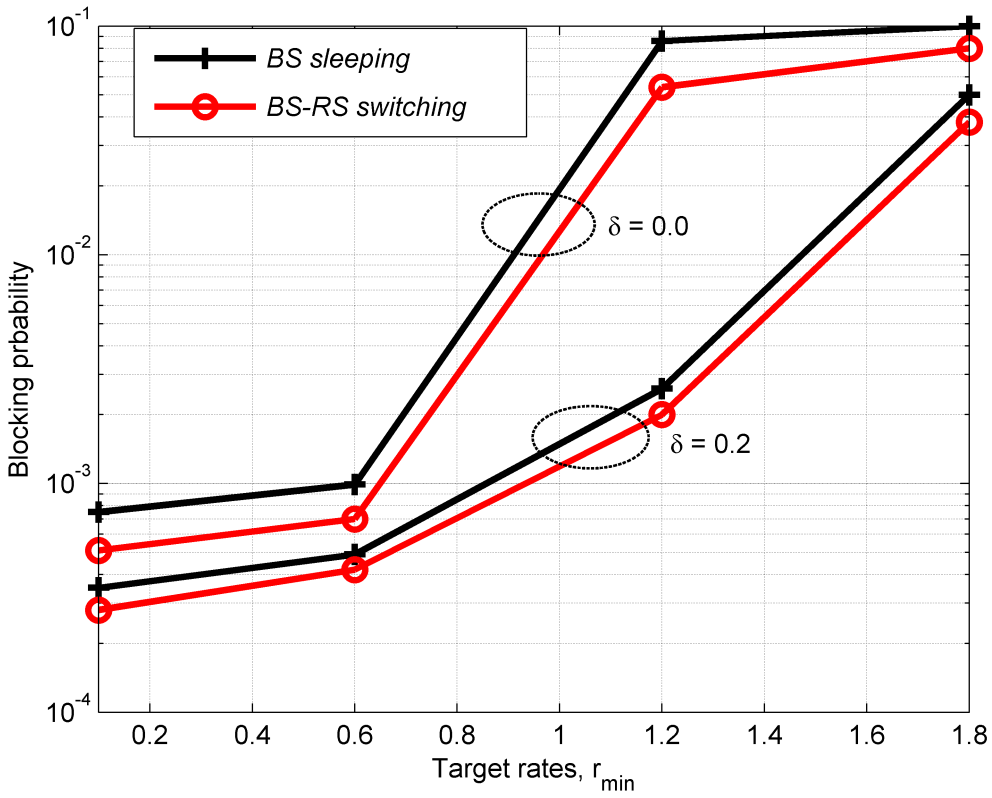

Figure 5-9: System blocking probability versus target data rates using the adaptive threshold based algorithm.

5.5.7 Blocking Probability

Figure 5-9 presents the system blocking probability for different target rates and tolerance margins for the proposed adaptive threshold based algorithm. It can be seen that an acceptable system blocking probability is achievable with both the *BS sleeping* and *BS-RS switching* models at low target data rates. For example, for $r_{\min}$ = 0.6 Mbps, the blocking probabilities are less than 10^{-3} for all cases. The results also show that the blocking probability can be reduced for both models by setting δ = 0.2. Setting the tolerance margin δ to higher value makes the network more conservative because the CC leaves higher idle traffic capacity for any sudden changes in traffic before setting a new threshold. It also illustrates that the *BS-RS switching* model always provides lower blocking probabilities than the *BS sleeping* model for all target data rates and δ values. However, for higher data rate requirements, both models suffer from higher blocking probabilities due to the transmit power constraint. For example, for $r_{\min}$ =1.8 Mbps, 4% and 5% of users

are in the blocking region with the *BS-RS switching* and *BS sleeping* models respectively for δ=0.2 while these are 8% and 10%, respective for δ=0.0. Moreover, as has been seen in Figure 5-5, both models allowed higher numbers of BSs into dormant mode for lower δ values, but the number of dormant mode BSs decreases with δ. Therefore, the most striking result to emerge from the figure is that a lower δ can be set for a lower rate requirement $r_{\min}$ and vice-versa while maintaining the blocking probabilities within a given target level.

5.6 Summary

This chapter has proposed a new adaptive threshold based *BS switching* algorithm for saving energy in relay-assisted cellular networks, which exploits the dynamic nature of cellular traffic. For reducing complexity, the algorithm was performed in clusters of seven-cells and a BS within each cluster has been selected as a controller that receives the traffic load information of all BSs within the cluster and calculates the switching threshold for the cluster at every time instant. System performance over asymmetric traffic loads, power model for relay-assisted networks, switching threshold variations, and off-cell users' data rates have been investigated. Energy savings can be controlled by tuning the tolerance margin, while setting the tolerance margin to zero provides higher energy savings. Moreover, higher savings are identified for the networks with low RS to BS power consumption ratio. Now, as neighbouring BSs are required to increase their transmit power to provide service coverage of dormant cells, interference can be a dominant factor for selecting a set of BSs to switch to dormant mode. Therefore, the next chapter will focus on developing energy efficient dynamic interference-aware *BS switching* mechanisms through cooperation among BSs.

Chapter 6

Dynamic Traffic-and-Interference-Aware Base Station Switching

6.1 Introduction

As discussed in Chapter 4, when a BS switches to dormant mode, neighbouring *active* BSs are required to increase their transmit power to cover the off-cell service areas and this can lead to increased interference to other users in the network (Tabassum et al., 2014). However, the impact of interference was not considered in the earlier *BS switching* algorithms where only traffic-aware switching algorithms have been employed. Moreover, during low traffic periods, most BSs will satisfy the switching conditions in (4.11) and (4.12) in order to switch to dormant mode, but not all can be switched to dormant mode due to QoS and coverage guarantees. This provided the motivation to investigate the nexus between the best selection of BSs to be placed into dormant mode and the corresponding network impact of increased interference. Therefore, it is important to consider the interference impact in taking switching decisions together with the traffic load.

This chapter presents a new *BS switching* algorithm, which considers both the impact of network interference and instantaneous traffic loads while still achieving energy savings. A new DTIA switching algorithm is introduced (Alam et al., 2013) which gives switching decision priority to those BSs that generate higher interference to other users, with the provision that the instantaneous traffic load of the cell must be below a certain threshold to satisfy (4.11). The DTIA algorithm can be seamlessly incorporated into both *BS sleeping* and *BS-RS switching* models, and its performance will be compared with the existing traffic only aware switching algorithm discussed in earlier chapters. For convenience, the traffic-aware dynamic BS switching in the earlier chapters can now be termed as a *dynamic traffic-aware* (DTA) algorithm in this chapter as it considered only the instantaneous traffic load information in taking dynamic switching decisions.

6.2 System Model

6.2.1 Network Layout

The regular hexagonal grid cellular network arrangement of N_{BS} (5x5) cells (BSs) illustrated in Figure 3-2(b) will be employed in this chapter, where it is assumed that each $\mathcal{B}_b$ is connected to its neighbouring BS set $\boldsymbol{\mathcal{N}}_b$ via backhaul connections, as shown in Figure 2-1(b), thereby ensuring cooperative sharing of information. For *BS-RS switching*, each cell includes a low-powered RS (*x-RS*), $\mathcal{R}_b \in \boldsymbol{\mathcal{R}} = \{\mathcal{R}_1, \cdots, \mathcal{R}_{N_{BS}}\}$, collocated with the corresponding BSs, as described in *Section 4.2.1*, characterized by the MAF $A_b(t)$. When $A_b(t) = 0$ for $\mathcal{B}_b$, the corresponding set of off-cell MS $\boldsymbol{\mathcal{M}}_b$ are redistributed amongst neighbouring *active* BSs $\boldsymbol{\mathcal{N}}_b$.

6.2.2 User Association Schemes

As has been mentioned previously (Section 5.4.3), the switching of a BS to dormant mode requires an association of off-cell MS to *active* BS. In this chapter, any MS of interest can select a BS from which it experiences the maximum instantaneous received signal power (Oh et al., 2013), so a MS, $m \in \boldsymbol{\mathcal{M}}$ is associated with and served by $\mathcal{B}_b^*$ which provides the strongest signal strength:

$$\mathcal{B}_b^* = \arg \max_{b' \in \boldsymbol{\mathcal{B}}^{\mathbf{on}}} g_{b'm} \cdot p_{tx,b'm}^{BS} \tag{6.1}$$

where $\boldsymbol{\mathcal{B}}^{\mathbf{on}} \subseteq \boldsymbol{\mathcal{B}}$ is the set of *active* BSs at any time instant, $g_{b'm}$ is the channel gain between $\mathcal{B}_{b'}$ and MS *m* and includes both PL and shadow fading; and $p_{tx,b'm}^{BS}$ is the transmit power of $\mathcal{B}_{b'}$ for *m* so that $\sum_{m \in \boldsymbol{\mathcal{M}}_b} p_{tx,b'm}^{BS} \le P_{tx,\max}^{BS}$, where $P_{tx,\max}^{BS}$ is the peak BS transmit power.

Now, if every *active* BS has a maximum bandwidth, W_{max}, then each sub-channel will have a bandwidth $W = W_{max} / N_{RB}$, where N_{RB} is the total number of PRB in each BS. The achievable throughput of $\mathcal{B}_b$ is then:

$$R_b = W \cdot \sum_{m \in \mathcal{M}_b} \log_2 \left(1 + \frac{g_{bm} \cdot p_{tx,bm}^{BS}}{\sum_{n \in \mathcal{N}_b} I_n + N_0} \right) \tag{6.2}$$

where the term $\sum_{n \in \mathcal{N}_b} I_n$ is the interference received at MS *m* from its direct neighbouring cells $n \in \mathcal{N}_b$, and N_0 is the noise power. Using the total power consumption of $\mathcal{B}_b$ in (4.1) and the achievable throughput in (6.2), the network EE can be rewritten as:

$$\eta_{EE} = \sum_{b \in \boldsymbol{\mathcal{B}}^{\mathbf{on}}} \frac{R_b}{P_{T_b}} \tag{6.3}$$

where P_{T_b} is the total power consumption of $\mathcal{B}_b$, which has been described in *Section 4.2.2*. The main goal of the BS switching algorithm is to reduce the number of *active* BSs $\boldsymbol{\mathcal{B}}^{\mathbf{on}}$ at each decision time, so as to reduce the overall energy consumption while increasing η_{EE}. Since only the *active* BSs are considered in (6.3) to avoid the unexpected zero value for P_{T_b} as in (4.7), the power consumption of each *active* BS includes the corresponding associated power consumption of *x-RS*. The corresponding throughput is calculated using (3.3) and (3.4) for direct and relay-assisted communications, respectively.

6.2.3 Traffic Model

While in previous chapters, an approximated sinusoidal traffic profile has been assumed for generating cellular traffic, due to the highly dynamic temporal and spatial nature of the traffic (Marsan et al., 2009; Oh et al., 2011), the call arrival process will instead be modelled as time-inhomogeneous. This is achieved by multiplying a homogeneous Poisson process with a traffic intensity parameter λ and a time-varying rate function $0 \le f(t) \le 1$

(Hossain et al., 2013a). If the call arrives in cell $\mathcal{B}_b$ according to a Poisson process with intensity λ_b [calls/sec] and constant service time h [sec/call], then the normalized traffic load of $\mathcal{B}_b$ at time t is:

$$\rho_b(t) = \frac{\mathcal{X}_b h \ell_b f(t)}{N_{RB}}, \qquad \forall b = 1, \cdots, |\boldsymbol{\mathcal{B}}| \tag{6.4}$$

where $\mathcal{X}_b \sim Poi(\lambda_b)$ is a Poisson random variable with parameter λ_b; ℓ_b is the required number of channels (PRB) and N_{RB} is the total number of PRB in each BS, with $\boldsymbol{\rho}(t) = \{\rho_1(t), \cdots, \rho_{|\boldsymbol{\mathcal{B}}|}(t)\}$ being the set of traffic loads at time t. The same rate function is assumed for all the BSs, with two typical rate functions $f_1(t)$ and $f_2(t)$ being shown in Figure 6-1, which closely reflect traffic patterns in real cellular networks (Oh et al., 2013; Peng et al., 2011).

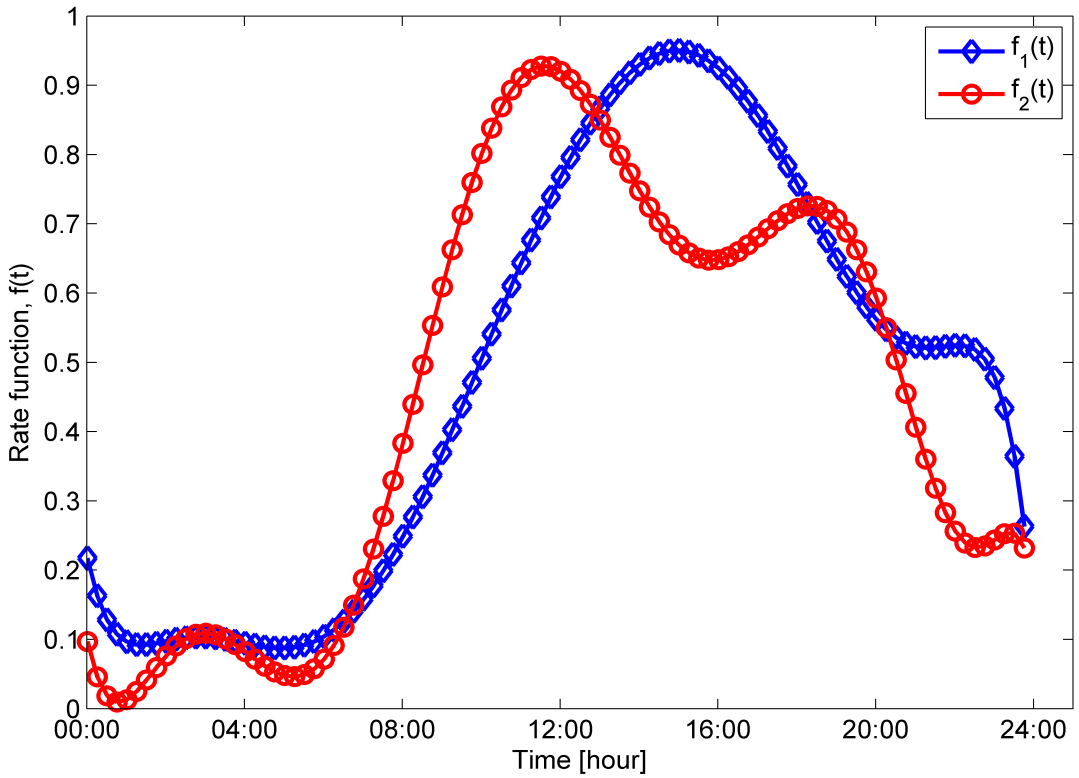

Figure 6-1: Rate functions for generating time-inhomogeneous traffic profiles.

6.2.4 Interference Estimation

While it is reasonable to assume that intra-cell interference can be neglected due to the use of orthogonal frequency bands, *BS switching* strategies can have a significant impact on ICI. For example, when some BSs are in dormant mode, the off-cell MS are served by *active* neighbouring BSs, which requires them to increase their transmit power (Tabassum et al., 2014). Therefore, the impact of interference in any switching strategy has to be incorporated, which correspondingly means that the level of interference must be estimated before making any switching decisions. One way of estimating ICI is to keep track of whether the same PRB is simultaneously assigned to the interfering BSs (Hossain et al., 2013b). However, it requires coordination among BSs for multi-user scheduling to PRB through a central coordinator to maintain PRB allocations for each BS, resulting in creating a large overhead on the system. Thus, for reducing the overhead, a PRB collision based model is considered to evaluate the ICI (Yarkan et al., 2010).

Since the non-coordinated PRB collision based scheme is considered in this chapter for simplicity, the indices of PRB allocated by a BS to its MS appear as random to the neighbouring BSs (Hossain, 2013). Under such scenario, if the upper bound of the probability of collision between two PRB is $P_C(\rho)$, the total estimated ICI undergone by MS *m* located in $\mathcal{B}_b$ is expressed as follows (Yarkan et al., 2010):

$$I_{m,\mathcal{B}_b} = \sum_{n \in \mathcal{N}_b} I_{nm} = \sum_{n \in \mathcal{N}_b} P_C(\rho) \cdot p_{rx,nm} \tag{6.5}$$

where $\mathcal{N}_b$ is the interfering (*active* neighbouring) BSs; and $p_{rx,nm}$ is the received power at MS *m* in $\mathcal{B}_n \in \mathcal{N}_b$. Note that the interference power received at a MS *m* depends on both the location of the MS and the distance between MS *m* and the interfering BSs, with the latter assumed to be known to each BS.

6.3 Interference-Aware Base Station Switching Strategy

The key objective of *BS switching* is to minimize the number of *active* BSs during low traffic periods, so reducing energy consumption of BS. This section firstly describes the dynamic BS switching strategy using the traditional traffic-only or the DTA algorithm before presenting the new DTIA algorithm which can be embedded into both the *BS sleeping* and the *BS-RS switching* models.

In switching a BS from *active* to dormant mode, the key challenge is to decide when the traffic load is sufficiently low that user performance can still be satisfactorily maintained following the mode change. Thus, the underlying premise of the DTA switching is that when the traffic load of $\mathcal{B}_b$ falls below a threshold ρ_{th}, it can switch to dormant mode provided the *active* neighbouring BSs $\mathcal{N}_b$ are able to handle the extra traffic generated from $\mathcal{B}_b$. This has already been formulated in (4.11) and (4.12), and proven that energy savings are achievable while satisfying the required QoS constraints. The value of ρ_{th} has been empirically shown to be in the range 0.5 to 0.6 (Oh et al., 2013; Alam et al., 2012) though adaptive threshold based switching allows higher energy savings as witnessed in *Chapter 5*. However, for simplicity, the fixed threshold based DTA switching algorithm is applied due to the high computational complexity of the former strategy, and compared with the new DTIA algorithm.

In the BS switching strategy, turning off certain BSs will apparently result in increasing traffic load for neighbouring BSs and this may bring a positive impact on the network due to reduced ICI, particularly for few MS. However, since the off-cell MS are expected to be further away from their new serving BSs, it is necessary to increase the transmit power of neighbour serving BSs, so increasing the ICI to other users. In addition, it is important to highlight that not all BSs can be switched to dormant mode even in the extreme case where the traffic profiles in every cell falls below ρ_{th}. In this situation, some low-load BSs must still be kept in *active* mode in order to support any users during the off-peak periods. It is

therefore a crucial design aim to select the best combination of BSs to switch to dormant mode at any particular time. Basing any BS switching strategy on traffic load alone (*i.e.*, DTA) however, may not lead to the best BS set being made dormant, because no cognisance is made of MS locations, which can lead to high interference in other cells. The new DTIA algorithm assimilates interference into the BS switching model, with each $\mathcal{B}_b$ comparing both the traffic load and received interference at each MS from *active* neighbouring BSs, with the requisite information being exchanged between neighbouring BSs via an X2 interface. The new algorithm will now be formally introduced.

6.3.1 Design Rationale

Assume each $\mathcal{B}_b \in \boldsymbol{\mathcal{B}}^{\mathbf{on}}$ with the corresponding traffic profile set $\boldsymbol{\rho}(t) = \left\{\rho_1(t), \cdots, \rho_{|\boldsymbol{\mathcal{B}}|}(t)\right\}$ co-operatively acquires instantaneous traffic load information from their neighbouring cells. The estimated received interference power from each user in the neighbouring cells is exchanged between the BSs. Represented as $\boldsymbol{w} = \left\{w_1, \cdots, w_{|\boldsymbol{\mathcal{B}}^{\mathbf{on}}|}\right\}$, a weighted vector is then formed of all the estimated received interference power $\sum_{m \in \mathcal{M}_b} I_{m,\mathcal{B}_b}$ in normalized form for each $\mathcal{B}_b \in \boldsymbol{\mathcal{B}}^{\mathbf{on}}$. The proposed DTIA algorithm employs a two-stage switching decision for any $\mathcal{B}_b \in \boldsymbol{\mathcal{B}}^{\mathbf{on}}$ to be switched into dormant mode:

i) The traffic load in $\mathcal{B}_b \in \boldsymbol{\mathcal{B}}^{\mathbf{on}}$ has to satisfy the switching conditions in (4.11) and (4.12);

ii) While many BSs will fulfil the above conditions, not all can be switched to dormant mode, so the new algorithm selects a combination of BSs, giving priority to those which have the highest estimated interference weighted vector, $\boldsymbol{w}$.

The combination of BSs selected is called the best set of BSs to be switched into dormant mode at that decision instant, as other *active* BSs will require lower transmission power to

serve off-cell MS. As a result, in order to encompass the impact of both traffic and interference in the switching decision, a *utility function* for each $\mathcal{B}_b$ is defined:

$$\mathcal{U}(\mathcal{B}_b) = \begin{cases} \dfrac{\rho_b}{w_b}, & \text{if } \rho_b \le \rho_{th} \\ \infty, & \text{otherwise} \end{cases} \tag{6.6}$$

When $\rho_b > \rho_{th}$, $\mathcal{B}_b$ cannot be switched to dormant mode so $\mathcal{U}(\mathcal{B}_b)$is set to ∞. Also as $0 > w_b \ge 1$, a higher w_b gives greater emphasis to the received interference component in DTIA switching, while conversely when $w_b = 1$, interference is not considered and DTIA reverts to the DTA algorithm. In other words, a BS whose MS receives higher interference, *i.e.*, higher w_b, will have the highest priority to switch to dormant mode, provided it satisfies the switching conditions in (4.11) and (4.12). Since each $\mathcal{B}_b$ shares their status amongst neighbours $\mathcal{N}_b$, the $\mathcal{B}_b^*$ with the lowest $\mathcal{U}(\mathcal{B}_b^*)$ in (6.6) is switched first into the dormant mode, with the corresponding MS $\mathcal{M}_b$ associated with $\mathcal{B}_b^*$ being redistributed among $\mathcal{N}_b$. In other words, the algorithm iteratively switches BSs from *active* to dormant mode on a one-by-one basis, starting from the BS with the lowest $\mathcal{U}(\mathcal{B}_b^*)$. The rationale of applying a higher priority to the BS with the lower $\mathcal{U}(\mathcal{B}_b^*)$ ensures the network interference will always tend to be reduced when a BS is switched to dormant mode. When all $\mathcal{M}_b$ have been successfully reassigned to their neighbours, $\mathcal{B}_b$ is then switched to dormant mode ($A_b(t) = 0$) and this process continues iteratively in each decision instant until all *active* BSs $\mathcal{B}^{\text{on}} \in \mathcal{B}$ have been checked.

The pseudo-code representation of the DTIA *BS switching* algorithm is presented in Algorithm 6.1. At each decision instant, the *utility function* $\mathcal{U}(\mathcal{B}_b)$ is calculated for all BSs (Line 3) after defining and initializing parameters in Line 1 and 2. Now, the switching decisions are made in Line 4-14, *i.e.*, set $A_b(t)$ either to 0 or 1 for all BSs. After sharing the

status of each BS that includes the load profile, the MAF and the interference weight among neighbours (Line 5), the algorithm then finds a BS with the lowest $\mathcal{U}(\mathcal{B}_b)$ (Line 6). Before switching the BS in dormant mode and updating status (Lines 11 & 12), the associated MS $\boldsymbol{\mathcal{M}}_b$ are then distributed among *active* neighbours (Line 8) based on the signal strength based user distribution discussed in *Section 6.2.2* and the corresponding pseudo-code is presented in Algorithm 6.2.

Algorithm 6.1: The DTIA BS switching algorithm.

1: **Inputs:** $\boldsymbol{\rho}$, ρ_{th}, $\boldsymbol{\mathcal{M}}$, $\boldsymbol{\mathcal{B}}$, $\boldsymbol{\mathcal{W}}$, **Outputs:** A_b

2: Initialize $\boldsymbol{\mathcal{B}}^{\mathbf{on}} \in \boldsymbol{\mathcal{B}}$, $\mathcal{M}_b \in \boldsymbol{\mathcal{M}}, \forall \mathcal{B}_b \in \boldsymbol{\mathcal{B}}^{\mathbf{on}}$

3: Calculate: $\mathcal{U}(\mathcal{B}_b)$, $\forall \mathcal{B}_b \in \boldsymbol{\mathcal{B}}^{\mathbf{on}}$ by (6.6)

4: **FOR** each $\mathcal{B}_b \in \boldsymbol{\mathcal{B}}^{\mathbf{on}}$ **DO**

5: Exchange status (ρ_b, A_b, w_b) among $\boldsymbol{\mathcal{N}}_b$ // Acknowledge status with other BSs

6: Find $\mathcal{B}_b^* = \arg \min_{\mathcal{B}_b \in \boldsymbol{\mathcal{N}}_b \cup \{\mathcal{B}_b\}} \mathcal{U}\left(\mathcal{B}_b^*\right)$ // Select a BS with the lowest utility

7: **IfF** $\mathcal{B}_b^* = \mathcal{B}_b$ **THEN**

8: Distribute $\boldsymbol{\mathcal{M}}_b$ among $\boldsymbol{\mathcal{N}}_b$ by **Algorithm 6.2** // Signal strength based user distribution

9: **END IF**

10: **IF** $\boldsymbol{\mathcal{M}}_b = \phi$ **THEN**

11: $A_b \leftarrow 0$, $\rho_b \leftarrow 0$, $w \leftarrow \infty$, $\boldsymbol{\mathcal{B}}^{\mathbf{on}} \leftarrow \boldsymbol{\mathcal{B}}^{\mathbf{on}} - \{\mathcal{B}_b\}$

12: Update status (ρ_b, A_b, w_b)

13: **END IF**

14: **END FOR**

The user distribution procedure from dormant mode BS to *active* mode neighbouring BSs is presented in Algorithm 6.2, and is based on (6.1). In this algorithm, every $m \in \boldsymbol{\mathcal{M}}_b$ is assigned to the $\mathcal{B}_n^* \in \boldsymbol{\mathcal{N}}_b$ which has the maximum signal strength (Line 3) as described in *Section 6.2.2*, provided the traffic load ρ_n of $\mathcal{B}_n^*$ is less than the maximum permitted $\rho_{\max}$

without compromising the QoS (Line 4-9). Any MS in $\mathcal{M}_b$ which is unable to handover to an *active* neighbouring BS is blocked (Line 10-12).

Algorithm 6.2: User Distribution of $\mathcal{B}_b$ among Neighbouring BSs $\mathcal{N}_b$.

1: **WHILE** $\mathcal{M}_b \neq \phi$ **DO**

2: Select a MS, $m \in \mathcal{M}_b$

3: Find $\mathcal{B}_b^* = \arg \max_{b' \in \mathcal{B}^{on}} g_{b'm} \cdot p_{tx,b'm}^{BS}$ // Associate a BS with the strongest signal

4: **IF** $\rho_n \geq \rho_{\max}$ **THEN** // $\rho_{\max}$ is max. load served by each BS

5: $\mathcal{N}_b = \mathcal{N}_b - \{\mathcal{B}_n\}$ // $\mathcal{B}_n$ has no capacity to serve *m*.

6: **ELSE**

7: Associate MS *m* to $\mathcal{B}_n$ // MS *m* is now handed over to $\mathcal{B}_n$

8: $\mathcal{M}_b = \mathcal{M}_b - \{m\}$ // Remove MS *m* from the set $\mathcal{M}_b$

9: **END IF**

10: **IF** $\mathcal{N}_b = \phi$ **THEN**

11: Any MS in $\mathcal{M}_b$ are blocked and $\mathcal{M}_b \leftarrow \phi$

12: **END IF**

13: **END WHILE**

To return $\mathcal{B}_b$ back to *active* mode, all neighbouring BSs must monitor their traffic loads and cooperate with each other to make the decision for the dormant mode BS $\mathcal{B}_b$. All neighbouring BSs record their own traffic loads as well as the handover traffic from $\mathcal{B}_b$. When the traffic load from $\mathcal{B}_b$ exceeds the switching threshold ρ_{th}, the dormant mode $\mathcal{B}_b$ receives a trigger signal from any of the *active* neighbouring BSs to switch back into *active* mode, so the condition for switching $\mathcal{B}_b$ back on is exactly the same as (4.13):

$$\rho_b > \rho_{th} \tag{6.7}$$

Once $\mathcal{B}_b$ receives the trigger, $\mathcal{B}_b$ wakes up and its MAF $A_b(t)$ is set to 1. Accordingly, the corresponding traffic load located within its possible serving area reverts back to the original BS $\mathcal{B}_b$.

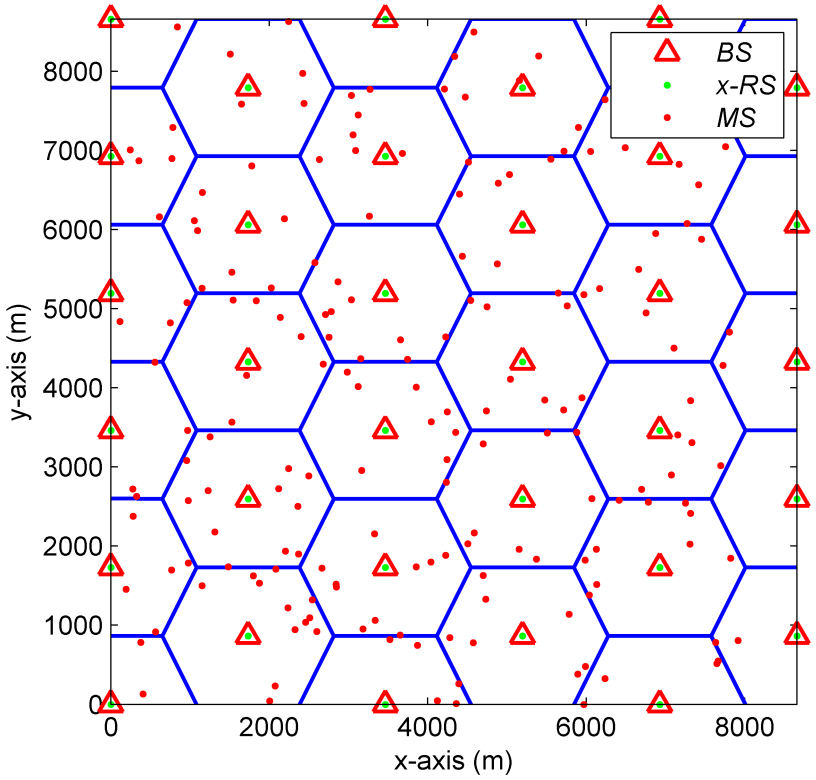

Figure 6-2: A snapshot of the network layout at an arbitrary time showing deployed BSs, collocated RS (*x-RS*) and MS.

6.4 Simulation Results

6.4.1 Simulation Settings

A simulation layout of 5 by 5 hexagon grid cells was used with an ISD of 1.732km and switching threshold ρ_{th}=0.6 (Oh et al., 2013). The call arrival rate λ_b was assumed to be 138.9×10^{-3} calls/sec, the service time was set at 180sec with ℓ_b=1PRB, which corresponds to a peak-time load of 25 PRB, while the time-inhomogeneous traffic used the rate function displayed in Figure 6-1 was used. A snapshot of the network layout is illustrated in Figure 6-2 at an arbitrary time. Two transmit power classes of 24dBm and 30dBm were assumed for *x-RS* while the rest of the simulation settings are based on Table 3.1. To critically evaluate the performance of the DTA algorithm by employing the same algorithms (Algorithm 6.1 and 6.2), the weighted vector $\boldsymbol{w} = \left\{w_1, \cdots, w_{|\mathcal{B}^{on}|}\right\}$ was set to 1, *i.e.*,

$w_b = 1, \forall b \in \mathcal{B}^{\mathbf{on}}$ in (6.6). In this experiment, both the DTIA and DTA algorithms are integrated into both the *BS-RS switching* and *BS sleeping* models for comparison purposes.

6.4.2 Impact of Interference on Base Station Selection

The motivation of the proposed DTIA algorithm is to select a set of BSs at each decision time, which will conserve more energy than the DTA algorithm as will be shown in the following section. Figure 6-3(a) now compares the performance of DTA and DTIA in terms of the average number of *active* BSs operating over a 24hr period, with the normalized traffic load being averaged in 15min slots (T_0=15min). The plots reveal that DTIA is able to maintain more BSs in dormant mode in the early morning, while conversely more BSs are *active* in the evening compared to DTA. However, the average number of *active* BSs across the day is the same for both DTA and DTIA algorithms. As a result, the static power consumption P_f^* in (4.1) with both algorithms will be approximately the same, while the transmit power requirements for the DTIA will be less as only those BSs, which generate higher interference to the network are selected to be switched into dormant mode. The remaining BSs are marked as the best set of BSs to be in *active* mode because they are less responsible for generating interference to other users, so they have better link qualities to users.

Figure 6-3(b) contrasts the selected BS sets chosen to be dormant at a specific time instant of the day (11.00am) for both DTA and DTIA respectively. It is clear that while both keep 12 *active* BSs, the chosen BS sets are very different. A similar snapshot taken at 22:00pm shown in Figure 6-3(c) again reveals that both algorithms keep different sets of *active* BSs. Furthermore, both algorithms do not always have the same number of *active* BSs, as for example at 22:00pm, there are 13 *active* BSs with the DTA algorithm, while the DTIA has 15 BSs in *active* mode, again with different BS selections. It needs to be stressed that DTIA, despite the opportunity, does not always allow a higher number of BSs to be in dormant mode when either the traffic variations or rate function change fast, due to the

potential abrupt changes in interference within the network. In contrast, DTA allows more BSs to switch to dormant mode in this scenario as the impact of interference is not a factor in the BS switching decision-making process. However, the important point to emphasise is that the DTIA BS set selected to remain *active* will always be better than that for DTA, because those BSs incurring the highest interference levels have priority to switch to dormant mode, hence leveraging better off-cell MS link quality. This is apparent in the higher throughput of off-cell MS (see Figure 6-6) and the lower transmission energy consumption (see Figure 6-7).

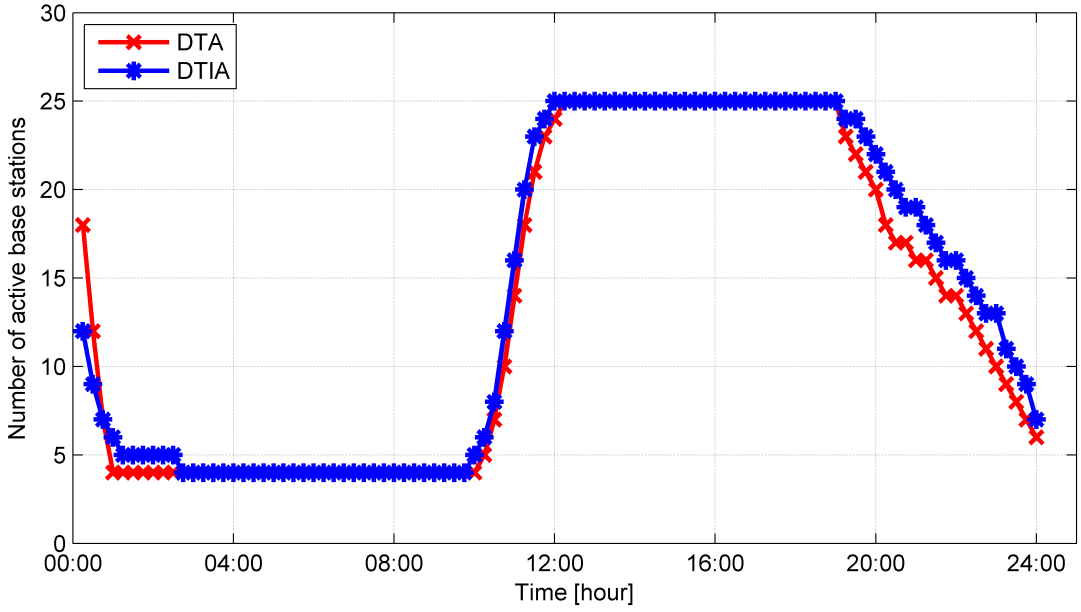

(a)

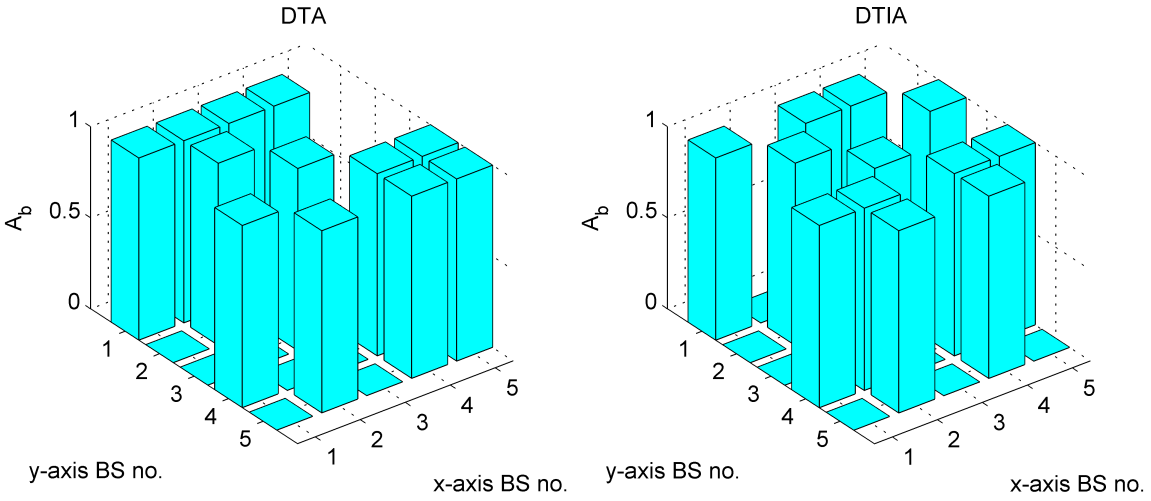

(b)

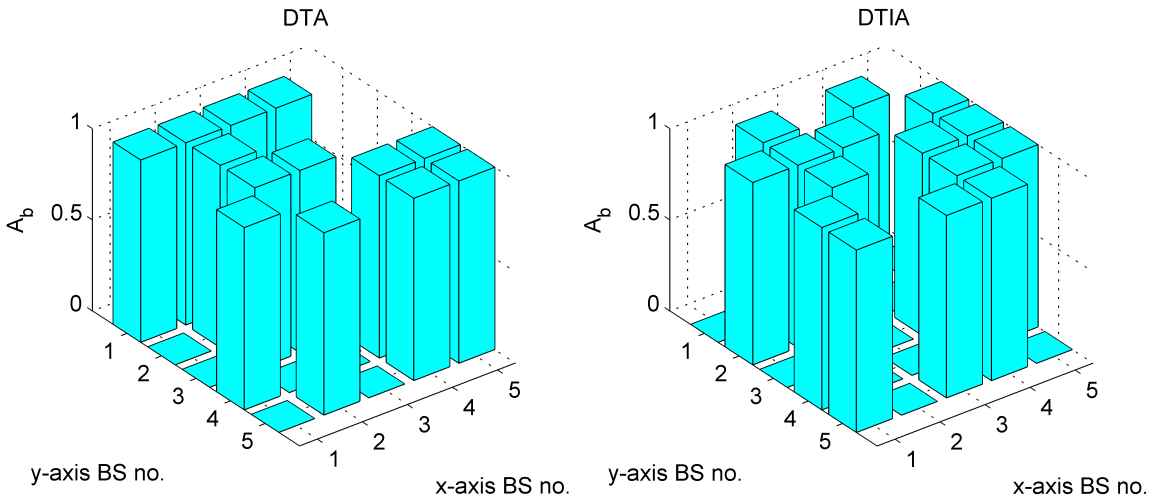

(c)

Figure 6-3: (a) Average number of *active* BSs over a 24hr interval; (b) DTA and DTIA comparison of the set of *active* BSs – snapshots at 11:00am; and (c) 22:00pm.

6.4.3 Daily Energy Savings

Using (3.8), the average network energy saving per day for the proposed DTIA algorithm is presented in Figure 6-4 in comparison with DTA, while also illustrating the impact of switching thresholds, rate functions and the *BS switching* models on the network energy savings. It is evident from Figures 6-4(a) and (b) that by increasing the low-load switching threshold ρ_{th}, a higher energy saving is attained. For instance, the energy savings with the DTIA algorithm for the *BS-RS switching* (or *BS sleeping*) model increased from 22% (or 18%) at ρ_{th} = 0.3 to 45% (or over 37%) at ρ_{th} = 0.6 as shown in Figure 6-4(a). Similar trends are observed for DTA, while the overall conclusion is that DTIA consistently performs better than the DTA for both the *BS sleeping* and the *BS-RS switching* models. This is because the DTIA keeps *active* those BSs that generate less interference to other users, *i.e.*, BSs with better link qualities are kept in *active* mode so they do not require to increase their transmit power greatly in order to continue to provide services to users.

The impact of rate functions on the energy savings using the DTIA algorithm is now analysed and it has been seen in Figure 6-4(c), where the rate function $f_2(t)$ is considered, that there are slightly lower energy savings by using the DTIA for both models than that

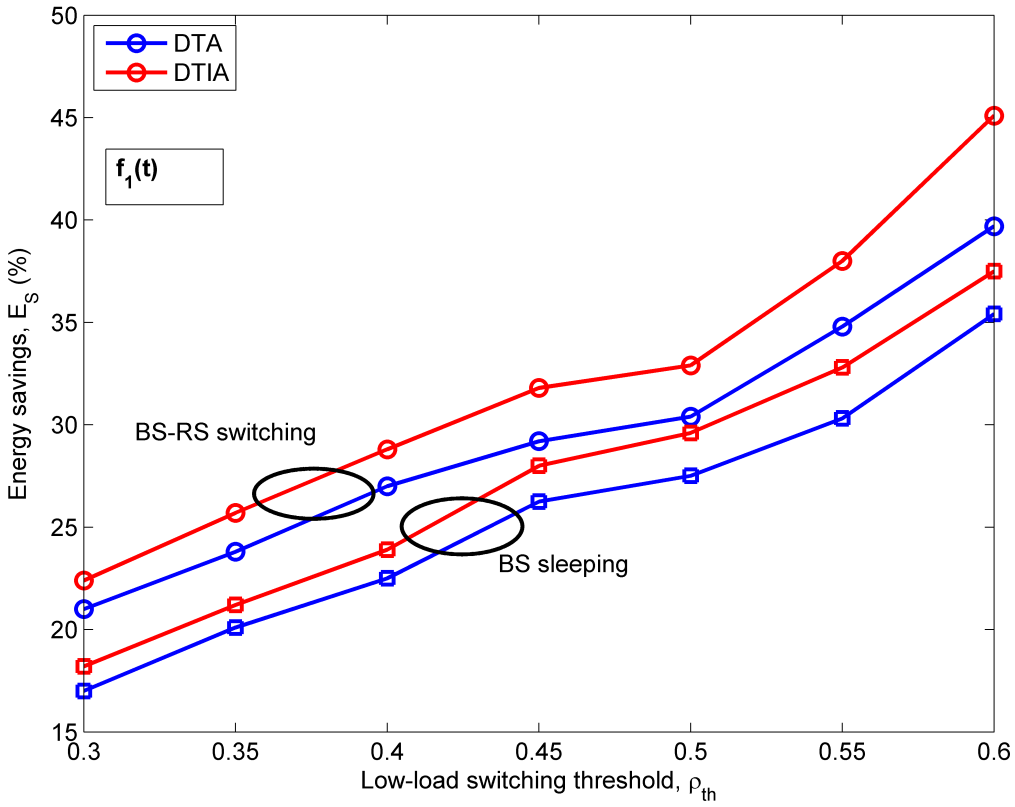

(a) Rate function, $f_1(t)$.

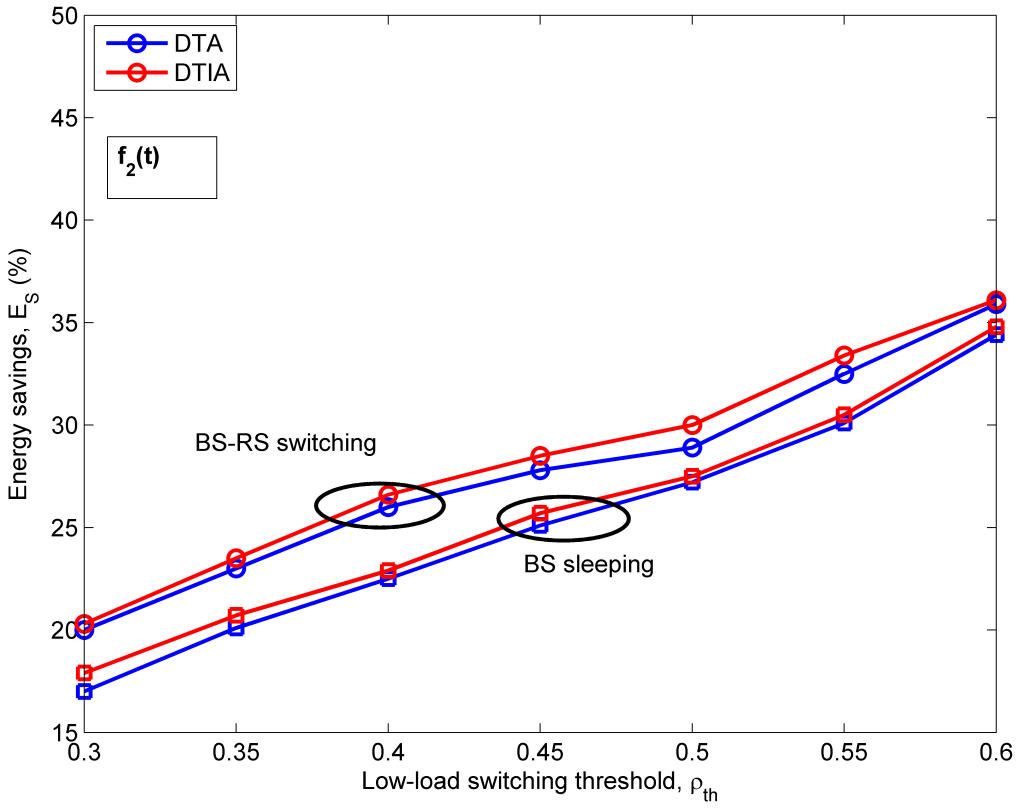

(b) Rate function, $f_2(t)$.

Figure 6-4: Daily energy savings with both DTA and DTIA strategies for both *BS-RS switching* and *BS sleeping* models.

when using $f_1(t)$ (Figure 6-4(a)). This is because $f_2(t)$ has a highly fluctuating characteristic and the DTIA is more sensitive to the traffic fluctuations than the DTA allowing a lower number of BSs to switch to dormant mode. For example, when applying the DTIA algorithm in the *BS-RS switching* model with ρ_{th}=0.6, over 45% energy was saved for $f_1(t)$ while only 36% energy was saved for $f_2(t)$. Similar trends for any ρ_{th} are also observed when both algorithms are employed in the *BS sleeping* model.

6.4.4 The EE Performance

Figure 6-5 compares the corresponding EE performance using (6.4) accomplished by both DTA and DTIA algorithms over an entire 24hr period. While the former considers only traffic load using ρ_{th} for switching, DTIA turns off those BSs suffering the highest interference first, so the overall interference in the network is attenuated. The minimum QoS is still achieved by incurring a small increase in the transmit power so the EE is improved during low-traffic load periods. For example, the EE for DTIA in the morning period (1:00am to 11:00am) is ≈22% higher than DTA because of the lower energy consumed as evidenced in Figure 6-4, leading to a smaller denominator in (6.3) thus augmenting the overall EE. Furthermore, by predicting the most appropriate *active* BS set based upon the received interference of each BS, the overall network throughput is increased which is another contributory factor to the superior EE performance of the DTIA algorithm. Figure 6-5 confirms *BS-RS switching* model consistently provides better performance than the *BS sleeping* using both the DTA and DTIA. This is a direct consequence of switching to RS mode, so the distance between the neighbouring BSs that are serving the off-cell MS, is reduced. This then lowers the additional transmission power requirements when BSs are switched to dormant mode (see Figure 4-5).

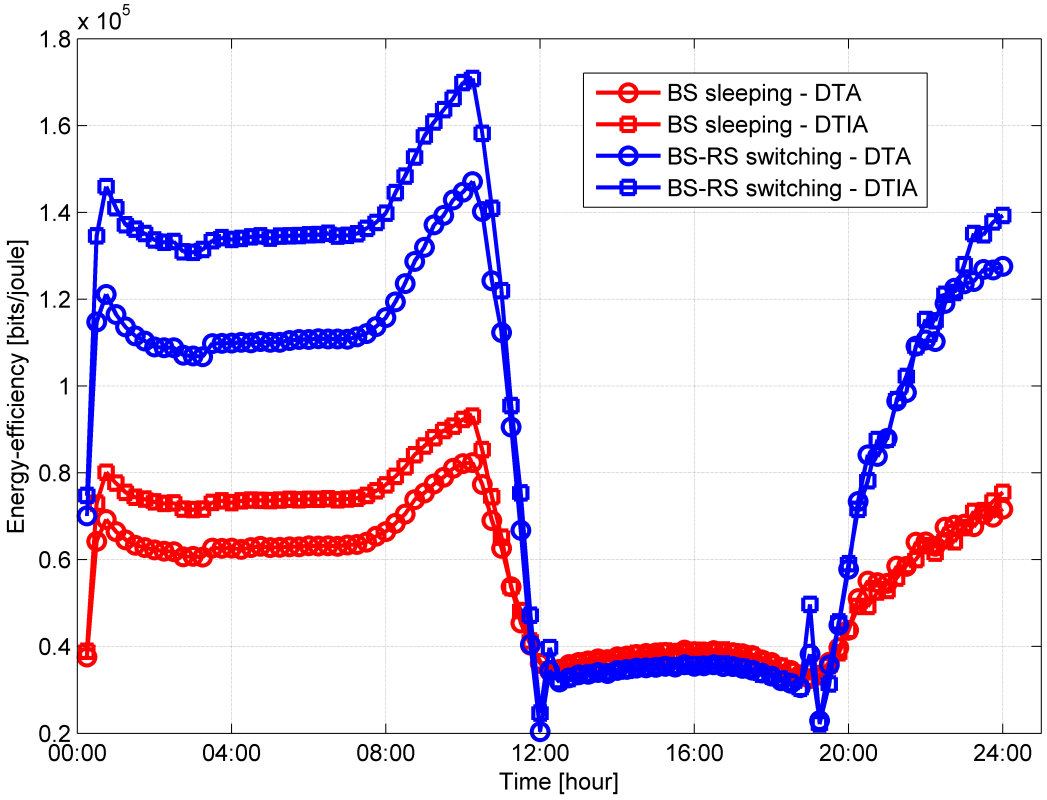

Figure 6-5: EE performance comparison of energy-efficient DTA and DTIA strategies for both *BS-RS switching* and *BS sleeping* models over a 24hr window under rate function $f_1(t)$.

6.4.5 Impact on Off-Cell MS Throughput and Power Consumption

The impact on off-cell MS throughput is analysed in Figure 6-6 with two power classes (24*dBm* and 30*dBm*) of RS being used for *x-RS* with the *BS-RS switching* case. The results are plotted with respect to the average number of off-cell MS per cell in the network. The graph shows that the off-cell MS throughput increased with the number of off-cell users with using both algorithms. Since the off-cell MS experienced better link quality to communicate with the *active* neighbour BS set using the DTIA algorithm, their achievable throughputs were higher than that with using the DTA for a given transmit power. For example, when the number of off-cell MS is 2 or more, the achievable throughput increased from typically 1Mbps to ≈1.1Mbps. In addition, the off-cell MS throughput is further improved when the DTIA is employed in the *BS-RS switching* model compared to that in the *BS sleeping*. The reason for this is the shorter distance between the BS and off-

cell MS by the *x-RS*. As expected, a higher off-cell MS throughput was achieved if a power class of 30dBm RS was used for the *x-RS*.

Due to the increased distance between the serving BS and off-cell MS, it is generally required to increase the transmit power of off-cell MS to achieve the minimum QoS provision. The UL power control is used to calculate the amount of average energy consumed per off-cell MS using (4.2), where P_0=-99dBm to ensure the minimum QoS is upheld. Figure 6-7 plots the power reduction performance for off-cell MS achieved by both the DTIA and DTA strategies. The former provides more than 5% improvement due to the reduced interference in the network, and/or better link qualities between off-cell MS and the serving neighbour BS, with the results showing that better MS power savings (≈30%) are consistently achieved using the *BS-RS switching* model, which is reflected in an enhanced UL quality between the serving BS and all off-cell MS.

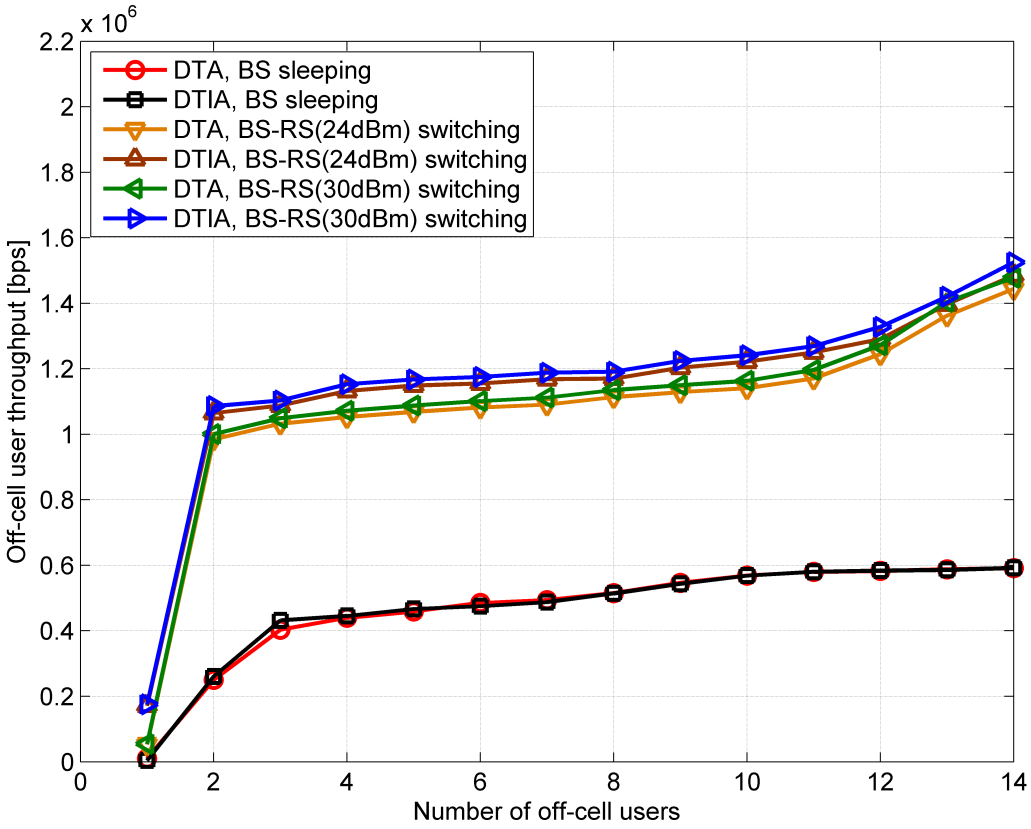

Figure 6-6: Average off-cell MS throughput verses the number of off-cell users.

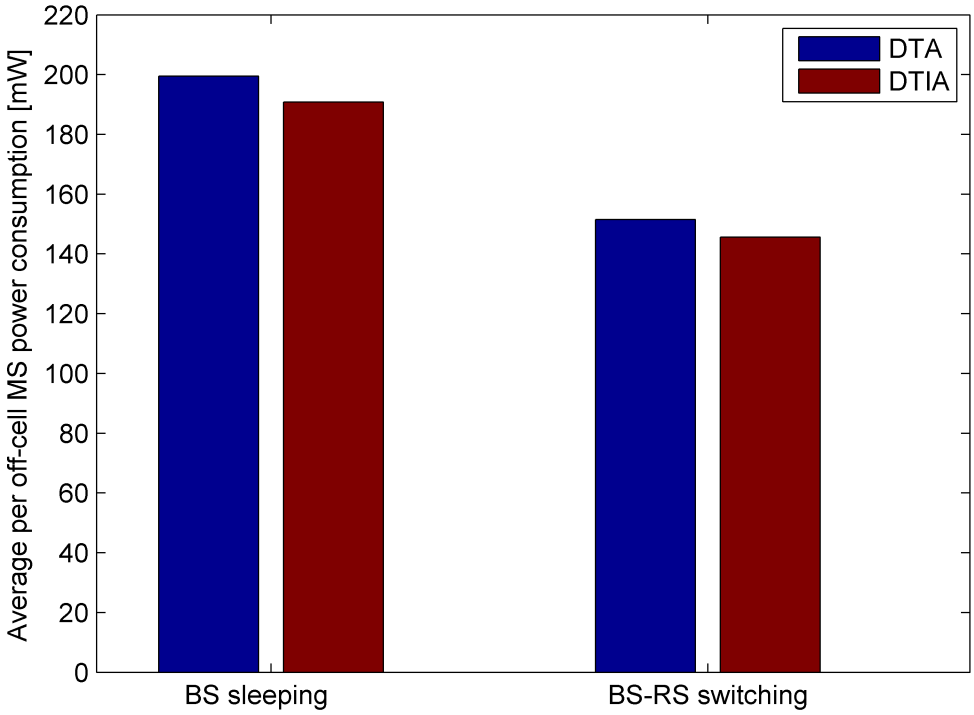

Figure 6-7: Average per off-cell MS power consumption with the *BS sleeping* and *BS-RS switching* models for DTA and DTIA.

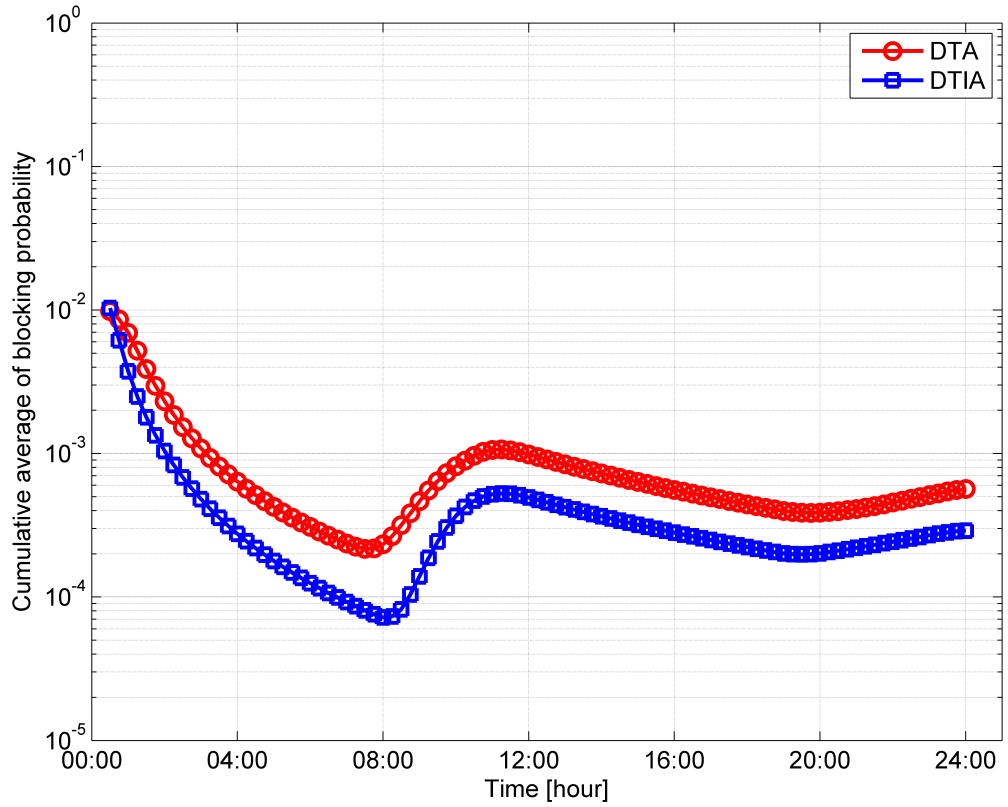

Figure 6-8: Cumulative average blocking probability for a 24hr period for the DTA and DTIA algorithms.

6.4.6 Blocking Probability Analysis

Finally, Figure 6-8 analyses the cumulative average blocking probability for every switching-decision occurrence during the day using (3.11). Results again confirm that the blocking probability in each decision time for both algorithms is maintained below the target (1%), while the DTIA provides a consistently lower blocking probability than the DTA, due to the better choice of BSs to remain *active* during the low-peak traffic periods. These results confirm that by incorporating interference alongside traffic in the switching decision in DTIA consistently provides superior energy savings both from both the BS and MS perspectives over the traditional DTA approach.

6.5 Summary

This chapter has proposed a DTIA *BS switching* algorithm for enhancing energy savings in cellular networks and is compared with the traditional DTA algorithm. The DTIA algorithm selects a set of BSs, which satisfy the traditional switching conditions, and it gives the priority to those BSs that are responsible for generating high interference to switch into dormant mode. For DTA, *BS switching* is founded only on the traffic load profile of each BS and uses a preset threshold, while DTIA in contrast, incorporates received interference along with traffic load to manage the switching decision. Thus, DTIA by virtue of choosing the better BS set to remain *active* affords improved network EE, and while DTA and DTIA use the same number of *active* BSs on average, they are dissimilar sets. However, the DTIA has performed better with traffic profiles with less variation. When both algorithms have been seamlessly integrated into both the *BS sleeping* and *BS-RS switching* models, the latter consistently provides superior performance for off-cell MS throughput, EE and MS power consumption.

So far dynamic *BS switching* models such as existing *BS sleeping* and the proposed *BS-RS switching* have been investigated with new switching algorithms being developed, *i.e.*, fixed and adaptive threshold based traffic-aware, and in this chapter traffic-and-

interference aware, to enhance the overall BS energy savings within a cellular network context. None of these however, have examined the potential energy savings which could be achieved by scaling the network capacity with traffic demand and energy consumption. The next chapter concentrates on developing a novel scalable solution for homogeneous network scenarios.

Chapter 7

A Multimode Base Station Switching Framework - A Scalable Cellular Network Design

7.1 Introduction

Since existing networks are normally dimensioned based upon peak-traffic load scenarios, *i.e.*, worst case conditions to ensure their guaranteed QoS, maximum BS efficiency can only be achieved during peak-traffic situations. However, due to the dynamic traffic variations of real cellular networks in both temporal and spatial domains, it is highly likely that most BSs are under-utilized whenever the traffic load is below its peak. Despite the availability of many *BS switching* energy-saving techniques (Oh et al., 2013; Alam et al., 2012) that have the potential to lower the energy consumed at low-traffic conditions, their operation can still be more energy efficient. The opportunity to secure further energy savings based on traffic dynamics is still an omission due to the ineffective exploitation of network capacity. For example, to guarantee the coverage for a given traffic demand, there must be a certain number of *active* BSs within a given area even though the capacity of the *active* BSs may not be necessary to meet such demand. This inevitably leads to BSs still being under-utilized while at the same time consuming high static power as shown in Figure 2-8, which is independent of traffic load during low, medium or below peak-traffic periods (Auer et al., 2012). Due to the inherent high static power overheads, BSs exhibit poor EE when they operate under either low or medium traffic loads, so in order to achieve tangible energy savings, it is necessary to develop a new architecture capable of scaling the network in terms of user traffic demand.

The switching decision (*active*/*sleep*) in existing *BS switching* techniques is dynamically taken when traffic load is sufficiently low that the QoS performance can still be maintained after switching. This decision is normally based on a threshold value, which is set either to a fixed value as in *Chapter 4* or is adaptively determined (*Chapter 5*) by taking cognisance

of the capability of neighbouring BSs to manage handover traffic without compromising network performance. While all existing energy saving strategies are efficacious to some extent, their underlying premise is of dual-mode (*active*/*sleep*) BS switching, though there are clearly situations where further savings are attainable by facilitating scalability by enabling BSs to operate in different power modes, so the static power consumption of BSs tracks the traffic demand.

This chapter proposes a *scalable MMBS framework* which exploits latent opportunities to lower energy consumption by changing the BS either from *active* to *low-power*[7] (LP) or LP to *sleep* modes when particular network conditions prevail, rather than only switching between *active* and *sleep* modes when the traffic load is low. In scenarios where the BS load is higher than the switching threshold, the decision is made to change if possible, to an intermediate LP mode, instead of keeping the macro BS *active* which expends much more static power. In these circumstances, a fraction of the traffic load is served by a LP mode BS which means the overall handover traffic to neighbouring BSs falls below the threshold. Pragmatically, this necessitates a LP microcell BS to be collocated with the macrocell BS, though with the evolution of *XG all-in-one* BS designs which are smarter, more energy cognisant and have cognitive capability; such a practical energy saving scalable multimode BS operation will become feasible. It is important to stress that the static power consumption of a macro BS is much larger in comparison to a micro BS, since the latter does not require the logistical overheads of either large power amplifiers or major cooling equipment, as discussed extensively in *Section 2.5*. As a result, the new framework presented in this chapter fulfils the objective 3 of this thesis as illustrated Figure 1-2, by dimensioning the network capacity into smaller scales depending on the traffic demand.

[7] The LP mode BSs can be defined as small-cell BSs that consume low power compared to the high power macro BSs. In this thesis, micro BSs are considered as LP mode BSs.

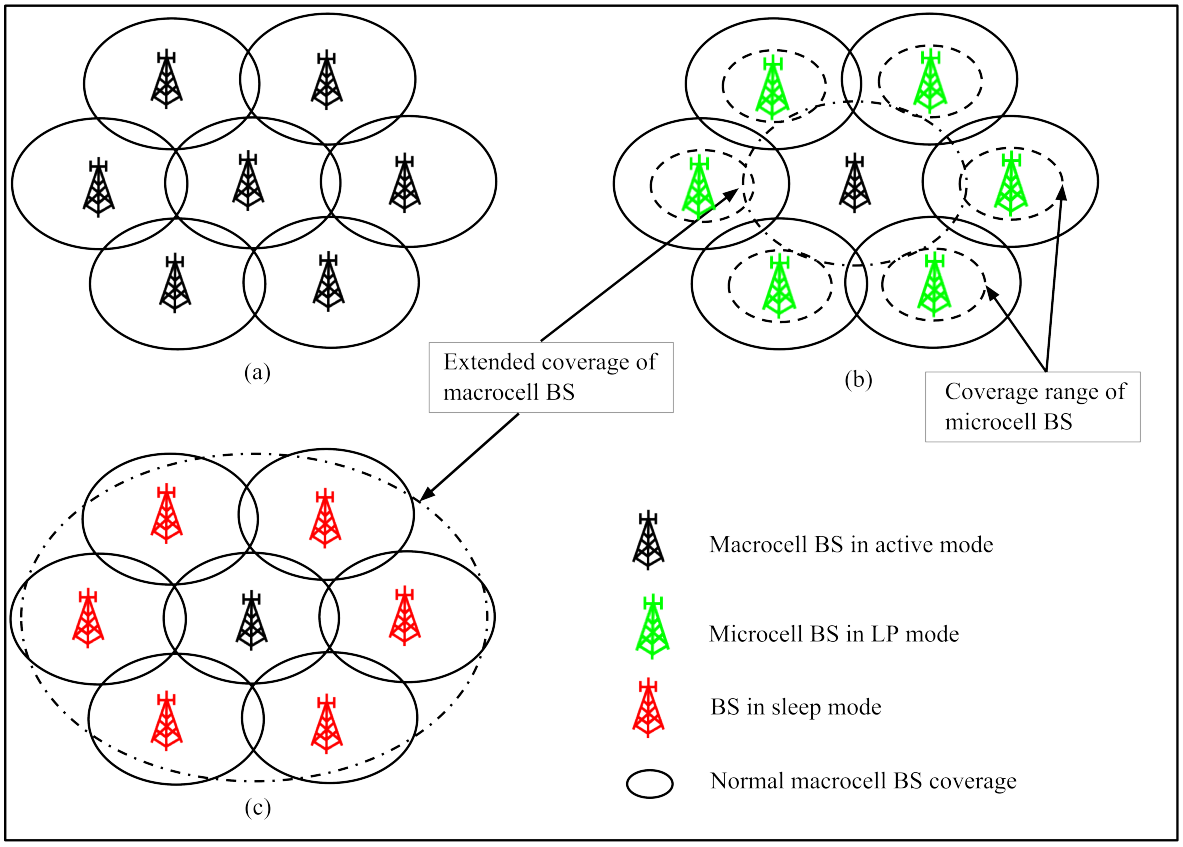

Figure 7-1: Example energy saving network arrangements reflecting different traffic variations: (a) all BSs in *active* mode (macro) during peak-traffic; (b) Certain BSs switched from *active* (macro) to LP (micro) mode and others in *active* mode (macro) during medium-traffic periods; and (c) some BSs in *sleep* and *active* modes during low-traffic.

7.2 Scalable System Model

A cellular network consisting a set of N_{BS} macrocell BSs, $\mathcal{B} = \{\mathcal{B}_1, \cdots, \mathcal{B}_{N_{BS}}\}$ is assumed within a two-dimensional area $\mathcal{A}$. It is assumed that a microcell BS, which normally consumes low static power compared to macro BSs (see Figure 2-8), is also deployed and collocated with each macro BS. Both collocated macro and micro BSs cannot be in *active* mode at the same time. This means if macro BS is in operating (*active*) mode, micro BS must be in *sleep* mode and vice-versa, so micro BS can also be denoted by the same set $\mathcal{B} = \{\mathcal{B}_1, \cdots, \mathcal{B}_{N_{BS}}\}$. If there are a set of N_{MS} MS, $\mathcal{M} = \{\mathcal{M}_1, \cdots, \mathcal{M}_{N_{MS}}\}$ located within $\mathcal{A}$, then $\mathcal{M}_b \in \mathcal{M}$ is the set of MS associated with $\mathcal{B}_b$ such that $\mathcal{M} = \mathcal{M}_1 \cup \cdots \cup \mathcal{M}_{N_{BS}}$ and $\mathcal{M}_i \cap \mathcal{M}_j = \phi$ for $i \neq j$. The new energy saving network model is illustrated in Figure 7-1.

Since the micro BS, as illustrated by uniform dashed circles in Figure 7-1(b) covers a smaller area compared to the macro BS coverage (solid circles), any remaining coverage has to be filled by extending the coverage of other *active* macro BS (non-uniform dashed circles) in Figure 7-1(b). It is assumed that each macro BS is able to extend its coverage up to double its original range, *i.e.*, it extends its range from its own cell to the neighbouring cells, if required, as illustrated in Figure 7-1(c). This is reasonable in urban scenarios, where BSs are densely deployed (Gong et al., 2012), so it can therefore be assumed that the considered network area can be covered by *active* macro and micro BSs, even when some of them are in *sleep* mode.

When a macro BS is in *active* mode, *i.e.*, the collocated micro BS is in *sleep* mode, the activity of the corresponding cell is known as *active* mode. On the other hand, when a macro BS is in *sleep* mode, the micro BS is *active* and the corresponding cell mode activity is known as LP mode, while when both macro and micro BSs are *sleep*, the condition for the corresponding cell is formally defined as in *sleep* mode. As a result, each cell has three different operating modes at any instant. As cells and BSs have been interchangeably used in previous chapters, for consistency, it is assumed that each BS can operate in three different modes: *active* (macro BS), *LP* (micro BS) and *sleep*. This is the reason for the new network design with multiple operating modes being referred to as *multimode switching* compared with the existing dual-mode switching (*active* and *sleep*) which has been the focus on earlier thesis chapters. The MAF of each BS changes over time depending upon the traffic variation within the cell. For example, all BSs are in *active* mode during peak periods as illustrated in Figure 7-1(a) while during medium traffic periods, some BSs are in LP mode and some are in *active* mode (see Figure 7-1(b)). During low traffic periods, most of the BSs are in *sleep* mode while *active* mode BSs are responsible for service coverage by extending their coverage as shown in Figure 7-1(c). Therefore, a *scalable* cellular design can be achieved by *multimode switching*, where the capacity of the network is scaled with respect to the traffic demand.

The operational time line (e.g. D = 24hr) is divided into N_t slots with each slot being of duration T_0 so $N_t.T_0$ = 24hr, and the mode switching decision is taken once per slot. When *active*, $\mathcal{B}_b$ functions as a full-power macro BS covering a large area and consuming high static power irrespective of the traffic load (see Figure 2-8), while in *sleep* mode, $\mathcal{B}_b$ is completely turned off. In the intermediate LP mode, $\mathcal{B}_b$ opportunistically operates as a micro BS covering a smaller area and it consumes low static power. When $\mathcal{B}_b$ switches from *active* to either LP or *sleep* mode, both the residual radio coverage and service provision of $\mathcal{B}_b$ must be guaranteed by its *active* neighbours as discussed above. The BS operating mode or the MAF, $A_b(t)$ of $\mathcal{B}_b$ at time t is then defined as:

$$A_b(t) = \begin{cases} 0, & \textit{Sleep}\ \text{mode} \\ 0.5, & \text{LP mode} \\ 1, & \textit{Active}\ \text{mode} \end{cases} \tag{7.1}$$

When $A_b(t)$ for each $\mathcal{B}_b, \forall b = \boldsymbol{\mathcal{B}}$ is set to a particular mode, $\mathcal{B}_b$ holds the mode during the interval T_0. The corresponding MS $\boldsymbol{\mathcal{M}}_b$ are then served by the currently *active* and LP mode BSs. At each decision time t, the BS decides whether to switch operating modes or not depending on current traffic conditions. Once the activity factor of each BS is fixed, a particular MS $m \in \boldsymbol{\mathcal{M}}$ is associated with and served by $\mathcal{B}_b$ which provides the best signal strength according to (6.1).

7.3 Power Consumption Model

As has been seen in *Section 2.5*, the static power consumption of a macro BS is large compared to that of a micro BS. This is also evidenced by the well-established power model parameters defined in Table 2.1. Since the power consumption of $\mathcal{B}_b$ depends on $A_b(t)$ and can hold a single state (*active*/LP/*sleep*) at any instant t, a straightforward

generalised power consumption model of $\mathcal{B}_b$ according to the power consumption model of BS (2.1) using $A_b(t)$ can be expressed as:

$$P_{T_b}(t, A_b) = \begin{cases} a_M . P_{tx,M}^{BS}(t) + P_{f,M}^{BS}, & \text{if } A_b(t) = 1, \\ a_L . P_{tx,L}^{BS}(t) + P_{f,L}^{BS}, & \text{if } A_b(t) = 0.5, \\ 0, & \text{if } A_b(t) = 0, \end{cases} \tag{7.2}$$

The power consumed in *sleep* mode is assumed to be zero, though in practice there will be a small amount of energy expended in reactivating a BS, though this is negligible compared with the BS power consumption in *active* mode (Gong et al., 2013).

7.4 Multimode Base Station Switching Framework

In the dual-mode (*active*/*sleep*) *BS sleeping* arrangement, $\mathcal{B}_b$ switches to *dormant* mode at a particular time instant only if it satisfies the switching conditions in (4.11) and (4.12). In this case, *active* neighbouring BSs of $\mathcal{B}_b$ play an important role in taking the switching decision as they are responsible for the service coverage of the switched-off cell $\mathcal{B}_b$. Usually, BSs operate in a conservative manner by setting a lower switching threshold to ensure there is no compromising in the QoS (Oh et al., 2013). While a higher switching threshold will afford improved energy savings, it also concomitantly will increase the blocking probability. This provided the motivation for the new *scalable MMBS framework* presented in this chapter, namely to enable the network to operate in a more energy efficient manner, while satisfying the required QoS. The potential to lower overall network energy consumption by adopting this *scalable MMBS framework* will now be described. Both dual-mode and multimode strategies are underpinned by the guiding precept that whenever a BS switches mode, the corresponding radio coverage and QoS provision must be guaranteed.

While existing energy saving *BS switching* techniques (Marsan et al., 2009; Zhou et al., 2009; Niu et al., 2010; Oh & Krishnamachari, 2010; Oh et al., 2013) operate in dual-mode

(*active*/*sleep*), the proposed *scalable MMBS framework* operates each BS in three different operating modes. As explained in *Section 4.3*, the condition to switch $\mathcal{B}_b$ to *sleep* mode is $0 \le \rho_b(t) \le \rho_{th}$, so when the load is greater than ρ_{th}, *i.e.*, during medium-to-high traffic periods, $\mathcal{B}_b$ can still conserve energy by switching to a LP mode. In these circumstances, if a portion of the load, $\rho'_b(t)$ is served by, for example, a gene, which can be an additional fixed or mobile BS, this fulfils the switching condition (4.11), *i.e.*, $0 \le \left(\rho_b(t) - \rho'_b(t)\right) \le \rho_{th}$ and $\mathcal{B}_b$ is allowed to switch to dormant mode. The LP mode collocated micro BS can play a role for the gene, which can also take some portion of the traffic load $\rho'_b(t) > \left(\rho_b(t) - \rho_{th}\right)$ to satisfy another switching condition (4.12) and to allow the macro BS to *sleep*. In other words, one can say if a portion of the traffic $\rho'_b(t) > \left(\rho_b(t) - \rho_{th}\right)$ in cell $\mathcal{B}_b$ can be served by the corresponding collocated micro BS and the remaining traffic $\left(\rho_b(t) - \rho'_b(t)\right)$ can be handed over to its neighbouring *active* macro BSs, the high-power consuming macro BS can then be switched to *sleep* mode. This is the rationale behind collocating micro BS deployment with the macro BS in each cell.

From (7.1), the MAF, $A_b(t)$ of $\mathcal{B}_b$ for the new *scalable MMBS framework* can be expressed as:

$$A_b(t) = \begin{cases} 0, & 0 \le \rho_b(t) \le \rho_{th} \\ 0.5, & \rho_b(t) > \rho_{th} \;\&\; \rho_b(t) - \rho'_b(t) \le \rho_{th} \\ 1, & \text{Otherwise} \end{cases} \tag{7.3}$$

The switching of $\mathcal{B}_b$ from *active* to either LP or *sleep* mode involves two conditions being fulfilled. Firstly, it checks whether it is permissible to switch directly to *sleep* mode, to attain the greatest energy saving. If this switch is not allowed, then the traffic load within the micro BS coverage range is calculated based upon the user locations and if the corresponding condition in (7.3) is upheld, $\mathcal{B}_b$ is switched to LP mode. In the MMBS algorithm, coordination amongst BSs is needed, so two sets $\mathcal{B}^{\text{on}}$ and $\mathcal{B}^{\text{off}}$ are respectively

maintained to track the total number of BSs in *active* mode and either in LP or *sleep* mode, and updated each set following each decision. The MMBS algorithm is described as follows, where without loss of generality the time index *t* has been omitted:

Step 1: Each BS obtains the information for traffic loads of its entire neighbour BSs through X2 interface.

Step 2: Each *active* BS $\mathcal{B}_b \in \boldsymbol{\mathcal{B}}^{\mathsf{on}}$ checks whether it satisfies conditions (4.11) and (4.12).

Step 3: If *Step 2* is satisfied, $\mathcal{B}_b$ is switched off and the associated users $\boldsymbol{\mathcal{M}}_b$ are distributed among *active* neighbours $\boldsymbol{\mathcal{N}}_b$ with updating sets $\boldsymbol{\mathcal{B}}^{\mathsf{on}}$, $\boldsymbol{\mathcal{B}}^{\mathsf{off}}$, and the MAF A_b.

Step 4: Otherwise, it calculates traffic ρ_b' within microcell coverage area and check switching condition (4.11) for the remaining traffic $(\rho_b - \rho_b')$.

Step 5: If (4.11) for traffic $(\rho_b - \rho_b')$ is satisfied, *i.e.*, $(\rho_b - \rho_b') \leq \rho_{th}$, $\mathcal{B}_b$ is switched to LP mode and $\boldsymbol{\mathcal{B}}^{\mathsf{on}}$, $\boldsymbol{\mathcal{B}}^{\mathsf{off}}$, and A_b are updated. In this case, the load ρ_b in $\mathcal{B}_b$ is then served by both the LP mode micro BS and the *active* neighbouring macro BSs $\boldsymbol{\mathcal{N}}_b$.

Step 6: Repeat *Steps 2-5* until all BSs in $\boldsymbol{\mathcal{B}}^{\mathsf{on}}$ have been checked.

The flowchart of the MMBS algorithm is displayed in Figure 7-2 for a single instant, where $sgn(x)$ is the sign function, with $sgn(x)$=1 when $x > 0$ and = 0 otherwise. The algorithm iterates $\left|\boldsymbol{\mathcal{B}}^{\mathsf{on}}\right|$ at each time instant and generates the corresponding A_b values for all BSs. Furthermore, in order to ensure the QoS, each off-cell MS will either achieve the minimum bit rate or be blocked. It is reasonable to assume that all BSs will co-operate with each other and serve any off-cell MS, provided they are not over-loaded.

To return $\mathcal{B}_b \in \boldsymbol{\mathcal{B}}^{\mathsf{off}}$ from *sleep* to either LP or *active* mode, all neighbouring BSs continually monitor their traffic loads and by sharing load information make the decision for the off-cell $\mathcal{B}_b$ to be reactivated to either LP or *active* modes. The priority is firstly to

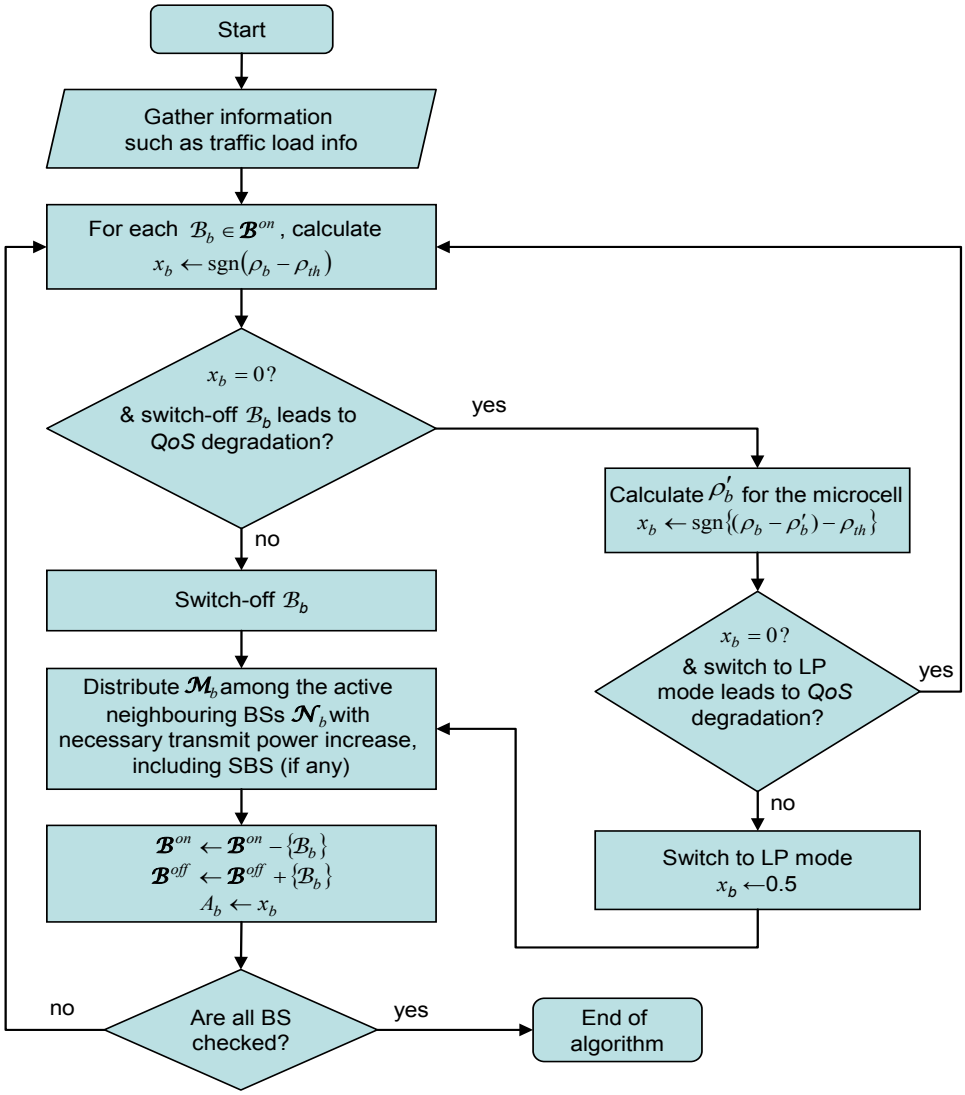

Figure 7-2: Flowchart of the MMBS (*active*/LP/*sleep*) algorithm.

switch from *sleep* to LP rather than directly to *active* mode according to (7.3), because of the lower static power consumed by LP mode micro BS. Once $\mathcal{B}_b$ is either in *active* (A_b = 1) or LP modes (A_b = 0.5) at any time instant, the corresponding traffic load respectively reverts to either the original macro BS or micro BS and its *active* neighbouring BSs $\boldsymbol{\mathcal{N}}_b$, $\mathcal{B}_b \in \boldsymbol{\mathcal{B}}^{\text{on}}$.

7.5 Results Discussion

To critically assess the performance of the new *scalable MMBS framework*, all simulation settings are exactly the same as that used for the *DTIA BS switching* algorithm presented in *Chapter 6*. An ISD of 1.5km between cells was considered with the microcell coverage radius being set at 200m. The corresponding micro BS settings were matched with those in

Table 3.1 and for this analysis *power model 2* defined in Table 2.1 was used for both macro and micro BSs. To maintain the QoS, the target blocking probability was set to 1% for $r_{\min}$=122kbps, while T_0= 15min is chosen giving a total of N_T = 96 time slots per day. It is assumed at least two neighbouring BSs will always be *active* to allow a BS to switch to either LP or *sleep* mode *i.e.*, $|\mathcal{N}_b| \geq 2$.

During the dynamic *BS switching* operation of the *scalable MMBS framework*, each BS can experience multiple switching between the three modes across a day. To demonstrate this, instantaneous traffic loads of two randomly chosen BSs ($\mathcal{B}_1$ and $\mathcal{B}_2$) are presented in Figure 7-3. As seen, both BSs are switched from either *active* to *sleep* or *active* to LP or LP to *sleep* or *sleep* to *active* or *sleep* to LP or LP to *sleep* mode for multiple times over the 24hr period. For example, both $\mathcal{B}_1$ and $\mathcal{B}_2$ go into *sleep* mode at 00:00 hours and remain in *sleep* mode until approximately 11:00 hours, while $\mathcal{B}_1$ with the MMBS stays in *sleep* mode longer than that with the *BS sleeping*. For $\mathcal{B}_1$, the MMBS model allows it to switch from *active* to LP mode much earlier at 18:30 than it is allowed by *BS sleeping* and stays in the LP mode for a long time (until 22:00) before it switches to *sleep* mode. Interestingly to

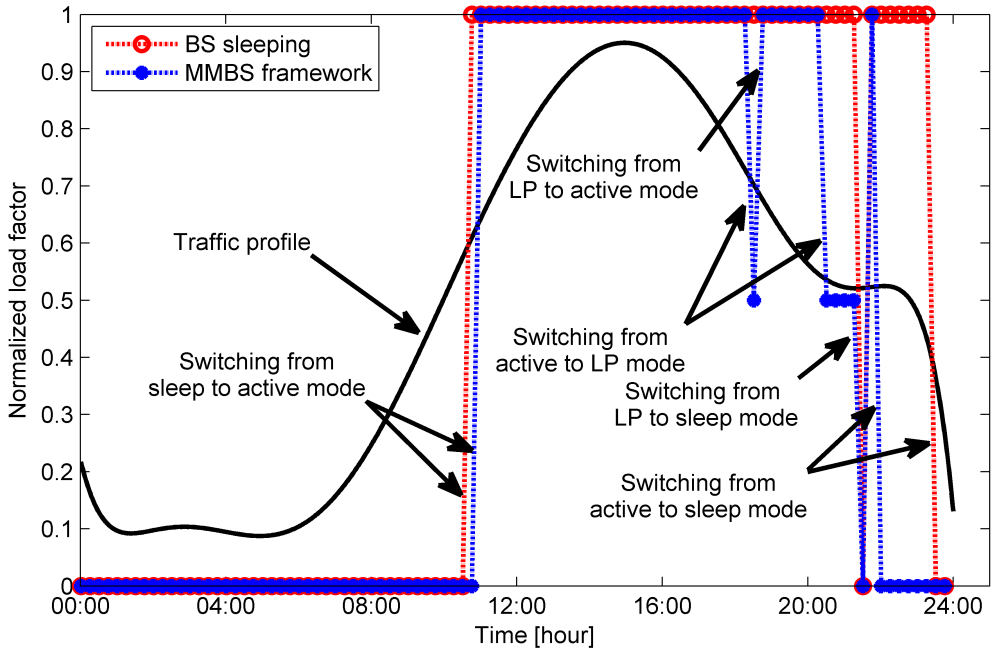

(a) Randomly chosen BS, $\mathcal{B}_1$.

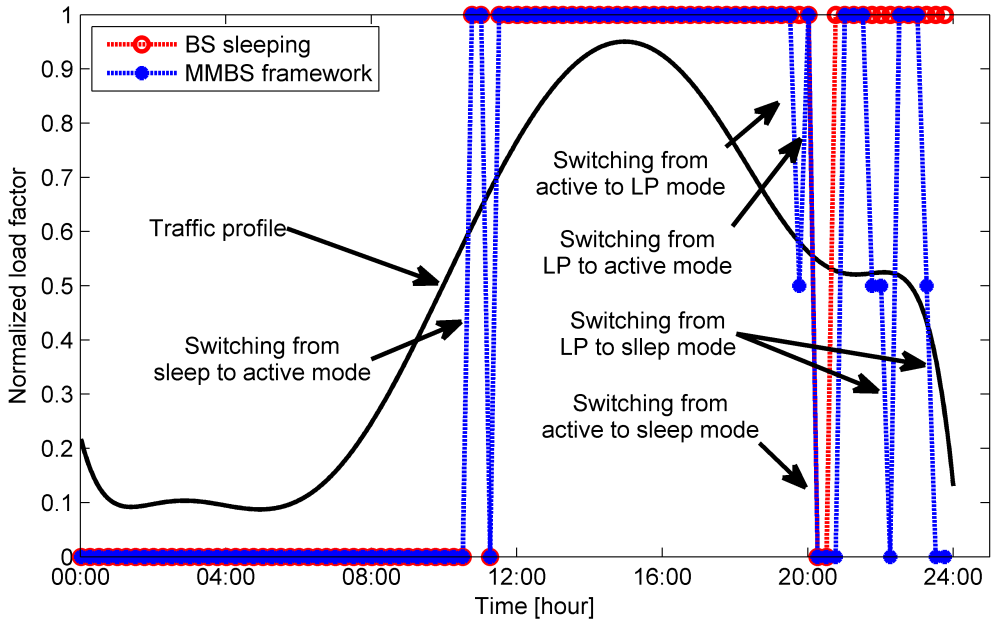

(b) Randomly chosen BS, $\mathcal{B}_2$.

Figure 7-3: Illustration of switching with both *BS sleeping* and the *scalable MMBS framework* for two arbitrary BSs across a day.

note that the *BS sleeping* model does not allow $\mathcal{B}_1$ to switch from *active* to *sleep* mode until 23:30 except a single switching shortly before 22:00, while in contrast the MMBS model switches $\mathcal{B}_1$ to LP mode, which is a better energy efficiency option than keeping it *active*. Therefore, keeping $\mathcal{B}_1$ in either LP or *sleep* mode for longer periods translates into a higher energy saving with the MMBS due to the lower static power consumption of LP mode micro BSs. Similar observations for $\mathcal{B}_2$ can be made on the performance of the MMBS model, which allows it to stay in either *sleep* or LP mode for a longer time period than the *BS sleeping*, which only allow BSs to switch between either *active* or *sleep* modes.

The number of *active* (macro) and LP (micro) mode BSs under the proposed MMBS framework is presented in Figure 7-4 for different normalized traffic loads per cell. For comparison purposes, results corresponding to the existing *BS sleeping* model are also included. The rate function of $f_1(t)$ is used to generate traffic as a load factor while the corresponding results for the other rate function $f_2(t)$ is displayed in Appendix C-1 for completeness. The key aim of the new framework is to reduce the number of *active* BSs

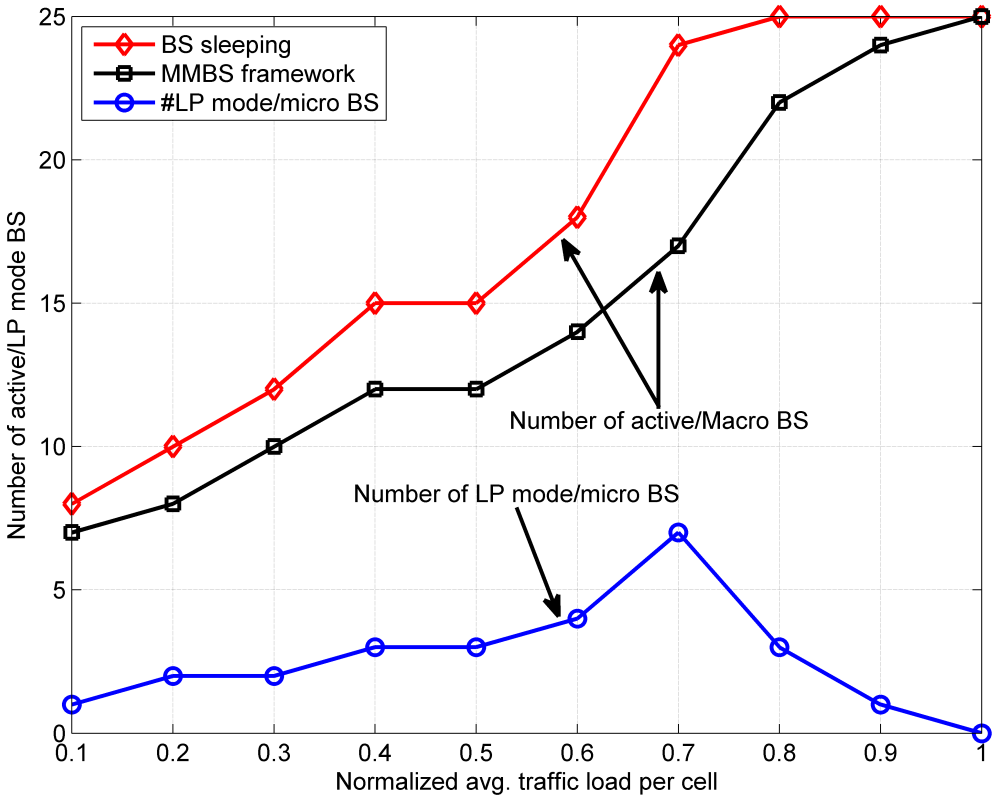

Figure 7-4: Number of *active* and LP mode BSs per day.

while providing the service coverage by means of LP mode micro BSs. The results show that the number of *active* BSs increases with the normalized cell traffic load both for the proposed MMBS and *BS sleeping* cases. It is evident that the number of *active* BSs, which are the high energy consuming macro BSs, is consistently lower with MMBS than with *BS sleeping*. For example, only 17 *active* and 7 LP mode BSs are enough to provide services to the considered area $\mathcal{A}$ for the MMBS model whereas the *BS sleeping* model requires 24 *active* BSs to provide the similar service coverage for the normalized cell traffic load of 0.7. The most revealing result in terms of energy conservation is that the new MMBS model is able to save considerably more energy due to the use of LP mode BSs that do not consume high static power. On the other hand, the *active* mode macro BS consumes high static power (see Figure 2-8) and the *BS sleeping* model requires a higher number of BSs in *active* mode to provide the similar service coverage. This means BSs are still under-utilized with the *BS sleeping* model at all traffic conditions as it had to keep the number of *active* BSs, which was actually not required for the given traffic load. These results also reveal that there was a larger number of LP mode BSs during medium to high traffic

conditions, specially at the normalized traffic load of 0.7, when the BS in *BS sleeping* model are mostly under-utilized as it requires a higher number of macro BSs to be kept in *active* mode.

In the *scalable MMBS framework*, the network is scaled by reducing the distance between two *active* BSs through the collocated micro BSs compared to the *BS sleeping* model, so the network power consumption relative to the coverage area can be evaluated as an elective performance measure. Figure 7-5 illustrates the APC for the three different BS switching strategies across an entire day. The results confirm that the MMBS consumed the lowest power per unit area (190 watts/km^2) compared with 400 watts/km^2 for *BS sleeping* and 580 watts/km^2 for the "*always-on*" strategy during low traffic periods. This saving is derived both from the lower transmit power required for microcell users and the reduced static power consumed by the LP mode micro BS in contrast with the high power consuming macro BS. As was evident in Figure 7-4, there exist more opportunities for the

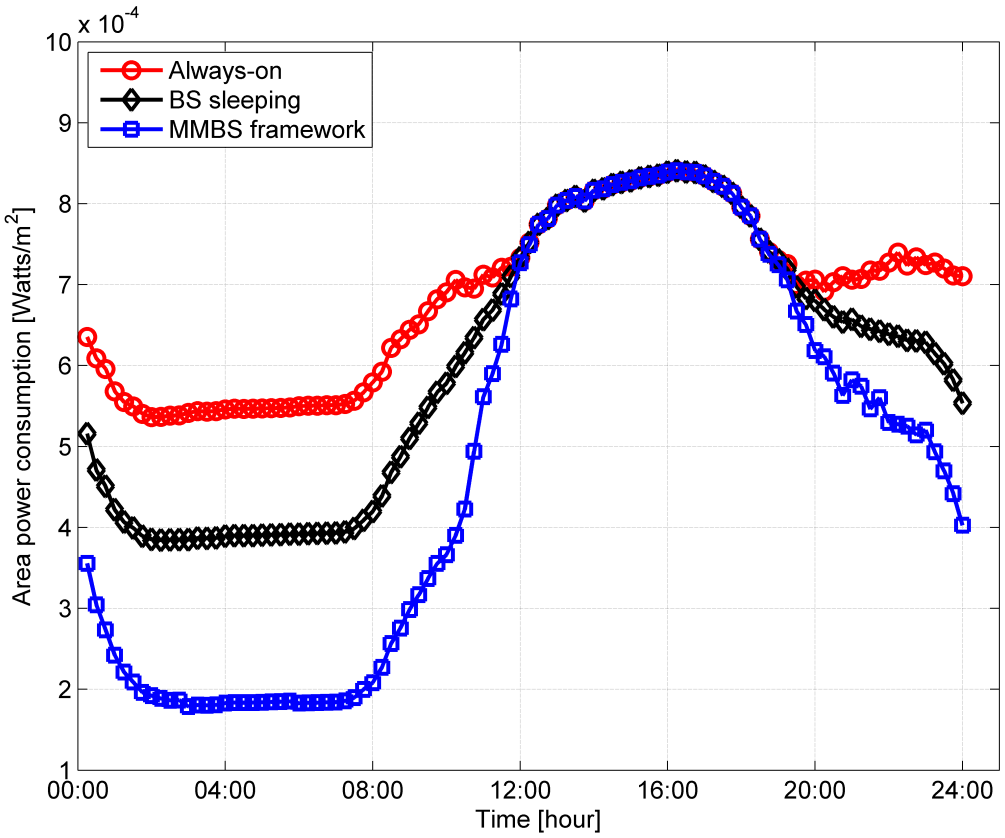

Figure 7-5: APC comparison for the *scalable MMBS framework*, *BS sleeping* and "*always-on*" models over a 24hr window.

MMBS to change mode to LP mode BS during the more demanding medium-to-high traffic periods, thereby securing further static power savings. Conversely, when no micro BSs are employed in *BS sleeping*, two scenarios can arise:

i) A BS is prevented from being put to *sleep* mode thus consuming high static power until the necessary condition is upheld, *i.e.*, the BS has to stay *active* for at least the next period and possible beyond.

ii) If the BS switches to *sleep* mode, the transmit power of neighbouring BSs must be increased to extend the coverage area for off-cell MS.

This means a higher number of *active* macro BSs are required to operate with the *BS sleeping* than in the new *scalable MMBS framework* and/or they require higher transmission power for off-cell MS. The results also reveal the APC for the "*always-on*" strategy is continually the highest except during the peak hours (12:00-19:00), and that the same level of power per unit area, *i.e.,* on average 790 watts/km^2, is consumed during the peak-traffic period for all three switching strategies.

The respective EE performances defined in (3.6) for the new power consumption model in (7.2) are given in Figure 7-6, which shows the number of bits delivered per unit energy for each switching strategy. For low-traffic periods, there is a noticeable improvement in EE for both the MMBS and *BS sleeping* models, which is especially significant for the new MMBS model, because the numerator term in (3.6), *i.e.*, the overall throughput is increased due to the collocated LP mode micro BS being activated instead of completely switching off the BS. Another reason is that wherever possible, the MMBS algorithm distributes off-cell MS among *active* and LP mode BSs, with the consequence that off-cell MS served by the LP mode BSs require lower transmit power while other off-cell MS served by neighbouring *active* macro BSs, incur comparatively higher transmit power. In contrast, in the *BS sleeping* all off-cell MS are required to be served by neighbouring *active* macro BSs that require higher transmit power to acquire the minimum QoS, due to the larger

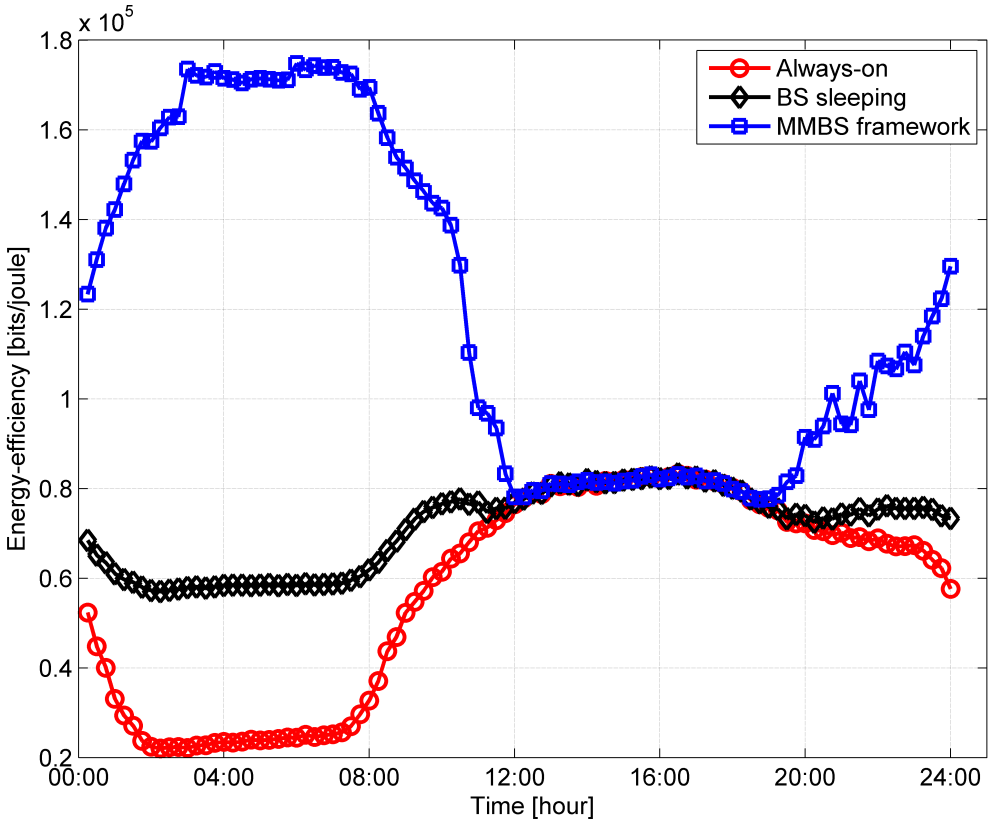

Figure 7-6: EE performance comparison of the new *scalable* MMBS *framework*, *BS sleeping* and "*always-on*" models over a 24hr window.

propagation distance between the off-cell MS and the neighbouring *active* BS. Thus, keeping certain BSs in LP mode instead of in *active* mode, result in lower energy consumption which ultimately translates into enhanced EE. For example, the EE for the MMBS during low-traffic period is on average 1.5×10^5 bits/joule higher than for *BS sleeping* (6.5×10^4 bits/joule), *i.e.*, on average over 56% EE improvement is achieved. As expected, the "*always-on*" mode consistently gave the poorest EE performance during low-traffic periods, while for the peak period, again no savings were feasible and all three strategies provided the same EE performance, an average 8×10^4 bits/joule.

Figure 7-7 compares the energy saving percentage of the new *scalable MMBS framework* and *BS sleeping* relative to the "*always-on*" strategy for different (normalized) traffic loads. The results reveal that a consistently higher percentage of energy savings is achieved by the MMBS (up to 55%) compared with *BS sleeping* (up to 52%), with the relative savings being greater at higher normalized traffic loads, which is a particular noteworthy

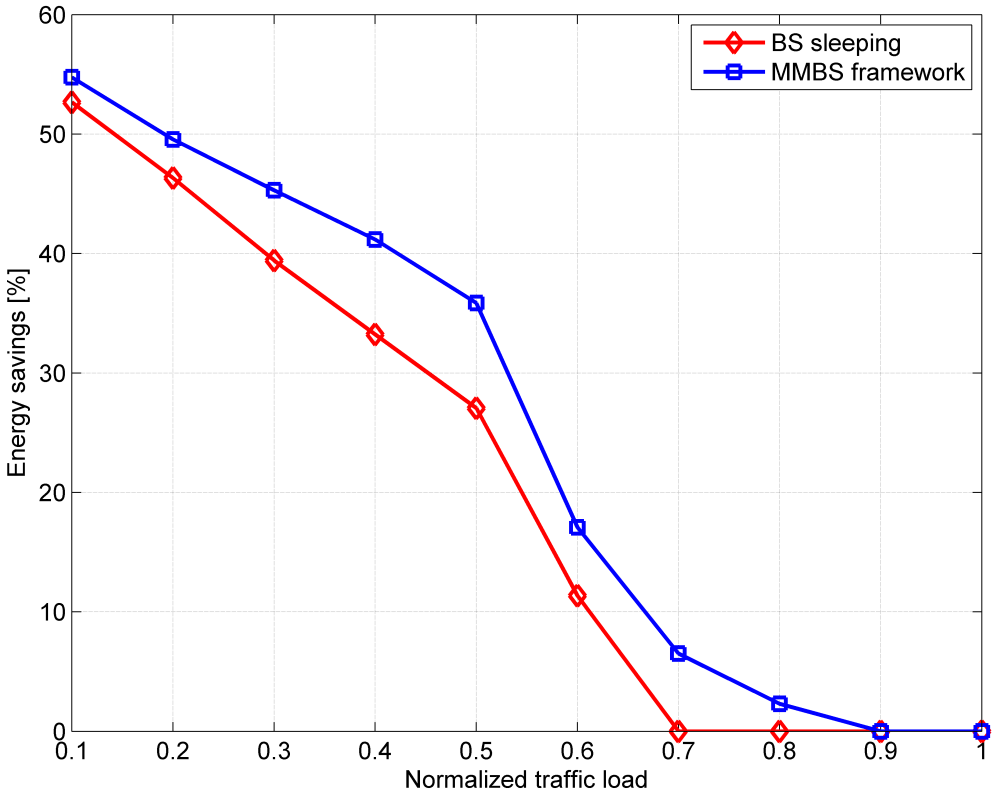

Figure 7-7: Comparison of the percentage of energy savings for the *scalable MMBS framework* and *BS sleeping* models relative to the "*always-on*" strategy.

feature of the new *scalable MMBS framework*. Note there are no savings with *BS sleeping* when the normalized traffic load is greater than 0.6 because this is the ρ_{th} value used in the simulations. Interestingly, the MMBS model can still save energy even when the normalized traffic load is higher than ρ_{th}, with ≈7% saving being achieved for traffic loads of 0.7 and even ≈3% at 0.8. The reason for this is a fraction of the traffic load is still able to be off-loaded to the switched LP mode BS rather than being kept in *active* mode, with the corollary being that the handed-over traffic load is then lower than the threshold.

Figure 7-8 plots the respective blocking probabilities averaged over 15min intervals across a 24hr time window. The average blocking performance for the MMBS and *BS sleeping* are consistently well below the 1% target at approximately 0.3% and 0.4% respectively. It is interesting to note that if the low blocking tolerance for the network is relaxed, then further significant energy savings are feasible by employing a higher switching threshold ρ_{th}. This means that there can be a higher number of *active* BSs to switch to either LP or

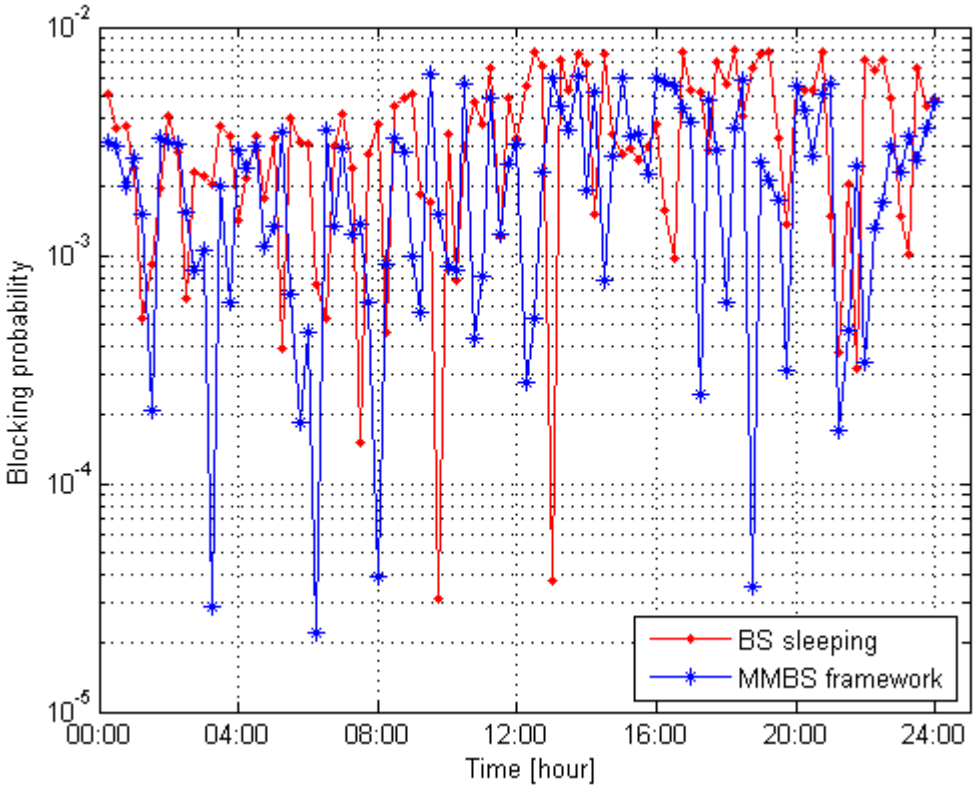

Figure 7-8: Blocking probability variations averaged over 15min intervals over a 24hr window.

sleep mode that translates into even a larger energy saving. For completeness, the corresponding blocking probability results for both ρ_{th}=0.7 and ρ_{th}=0.8 have been included in Appendix C-2, and they again demonstrate that they are also always within the target range at every instant, except during medium-to-high traffic conditions.

With the introduction of multimode switching, the number of switching instances defined in *Section 3.6.7* will in all probability increase and thus a higher energy cost will be incurred in comparison to existing dual-mode switching techniques like *BS sleeping* and *BS-RS switching*, although the switching energy cost has generally been ignored in the overall network energy consumption of these techniques, because it neither has a known energy cost value nor significant compared to the amount of energy saved. Figure 7-9 presents the CDF results of the number of switching instances for each BS per day for: i) switching from *active* to *sleep* mode for the *BS sleeping*, and ii) switching from *active* to LP or from *active* and/or LP to *sleep* for the MMBS model. The results clearly show for

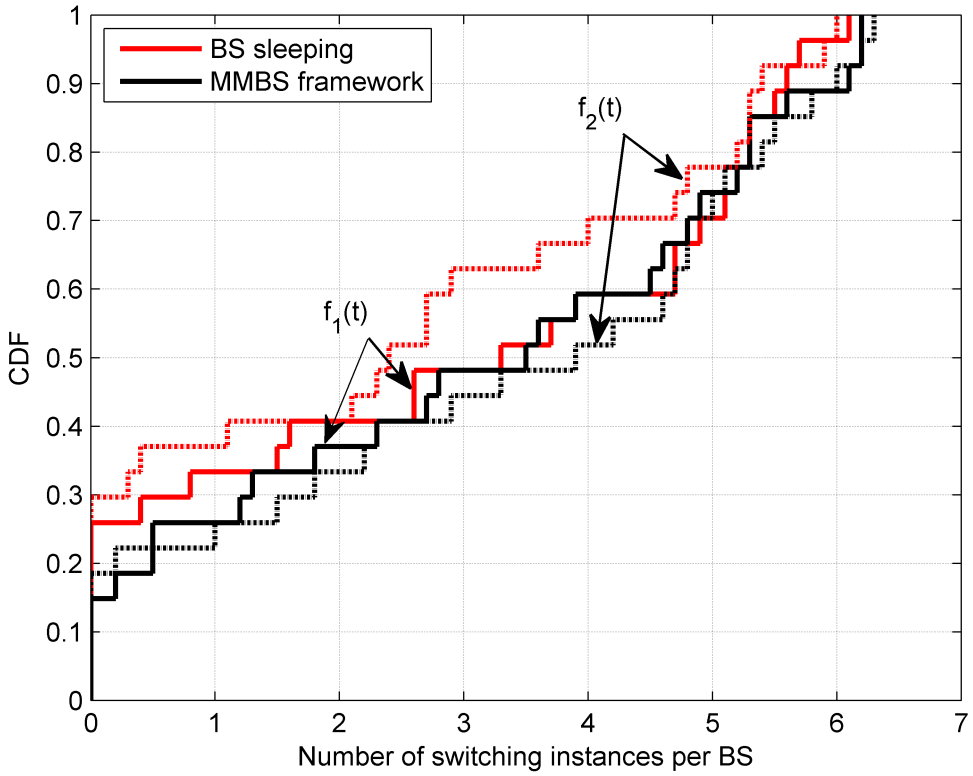

Figure 7-9: The cumulative distribution function of number of BS switching instances per day.

the $f_1(t)$ rate function that only 15% of BSs in the MMBS model never switch to *sleep* mode, while this falls to over 25% of BSs in *BS sleeping*, and these BSs conserve no energy for themselves. They do however contribute savings by sharing the traffic of other BSs and allowing them to remain in either *sleep* or LP modes for longer periods. This means the MMBS model switches an extra 10% of BSs into either LP or *sleep* modes, thereby resulting in greater energy savings. Closer analysis also reveals that 48% and 40% of BSs switched their modes four or more times each in 24hr period respectively for the $f_2(t)$ and $f_1(t)$ rate functions when MMBS is applied. Thus each of these BSs switches their modes at least four times out of a possible $N_T = 96$ decision slots each day. The corresponding switching percentages for the *BS sleeping* model are lower for both $f_2(t)$ (over 40%) and $f_1(t)$ (below 30%). While the higher number of BSs switching into either *sleep* or LP mode means to an overall conserving of energy, there will inevitably be some additional switching costs, though from the rigorous experiments undertaken, it is

Table 7.1: Total number of switching instances in the network per day.

Rate functions / Frameworks	$f_1(t)$ □	$f_2(t)$
BS sleeping	103	113
MMBS framework	123	127

important to stress that none of the BSs switched more than six times in any 24hr period for both models.

The average number of switching instances in the network per day for both models is summarised in Table 7.1 using (3.13). This interestingly reveals that the total number of switching instances incurred by the MMBS model for $f_1(t)$ and $f_2(t)$, represent a less than 10% and 12% increase respectively, with a correspondingly small increase in the total energy consumed. When this is pragmatically judged against both the overall network energy savings (Figure 7-6) and improved EE performance (Figure 7-7) achieved by the *MMBS framework*, it is still a notably superior solution compared to *BS sleeping*. It above all illustrates how this framework is able to effectively balance between energy saving by exploiting the LP and *sleep* modes, while only experiencing a small overhead in terms of the total energy consumed per-switching.

In collectively analysing these results, it is apparent the *scalable MMBS framework* offers a number of benefits for greener cellular networks. Firstly, it saves energy even in medium-to-high traffic load scenarios and makes the network scalable with respect to traffic demand by changing certain BSs modes accordingly. Secondly, the idea behind MMBS can be further exploited for *load balancing* by readily transferring traffic from one cell to another. Finally, even greater energy savings are achievable during low-traffic periods if the network is scaled down using further modes such as pico mode, though in introducing more modes, caution must be exercised as the potential energy savings may not necessarily improve significantly if the corresponding number of switching instances becomes

appreciably higher. There will also be the correspondingly impact on the switching energy costs of the *MMBS framework*, so reinforcing the observation made obviously on striking a judicious balance between energy savings and per-switching overheads.

7.6 Summary

A novel *BS switching* mechanism called the *MMBS framework* has been presented in this chapter for enhanced EE by deploying multiple BSs in each cell of a cellular network. The strategy is founded on the assumption each BS acts in a scalable fashion *i.e.*, can switch from high-power (macro) to intermediate LP (micro) or to *sleep* mode without incurring significant switching costs. Depending on current traffic conditions, when a BS changes its operating mode, priority is given to switching firstly to *sleep* mode and then to the new LP mode, so the BS is scalable in terms of traffic demands. While there may be some philosophical debate about the cost of deploying multiple BSs within a cell, the quantitative results analysis confirms up to 55% energy savings are feasible across an entire day with consistently superior APC and EE performance compared with the "*always-on*" and existing *BS sleeping* approaches, which is noteworthy when offset against the one-off deployment expenditure. Additionally, on average over 9% energy savings are also feasible by the *MMBS framework* during medium-to-high traffic conditions while the *BS sleeping* is unable to conserve any energy during those periods. The scalability solution also means higher energy saving percentages are envisaged with more switching modes *i.e.*, macro/micro/pico and *sleep*, though there is a potential trade-off with the resulting switching overheads. Moreover, this multimode model provides impetus to vendors to design and implement smarter *scalable XG* '*all-in-one*' BSs which more effectively adapt their operating modes to current traffic loads in order to reduce energy consumption.

Chapter 8

Future Work

There are a number of potential opportunities, both to enhance and extend the *BS switching framework*, which has been presented in this thesis in various productive directions. Some of these potential research openings will now be discussed.

- The research had the clear overarching objective of reducing energy consumption of the RAN in cellular networks by switching BSs between macro/micro and *sleep* modes. The *scalable MMBS framework* which has been developed can be extended to embrace more switching modes so improving the overall network EE at smaller scales. For example, each BS can have the capability to switch to any of the following modes: macro, micro, pico and *sleep* depending upon the prevailing cell traffic and interference conditions. The energy consumption impact on both BS and MS will be more readily apparent in the new *BS switching framework* as the number of *active* macro BSs will be reduced, while other low-power BSs take on the responsibility of maintaining service coverage. Despite the one-off overhead of deploying multiple BSs in each cell in the *scalable MMBS framework*, the emerging low-cost smarter '*all-in-one*' BSs and the amount of energy saved will reduce this cost. Importantly, this new model provides impetus to vendors to design and implement intelligent BSs which more adaptively adjust their operating modes to current traffic loads to reduce energy consumption.

- To overcome several performance limitations including the *spectrum efficiency* (SE) and coverage of the conventional macrocell networks, the notion of multi-tier heterogeneous networks deploying small cell BS within the macrocell coverage has gained universal recognition (Hu & Qian, 2014; Soh et al., 2013). This thesis proposed and investigated energy saving mechanisms for homogeneous cellular networks having macrocells only. One potentially interesting research project would be to investigate

extending the proposed *BS switching framework* to more complex scenarios of heterogeneous networks. However, one of the major challenges in heterogeneous networks is the incursion of ICI due to aggressive frequency reuse, which can reduce the effectiveness of the heterogeneous networks (Soh et al., 2013). This challenge can even be severe when some BSs switch to *sleep* while others increase their transmit power. As a result, it would be interesting to assess the DTIA algorithm for the new *BS switching framework* in such a complex scenario as well as developing advanced traffic-aware and spectrum-aware joint cognitive BS switching techniques in improving both EE and SE.

- To improve EE while guaranteeing coverage and services, the recently proposed concept of separation architecture by Xu et al., (2013) and Wang et al., (2014) seems to offer a promising alternative compared to conventional cellular networks, wherein the macrocell BS provides a wide coverage for control signals whereas small-cell traffic BS dynamically handles only the user traffic. This means there is a logical separation of data and control planes within the system architecture. As has been well documented, cellular traffic varies both temporally and spatially, so coordinated switching of some small-cell BSs on and off, depending on necessity, would represent a valuable extension of the work presented in this thesis.

  Since wireless users are indoors for around 80% of time while only being outdoors about 20% of the time (C.-X. Wang et al., 2014), the wireless signals for indoor users communicating with outdoor BSs have to endure potentially very high penetration losses due to buildings and walls, leading to significantly degraded data rates, EE and SE of wireless transmissions. An alternative cellular architecture design strategy (C.-X. Wang et al., 2014) would be to separate outdoor and indoor scenarios so that penetration losses due to buildings, etc. can be avoided. DAS and massive MIMO technologies (Joung, Chia, et al., 2014), where geographically distributed antenna arrays

with tens or hundreds of antenna elements are deployed, will assist in achieving the goal.

- Another attractive option for reducing energy consumption is to offload cellular traffic onto direct *device-to-device* (D2D) connections and/or Wi-Fi connections whenever the users involved are in close proximity (Andreev et al., 2014). Despite the undoubted commercial success, Wi-Fi connections often suffer from a number of drawbacks including stringent session continuity limitations, excessive user contention, and cumbersome manual setup/security procedures. As a result, D2D communications with their advantage of using *millimetre wave* (mmWave) spectrum, higher data rates, lower transfer delays, and better EE has given impetus to academic and industrial activities aimed at the standardization of D2D communications (3GPP, 2013). Academia and industry have aggressively pursued research standardization of D2D communications over the past couple of years (Astely et al., 2013). In this context, both the BS and MS need to incorporate a greater intelligence capability compared to traditional units, while a robust channel model for D2D communications also needs to be formulated, so rigorous investigation can be undertaken to achieve those D2D benefits in practice, for future 5G cellular networks.

- Due to the high energy consumption by the network itself, future generation networks will face even great challenges to providing electricity for networks, especially in remote areas. It is also anticipated that future BSs will be powered by multiple renewable energy sources like solar and wind energy together with on-grid energy sources. However, climate conditions and as a consequence, renewable green energy generation can vary from location to location so there will be a requirement to optimize the energy usage in such a way that BSs are first powered by renewable energy if they have enough renewable energy storage. Otherwise, the BS will have to switch to on-grid energy in order to serve mobile users. Another possible way to maximize the energy

utilization is to adjust cell sizes depending upon the available renewable energy. For example, some BSs may run out of green energy and switch to on-grid energy supplies by shrinking their cell sizes or switching to *sleep* mode while the other BSs may have surplus green energy stored in their batteries, and so are able to expand their cell sizes. This additional *green energy availability* parameter in a BS can then be considered as possibly an extra decision parameter within the presented *BS switching framework*. Therefore, development of hybrid energy sources scheduling and equipment switching strategies for minimizing the on-grid energy usage will increasingly assume importance both from the environmental and economic perspectives.

Chapter 9

Conclusions

The unprecedented growth in data traffic has led to the issue of energy consumption in cellular networks becoming a major political, financial, environmental and social issue for network vendors and regulators alike, with ever more demands and targets for greener networks. A by-product of this traffic growth is that both the number of connected devices and density of cellular networks have correspondingly increased, with the consequence that their carbon footprint is expected to triple between 2007 and 2020. The task of achieving 'greener' communications has to be addressed from a range of diverse perspectives. While BSs are the most energy intensive equipment (typically 60%-80% of total network energy consumption), they are generally under-utilized for large parts of the day because of their traditional "*always-on*" operating mode. This provided the key motivation to investigate minimizing the energy consumption of cellular BSs by innovatively developing *BS switching* strategies without compromising the requisite QoS. Existing energy-aware *BS switching* strategies invariably compromise the overall QoS, which means new *BS switching* strategies are required to ensure greener cellular networks can operate more energy efficiently, while maintaining QoS.

This thesis has presented a new *BS switching framework* which comprises a suite of innovative cellular models and algorithms to reduce BS energy consumption by exploiting the natural temporal-spatial traffic diversity in dynamically switching BSs between different power modes (*active*/*dormant*), while always upholding requisite QoS provision. The new *BS switching framework* has been tested by faithfully following the guidelines provided in the 3GPP LTE and IEEE 802.16 standards, with most system parameter settings being defined according to the 3GPP LTE standard for validation and comparative performance analysis purposes.

The new *BS switching framework* includes four original scientific contributions to green cellular networks, which are summarised as follows:

i) The most significant is a *scalable MMBS framework* which adapts network capacity and dynamic traffic demands to facilitate BS switching to different power modes. Unlike traditional dual-mode *BS sleeping*, the *MMBS framework* consists of multiple collocated BSs in every cell, with each having different BS power modes, *i.e.*, *active* (macro), LP (micro) or *sleep*, so each BS is able to operate in multimodal fashion. In this framework, many BSs which are not allowed to switch to *sleep* mode using the traditional dual-mode *BS sleeping* model because of QoS constraints, are permitted to switch to LP mode rather than being kept in an *active* or high-power macrocell BS mode. As a result, a large number of *active* BSs is switched to LP or microcell BSs mode that alone provide the required service coverage together with the remaining *active* BS. A noteworthy feature of MMBS is that energy savings are achieved even during high traffic load conditions, by always keeping a minimum number of *active* BSs whilst prioritising the BS to be switched first into either *sleep* or LP mode, so reducing the high static power consumption of the macro BS. Rigorous quantitative results confirm the new model provides on average up to 55% energy savings across a full day compared with the traditional "*always-on*" cellular operation, while still guaranteeing minimum QoS.

ii) A new BS to RS (*BS-RS*) *switching* model together with its power model has been proposed to address the coverage hole problem in *BS sleeping*, while maximizing the EE by switching BS to a collocated RS or *x-RS* instead of turning it to *sleep* mode. This model ensures uninterrupted communications between BS and MS as well as providing similar QoS level to the "*always-on*" mode of operation. A particular challenge to be resolved is that of off-cell user throughout close the centre of a sleeping cell in the *BS sleeping* model, which can become degraded due to severe

propagation attenuation. The new *BS-RS switching* model significantly improves the throughput with the switching between *active* and RS modes being dynamically taken based on temporal traffic variations on an hourly basis. By initially adopting a *fixed threshold based BS switching* mechanism, which is then subsequently generalised to afford greater flexibility and robustness in the switching process, results confirm the energy consumed by both BS and MS can be reduced by up to 30% and 38% respectively, compared with existing approaches, without compromising the user throughput.

iii) Founded upon the rigorous analysis of the *BS-RS switching* model using a *fixed threshold based BS switching* algorithm, which only exploits temporal traffic diversity, a new *adaptive threshold based BS switching* algorithm exploiting both temporal and spatial traffic diversity was developed and critically evaluated. This adaptive solution not only has the capability to adjust the threshold flexibly in making switching decisions, but also consistently provides enhanced energy savings across an entire day in a relay-deployed cellular network. The algorithm has been designed based on a seven-cell cluster arrangement with the BS considered as a CC in the management of switching decisions. A strategy on how best to distribute off-cell MS amongst neighbouring BSs has been formulated in which higher-load BSs in *active* mode allow lower-load BSs to be switched to dormant mode. The new algorithm has been successfully integrated into both *BS sleeping* and *BS-RS switching* models, with the later providing consistently superior performance. To maintain a desired target blocking probability, the impact of a *tolerance margin* δ has been analysed. By gradually increasing this margin, the corresponding effect on the overall energy savings performance was assessed, with results verifying energy reductions up to 53% achieved at $\delta = 0.1$, and while even greater savings are feasible with a zero tolerance margin, this comes at the cost of much higher blocking probabilities.

iv) Finally, the *BS switching framework* has been extended further to incorporate the impact of interference in making the BS switching decisions via the development of a novel DTIA algorithm. Unlike traditional DTA algorithms, DTIA employs a two-stage switching decision-making process for any BS to change to dormant mode, combining the switching criteria of the existing DTA techniques with the interference level in each cell, and giving priority to those BSs which have the highest estimated interference. DTIA has a significant influence on both energy savings and the performance of off-cell user's throughput. It is important to stress that on average both DTIA and DTA algorithms switch the same number of BSs to dormant mode, but their respective selections are very different. DTIA chooses the best BS set to be *active* from an interference context thereby affording improved EE as a result of improved UL and DL qualities. DTIA has been seamlessly incorporated into both the *BS sleeping* and *BS-RS switching* models to determine the best BS set to be kept *active*, with DTIA consistently performing better in both models. Results also confirm the DTIA algorithm provides more than 22% EE improvement over DTA, while at the same time reducing by more than 5% of the net energy consumption by MS.

The presented *BS switching framework* is a scalable green solution to lower energy consumption in cellular networks. The models and algorithms developed to answer the overarching research question are compatible with current cellular infrastructure (LTE) through the co-deployment of additional micro BSs and RSs. The framework dynamically manages cellular BSs in an energy efficient manner, while crucially upholding QoS provision so overcoming a major bottleneck in existing green networks. Most importantly, the *BS switching framework* provides reliable energy savings from both a BS and MS perspective, even for challenging high-traffic scenarios, where existing *BS sleeping* techniques fail. Finally in the broader context, the presented framework makes a notable contribution to the on-going debate amongst key network stakeholders, into how best to lower energy consumption while accommodating the predicted growth in cellular traffic. It

above all delivers impetus to vendors to design and implement smarter '*all-in-one*' BS solution for multiple purposes as part of their XG network strategies.

Appendix

Appendix A: Comparative transmission strategies of *BS sleeping* and *BS-RS switching*

When a BS switches into *sleep* mode (Figure A-1(a)), any off-cell MS which is required to communicate with an *active* neighbouring BS, experiences a high propagation PL due to the increased propagation distance between them resulting in higher transmission power requirements. On the other hand, in the *BS-RS switching* model, the *active* neighbouring BS communicates with the off-cell MS via the collocated *x-RS* as shown in Figure A-1(b).

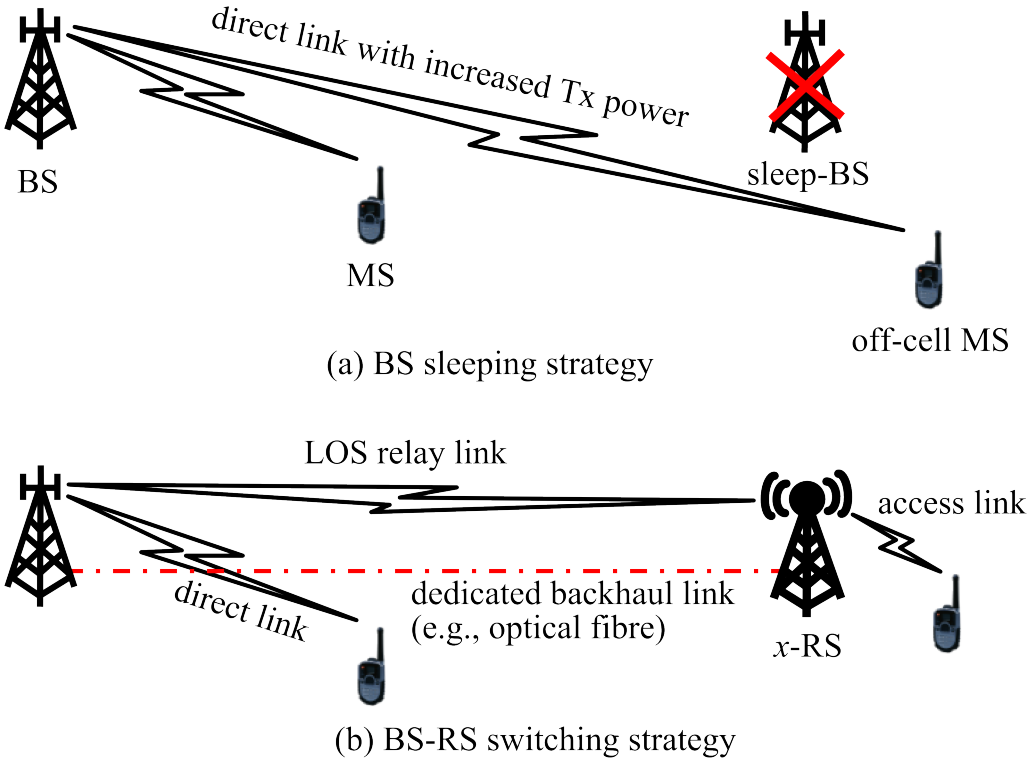

Figure A-1: (a) The BS has to increase its transmit power for serving the off-cell MS in the case of *BS sleeping* strategy; (b) The BS can communicate to the off-cell MS via the *x-RS* while the lower amount of BS transmission is required for the line-of-sight (LOS) relay link, which can be negligible if a dedicated link is used as the relay link.

Appendix B: The percentage of power consumption for tolerance margins δ=0 and 0.2.

The percentage of energy savings is highly dependent upon the tolerance margin. For δ=0.0, a higher energy saving was achievable as shown in Figure B-1(a) with a higher cost of blocking probabilities (see Figure 5-9). On the other hand, for δ=0.2 the *adaptive threshold based* algorithm still provided a feasible percentage of energy savings as shown in Figure B-1(b)while the blocking probability was low.

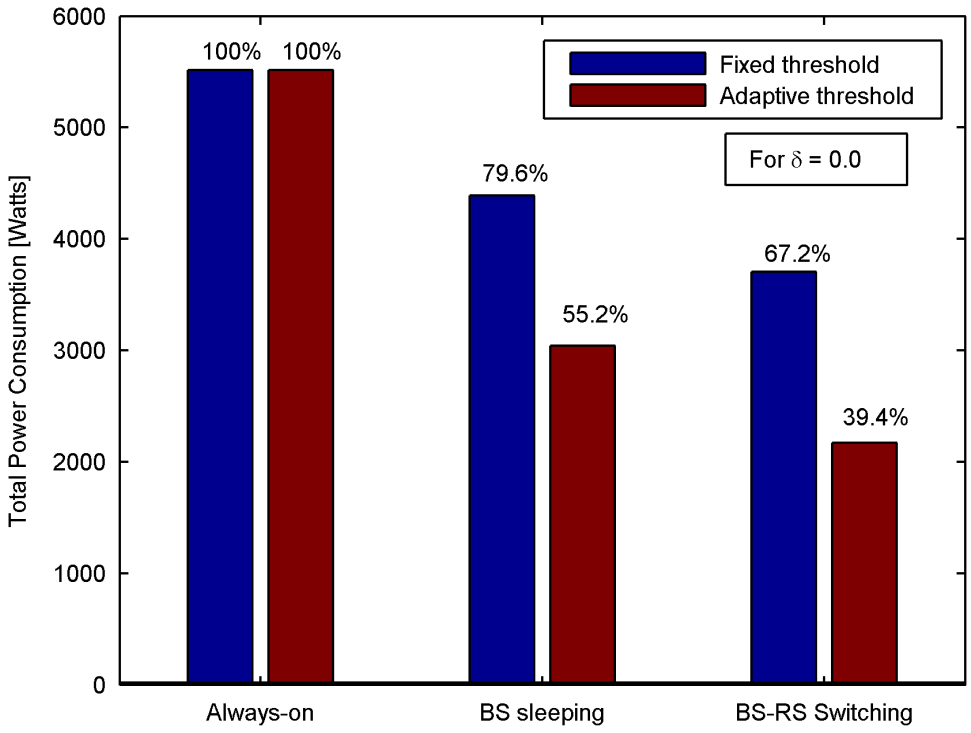

(a)

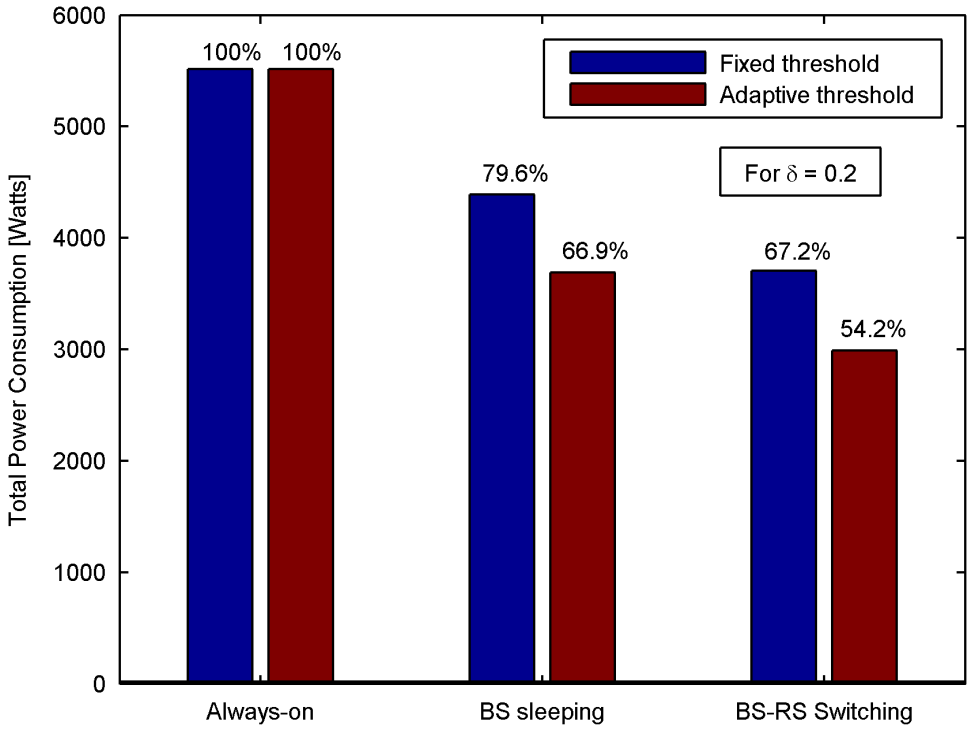

(b)

Figure B-1: The percentage of energy consumption in different BS operation modes for a whole day period for δ = 0.0 and 0.2.

Appendix C: The performance results of the *scalable MMBS framework* for the rate function $f_2(t)$ and different switching threshold values.

Due to the high fluctuation of the considered traffic profiles using the rate function $f_2(t)$, the number of *active* BSs in both models is higher for using $f_2(t)$ than for using $f_1(t)$ as shown in Figure C-1.

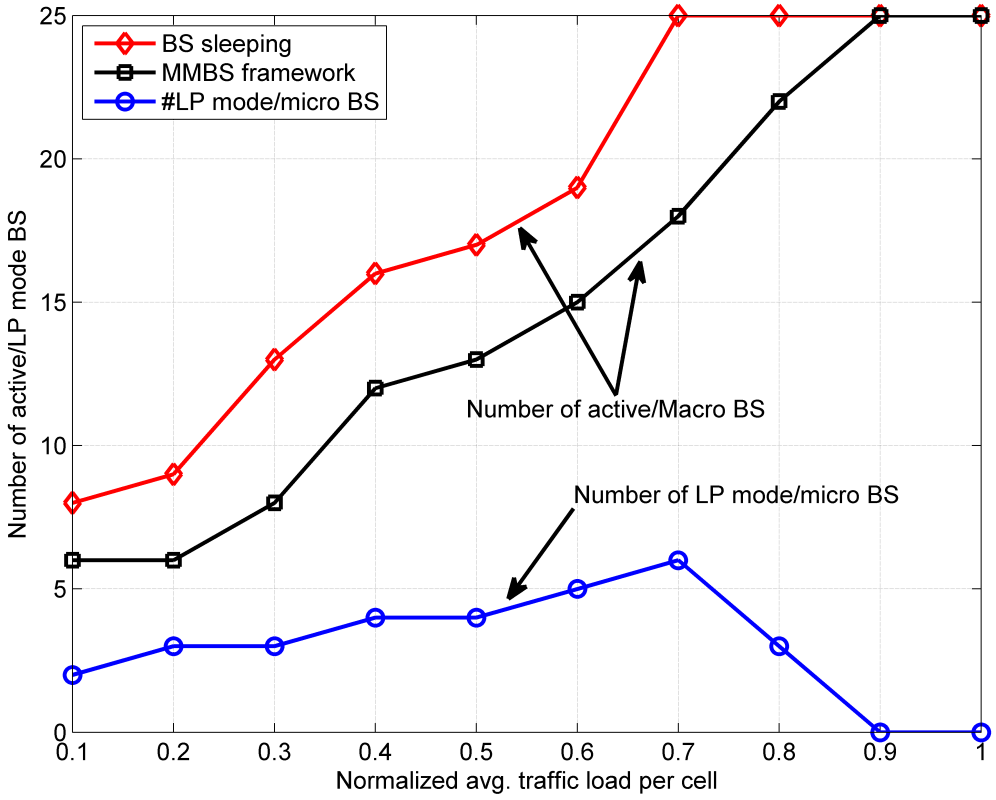

Figure C-1: Number of *active* (macro) and LP mode (micro) BSs per day for $f_2(t)$.

The following set of graphs as shown in Figure C-2 represent the blocking probability performances of the *scalable MMBS framework* and the existing *BS sleeping* model for higher switching thresholds, ρ_{th}=0.7 and 0.8. Both graphs show that the blocking probabilities increased for both ρ_{th}=0.7 and 0.8 compared with it for both ρ_{th}=0.6 (See Figure 7-8), the blocking probability is higher for ρ_{th}= 0.8 (Figure C-2(b)) than that for ρ_{th}=0.7 (Figure C-2(b)).

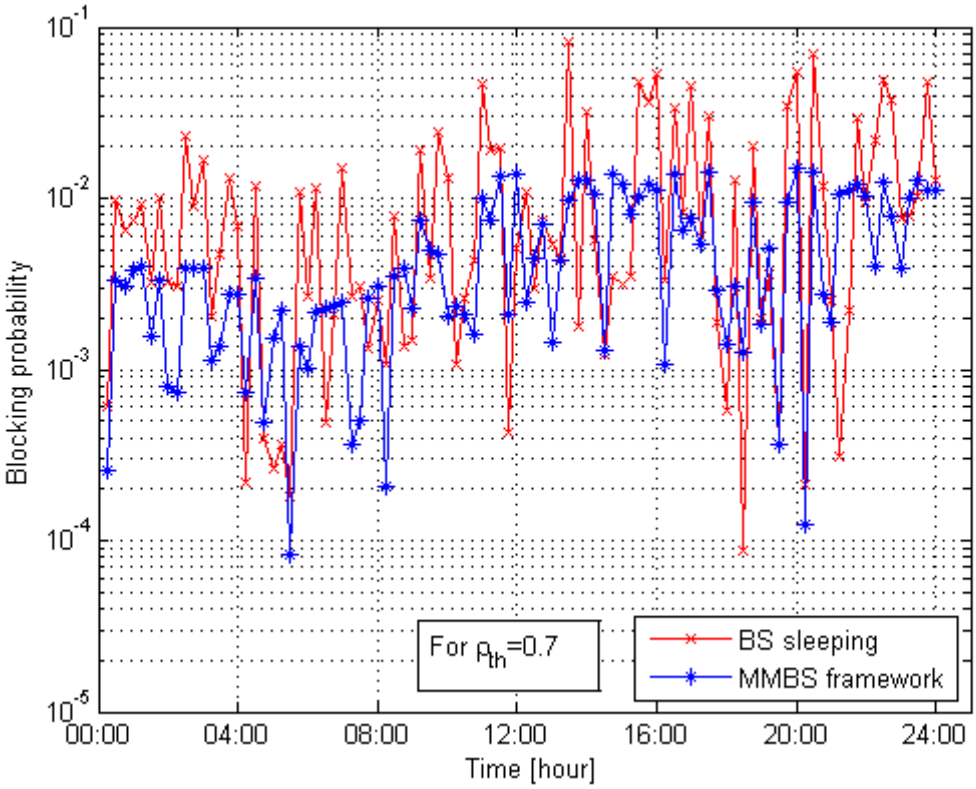

(a) For switching threshold, ρ_{th}=0.7

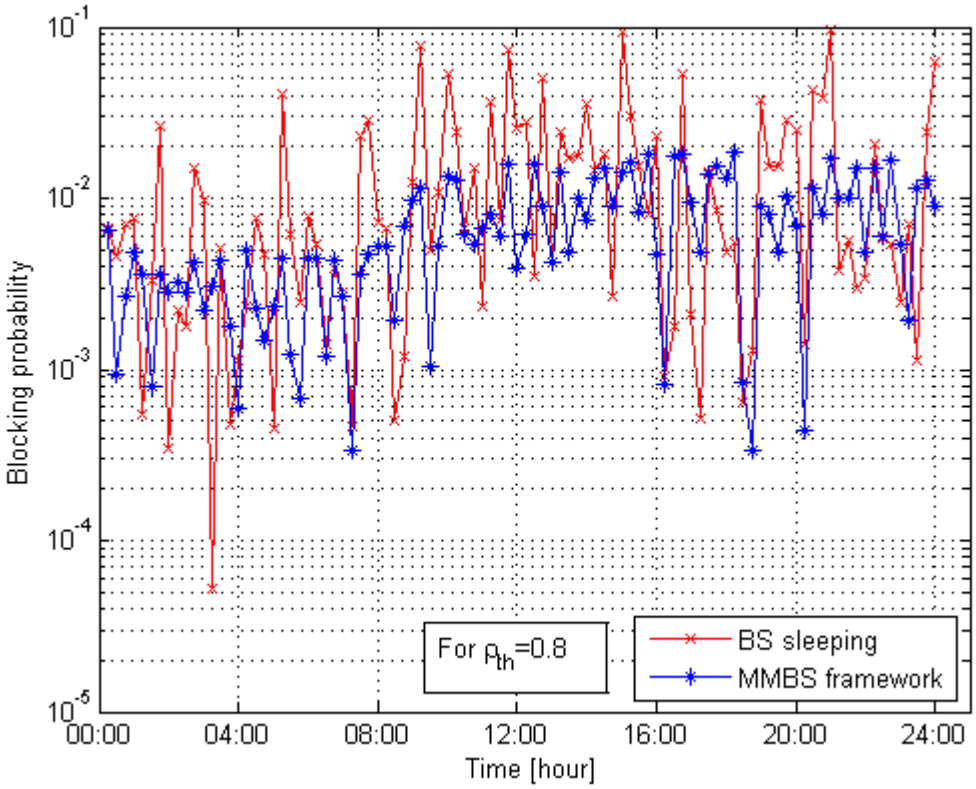

(b) For switching threshold, ρ_{th}=0.8

Figure C-2: Blocking probability variations for different switching thresholds.

References

3GPP (2013) “TR 22.803, Feasibility study for Proximity Services (ProSe) (Release 12) v12.2.0,” ETSI.

3GPP (2006) “TR 25.814, Radio Access Network, Physical layer aspects for evolved Universal Terrestrial Radio Access (UTRA) (Release 7) v7.1.0,” *ETSI*.

3GPP (2010a) “TR 32.826, Study on Energy Savings Management (ESM) (Release 10) v10.0.0,” *ETSI*.

3GPP (2010b) “TR 36.806, Evolved Universal Terrestrial Radio Access (E-UTRA) - Relay architectures for E-UTRA (LTE-Advanced) (Release 9) v9.0.0,” *ETSI*.

3GPP (2010c) “TR 36.814, Evolved Universal Terrestrial Radio Access (E-UTRA), Further advancements for E-UTRA physical layer aspects (Release 9) v9.0.0,” ETSI.

3GPP (2011a) “TR 36.912, Feasibility study for further advancements for E-UTRA (LTE-Advanced) (Release 10) v10.0.0,” *ETSI*.

3GPP (2010d) “TR 36.942, Radio frequency system scenarios (Release 9)”, V9.2.0,”.

3GPP (2009a) “TS 102 706, Environmental engineering, energy efficiency of wireless access network equipment, V1.1.1,” *ETSI*.

3GPP (2011b) “TS 36.101, Evolved Universal Terrestrial Radio Access (E-UTRA) User Equipment (UE) radio transmission and reception (Release 10) v10.3.0,” ETSI.

3GPP (2009b) “TS 36.213, Evolved Universal Terrestrial Radio Access (E-UTRA) Physical layer procedures (Release 8) v8.8.0,” *ETSI*.

3GPP (2008) “TS 36.420, Evolved Universal Terrestrial Radio Access Network (E-UTRAN), X2 general aspects and principles (Release 8) v8.0.0,” ETSI.

Alam, A. S. (2011) “Cognitive radio – an enabling technology for green wireless communications?,” Milton Keynes, The Open University.

Alam, A. S. ., Dooley, L. S. . and Poulton, A. S. . (2011) “Dynamic spectrum access based on cognitive radio within cellular networks,” In *IEEE Wireless Advanced (WiAd)*, London, pp. 85–89.

Alam, A. S. ., Dooley, L. S. . and Poulton, A. S. . (2012) “Energy efficient relay-assisted cellular network model using base station switching,” In *IEEE Global Communications Conference (GLOBECOM) Workshop*, pp. 1155–1160.

Alam, A. S. ., Dooley, L. S. . and Poulton, A. S. . (2013) “Traffic-and-interference aware base station switching for green cellular networks,” In *IEEE CAMAD*, Berlin, German, pp. 1–6.

Alam, A. S. and Dooley, L. S. (2015) “A scalable multimode base station switching model for green cellular networks,” In *IEEE Wireless Communication and Networking Conference (WCNC)*, pp. 1–6.

Alam, A. S., Dooley, L. S., Poulton, A. S. and Ji, Y. (2012) “Energy savings using an adaptive base station-to-relay station switching paradigm,” In *International Conference on Wireless Communications and Signal Processing (WCSP)*, Huanshan, China, pp. 1–6.

Ambrosy, A., Auer, G., Blume, O., Caretti, M., Eilenberger, G., Erdem, A., Fantini, R., Fazekas, P., Fehske, A. J., Gódor, I., Héliot, F., Holtkamp, H., Imran, M. A., Marsch, P., Maugars, P., Olsson, M., Pellón, A., Rubio, J. A., Sabella, D. and Skillermark, P. (2012) “Definition and Parameterization of Reference Systems and Scenarios,” *EARTH Project D.2.2*.

Andreev, S., Pyattaev, A., Johnsson, K., Galinina, O. and Koucheryavy, Y. (2014) "Cellular traffic offloading onto network-assisted device-to-device connections," *IEEE Communications Magazine*, IEEE, 52(4), pp. 20–31.

Anon (2012a) "Digital agenda: EU research breakthrough will cut 4G/LTE mobile network energy use in half," European Commission - MEMO/12/327.

Anon (2010a) "EARTH: energy aware radio and networks technologies," [online] Available from: https://www.ict-earth.eu/ (Accessed 20 March 2014).

Anon (2013) "Flatten network energy consumption," *White paper*, [online] Available from: http://nsn.com//file/28586/nsn-tv2020-flatten-network-energy-white-paper (Accessed 30 December 2013).

Anon (2011) "GREENET," [online] Available from: http://www.fp7-greenet.eu/default.php (Accessed 20 June 2012).

Anon (2010b) "GreenTouch," [online] Available from: http://www.greentouch.org/index.php?page=about-us (Accessed 1 February 2012).

Anon (n.d.) "IEEE ComSoc Best Reading Topics on Green Communications," [online] Available from: http://www.comsoc.org/best-readings/topics/green (Accessed 20 March 2014a).

Anon (2010c) "IEEE P802.3az: Energy Efficient Ethernet Task Force," [online] Available from: http://www.ieee802.org/3/az/ (Accessed 18 January 2014).

Anon (2012b) "IEEE Standard 802.16 for air interface for broadband wireless access systems," IEEE Computer Society.

Anon (2012c) “MIMO and smart antennas for mobile broad systems,” [online] Available from: http://www.4gamericas.org/documents/MIMO and Smart Antennas for Mobile Broadband Systems Oct 2012x.pdf (Accessed 12 April 2013).

Anon (n.d.) *Mobile Energy Efficiency (MEE) Benchmarking*, [online] Available from: http://www.gsma.com/publicpolicy/mobile-energy-efficiency/mobile-energy-efficiency-benchmarking (Accessed 5 September 2013b).

Anon (n.d.) “MVCE Green Radio,” [online] Available from: http://www.mobilevce.com/green-radio (Accessed 20 March 2014c).

Anon (n.d.) “OPERA-Net 2: Optimising Power Efficiency in mobile RAdio Networks 2,” [online] Available from: http://www.celticplus.eu/Projects/Celtic-Plus-Projects/2011/OPERA-NET2/operanet2-default.asp (Accessed 12 December 2011d).

Anon (n.d.) “OPERA-Net: Optimising Power Efficiency in mobile RAdio Networks,” [online] Available from: http://www.celticplus.eu/pub/Project-leaflets/Webquality/opera-net-lq.pdf (Accessed 20 February 2011e).

Anon (2012d) “Sustainability 2012 Summary Report by Vodafone,” *Vodafone Group*, Vodafone Group, [online] Available from: http://www.vodafone.com/content/dam/vodafone/about/sustainability/reports/2011_12/vodafone_sustainability_report.pdf (Accessed 14 June 2013).

Anon (2014) “US wireless and wireline voice: threats and opportunities,” *The Insight Research Corporation*, The Insight Research Corporation.

Arnold, O., Richter, F., Fettweis, G. and Blume, O. (2010) “Power consumption modeling of different base station types in heterogeneous cellular networks,” In *Future Network and Mobile Summit*, pp. 1–8.

Ashraf, I., Boccardi, F. and Ho, L. T. W. (2011) “SLEEP mode techniques for small cell deployments,” *IEEE Communications Magazine*, 49(8), pp. 72–79.

Astely, D., Dahlman, E., Fodor, G., Parkvall, S. and Sachs, J. (2013) “LTE release 12 and beyond,” *IEEE Communications Magazine*, 51(7), pp. 154–160.

ATIS (2010) “ATIS report on wireless network energy efficiency,” *Alliance for Telecommunications Industry Solutions,*.

Auer, G., Blume, O., Giannini, V. and Godor, I. (2012) “Energy efficiency analysis of the reference systems, areas of improvements and target breakdown,” *EARTH Project D.2.3*.

Badic, B., O’Farrrell, T., Loskot, P. and He, J. (2009) “Energy efficient radio access architectures for green radio: large versus small cell size deployment,” In *2009 IEEE 70th Vehicular Technology Conference Fall*, pp. 1–5.

Bhat, P., Nagata, S., Campy, L., Berberana, I., Derham, T., Liu, G., Shen, X., Zong, P. and Yang, J. (2012) “LTE-advanced: an operator perspective,” *IEEE Communications Magazine*, 50(2), pp. 104–114.

Bhaumik, S., Narlikar, G., Chattopadhyay, S. and Kanugovi, S. (2010) “Breathe to stay cool: adjusting cell sizes to reduce energy consumption,” In *1st ACM SIGCOMM workshop on Green networking*, pp. 41–46.

Bianzino, A. P., Chaudet, C., Rossi, D. and Rougier, J.-L. (2012) “A survey of green networking research,” *IEEE Communications Surveys & Tutorials*, 14(1), pp. 3–20.

Blume, O., Eckhardt, H. and Klein, S. (2010) “Energy savings in mobile networks based on adaptation to traffic statistics,” *Bell Labs Technical Journal*, 15(2), pp. 77–94.

Boiardi, S., Capone, A. and Sansò, B. (2014) "Planning for energy-aware wireless networks," *IEEE Communications Magazine*, 52(2), pp. 156–162.

Bolla, R. and Bruschi, R. (2011) "Energy efficiency in the future internet: a survey of existing approaches and trends in energy-aware fixed network infrastructures," *IEEE Communications Surveys & Tutorials*, 13(2), pp. 223–244.

Bou Saleh, A., Redana, S., Hämäläinen, J. and Raaf, B. (2010) "On the coverage extension and capacity enhancement of inband relay deployments in LTE-Advanced networks," *Journal of Electrical and Computer Engineering*, 2010, pp. 1–12.

Bousia, A., Antonopoulos, A., Alonso, L. and Verikoukis, C. (2012) "'Green' distance-aware base station sleeping algorithm in LTE-Advanced," In *IEEE International Conference on Communications (ICC)*, IEEE, pp. 1367–1371.

Bousia, A., Kartsakli, E., Alonso, L. and Verikoukis, C. (2012) "Dynamic energy efficient distance-aware base station switch on-off scheme for LTE-Advanced," In *2012 IEEE Global Communications Conference (GLOBECOM)*, pp. 1532–1537.

Brubaker, D. (2009) *Optimizing performance and efficiency of PAs in wireless base stations*, White Paper, Texas Instruments, [online] Available from: http://www.ti.com/lit/wp/slwy002a/slwy002a.pdf (Accessed 19 September 2013).

Bulakci, Ö., Awada, A., Saleh, A., Redana, S. and Hämäläinen, J. (2013) "Automated uplink power control optimization in LTE-Advanced relay networks," *EURASIP Journal on Wireless Communications and Networking*, Springer, 2013(1), p. 8.

Caire, G., Knopp, R. and Humblet, P. (1998) "System capacity of F-TDMA cellular systems," *IEEE Transactions on Communications*, 46(12), pp. 1649–1661.

Cao, D., Zhou, S., Zhang, C. and Niu, Z. (2010) “Energy saving performance comparison of coordinated multi-point transmission and wireless relaying,” In *IEEE Global Communications Conference (GLOBECOM)*, IEEE, pp. 1–5.

Chandwani, G., Datta, S. N. and Chakrabarti, S. (2010) “Relay assisted cellular system for energy minimization,” In *Annual IEEE India Conference (INDICON)*, pp. 3–6.

Chen, Y., Zhang, S. and Xu, S. (2010) “Characterizing energy efficiency and deployment efficiency relations for green architecture design,” In *IEEE International Conference on Communications (ICC) Workshops*, IEEE, pp. 1–5.

Chen, Y., Zhang, S., Xu, S. and Li, G. (2011) “Fundamental trade-offs on green wireless networks,” *IEEE Communications Magazine*, 49(6), pp. 30–37.

Chiaraviglio, L., Ciullo, D., Koutitas, G., Meo, M. and Tassiulas, L. (2012) “Energy-efficient planning and management of cellular networks,” In *9th Annual Conference on Wireless On-Demand Network Systems and Services (WONS)*, Ieee, pp. 159–166.

Chiaraviglio, L., Ciullo, D., Meo, M., Marsan, M. A. and Torino, I. (2008) “Energy-aware UMTS access networks,” In *11th International Symposium on Wireless Personal Multimedia Communications (WPMC)*, IEEE, pp. 1–5.

Chiaraviglio, L., Mellia, M. and Neri, F. (2008) “Energy-aware UMTS core network design,” In *11th International Symposium on Wireless Personal Multimedia Communications (WPMC)*, IEEE, pp. 1–5.

Cho, Y. S., Kim, J., Yang, W. Y. and Kang, C. G. (2010) *MIMO-OFDM wireless communications with MATLAB*, John Wiley & Sons.

Choi, W. and Andrews, J. G. (2007) “Downlink performance and capacity of distributed antenna systems in a multicell environment,” *IEEE Transactions on Wireless Communications*, 6(1), pp. 69–73.

Christensen, K., Reviriego, P., Nordman, B., Bennett, M., Mostowfi, M. and Maestro, J. A. (2010) “IEEE 802.3az: the road to energy efficient ethernet,” *IEEE Communications Magazine*, 48(11), pp. 50–56.

Cisco (2013) *Cisco Visual Networking Index: Global Mobile Data Traffic Forecast Update, 2012 – 2017*, white paper, Cisco.

Correia, L., Zeller, D., Blume, O., Ferling, D., Jading, Y., Gódor, I., Auer, G. and Der Perre, L. (2010) “Challenges and enabling technologies for energy aware mobile radio networks,” *IEEE Communications Magazine*, 48(11), pp. 66–72.

Cui, S., Goldsmith, A. J. and Bahai, A. (2005) “Energy-constrained modulation optimization,” *IEEE Transactions on Wireless Communications*, 4(5), pp. 2349–2360.

Deruyck, M., Joseph, W. and Martens, L. (2014) “Power consumption model for macrocell and microcell base stations,” *Transactions on Emerging Telecommunications Technologies*, 25(3), pp. 320–333.

Desset, C., Debaillie, B., Giannini, V., Fehske, A., Auer, G., Holtkamp, H., Wajda, W., Sabella, D., Richter, F., Gonzalez, M. J., Klessig, H., Godor, I., Olsson, M., Imran, M. A., Ambrosy, A. and Blume, O. (2012) “Flexible power modeling of LTE base stations,” In *IEEE Wireless Communications and Networking Conference (WCNC)*, IEEE, pp. 2858–2862.

Dufková, K., Le Boudec, J.-Y., Popović, M., Bjelica, M., Khalili, R. and Kencl, L. (2011) “Energy consumption comparison between macro-micro and public femto deployment in a

plausible LTE network," In *2nd International Conference on Energy-Efficient Computing and Networking*, ACM, pp. 67–76.

Edler, T. and Lundberg, S. (2004) "Energy efficiency enhancements in radio access networks," *Ericsson Review*, (1), pp. 42–51.

Elayoubi, S.-E., Saker, L. and Chahed, T. (2011) "Optimal control for base station sleep mode in energy efficient radio access networks," In *IEEE INFOCOM*, IEEE, pp. 106–110.

Fallgren, M. (2012) "An optimization approach to joint cell, channel and power allocation in multicell relay networks," *IEEE Transactions on Wireless Communications*, 11(8), pp. 1–8.

Fehske, A., Fettweis, G., Malmodin, J. and Biczok, G. (2011) "The global footprint of mobile communications: the ecological and economic perspective," *IEEE Communications Magazine*, 49(8), pp. 55–62.

Fehske, A. J., Richter, F. and Fettweis, G. P. (2009) "Energy efficiency improvements through micro sites in cellular mobile radio networks," In *IEEE Global Communications Conference (GLOBECOM) Workshops*, Ieee, pp. 1–5.

Feng, D., Jiang, C., Lim, G., Cimini, L. J., Feng, G. and Li, G. Y. (2013) "A survey of energy-efficient wireless communications," *IEEE Communications Surveys & Tutorials*, 15(1), pp. 167–178.

Ferling, D., Ambrosy, A., Petersson, S., Hashemi, M., Burstrom, P., Erdem, A., Maugars, P., Retrouvey, J.-M., Mizuta, S., Dietl, G., Boldi, M., Giry, A., Bories, S., Debaillie, B., Torrea, R., Goncalves, T., Cardoso, F., Correia, L., Peixeiro, C., Leinonen, J. and Fernandez, Y. (2012) "Green radio technologies," *EARTH Project D.4.3*.

Ferling, D., Bohn, T. and Zeller, D. (2010) “Energy efficiency approaches for radio nodes,” In *Future Network and Mobile Summit*, Florence, pp. 1–9.

Fettweis, G. and Zimmermann, E. (2008) “ICT energy consumption - trends and challenges,” In *11th International Symposium on Wireless Personal Multimedia Communications (WPMC)*, pp. 1–4.

Frenger, P. and Moberg, P. (2011) “Reducing energy consumption in LTE with cell DTX,” In *IEEE 73rd Vehicular Technology Conference (VTC Spring)*, pp. 1–5.

Ge, X., Cao, C., Jo, M., Chen, M., Hu, J. and Humar, I. (2010) “Energy efficiency modelling and analyzing based on multi-cell and multi-antenna cellular networks,” *KSII Transactions on Internet and Information Systems*, 4(4), pp. 560–574.

Ghosh, A., Mangalvedhe, N., Ratasuk, R., Mondal, B., Cudak, M., Visotsky, E., Thomas, T. A., Andrews, J. G., Xia, P., Jo, H. S., Dhillon, H. S. and Novlan, T. D. (2012) “Heterogeneous cellular networks: from theory to practice,” *IEEE Communications Magazine*, 50(6), pp. 54–64.

Goldsmith, A., Jafar, S. A., Maric, I. and Srinivasa, S. (2009) “Breaking spectrum gridlock with cognitive radios: an information theoretic perspective,” *Proceedings of the IEEE*, 97(5), pp. 894–914.

Gong, J., Thompson, J., Zhou, S. and Niu, Z. (2013) “Base station sleeping and resource allocation in renewable energy powered cellular networks,” *IEEE Transactions on Wireless Communications, submitted*, pp. 1–30, [online] Available from: http://arxiv.org/abs/1305.4996 (Accessed 28 May 2013).

Gong, J., Zhou, S. and Niu, Z. (2012) “A dynamic programming approach for base station sleeping in cellular networks,” *IEICE Transaction on Communications*, IEICE, E95-B(2), pp. 551–562.

Grace, D., Chen, J., Jiang, T. and Mitchell, P. D. (2009) “Using cognitive radio to deliver ‘Green’ communications,” In *4th International Conference on Cognitive Radio Oriented Wireless Networks and Communications*, pp. 1–6.

Grangeat, C., Grandamy, G. and Wauquiez, F. (2010) “A solution to dynamically decrease power consumption of wireless base stations and power them with alternative energies,” In *Intelec 2010*, Ieee, pp. 1–4.

GSMA (2013) *The Mobile Economy 2013*, *GSM Association*, GSMA mobile economy, [online] Available from: http://www.gsmamobileeconomy.com/read/ (Accessed 9 October 2013).

Guo, W. and O’Farrell, T. (2013) “Dynamic cell expansion with self-organizing cooperation,” *IEEE Journal on Selected Areas in Communications*, 31(5), pp. 851–860.

Gür, G. and Alagöz, F. (2011) “Green wireless communications via cognitive dimension: an overview,” *IEEE Network*, 25(2), pp. 50–56.

Han, C., Harrold, T., Krikidis, I., Ku, I., Le, T. A., Videv, S., Zhang, J., Armour, S., Grant, P. M., Haas, H., Hanzo, L., Nakhai, M. R., Thompson, J. S. and Wang, C.-X. (2011) “Green radio: radio techniques to enable energy efficient wireless networks,” *IEEE Communications Magazine*, 49(6).

Han, F., Safar, Z. and Liu, K. (2013) “Energy-efficient base-station cooperative operation with guaranteed QoS,” *IEEE Transaction on Communications*, IEEE, 61(8), pp. 3505–3517.

Han, T. and Ansari, N. (2012) “Optimizing cell size for energy saving in cellular networks with hybrid energy supplies,” In *IEEE Global Communications Conference (GLOBECOM)*, IEEE, pp. 5189–5193.

Hasan, Z. and Bhargava, V. K. (2013) “Relay selection for OFDM wireless systems under asymmetric information: a contract-theory based approach,” *IEEE Transactions on Wireless Communications*, 12(8), pp. 3824–3837.

Hasan, Z., Boostanimehr, H. and Bhargava, V. K. (2011) “Green cellular networks: a survey, some research issues and challenges,” *IEEE Communications Surveys & Tutorials*, 13(4), pp. 524–540.

Haykin, S. (2005) “Cognitive radio: brain-empowered wireless communications,” *IEEE Journal on Selected Areas in Communications*, 23(2), pp. 201–220.

He, A., Srikanteswara, S., Newman, T. R., Reed, J. H., Tranter, W. H., Sajadieh, M. and Marian Verhelst (2009) “System power consumption minimization for multichannel communications using cognitive radio,” In *IEEE International Conference on Microwaves, Communications, Antennas and Electronics Systems*.

He, G., Zhang, S., Chen, Y. and Xu, S. (2012) “Energy efficiency and deployment efficiency tradeoff for heterogeneous wireless networks,” In *IEEE Global Communications Conference (GLOBECOM)*, IEEE, pp. 3189–3194.

Heliot, F., Imran, M. A. and Tafazolli, R. (2011) “Energy efficiency analysis of idealized coordinated multi-point communication system,” In *IEEE 73rd Vehicular Technology Conference (Spring)*, IEEE, pp. 1–5.

Hirata, H., Totani, K., Maehata, T., Shimura, T., Take, M., Kurokawa, Y., Onishi, M., Ada, Y. and Hirata, Y. (2010) "Development of high efficiency amplifier for cellular base stations," *SEI Tech. Review*, 70(November), pp. 47–52.

Holland, O., Friderikos, V. and Aghvami, a. H. (2010) "Green spectrum management for mobile operators," In *IEEE Global Telecommunications Conference (GLOBECOM) Workshops on Green Communications*, IEEE, pp. 1458–1463.

Hossain, E., Bhargava, V. K. and Fettweis, G. P. (2012) *Green radio communication networks*, Cambridge University Press.

Hossain, E., Kim, D. I. and Bhargava, V. K. (eds.) (2011) *Cooperative cellular wireless networks*, Cambridge, Cambridge University Press.

Hossain, F., Munasinghe, K. S., Jamalipour, A. and Hossain, M. F. (2012) "Two level cooperation for energy efficiency in multi-RAN cellular network environment," In *2012 IEEE Wireless Communications and Networking Conference (WCNC)*, IEEE, pp. 2493–2497.

Hossain, M. F. (2013) "Traffic-driven energy efficient operational mechanisms in cellular access networks," The University of Sydney, [online] Available from: http://ses.library.usyd.edu.au/handle/2123/10084 (Accessed 7 March 2014).

Hossain, M. F., Munasinghe, K. S. and Jamalipour, A. (2013a) "On the eNB-based energy-saving cooperation techniques for LTE access networks," *Wireless Communications and Mobile Computing*.

Hossain, M. F., Munasinghe, K. S. and Jamalipour, A. (2012) "On the energy efficiency of self-organizing LTE cellular access networks," In *IEEE Global Communications Conference (GLOBECOM)*, pp. 5314–5319.

Hossain, M. F., Munasinghe, K. S. and Jamalipour, A. (2013b) "Toward self-organizing sectorization of LTE eNBs for energy efficient network operation under QoS constraints," In *IEEE Wireless Communications and Networking Conference (WCNC)*, pp. 1279–1284.

Hosseini, K., Hoydis, J., ten Brink, S. and Debbah, M. (2013) "Massive MIMO and small cells: How to densify heterogeneous networks," In *IEEE International Conference on Communications (ICC)*, IEEE, pp. 5442–5447.

Hu, R. and Qian, Y. (2014) "An energy efficient and spectrum efficient wireless heterogeneous network framework for 5G systems," *IEEE Communications Magazine*, 52(5), pp. 94–101.

Huawei (2011) "Improving energy efficiency, lower CO2 emission and TCO," *White paper*, [online] Available from: http://www.huawei.com/uk/static/hw-076768.pdf (Accessed 5 December 2012).

IEEE (2009a) "IEEE 802.16's relay task group," *IEEE*, [online] Available from: http://www.ieee802.org/16/relay (Accessed 21 May 2013).

IEEE (2009b) "IEEE 802.16m evaluation methodology document," *IEEE 802.16 WG*.

IEEE (2007) "Multi-hop relay system evaluation methodology (channel model and performance metric)," *IEEE C802.16j-06/013r3*.

Imran, M. A., Alonso-Rubio, J., Auer, G., Boldi, M., Braglia, M., Fazekas, P., Ferling, D., Fehske, A., Frenger, P., Gupta, R., Katranaras, E., Manosha, S., Pirinen, P., Rajatheva, N., Sabella, D., Skillermark, P., Perre, L. Van der, Vidács, A. and Wajda, W. (2012) "Most suitable efficiency metrics and utility functions," *EARTH Project D.2.4*.

Irmer, R., Droste, H., Marsch, P., Grieger, M., Fettweis, G., Brueck, S., Mayer, H. and Theiele, L. (2011) "Coordinated multi-point: concepts, performance, and field trial results," *IEEE Communications Magazine*, 49(2), pp. 102–111.

Ismail, M. and Zhuang, W. (2011) "Network cooperation for energy saving in green radio communications," *IEEE Wireless Communications*, 18(5), pp. 76–81.

ITU-R (2009) *Guidelines for evaluation of radio interface technologies for IMT-Advanced*, [online] Available from: http://www.itu.int/dms_pub/itu-r/opb/rep/R-REP-M.2135-1-2009-PDF-E.pdf (Accessed 12 April 2012).

ITU-T (2010) "Overview of energy saving of networks," *ITU-T Focus Group on Future Networks (FG-FN), FG-FN OD-66, Draft Deliverable*, [online] Available from: http://www.itu.int/dms_pub/itu-t/oth/3A/05/T3A050000740001MSWE.doc (Accessed 15 April 2012).

Iwamura, M., Takahashi, H. and Nagata, S. (2010) "Relay technology in LTE-Advanced," *NTT DoCoMo Technical Journal*, 12(2), pp. 29–36, [online] Available from: http://www.nttdocomo.co.jp/english/binary/pdf/corporate/technology/rd/technical_journal/bn/vol12_2/vol12_2_029en.pdf (Accessed 2 January 2014).

Jain, R., Katiyar, S. and Agrawal, N. (2011) "Smart antenna for cellular mobile communication," *International Journal of Electrical, Electronics & Communication Engineering*, 1(9), pp. 530–541.

Joung, J., Chia, Y. K. and Sun, S. (2014) "Energy-efficient, large-scale distributed-antenna system (L-DAS) for multiple users," *IEEE Journal of Selected Topics in Signal Processing*, PP(99), pp. 1–12.

Joung, J., Ho, C. and Sun, S. (2014) “Spectral efficiency and energy efficiency of OFDM systems: Impact of power amplifiers and countermeasures,” *IEEE Journal on Selected Areas in Communications*, 32(2), pp. 208–220.

Jovicic, A. and Viswanath, P. (2009) “Cognitive radio: an information-theoretic perspective,” *IEEE Transactions on Information TheoryInformation Theory*, 55(9), pp. 3945–3958.

Kanesan, T. and Ng, W. (2012) “Theoretical and experimental design of an alternative system to 2× 2 MIMO for LTE over 60 km directly modulated RoF link,” In *IEEE Global Communications Conference (GLOBECOM)*, IEEE, pp. 2959–2964.

Kasch, W. T., Ward, J. R. and Andrusenko, J. (2009) “Wireless network modeling and simulation tools for designers and developers,” *IEEE Communications Magazine*, 47(3), pp. 120–127.

Khirallah, C., Thompson, J. S. and Rashvand, H. (2011) “Energy and cost impacts of relay and femtocell deployments in long-term-evolution advanced,” *IET Communications*, 5(18), p. 2617.

Kim, J., Hwang, J. and Han, Y. (2010) “Joint processing in multi-cell coordinated shared relay network,” In *IEEE International Symposium on Personal, Indoor and Mobile Radio Communications (PIMRC)*, IEEE, pp. 702–706.

Ku, I., Wang, C. and Thompson, J. (2013) “Spectral-energy efficiency tradeoff in relay-aided cellular networks,” *IEEE Transaction on Wireless Communications*, 12(10), pp. 4970–4982.

Lannoo, C. B., Lambert, S., Heddeghem, W. Van, Pickavet, M., Tudelft, F. K., Koutitas, G., Niavis, H., Certh, A. S., Till, M., Fischer, A., Meer, H. De, Passau, U. N. I., Ulanc, P.

A., Epfl, P., Viet, N. H., Uio, T. P. and Uam, J. A. (2013) "Overview of ICT energy consumption," *Network of Excellence in Internet Science, D8.1*, iMinds.

Lee, B. and Kim, S. (2012) "Characterizing energy and deployment efficiency relations in cellular systems," In *6th International Conference on Signal Processing and Communication Systems*, IEEE, pp. 1–5.

Lee, D., Zhou, S. and Niu, Z. (2011) "Multi-hop relay network for base station energy saving and its performance evaluation," In *IEEE Global Communications Conference (GLOBECOM)*, IEEE, pp. 1–5.

Lee, D., Zhou, S. and Niu, Z. (2013) "Spatial modeling of Scalable Spatially-correlated log-normal distributed traffic inhomogeneity and energy-efficient network planning," In *IEEE Wireless Communications and Networking Conference (WCNC)*, IEEE, pp. 1303–1308.

Lee, J., Kim, Y., Lee, H., Ng, B. L., Mazzarese, D., Liu, J., Xiao, W. and Zgou, Y. (2012) "Coordinated multipoint transmission and reception in LTE-advanced systems," *IEEE Communications Magazine*, 50(11), pp. 44–50.

Leem, H., Baek, S. Y. and Sung, D. K. (2010) "The effects of cell size on energy saving, system capacity, and per-energy capacity," In *IEEE Wireless Communication and Networking Conference (WCNC)*, IEEE, pp. 1–6.

Letaief, K. and Zhang, W. (2009) "Cooperative communications for cognitive radio networks," *Proceedings of the IEEE*, 97(5).

Li, G., Xu, Z., Xiong, C., Yang, C., Zhang, S., Chen, Y. and Xu, S. (2011) "Energy-efficient wireless communications: tutorial, survey, and open issues," *IEEE Wireless Communications*, 18(6), pp. 28–35.

Li, L., Zhou, X., Xu, H., Li, G. Y., Wang, D. and Soong, A. (2010) "Energy-efficient transmission in cognitive radio networks," In *7th IEEE Consumer Communications and Networking Conference (CCNC)*, IEEE, pp. 1–5.

Lin, B., Ho, P. and Xie, L. (2010) "Optimal relay station placement in broadband wireless access networks," *IEEE Transactions on Mobile Computing*, 9(2), pp. 259–269.

Lister, D. (2009) "An operator's view on green radio," In *Keynotes, IEEE ICC Workshop on GreenComm*, Dresden, Germany.

Louhi, J. T. (2007) "Energy efficiency of modern cellular base stations," In *29th International Telecommunication Energy Conference (INTELEC)*, pp. 475–476.

Mancuso, V. and Alouf, S. (2011) "Reducing costs and pollution in cellular networks," *IEEE Communications Magazine*, IEEE, 49(8), pp. 63–71.

Marsan, M. A., Chiaraviglio, L., Ciullo, D. and Meo, M. (2009) "Optimal energy savings in cellular access networks," In *IEEE International Conference on Communications (ICC) Workshops*, IEEE, pp. 1–5.

Marsan, M. A., Chiaraviglio, L., Ciullo, D. and Meo, M. (2011) "Switch-off transients in cellular access networks with sleep modes," In *IEEE International Conference on Communications (ICC) Workshops*, IEEE, pp. 1–6.

Marsan, M. A. and Meo, M. (2010) "Energy efficient management of two cellular access networks," *ACM SIGMETRICS Performance Evaluation Review*, 37(4), pp. 69–73.

Marsan, M. A. and Meo, M. (2011) "Energy efficient wireless Internet access with cooperative cellular networks," *Computer Networks*, Elsevier, 55(2), pp. 386–398.

Marzetta, T. L. (2010) “Noncooperative cellular wireless with unlimited numbers of base station antennas,” *IEEE Transactions on Wireless Communications*, IEEE, 9(11), pp. 3590–3600.

Mathworks (n.d.) “Design and code verification using formal mathematics,” [online] Available from: http://www.mathworks.co.uk/discovery/formal-verification.html (Accessed 12 January 2013).

McLaughlin, S. S., Grant, P. M., Thompson, J. S., Haas, H., Laurenson, D. I., Khirallah, C., Hou, Y. and Wang, R. (2011) “Techniques for improving cellular radio base station energy efficiency,” *IEEE Wireless Communications*, IEEE, 18(5), pp. 10–17.

Miao, G., Himayat, N., Li, G. and Talwar, S. (2009) “Interference-aware energy-efficient power optimization,” In *2009 IEEE International Conference on Communications*, pp. 0–4, [online] Available from: http://ieeexplore.ieee.org/xpls/abs_all.jsp?arnumber=5199096 (Accessed 17 April 2013).

Mietzner, J., Schober, R., Lampe, L., Gerstacker, W. H. and Hoeher, P. A. (2009) “Multiple-antenna techniques for wireless communications - a comprehensive literature survey,” *IEEE Communications Surveys & Tutorials*, IEEE, 11(2), pp. 87–105, [online] Available from: http://ieeexplore.ieee.org/xpls/abs_all.jsp?arnumber=5039585 (Accessed 14 March 2014).

Mitola, J. and Maguire, G. Q. (1999) “Cognitive radio: making software radios more personal,” *IEEE Personal Communications*, IEEE, 6(4), pp. 13–18.

Morosi, S., Piunti, P. and Re, E. Del (2013) “Sleep mode management in cellular networks: a traffic based technique enabling energy saving,” *Transactions on Emerging Telecommunications Technologies*, 24(3), pp. 331–341.

Nekovee, M. (2010) “A survey of cognitive radio access to TV white spaces,” *International Journal of Digital Multimedia Broadcasting*, 2010, pp. 1–11.

Neves, L. and Krajewski, J. (2012) “SMARTer 2020: the role of ICT in driving a sustainable future,” *Global eSustainability Initiative (GeSI)*.

Ng, T. and Yu, W. (2007) “Joint optimization of relay strategies and resource allocations in cooperative cellular networks,” *IEEE Journal on Selected Areas in Communications*, IEEE, 25(2), pp. 328–339.

Niu, Z., Wu, Y., Gong, J. and Yang, Z. (2010) “Cell zooming for cost-efficient green cellular networks,” *IEEE Communications Magazine*, IEEE, 48(11), pp. 74–79.

Niu, Z., Zhang, J., Guo, X. and Zhou, S. (2012) “On energy-delay tradeoff in base station sleep mode operation,” In *IEEE International Conference on Communication Systems (ICCS)*, IEEE, pp. 235–239.

Norris, J. R. (1998) *Markov chains*, Cambridge University Press.

Novlan, T. D., Ganti, R. K., Ghosh, A. and Andrews, J. G. (2011) “Analytical evaluation of fractional frequency reuse for OFDMA cellular networks,” *IEEE Transactions on Wireless Communications*, IEEE, 10(12), pp. 4294–4305.

Oh, E. and Krishnamachari, B. (2010) “Energy savings through dynamic base station switching in cellular wireless access networks,” In *IEEE Global Telecommunications Conference (GLOBECOM)*, IEEE, pp. 1–5.

Oh, E., Krishnamachari, B., Liu, X. and Niu, Z. (2011) “Toward dynamic energy-efficient operation of cellular network infrastructure,” *IEEE Communications Magazine*, IEEE, 49(6), pp. 56–61.

Oh, E., Son, K. and Krishnamachari, B. (2013) “Dynamic base station switching-on/off strategies for green cellular networks,” *IEEE Transactions on Wireless Communications*, IEEE, 12(5), pp. 2126–2136.

Olsson, M., Cavdar, C., Frenger, P., Tombaz, S., Sabella, D. and Jantti, R. (2013) “5GrEEn: towards green 5G mobile networks,” In *IEEE 9th International Conference on Wireless and Mobile Computing, Networking and Communications (WiMob)*, IEEE, pp. 212–216.

Pabst, R., Walke, B. H., Schultz, D. C., Herhold, P., Yanikomeroglu, H., Mukherjee, S., Viswanathan, H., Lott, M., Zirwas, W., Dohler, M., Aghvami, H., Falconer, D. D. and Fettweis, G. P. (2004) “Relay-based deployment concepts for wireless and mobile broadband radio,” *IEEE Communications Magazine*, IEEE, 42(9), pp. 80–89.

Pace, P. (2012) “Green antenna switching to improve energy saving in LTE networks,” In *IEEE Online Conference on Green Communications (GreenCom)*, IEEE, pp. 92–97, [online] Available from: http://ieeexplore.ieee.org/lpdocs/epic03/wrapper.htm?arnumber=6519622.

Palicot, J. (2009) “Cognitive radio: an enabling technology for the green radio communications concept,” In *International Conference on Wireless Communications and Mobile Computing*, ACM, pp. 489–494.

Panah, A. Y., Truong, K. T., Peters, S. W. and Heath, R. W. (2011) “Interference management schemes for the shared relay concept,” *EURASIP Journal on Advances in Signal Processing*, 2011(1), pp. 1–14.

Peng, C., Lee, S.-B., Lu, S., Luo, H. and Li, H. (2011) “Traffic-driven power saving in operational 3G cellular networks,” In *ACM 17th Annual International Conference on Mobile Computing and Networking (MobiCom)*, ACM, pp. 121–132.

Pescovitz, D. (2004) “Wireless ways to go green,” [online] Available from: http://coe.berkeley.edu/labnotes/0904/horvath.html (Accessed 1 April 2012).

Peters, S. W., Panah, A., Truong, K. and Heath, R. W. (2009) “Relay architectures for 3GPP LTE-Advanced,” *EURASIP Journal on Wireless Communications and Networking*, 2009(1), p. 618787.

Rao, J. and Fapojuwo, A. (2013) “A survey of energy efficient resource management techniques for multicell cellular networks,” *IEEE Communications Surveys & Tutorials*, IEEE, 16(1), pp. 154–180.

Rappaport, T. S. (2001) *Wireless communications - principles and practice*, Second. Pearson Education.

Richter, F., Fehske, A. J. and Fettweis, G. P. (2009) “Energy efficiency aspects of base station deployment strategies for cellular networks,” In *IEEE 70th Vehicular Technology Conference (Fall)*, IEEE, pp. 1–5.

Richter, F., Fehske, A. J., Marsch, P. and Fettweis, G. P. (2010) “Traffic demand and energy efficiency in heterogeneous cellular mobile radio networks,” In *IEEE 71st Vehicular Technology Conference (Spring)*, IEEE, pp. 1–6.

Richter, F. and Fettweis, G. (2010) “Cellular mobile network densification utilizing micro base stations,” In *IEEE International Conference on Communications (ICC)*, IEEE, pp. 1–6.

Roche, G. de la, Glazunov, A. A. and Allen, B. (eds.) (2013) *LTE-advanced and next generation wireless networks: channel modelling and propagation*, John Wiley & Sons.

Sachs, J., Maric, I. and Goldsmith, A. (2010) “Cognitive cellular systems within the TV spectrum,” In *IEEE Symposium on New Frontiers in Dynamic Spectrum (DySPAN)*, IEEE, pp. 1–12.

Sawahashi, M., Kishiyama, Y., Morimoto, A., Nishikawa, D. and Tanno, M. (2010) “Coordinated multipoint transmission/reception techniques for LTE-advanced,” *IEEE Wireless Communications*, IEEE, 17(3), pp. 26–34.

Shafiq, M. Z., Ji, L., Liu, A. X. and Wang, J. (2011) “Characterizing and modeling internet traffic dynamics of cellular devices,” *ACM SIGMETRICS Performance Evaluation Review*, ACM, 39(1), p. 265.

Shannon, C. (1948) “A mathematical theory of communication,” *The Bell System Technical Journal*, 27(July 1948), pp. 379–423, [online] Available from: http://dl.acm.org/citation.cfm?id=584093 (Accessed 21 February 2014).

Shen, X. (2013) “Green Wireless Communication Networks [Editor’s Note],” *IEEE Network*, 27(2), pp. 2–3.

Soh, Y. S., Quek, T. Q. S., Kountouris, M. and Shin, H. (2013) “Energy efficient heterogeneous cellular networks,” *IEEE Journal on Selected Areas in Communications*, IEEE, 31(5), pp. 840–850.

Son, K., Chong, S. and Veciana, G. (2009) “Dynamic association for load balancing and interference avoidance in multi-cell networks,” *IEEE Transactions on Wireless Communications*, IEEE, 8(7), pp. 3566–3576.

Son, Kyuho, Kim, H., Yi, Y. and Krishnamachari, B. (2011) “Base station operation and user association mechanisms for energy-delay tradeoffs in green cellular networks,” *IEEE Journal on Selected Areas in Communications*, IEEE, 29(8), pp. 1525–1536.

Son, Kyuho, Oh, E. and Krishnamachari, B. (2011) “Energy-aware hierarchical cell configuration: from deployment to operation,” In *IEEE Conference on Computer Communications Workshops (INFOCOM Workshop)*, IEEE, pp. 289–294.

Son, Kyuho;, Oh, E. and Krishnamachari, B. (2011) “Normalized cellular traffic trace recorded during one week,” *ANRG*, [online] Available from: http://anrg.usc.edu/www/index.php/Downloads/ (Accessed 24 August 2011).

Song, Y., Yang, H., Liu, J., Cai, L., Li, D., Zhu, X., Wu, K. and Liu, H. (2008) *Relay station shared by multiple base stations for inter-cell interference mitigation*, *IEEE 802.16 Broadband Wireless Access Working Group (C802. 16m-08/1436r1)*.

Tabassum, H., Siddique, U., Hossain, E. and Hossain, M. J. (2014) “Downlink performance of cellular systems with base station sleeping, user association, and scheduling,” *IEEE Transactions on Wireless Communications*, PP(99), pp. 1–15.

Tariq, F. (2012) “Interference aware cognitive femtocell networks,” PhD thesis, The Open University, [online] Available from: http://oro.open.ac.uk/37461/ (Accessed 13 July 2013).

Tran, T.-T., Shin, Y. and Shin, O.-S. (2012) “Overview of enabling technologies for 3GPP LTE-advanced,” *EURASIP Journal on Wireless Communications and Networking*, Springer, 2012(1), p. 54.

Tranter, W. H., Shanmugan, K. S., Rappaport, Th. S. and Kosbar, K. L. (2003) *Principles of communication systems simulation with wireless applications*, Prentice Hall.

Tse, D. and Viswanath, P. (2005) *Fundamentals of wireless communication*, Cambridge University Press.

Uddin, M. F., Assi, C. and Ghrayeb, A. (2012) “Joint optimal relay selection and power allocation in multicast cooperative networks,” In *IEEE International Conference on Communications (ICC)*, IEEE, pp. 5086–5091.

Wang, C.-X., Haider, F., Gao, X., You, X.-H., Yang, Y., Yuan, D., Aggoune, H. M., Haas, H., Fletcher, S. and Hepsaydir, E. (2014) “Cellular architecture and key technologies for 5G wireless communication networks,” *IEEE Communications Magazine*, IEEE, 52(4), pp. 122–130.

Wang, X., Chen, M., Taleb, T., Ksentini, A. and Leung, V. C. M. (2014) “Cache in the air: exploiting content caching and delivery techniques for 5G systems,” *IEEE Communications Magazine*, IEEE, 52(2), pp. 131–139.

Webb, M. (2008) “SMART 2020: Enabling the low carbon economy in the information age,” *The Climate Group, London*, [online] Available from: http://www.smart2020.org/_assets/files/02_Smart2020Report.pdf (Accessed 1 April 2014).

Weng, X., Cao, D. and Niu, Z. (2011) “Energy-efficient cellular network planning under insufficient cell zooming,” In *IEEE 73rd Vehicular Technology Conference (Spring)*, IEEE, pp. 1–5.

Willkomm, D., Machiraju, S., Bolot, J. and Wolisz, A. (2009) “Primary user behaviour in cellular networks and implications for dynamic spectrum access,” *IEEE Communications Magazine*, IEEE, 47(3), pp. 88–95.

Willkomm, D., Machiraju, S., Bolot, J. and Wolisz, A. (2008) “Primary users in cellular networks: a large-scale measurement study,” In *3rd IEEE Symposium on New Frontiers in Dynamic Spectrum Access Networks (DYSPAN)*, IEEE, pp. 1–11.

Wu, G. and Feng, G. (2012) “Energy-efficient relay deployment in next generation cellular networks,” In *IEEE International Conference on Communications (ICC)*, IEEE, pp. 5757–5761.

Wu, J. (2012) “Green wireless communications: from concept to reality [Industry Perspectives],” *IEEE Wireless Communications*, IEEE, 19(4), pp. 4–5.

Wu, J., Zhou, S. and Niu, Z. (2013) “Traffic-aware base station sleeping control and power matching for energy-delay tradeoffs in green cellular networks,” *IEEE Transactions on Wireless Communications*, IEEE, 12(8), pp. 4196–4209.

Xu, X., He, G., Zhang, S., Chen, Y., Xu, S. and Technologies, H. (2013) “On functionality separation for green mobile networks: concept study over LTE,” *IEEE Communications Magazine*, IEEE, 51(5), pp. 82–90.

Yang, Y., Hu, H., Xu, J. and Mao, G. (2009) “Relay technologies for WiMAX and LTE-advanced mobile systems,” *IEEE Communications Magazine*, IEEE, (October), pp. 100–105.

Yang, Z. and Niu, Z. (2013) “Energy saving in cellular networks by dynamic RS-BS association and BS switching,” *IEEE Transactions on Vehicular Technology*, IEEE, (c), pp. 1–12.

Yarkan, S., Teo, K. H., Arslan, H., Zhang, J. and Qaraqe, K. a. (2010) “Upper and lower bounds on subcarrier collision for inter-cell interference scheduler in OFDMA-based systems: voice traffic,” *Physical Communication*, Elsevier, 3(4), pp. 265–275, [online] Available from: http://linkinghub.elsevier.com/retrieve/pii/S1874490710000182 (Accessed 18 May 2014).

Yeh, S., Talwar, S. and Wu, G. (2011) “Capacity and coverage enhancement in heterogeneous networks,” *IEEE Wireless Communications*, 18(3), pp. 32–38, [online] Available from: http://ieeexplore.ieee.org/xpls/abs_all.jsp?arnumber=5876498 (Accessed 1 January 2014).

Yvetot, B. (2010) *Orange development strategy in Africa*, [online] Available from: http://euroafrica-ict.org/wp-content/plugins/alcyonis-event-agenda/files/Orange_development_strategy_in_Africa.pdf (Accessed 28 August 2012).

Zeng, H. and Zhu, C. (2008) “System-Level modeling and performance evaluation of multi-hop 802.16j systems,” In *International Wireless Communications and Mobile Computing Conference*, pp. 354–359.

Zhou, S., Goldsmith, A. J. and Niu, Z. (2011) “On optimal relay placement and sleep control to improve energy efficiency in cellular networks,” In *2011 IEEE International Conference on Communications (ICC)*, IEEE, pp. 1–6, [online] Available from: http://ieeexplore.ieee.org/xpl/articleDetails.jsp?arnumber=5963235 (Accessed 13 July 2012).

Zhou, S., Gong, J., Yang, Z., Niu, Z., Yang, P. and Corporation, D. (2009) “Green mobile access network with dynamic base station energy saving,” In *ACM MobiCom*, ACM, pp. 10–12.